U.S. Department of the Interior
Bureau of Land Management

BLM-Alaska Open File Report 78
BLM/AK/ST-00/018+3091+932
May 2000

Alaska State Office
222 W. Seventh Avenue, #13
Anchorage, Alaska 99513

Geology and Gold Mineralization of the Nolan Area in the Brooks Range, Alaska

Karsten Eden

Geology and Gold Mineralization of the Nolan Area in the Brooks Range, Alaska

by
Karsten Eden

BLM-Alaska Open File Report 78
May 2000

U.S. Department of Interior
Bureau of Land Management
Alaska State Office
222 W. 7th Avenue, #13
Anchorage, Alaska 99513

Mission Statement

The Bureau of Land Management sustains the health, diversity, and productivity of the public lands for the use and enjoyment of present and future generations.

Authors

Karsten Eden is a geologist who volunteered for the BLM in 1998. He recently completed his Master's Thesis with the Institute of Deposits, the Institute of Geology, and the Institute of Mining Engineering at the Technical University of Clausthal in Germany.

Cover

West-facing view of the Brooks Range, the confluence of Smith and Nolan Creeks is right of photo center. Photo by Joseph Kurtak of the BLM.

Open File Reports

Open File Reports issued by the Bureau of Land Management-Alaska present the results of inventories or other investigations on a variety of scientific and technical subjects that are made available to the public outside the formal BLM-Alaska technical series. These reports can include preliminary or incomplete data and are not published and distributed in quantity.

The reports are available while supplies last from BLM External Affairs, 222 West 7th Avenue #13, Anchorage, Alaska 99513 and from the Juneau Minerals Information Center, 100 Savikko Road, Mayflower Island, Douglas, AK 99824, (907) 364-1553. Copies are also available for inspection at the Alaska Resource Library and Information Service (Anchorage), the USDI Resources Library in Washington, D.C., various libraries of the University of Alaska, the BLM National Business Center, and other selected locations.

A complete bibliography of all BLM-Alaska scientific reports can be found on the Internet at: http://www.ak.blm.gov/affairs/sci_rpts.html. Related publications are also listed at http://juneau.ak.blm.gov

ABSTRACT

The purpose of this thesis study is to examine the Geology and Gold Mineralization of the Nolan area in the Brooks Range of Alaska.

The Nolan area is comprised of metasedimentary rocks of the Coldfoot subterrane and Hammond subterrane of the Arctic Alaska terrane. The metasedimentary rocks have been assigned to Middle to Upper Devonian age. The metabasite dyke mapped in the study area is believed to be Upper Devonian to Jurassic in age.

During Late Jurassic to Early Cretaceous time the Middle Devonian metasedimentary rocks of the Coldfoot subterrane were thrust northward onto the Middle to Upper Devonian metasedimentary rocks of the Hammond subterrane. This is represented by a large thrust belt in the study area. This event produced regional metamorphism of the continental rocks that were overridden.
Thrusting led to north-northwest-vergent folding of the metasedimentary rocks, as evidenced by mapping.

A second major tectonic event in the study area is represented by post-Early Cretaceous, west-trending, strike-slip faulting that displaces the thrust faults.
Moreover, this east-west compression has produced a series of small north-south trending folds.

Two prominent joint systems are developed in the study area. These are interpreted to be tension fractures. Analogous to the prominent joint systems, two different striking gold-bearing vein systems occur in the Nolan-Hammond area. The NW-striking quartz-gold and NE-striking stibnite-quartz-gold vein systems were emplaced in these tension fractures (post-metamorphic structures) during uplift at temperatures below 300°C.
The composition of gold in both vein systems is different. Gold from the stibnite-quartz-gold veins is characterized by its low silver content, whereas gold from the quartz-gold veins shows a high silver content. Gold is believed to have been mobilized from metasedimentary rocks at lower crustal levels by metamorphic hydrothermal fluids. Gold-bearing vein systems were emplaced during Albian and Campanian time periods.

Placer gold from the Nolan-Hammond area can directly be related to the two different gold-bearing vein systems occurring in the area. Analogous to lode gold, placer gold can also be distinguished into two different populations characterized by a low silver type and a high silver type. The fact that productive placer deposits in the Nolan-Hammond area are located around or nearby auriferous veins, and the occurrence of both populations in lode and placer gold is evidence that placer gold in the Nolan-Hammond area has been derived by the erosion of the two different gold-bearing vein systems occuring in the area.

ACKNOWLEDGEMENTS

I would like to thank my advisors Prof. Dr. Bernd Lehmann, Prof. Dr. Gerhard Reik, and Prof. Dr.-Ing. Wolfgang Helms from the Technical University of Clausthal for their support and encouragement during the course of this study.

I am indebted to Mr. Joseph Kurtak (Alaska Mineral Resource Team, Bureau of Land Management), Mr. Mike Balen (President of Tri-con Mining Alaska), and Mr. Ed Armstrong (President of Silverado Mines (U.S.) Inc.) for giving me this great project and for allowing me the privilege of working in the Brooks Range. I cannot thank them enough for their tremendous support by providing office space, transportation, sample analysis, technical assistance, and room and board during field work. Furthermore, I have to thank them for the many hours we spent in inspirational discussion on geology. Thanks again to Joseph Kurtak for his continued assistance and support during my research and availability for consultation, and finally for his critical review of earlier versions of this manuscript.

I would also like to thank Prof. Dr. Rainer Newberry (University of Alaska Fairbanks), Dr. Kenneth Severin (University of Alaska Fairbanks), Mr. Rocky R. Reifenstuhl (Alaska Division of Geological and Geophysical Surveys, Fairbanks), and Dr. Richard Goldfarb (U.S. Geological Survey, Denver, Colorado) for their enormous support and availability for consultation. Moreover, I would like to thank Mr. Jack DiMarchi (Project Geologist, Teck Corp.) for the inspirational discussions on Nolan geology.

Special thanks go to Dr. E. Gierth, Dr. A. K. Schuster, and Dr. H.J. Franzke for their assistance during research at the Technical University of Clausthal.

I am also indebted to Mr. Jeff Lund for his tremendous extraordinary support out at Nolan, for the inspirational discussions we had about the meaning life, for his instructions of survival, and finally for being a very good friend. Thanks for introducing me to the "Airport Lounge" at Coldfoot.
Thanks go to Mr. Myron Wagoner for his enormous support out at Nolan and for being a very good friend.
Special thanks go to our lovely cook Mrs. Marie Mead, not only for her wonderful cooking, but also for making camp life more pleasant. I still miss your wonderful cooking.
Thanks to all the people at Tri-con Mining in Fairbanks for their great support, especially to Mr. Roger Burggraf.

I am also indebted to Mr. Steve Wells and Mrs. Sharon Wells for their tremendous support and their warm hospitality in Anchorage. I would not have made it without their support.
Very special thanks go to Sydney J. Wells for believing in my work and for her patience with me.

Special thanks to the guys from EDEN, VORRATH & PARTNER (Scientific-Technical Services and Consultancy) for their technical assistance during my research and for the many inspirational discussions we had.

My gratitude to the helicopter pilot Ed Bartoli (Air Logistics) for safely transporting me to peaks, ridges and valleys during field work.

Very special thanks to my friends Mr. Robert Klieforth, Mr. Darrel Vandeweg, and Mr. John Clark from BLM for their tremendous support, continuing assistance, and for their friendship. I especially enjoyed the great discussions we guys had at Humpie`s and at the Pioneer Bar over a few pints of Newcastle Ale and Alaskan Amber. Remember, the next shout is on me. It has been a pleasure working together with you guys.

Thanks to my friend and colleague Mr. Mark Siebigteroth for his assistance and the many discussions we had on geologic problems. Furthermore, I would like to thank him for being a very good friend, for the all the fun we have had so far, and for the long inspirational discussions about life at the "Kellerbar".

Thanks to my brothers Jörg, Hendrik, and Torsten Eden for their support and simply for being there when needed. Special thanks go to Torsten for his critical review of this manuscript as well as for providing me with EDEN 21:30 homebrew, when necessary.

Finally, thanks and appreciation go to my parents Berend and Hilke Eden who believed that all these years of education would finally culminate in the following thesis.

TABLE OF CONTENTS

LIST OF FIGURES

LIST OF TABLES

I. Introduction

I.I Geography

Location: Nolan is located in the Koyukuk Mining District, situated about six miles north-northwest of Wiseman in the middle fork of the Koyukuk River (southern Brooks Range), 263 miles (408 km) north of Fairbanks.
The map and study area, containing 42 square miles (107.5 km^2), is situated between Latitude 67°26' - 67°32' and Longitude 150°02' - 150°15.5', covered by the Wiseman B-1 and Wiseman C-1 Quadrangle maps.

Access: Access to Nolan is by surface transportation on the Dalton Highway to Wiseman and then by mine access road to the camp. An airstrip suitable for light aircraft is located below the confluence of Smith Creek with Nolan Creek.

Apart from the five mile mine access road, which leads from Wiseman to the Nolan Camp and a bit further to Thompson Pup, and a second road leading from the Wiseman turn-off to Vermont Creek along the Hammond River, there are no trails in the study area suitable for Pick-Up Trucks. In order to reach remote places, like for example the other side of the Hammond River or mountain tops, helicopter transportation is necessary. Four-wheelers are required to reach locations between Nolan Creek and the Hammond River and difficult accessible places. This kind of transportation is necessary to work economically as field season is very short north of the arctic circle.

Topography: The Nolan area consists of rugged, and glacially sculptured mountains and ridges, such as Smith Creek Dome (4005 ft), Butte Mountain (3854 ft), Vermont Dome (4635 ft), and Midnight Dome (3585-3860 ft). The vertical range is almost a thousand meters (3000 ft). Where bedrock has been glaciated, bench slopes have formed (Fig.1).
Very common are the V-shaped valleys in which the creeks and gulches are located.
The Koyukuk River and the Hammond River (Fig.2), which leads in the Koyakuk River flow in the wide flat-floored, glaciated valleys (U-shaped).

Outcrop exposures are not the best in the area, mostly confined to ridgetops, gully, and creek bottoms, but even on ridgetops it is difficult to take representative data as, due to the glaciation, most of the outcrop is rugged and sculptured. Very often outcrop is displaced by solifluction.

Vegetation: On south facing-slopes at altitudinal treeline up to 2700 ft, mixed black and white spruce stands are open and dominated by nearly continuous shrub layers of birch and alder. Grass grows on the valley bottoms.
All country above 2000 ft in elevation is covered with mosses and lichens, an area of typical tundra. The common most berry is the blueberry. The lowbush cranberry is the second most common.

Wildlife: Wildlife is often seen in the study area. The area, as a whole, contains moose, dall sheep, and bears. Of these bears and sheep are the most abundant. Grizzly bears are common at Midnight Dome, the Hammond River, Montana Mountain and Vermont Creek, whereas dall sheep can often be seen on the top of

Butte Mountain. Other mammals in the area include wolves, foxes, rabbits, and ground squirrels. Mosquitoes and horse flies are prevalent during summer months.

Fig.1: View from Montana Mountain southwards to Nolan Valley and Nolan Camp.

Fig.2: View from the head of Gold Bottom Gulch westwards along the Hammond River. Vermont Dome is seen in the distance (4635 ft).

Climate: The Nolan area has a sub Arctic climate with a short, hot summer and long cold winter. Most precipitation occurs during the summer when storms track through the area from the south southwest. During the winter, the interior is dominated by relatively dry, continental polar-air masses; although infrequently, maritime air intrudes the area from the west or southwest, causing major snowstorms and, occasionally, winter rain. Overall, precipitation in the interior is convectional, widely scattered, and variable.

Temperature: Temperature regime in the area is extreme. It ranges from winter extreme minimum temperatures around -65°F (-54°C) and summer maximum temperatures above 89°F (32°C), a range of more than 154°F (86°C).

Permafrost: Permafrost is defined as a thickness of soil or other superficial deposit (or even bedrock) that has been colder than 32°F (0°C) for at least 2 years (MULLER, 1947). Permafrost occurs in the study area. In summertime it melts down to one meter deep from top, but is permanently frozen in fall, winter, and spring.

I.II Previous Geologic Investigations

Geologic investigations of the Wiseman Quadrangle began as early as 1899, when SCHRADER (1900) of the U.S.G.S. conducted reconnaissance geologic investigations along the Chandalar and Koyakuk Rivers. BROOKS (1904) discussed the early mining activities in the area and described the gold placer deposits found along the middle fork of the Koyakuk River at Tramway Bar, about 30 miles north of Nolan Creek camp. MADDREN (1913) and REED (1938) described the Koyukuk and Chandalar region. The U.S.G.S. have continued investigations in the area to the present with recent work orientated towards evaluating the resource potential of the area. The ALASKA STATE GEOLOGICAL SURVEY, DIVISION OF GEOLOGICAL AND GEOPHYSICAL SURVEYS, BUREAU OF MINES, and BUREAU OF LAND MANAGEMENT have carried out geological and geochemical programs in the Wiseman Quadrangle in recent years. Further, geologic investigations in the Wiseman quadrangle have been done by the UNIVERSITY OF ALASKA FAIRBANKS and RICE UNIVERSITY at Houston.

I.III Mining History and Economic Geology

The Nolan-Hammond area is located within the Upper Koyukuk Mining District, the most productive gold district in the Brooks Range (DILLON & REIFENSTUHL, 1990).

Placer mining in the Nolan Creek area dates from 1901 when shallow gravels were discovered in Fay Creek a short distance above its confluence with Nolan Creek (Fig.3). Actual mining was not actively begun until 1903 when the small amount of shallow ground on Fay, Archibald, and Smith Creeks was worked (MADDREN, 1913).
In 1905-1906 when boilers and steam thawing equipment was brought into the camp, mining started to concentrate on the deeper frozen gravels. In 1906 the first successful prospect shaft in the Nolan valley was sunk 135 feet (42 meters) to bedrock. Rich gold-bearing gravels were found at the bottom of this shaft (MADDREN,

1913). During 1906 to 1913 placer drift mining in the deep frozen deposits of Nolan valley was actively conducted by about 100 men. The bedrock deposits proved to be rich and were worked extensively until gold mine closure in 1942 (ED ARMSTRONG, Tri-con Mining). Placer mining has continued on Nolan Creek to the present day.

Fig.3: The mining camp of Nolan, 1909. Looking upstream from the east side of Nolan Creek valley near the mouth of Smith Creek. Gold was discovered here in 1901 and during the peak of the rush at least 100 miners were working its gravels. The creek has been the largest gold producer in the Koyukuk Mining District. Acme Creek lies on photo left. U.S. Geological Survey photograph, August 1909.

Fig.4: Placer mining activity at Archibald Creek, 1998.

During 1994 Silverado Mines (U.S.) Inc. / Tri-con Mining Alaska Inc. operated the largest gold mine in the northern region (Nolan Creek Mine), and the fourth largest gold mine in Alaska. During summer 1998 placer mining activity concentrated on Archibald Creek (Fig.4). During fall and winter 1998/99 placer mining activity focused on underground mining at Swede channel (Fig.5).

Since mining began, 135437.70 oz of gold have been mined from Nolan Creek, 15141.30 oz from Smith Creek, 5429.90 oz from Archibald Creek, 1865.41 oz from Fay Creek, and 3100 oz from Thompson Pup.
9145.40 oz have been reported from Vermont Creek, and 17255.90 oz from the Hammond River (AMRT (BLM) and TRI-CON MINING, written communication 1999).
That makes a total of 187375.61 oz gold for the Nolan-Hammond area since the beginning of this century.
Nolan has always played an important role in the Alaskan Mining Industry and history.

Placer gold deposits are found in close proximity to areas with auriferous veins. They are usually confined to Quaternary alluvial deposits just above bedrock in deeply cut valleys. In the Upper Koyukuk district occur three varieties of gold-bearing stream gravels (DILLON & REIFENSTUHL, 1990): active stream gravels (Qa), elevated bench gravels (Qa), and deeply buried gravels (Qg).

Fig.5: Swede underground placer mine, 1998.

The only record of lode mining in the Nolan area was antimony-bearing veins.

Berg & Cobb (1967) and Cobb (1973) report that during World War II about 6 tons of stibnite were mined from a prospect on the east side of Nolan Creek (on the right limit of Smith Creek above the confluence with Nolan Creek).

I.IV Objectives of Study

The purpose of this master's thesis study (Diplomkartierung-Diplomarbeit) is to examine the Geology and Gold Mineralization of the Nolan area in the Brooks Range, Alaska. This project was sponsored by the Technical University of Clausthal in Germany, the Alaska Mineral Resource Team Anchorage (Bureau of Land Management) and Tri-con Mining Alaska Inc. / Silverado Mines Ltd.
This project is part of a four year's reconnaissance program in the northern region undertaken by the Bureau of Land Management (BLM).
In particular this study focuses on:

1. The Geology of the Nolan area:

- Detailed geologic mapping and structural analysis of the Nolan area in order to reach a more thorough understanding of the geologic processes that shaped the region.

2. Gold Mineralization of the Nolan area:

- Geochemical reconnaissance sampling.
- Examining the occurrence of gold in quartz veins and veinlets in the area.
- Examining placer gold of the area to determine if placer has been derived from nearby lode occurrences.

II. Geologic Mapping of the Nolan Area

1. Procedures

To study the relationships of the geologic processes that shaped the study area, the entire Nolan-Hammond area of 42 square miles (107.5 km^2) was mapped during summer 1998. Geology was mapped at a scale of 1:21,000 based on U.S. Geological Survey topographic base maps of the Wiseman B1 and C1 quadrangles at a scale of 1:63, 360.

The Geologic map (Appendix 1) and Structural Geologic map (Appendix 2) were made by intense field mapping and by interpretation of infra-red aerial photographs from USGS (1997) and black and white aerial photographs from USGS (1955).

Thin sections were examined for mineral identification and for textural and structural analysis. X-ray diffraction was carried for mineral identification at the Colorado School of Mines (USA).

2. Regional Geologic Overview of the Southern Brooks Range

The southern Brooks Range and the northern Koyukuk basin are divided into four fault-bounded tectonostratigraphic or lithotectonic terranes: the Ruby, Mosquito, Angayucham, and Arctic Alaska terrane (DILLON, 1989). The rocks of the southern Brooks Range and the northern Koyukuk basin range in age from Proterozoic (?) to Cretaceous and in metamorphic grade from completely unmetamorphosed rocks to possibly polymetamorphic gneiss and schist of the amphibolite facies (DILLON, 1989).

Rock units of the Nolan area belong to the Hammond- and Coldfoot subterrane which compose with the North Slope subterrane and Endicott Mountains subterrane the Arctic Alaska terrane (Fig.6).

All rocks of the Arctic Alaska terrane in the southern Brooks Range have been significantly displaced by north-vergent thrusts. During Late Jurassic and Neocomian time (DILLON, 1989) the Angayucham terrane in the Koyukuk basin, composed of oceanic rocks that include diabase, pillow basalt, tuff, chert , and graywacke, was thrust and obducted northward onto the continental rocks of the Arctic Alaska terrane. This event produced regional metamorphism of the continental rocks that were overridden.

The Coldfoot subterrane is composed of Proterozoic (?) to Lower to Middle Devonian polymetamorphic metasedimentary rocks which are intruded by Devonian (?) granitic and mixed felsic-mafic intrusive complexes and are overlain locally by bimodal volcanics (DILLON, 1989). During Late Jurassic and Neocomian time rocks of the Coldfoot subterrane were thrust northward onto Middle and Upper Devonian rocks of the Hammond subterrane of the Arctic Alaska terrane. Rocks of the Hammond subterrane are composed of greenschist-facies metasedimentary and metavolcanic rocks. They were intruded by Devonian or Jurassic mafic plutons and by Devonian granitic bimodal plutons (DILLON, 1989).

A second deformation event in the southern Brooks Range is represented by post-Early Cretaceous, high angle, west-trending strike-slip faults with right-lateral separation that displace the thrust faults.

The study area is comprised of rocks of the Coldfoot subterrane and Hammond subterrane of the Arctic Alaska terrane. In the Nolan area the episodes of amphibolite facies-, and retrograde greenschist facies metamorphism, the scarcity of fossils, and the complex folding history have hindered the dating and stratigraphic control of the units. The rocks in the Nolan area have been assigned to Middle to Upper Devonian age (DILLON & REIFENSTUHL, 1990).

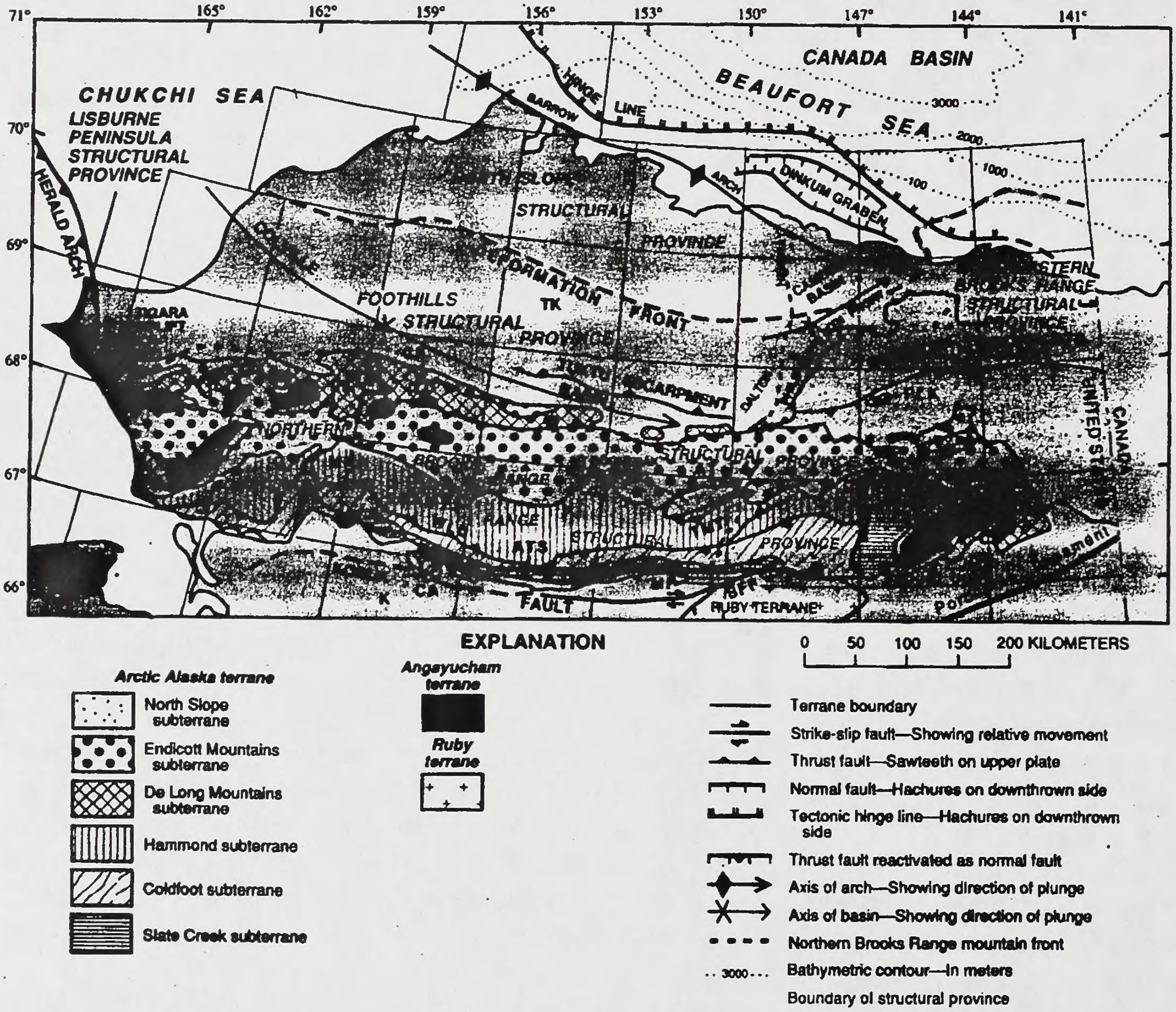

Fig.6: Structural provinces and major tectonic elements of northern Alaska. Map by MOORE ET AL. (1994). AT, Amawk thrusts; ATS, Angayucham "thrust" system; BTS, Bathub syncline; CA, Cosmos arch; CF, Cutaway fenster; K, Cretaceous rocks of Koyukuk basin; MAA, Mount Angayukaqsraq antiform; MF, Malamute fault; PF, Picnic Creek fenster; PLK, Porcupine Lake klippe; SFF, South Fork fault; TK, Cretaceous and Tertiary rocks of Brookian sequence; TMT, Table Mountain thrust; WLL, Walker Lake lineament.

3. Stratigraphy and Petrography

A detailed differentiation of all the lithologic map units, including subunits, and differentiated subunits is presented on the Geologic map (Appendix 1). A simplified version of main units, and subunits is presented on the Structural Geologic map (Appendix 2). Therefore I suggest the reader to take a first quick look at the Structural Geologic map to get a general overview of the main lithologic map units.

Beforehand, it should be noted that the Devonian metasedimentary and igneous rocks in the study area have been affected by at least two episodes of regional metamorphism (M_2, and M_3).

3.1 Metasedimentary Rocks

3.1.1 Dcc: Chloritic and carbonate metasedimentary rocks, Middle Devonian?

This unit crops out in the southern part of the study area, on the south trending ridge of Midnight Dome and south of Bluff Gulch in the southeast corner of the map area.

The Dcc unit is composed of chloritic pelitic metasiltstone and medium to fine-grained chloritic metasandstone with finely marble interlayers, interbedded with green, gray, and black phyllite; and chloritic, calcareous schist, quartzite clast conglomerate with some carbonate clasts.

The metasedimentary unit is composed chiefly of a poorly sorted, medium to fine grained chloritic metasandstone consisting of angular to subangular grains of quartz (50 to 70%) and chert (30 to 50%) (GOTTSCHALK, 1987). On fresh surfaces, metasandstones are light gray, weathering to a buff or green to brown colour.
Outcrops are massive and structureless, with bedding surfaces difficult to distinguish, but sedimentary structures are occasionally observed on weathered surfaces. The metasiltstones are gray in color, pelitic and also contain chlorite.
Chloritic metasiltstone, metasandstone, and quartzite conglomerate with some carbonate clasts contain interlayers of marble, less than 1 cm thick; calcareous schist; gray, green phyllite; chlorite quartz grit, and felsic volcaniclastic (?) rocks.

Phyllites are subordinate to the metasand- and siltstones. In general, phyllites occur as interbeds which range from a few centimeters to as much as a meter in thickness. Fine grained horizons are thinly laminated, with individual laminae ranging from 1 or 2 millimeters, to beds up to 2 centimeters in thickness; no other sedimentary structures were noted due to the prominence of cleavage and metamorphic foliation. Phyllites are commonly dark-gray to black in color, owing to the abundance of organic material.

The conglomerate is composed of subangular quartz grains (40%), albite (10%) and rock fragments (35%) in a microcrystaline matrix (15%) of silica (GOTTSCHALK, 1987). The clasts consist mostly of quartzite and carbonate.

The thickness of the Dcc unit in the study area is approximately 600 meters (1800 feet).

3.1.2 Dcss: Chloritic sandstone and conglomerate, Middle Devonian

This unit crops out in the southern part of the study area, southwest of Wiseman Creek and south of Bluff Gulch in the southeast corner of the map area.
This unit consists of gray-green chloritic quartz-mica schist, calcareous quartz-mica schist, and chloritic quartzite with interlayers of carbonate clast conglomerate.

The Dcc unit meshes into the Dcss unit. The rocks of this unit consist of chloritic quartzite and (calcareous) chlorite-quartz-mica schist that together may represent a basal sandstone. These clastic rocks are green- to buff- weathering. They contain interlayers of marble; gray, green phyllite, graphitic schist; chlorite quartz grit; and probably felsic volcaniclastic rocks.
Quartz-mica schists are well exposed on the south trending ridge of Midnight Dome. They occur in dark-gray blocky outcrops which are foliated and often partially slumped due to frost heave. Outcrops of quartz-mica schist are lithologically heterogeneous, consisting predominantly of pelitic schist with interlayered semi-pelitic (> 50% quartz) schist layers a few centimeters to several meters thick.
Pelitic layers are conspiciously banded, with numerous metamorphic quartz segregations and quartz veinlets separating dark-gray to black mica-rich bands. The semi-pelitic schists are relatively rich in quartz with a less prominent foliation than that of the pelitic schists; they are commonly diffusely banded due to changes in the proportions of quartz and micas.

Fine-grained quartz-mica schists and phyllites consist of metamorphic quartz, white mica, and chlorite. Graphite occurs in gray phyllites.
Quartz in the quartz-mica schists comprises between 15 to 90% of the rock, where it occurs as quartz-rich metamorphic segregations and as dispersed grains in mica-rich bands. White micas are the chief foliation forming mineral in the quartz-mica schists, occuring as idioblastic flakes up to 2 mm. Chlorite is the only other mineral whose presence is ubiquitous in the quartz-mica schists. It is conspicuous in hand specimen as green flakes intergrown with white mica and quartz on the foliation planes. Chlorite occurs primarily in the mica-rich segregations of the quartz-mica schists, but is also present in quartz-rich bands in minor amounts. Garnet in pelitic schists typically occurs as tiny idioblastic grains.

Chloritic quartzite occurs granoblastic with interlayers of carbonate clast conglomerates of various thickness. Those carbonate clast conglomerates are basically the same as described in the chapter above.
The conglomerate is composed of subangular quartz grains (40%), albite (10%) and rock fragments (35%) in a microcrystaline matrix (15%) of silica (DILLON, 1989). These clasts consist mostly of carbonate. The clasts vary in size, from 2 or 3 mm up to 1 cm. Clasts normally show a dark-grayish color.
Conglomerates are less prominent foliated than the pelitic schists. They show a red-brown weathering color, on fresh surfaces a grayish to dark gray color.

The thickness of this unit is approximately 180 meters (600 feet).

3.1.3 Dbss 1: Black metasiltstone with interlayers of phyllite and fine grained black quartzite, Beaucoup Formation?, Middle to Upper Devonian

This unit is exposed on the south trending ridge of Midnight Dome and south west of Wiseman Creek. The Dbss 1 unit is composed of fine black pelitic metasiltstone, interlayered with gray phyllite and gray pelitic quartz-mica schist, and small bands of fine grained black quartzite.

The main part of this unit consists of pelitic black metasiltstone of various thickness. Interlayered within this metasiltstone are gray graphitic phyllites and fine-grained gray quartz-mica schists, containing thin calcareous interlayers. Fine-grained quartz-mica schists and phyllites consist of metamorphic quartz, white mica, and chlorite. Graphite also occurs in gray schists.
Also interlayered within these metasiltstones are bands of fine grained black quartzite. These bands vary in thickness, from a few centimeters up to 40 centimeters as seen on Midnight Dome.

Unfortunately, the Dbss 1 occurs in dark-gray blocky outcrops, slumped due to frost heave. As rocks of this unit are heavily fractured and often covered with float consisting of rocks of the same unit, a more detailed differentiation could not be undertaken.

The thickness of this package is approximately 900 meters (2800 feet).

3.1.4 Dbss 2: Black metasiltstone and phyllite, Beaucoup Formation? Middle to Upper Devonian?

This unit is exposed southwest of Wiseman Creek, and on the west side of Nolan Creek on Montana Mountain which is mostly formed of this unit. A small portion is also exposed on the east side of Nolan Creek, north of Fay Creek, and south of Smith Creek (Workmen's Bench). Further, it crops out around Acme Creek, and on the south leading ridge of Midnight Dome.

This unit consists of gray and black, laminated metasiltstone and locally gray-black, partly calcareous phyllite and schist with thin calcareous interlayers which are well exposed on the southwest side of Acme Creek.

The Dbss 2 unit shows strong similarities to the Dbss 1 unit. The main difference between these units is first of all the abundance of gray phyllite and schist, which can reach large thickness up to more than 30 meters in Dbss 2 and secondly, the non-occurrence of fine grained black quartzite in Dbss 2. Therefore I distinguished Dbss into Dbss 1 and Dbss 2.

Dbss 2 consists of three subunits. The base unit is well exposed in the Nutmeg Gulch area, north-west of the mouth of Nolan Creek. The base unit consists of gray and black, laminated metasiltstones, interlayered with graphitic schist.
As a matter of fact, the base unit can be divided into three parts as well.

The bottom part of the base unit crops out in Location 288, 600 meters north-west of the mouth of Nutmeg Gulch. The bottom part of the base unit consists of gray-black pelitic metasiltstones. Borders to Dbss 1 and the middle part of the base unit of Dbss 2 are not exposed in the study area.
The middle part of the base unit consists of alternating layers of fine grained black laminated metasiltstone and graphitic phyllite in various thickness. A fraction of the middle part is exposed 1000 meters north-west of the mouth of Nutmeg Gulch (Loc. 290 and 291).
The top part of the base unit is exposed near the head of Nutmeg Gulch (Loc. 289) consisting of pelitic gray and black metasiltstone with interbeds of graphitic phyllite. These interbeds vary in thickness from a few centimeters up to 20 to 30 centimeters. Quartz veinlets (< 1mm) occur within the metasiltstones and are parallel to foliation.

The middle unit of Dbss 2 is well exposed on the south-west side of Acme Creek (Loc. 283 to 286). Also, in Loc. 292 and 293, on the east side of Montana Mountain where a small portion of this unit crops out.

The middle unit of Dbss 2 consists of thinly bedded, laminated, gray and green phyllites, and pelitic muscovite schists, with partly calcareous interlayers. Fine-grained calcareous felsic schist may have been derived from distal airfall tuff.
Within the pelitic metasediments are thin beds of metasandstone, sometimes up to 2 centimeters in thickness. Outcrops in this area are more than 30 meters in altitude.
A phenomena occuring in the Gulches south-east of Acme Creek is the yellowish to gray-brown dusty weathering of phyllites and schists. This dust is believed to be a sulfur salt.
Graphitic schist and phyllite also occur within this middle unit and are exposed on the east side of Montana Mountain (Loc. 292 and 293).

The top unit of Dbss 2 is exposed on Montana Mountain, where it forms large dark-gray blocky outcrops, easily visible from the distance.

The top unit of Dbss 2 consists of thinly bedded, laminated gray phyllites, and fine grained (pelitic) quartz-mica schists with chlorite on foliation planes. Interlayers of dark-gray metasiltstone are visible, sometimes up to a few centimeters in thickness. These rocks show a gray weathering color.
The metasedimentary rocks change from the bottom to the top of outcrop on Montana Mountain. The lower and middle parts are more pelitic in grain size , the top is more silty to sandy in grain size as exposed by coarse grained metasiltstone and fine grained metasandstone layers near the top. Within those coarser grained bands occur boudins of metasiltstone.

Dbss 2 on the south trending ridge of Midnight Dome is presumed to belong to the top unit of Dbss 2. Evidence is given in the occurrence of gray phyllites, coarse grained metasiltstones, and fine grained metasandstone interbeds.

Dbss 2 around Workmen's Bench is also presumed to belong to the top unit of Dbss 2. Evidence is given in the occurrence of gray quartz-mica schist, with interlayers of gray phyllite, metasandstone, and gray-brown pelitic mica schist.
The thickness of Dbss 2 in the study area is approximately 1000 meters (3050 feet).

3.1.5 "Butte Mountain Slate": Beaucoup Formation?, Middle to Upper Devonian?

This unit is well exposed on top of Butte Mountain, on the east side of the Hammond River, occuring on a low angle southeast dipping thrust plate. Butte Mountain Slate occurs in gray-black blocky outcrops which are foliated and often partially slumped due to frost heave. The stratigraphic setting of this unit is not quite certain to determine. As this unit shows strong similarities to the laminated black metasiltstone of Dbss 2 and the black slate of the Dbs unit, I suggest that this unit may be located in between these two units, or interfingering between these units. Therefore it represents a facies change as shown in correlation of map units on the Geologic map (Appendix 1).

Butte Mountain slate consists of laminated black slate and low micaceous gray-black schist. Slate bands reach various thickness, up to a few meters in width and are interlayered by low micaceous gray-black schist.
The black slate is pelitic in grain size and stands out due to its remarkable hardness, which leads to sharp edged fragments.
As mentioned above, Butte Mountain slate occurs as foliated gray-black blocky outcrops. Blocks break apart on low micaceous schist interlayers. Slate itself also breaks apart on foliation planes into thin plates.
Also, thin black metasiltstone interbeds appear within this unit.

The thickness of the Butte Mountain slate unit is approximately 200 meters (610 feet).

3.1.6 Dbs: Phyllite, pelitic schist, and black slate, Beaucoup Formation? Upper Devonian?

The Dbs unit crops out in the mid-west part of the map area. Dbs is exposed on top of Montana Mountain and north of it on a thrust plate, and on top of the ridge south-west of Acme Creek. Further, this unit is exposed on the east-side of Nolan Creek, in Smith Creek, Archibald Creek, Fay Creek, and Thompson Pup; and on the east side of the Right Fork of Vermont Creek.
Dbs is noted twice on the Geologic Map, first of all as Dbs undifferentiated where no differentiation could be made, and secondly as Dbs differentiated (Dbs 1 to Dbs 10) where a differentiation could be undertaken.

North of the Montana thrust fault, a small area north and south of Fay Creek, and a small part south of Workmen's Bench, a differentiation of Dbs could not be undertaken. On the thrust plate north of Montana Mountain, Dbs occurs as thinly bedded gray-black micaceous schist, gray-black phyllite, and black graphitic slate (Loc. 199, 200, 287, and 327).

A differentiation of Dbs can be undertaken on the east side of Nolan Creek (Dbs 1 to Dbs 10).

Basically, the pelitic schists, slates and phyllites of the Dbs unit do not vary much, except for their color and content of pyrite. Therefore, a detailed differentiation was undertaken due to changes of colors, grain size, and pyrite content.

South of Smith Creek, east of Workmen's Bench, the base layer of the Dbs unit is exposed, lying conform on top of Dbss 2. The base layer consists of gray-black micaceous schist with metasiltstone interbeds and black slate. The base layer is similar to the one on top of Montana Mountain which is also lying conform on Dbss 2, also consisting of thinly bedded gray-black micaceous schist and phyllite with interbedded thin metasiltstone, and black slate(Loc. 202, 203, 325, and 326). This is enough evidence to confirm these layers to be the base layer of the Dbs unit, therefore named Dbs 1.

Dbs 2 is exposed east of Workmen's Bench (Loc. 213), consisting of gray-black slate and brown slate. Dbs 3 crops out in Archibald Creek (Loc. 124 and 125), consisting of pyritic black micaceous schist. Pyrite cubes are up to 3 millimeters in size. Dbs 4 is exposed south of Gobblers Knob (Loc. 334, 359, and 364), consisting of thinly bedded brown micaceous schist and phyllite. Dbs 5 crops out on Gobblers Knob (Loc. 267 and 268), in Archibald Creek (Loc. 126), in Fay Creek, and the lower part of Thompson Pup. Dbs 5 consists of phyllites and schists of various color, mostly gray-black, and greenish. In Fay Creek, some layers of Dbs 5 contain pyrite cubes up to 3 millimeters in size (Loc. 2, 6, and 8). Further, it should be noted that some layers in Fay Creek contain interlayers of metasiltstone and fine grained quartzite.

Dbs 6 is located in Thompson Pup, consisting of gray-black micaceous schists and metasiltstones. Dbs 7, consisting of chlorite schist, and Dbs 8, consisting of brown micaceous schist and metasiltstone are exposed in the middle and upper part of Thompson Pup. Dbs 9 crops out at the head of Thompson Pup. Dbs 9 (Loc. 49) consists of thinly bedded, pyritic gray-brown micaceous schist and phyllite. Dbs 10 is exposed east of the Right Fork of Vermont Creek (Loc. 65, 172) consisting of gray-black pyritic phyllite and micaceous schist, and further black slate.

A more detailed example of bedrock change of Dbs can be given in the description of sequence of layers in Thompson Pup. At the mouth of Thompson Pup (leading into Fay Creek) the bedrock consists of green chlorite schist (phyllite?) and green metasiltstone interlayers (Loc. 255). Above occurs a package of gray-green and brown micaceous chlorite schist with metasiltstone interlayers (Loc. 252 and 253). On top of that appears a package of gray-black graphitic schist and phyllites with disseminated pyrite cubes up to 8 mm (Loc. 249, 250, 251), interlayered by chloritic schist.

Above the previous described occurs a layer of gray-black micaceous schist with interbedded gray-brown mica schist and phyllite (Loc. 247 and 248). On top of that is situated a thinly bedded graphitic black mica schist with interbeds of black metasiltstone (Loc. 246). Above occurs a package of gray- black pelitic mica schist (Loc. 245). On top of that appears pelitic chlorite schist (Loc. 244). The head of Thompson Pup consists of gray-brown phyllites and brown micaceous metasiltstones and pelitic schist (Loc. 241, 242, 243).

Dbs in the study area has an approximate thickness of 600 meters (1800 feet).

3.1.7 Dbps 1-4: Phyllite and pelitic mica schist, Beaucoup Formation, Upper Devonian

The Dbps unit crops out on the right side of the head of Nolan Creek, Vermont Pass, Webster Gulch, on the west side of the Right Fork of Vermont Creek, Vermont Creek itself, Vermont Dome, and on the east side of the Hammond River north of Butte Mountain.

Dbps mainly consists of gray-brown phyllites and schists and gray-black phyllites and schists. This unit can be divided into four subunits, Dbps 1 to Dbps 4, as presented on the Geologic map (Appendix 1) and on the Structural Geologic Map (Appendix 2).

Dbps 1 is well exposed at the head of Nolan Creek, Webster Gulch, Vermont Pass, the Right Fork of Vermont Creek, Vermont Creek, and on both sides of the Hammond River north of Butte Mountain.
This subunit consists of gray-brown phyllite containing minor graphite and disseminated cubes of pyrite, graphitic schist, and quartz phyllite. Quartz phyllite consists mainly of fine grained quartz with some fine muscovite and chlorite on foliation planes. Another rock type occuring within this subunit is sericite-quartz-pyrite phyllite. This rock consists of fine grained quartz, sericite and pyrite or iron oxide after pyrite. It is white, yellow or brown from iron oxide staining. It may have been a volcanic tuff.
This subunit forms cliffs which can be seen perfectly in Vermont Creek. Significant of this unit is the yellowish-brown dusty weathering of this unit. X-ray diffraction analysis was carried out on this powdery mineral, suggesting the dusty minerals to be hydrated iron sulfate (e.g. Rozenite $Fe_2SO_4 \cdot 4(H_2O)$) and perhaps hydrated magnesium sulfite (Starkeyite $MgSO_4 \cdot 4(H_2O)$, (John Clark, written communication 1999).

A small view of this unit is exposed in Vermont Creek. The base of Dbps 1 consists of black pelitic pyrite schist. Above this base layer occur several meters of thinly bedded quartz phyllite and schist, and sericite-quartz-pyrite phyllite. Within the quartz schist occur quartz-bands with thickness up to 1 cm.
On top of the quartz phyllites follows a layer of thinly bedded gray graphitic phyllite. It usually contains disseminated pyrite. The top of this Dbps 1 is exposed by thinly bedded gray-brown phyllite, containing minor carbonate.
The approximate thickness of this subunit is 200 meters (610 feet).

Dbps 2 is exposed on the right side of the Hammond River north of Butte Mountain and on the plateaus north and south of Vermont Creek. This subunit consists of thinly bedded gray-black graphitic phyllites, interbedded with gray pelitic mica schist. The rocks of this subunit are less resistant in weathering than the ones described in Dbps 1, as this subunit forms slopes in the Vermont Creek area.
The approximate thickness of this subunit is 330 meters (1100 feet).

Dbps 3 is exposed near the top of Vermont Dome. Dbps 3 consists of thinly bedded gray graphitic phyllites and gray pelitic schists. This subunit is more resistant in weathering than Dbps 2, forming cliffs on Vermont Dome. This criteria led me to define this package as a separate subunit.
The approximate thickness of Dbps 3 is 105 meters (320 feet).

Dbps 4 is exposed underneath the top of Vermont Dome where it lies conformable underneath the Dbcs unit. The Dbps 4 subunit consists of gray-brown phyllites and gray-mica schists. Significant is the yellowish-brown weathering color of this subuint which comes from iron oxide. Iron oxide derives from weathering of pyrite which also exists in this rock type.
This subunit is quite resistant in weathering, forming cliffs and blocky outcrops.
The approximate thickness of this subunit is 120 meters (365 feet).

3.1.8 Dbcs: Chloritic quartzite and coarse grained quartz-mica schist, interlayered with phyllites, schists, and chloritic metasiltstones; Beaucoup Formation, Upper Devonian

This unit covers most of the central part of the map area. Dbcs occurs on Midnight Dome, Smith Creek Dome, and on the ridge leading towards the mouth of Vermont Creek. Further, underneath the Butte Mountain thrust east of the Hammond River, and on top of Vermont Dome.

This unit consists of chloritic quartzite and coarse grained quartz-mica schist, interlayered with phyllites, schists, and chloritic metasiltstones; and locally banded chloritic quartzite. Quartzites and quartz-mica schists are very resistant rocks which occur with softer phyllites and schists. When Midnight Dome is viewed from the North or Northwest at a distance, this unit stands out and clearly delineates the sedimentary bedding, and dips gently to the Northeast from Smith Creek to the Hammond River. The sedimentary bedding is well preserved in the quartzites.

Dbcs is noted twice on the Geologic Map, first of all as Dbcs undifferentiated where no differentiation could be made as on Butte Mountain, and secondly as Dbcs differentiated where a differentiation could be undertaken.
As the Dbcs unit is divided by a number of faults, a detailed stratigraphic sequence cannot be given. Therefore I divided Dbcs into five subunits as described on the Geologic map (Appendix 1) with a further differentiation given of the subunits. Note that a simplified version of lithologic map units is presented on the Structural Geologic map (Appendix 2) and should be looked at beforehand to get a general overview of map units before going into more specific detail.

The base layer of Dbcs, **Vermont Dome Subunit (Dbcs 1)** is exposed on top of Vermont Dome where it lies conformable on top of Dbps 4. The base layer consists of foliated granoblastic chloritic quartzite, fine to medium in grain size with pyrite cubes. Larger single quartz grains were also determined within the quartzite. This quartzite looks more like a chlorite schist due to the abundance of chlorite and mica on weathering surface, but on fresh surface the quartz grains are clearly visible. The base layer of Dbcs occurs in green-gray blocky outcrops on Vermont Dome.

The **Nolan-Hammond Subunit (Dbcs 2 to Dbcs 12)** consists at its base of gray-black pelitic micaceous schist and phyllite (Smith Creek), followed by micaceous chlorite schist with interbeds of gray phyllite. Above this package occurs a thick layer of gray micaceous schist and phyllite. This is overlain by a package of banded fine grained quartz-mica schists with interbeds of phyllite and chlorite schist, and also quartzite (Loc. 264). On top of that appears green gray chloritic quartz-mica schist.

This layer can only be seen at the mouth of Buckeye Gulch (Loc. 328) where it contains pyrite cubes up to 3 mm in size, and south of Smith Creek Dome (Loc. 239). Above that unit occurs in Buckeye Gulch a package of biotite quartzite which forms blocky outcrops. This phenomena is only local. The biotite quartzite is gray to white in color, banded, fine grained and has small thinly interbeds of biotite along foliation planes.
Above that unit comes a package of thinly bedded gray phyllites and fine grained quartz-mica schists (Loc.48). This package is believed to lie on top of the banded fine-grained quartz-mica schists described above north of Smith Creek Dome as the chloritic quartz-mica schist and biotite-quartzite are not exposed, maybe due to covering by tundra. On the other hand, the blocky outcrops of biotite-quartzite could be seen in topography even if covered by tundra. Therefore the occurrence of biotite-quartzite is believed to be only local at Buckeye Gulch.
Above the previous described thinly bedded phyllites and fine grained quartz mica schist occurs a package of various gray, brown, and black mica schists and phyllites, interbedded with coarser grained quartz-mica schist.
On top of that package appears a significant package consisting of coarse grained banded gray chloritic quartz-feldspar-mica schist called the "Fortress Formation" (Loc.43, 44, and 45). The Fortress Formation shows a brown weathering color on surface due to iron oxide derived from pyrite oxidation. This schist contains metamorphic quartz, white mica (sericite?) and chlorite. This formation may have derived from a volcanic tuff.
Above the Fortress Formation occurs a package of gray-black pelitic micaceous schist (Loc. 75, 76, and 274). The top of the Nolan-Hammond subunit is composed of thinly bedded gray phyllites (Loc. 46 and 47).

The **Swift Creek Subunit (Dbcs 13 to Dbcs 19)** consists of fine grained gray-brown quartz-mica schists and phyllites with chlorite on foliation planes, fine grained black quartz-mica schist with pyrite cubes and interbedded chlorite schist (Loc.133 and 139), and fine grained gray-black quartz-mica schist with interbedded foliated black metasiltstone (Loc. 207 and 208). Fine grained quartz-mica schists and phyllites are composed of metamorphic quartz, white mica and chlorite. In minor amounts graphite is present.

The **Midnight Dome Subunit (Dbcs 20 to Dbcs 44)** mainly consists of chloritic quartzite and coarse grained quartz-mica schist with interlayered schists and phyllites.
The base of the Midnight Dome subunit (area west of Union Gulch Fault) consists of a sequence of different chloritic schists and phyllites of various color. Above this package, the metasediments become more sandy in grain size, as they turn into coarser grained chloritic quartz-mica schists.
Near the top of Midnight Dome (Loc. 230, altitude 3860 ft), banded chloritic granoblastic quartzite crops out with interbeds of pelitic chlorite schist.
The middle part of Midnight Dome (area between Union Gulch Fault and Confederate Gulch Fault) consists of chloritic quartzite and banded quartzite, which are interlayered by thick packages of different pelitic schists and phyllites of various color.
The upper part of Midnight Dome subunit (area east of the Confederate Gulch Fault) consists of a package of quartz mica schist, including bands of chlorite schist, phyllite and metasiltstone. Further, consisting of packages of chloritic granoblastic quartzite, including bands of quartzite, metasiltstone, and phyllite.

Sedimentary features such as bedding are well preserved on Midnight Dome. It should be noted that some of the quartzites and coarse grained quartz-mica schists have knotty texture, probably caused by two superimposed metamorphic fabrics. Also, quartzite rods were found in place (Loc. 346), probably caused by intersection of the different foliations. Moreover, crenulation cleavage and tight isoclinal folds, as well as ptygmatic folds are well exposed on Midnight Dome.

The **Smith Creek Dome Subunit (Dbcs 45)** is mapped as a low angle dipping thrust sheet. This unit strongly correlates with the banded chlorite quartzite and coarse grained quartz-mica schist of the Midnight Dome Subunit. Therefore I suggest that Smith Creek Dome is part of the Dbcs unit and has been given the status of a separate subunit.

Smith Creek Dome Subunit occurs in gray blocky outcrops. The base of Smith Creek Dome consists of coarse grained large isoclinal folded quartz-mica schists to quartz-schists, interbedded by thin phyllitic layers (Loc. 31 to 34). The top of Smith Creek Dome consists mainly of chloritic quartzite with sequences of white fine grained banded quartzite with thickness up to 20 centimeters. Further, it consists of gray banded quartzite with bands of thickness of up to 1 cm. In between these bands occur layers of mica and fine grained black quartzite. These rocks show managanese stains on weathered surface. Coarse grained folded quartz-mica schists to quartz schists with thin phyllitic interlayers are also present on top of Smith Creek Dome. Thin bands of chlorite quartz-mica schist, fine to medium grained also occur within that package.

Sedimentary features such as bedding are well preserved on Smith Creek Dome. It should be noted that some of the quartzites and coarse grained quartz-mica schists have knotty texture, probably caused by two superimposed metamorphic fabrics. Further, crenulation cleavage and tight isoclinal folds in various size are well preserved on Smith Creek Dome. Within the folds, minor folds such as parasitic folds occur also.

A differentiation of Dbcs could not be undertaken on Butte Mountain. Dbcs occurs there as brown micaceous schist (Loc. 212a) and quartzite, sometimes chloritic quartzite (Loc. 212b). Because these rocks show strong similarities to the ones on Midnight Dome I mapped them as Dbcs undifferentiated.

An approximate thickness of Dbcs in the study area can not be given. It is believed to be more than 2000 meters.

3.2 Metamorphosed Igneous Rocks

3.2.1 Metabasite ("Greenstone"), Devonian to Jurassic

Only one metabasite dyke was found in place near the mouth of Steep Gulch on the Hammond River. This dyke has an approximate thickness of 3 meters.
This rock is quite rare in the area. According to DENNIS STACEY, President of Alaska Mining Co. Inc., there is also a "greenstone" dyke exposed in Vermont Creek. The only evidence I found there were big "greenstone" boulders on bottom of Vermont Creek, but no dyke in place has been found.

The metabasite is green in color, massive to slightly schistose, and consists of medium to coarse grained chlorite, green amphibole, and possibly muscovite and plagioclase. Further, this rock contains disseminated pyrite. Pyrite cubes up to 5 millimeters in size can be observed within the rock. Original texture is not preserved but was probably derived by metamorphism of basaltic intrusives. This rock is quite different from the "greenstone" boulders found in the gravels of the area, which are much less metamorphosed.

A thin section made from this rock type was examined petrographically for mineral identification (Fig. 7).

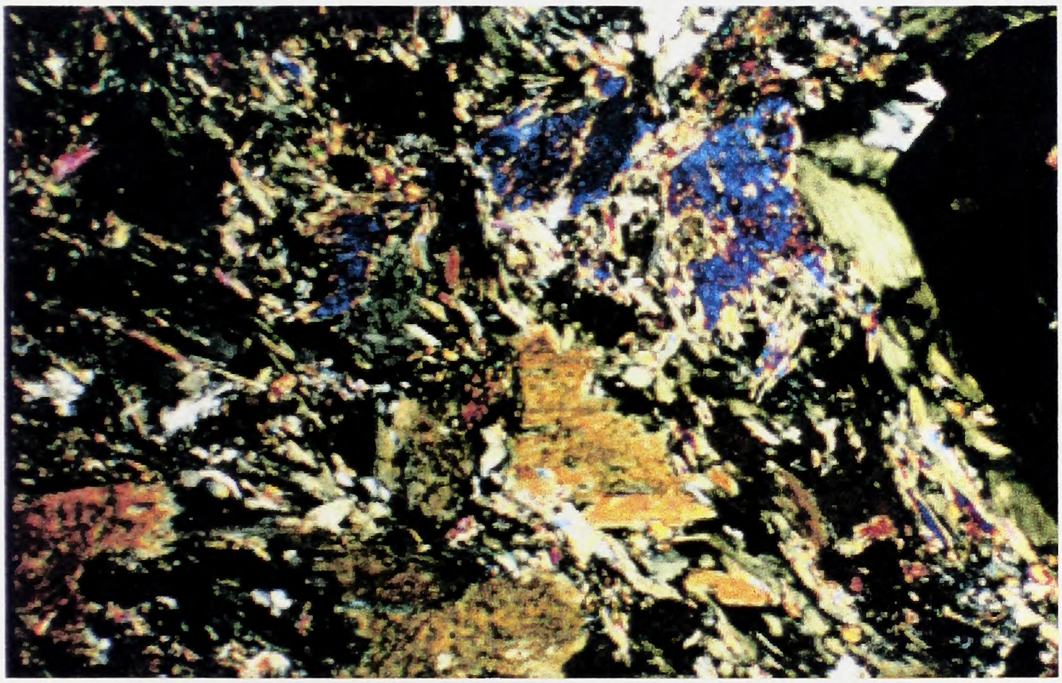

Fig. 7: Crossed-polar photomicrograph of the metabasite. Amphiboles of the amphibolite-facies are partly destroyed by retrograde greenschist-facies and turned into chlorite. Bottom edge of picture is 5.1 mm in length.

It is difficult to determine whether the rock was originally a basalt, but it definitely belonged to the group of basaltoids. Therefore it must have been a mafic to intermediary dyke. The metabasite dyke underwent two different stages of metamorphism. First of all, it was affected by the amphibolite-facies as garnet, tschermakite and the amphiboles in general (hornblende) prove. The second metamorphic event overprinting the rock happened to be under retrograde greenschist-facies as the typical greenschist facies minerals show (clinozoisite-epidote, chlorite, and actinolite). The amphiboles got partly destroyed during retrograde metamorphism and turned into chlorite. There is a small amount of quartz within the metabasite, but it is secondary and formed during retrograde greenschist-facies. Also, the amount of feldspar is very low in the rock, and if feldspar is present it consists mainly of plagioclase. Mica, possibly muscovite is also present in this rock. Other minerals which occur in the metabasite in subsidiary amounts include titanite (sphene), calcite, pyrite, and rutile. Epidote also occurs whithin pyrite.

3.3 Quaternary Deposits

3.3.1 Glacial deposits (Qg), Quaternary

Glacial deposits in the area are poorly sorted to moderately well sorted. Drift consists of silty, sandy gravel (with boulders) to clayey, stony silt with locally well stratified gravel. Gravel consists of local bedrock and rocks from distant areas. Glacial deposits form benches and terraced remnants of aprons and valley trains.

3.3.2 Alluvial deposits (Qa), Quaternary

Alluvial deposits are poorly to moderately sorted and consist of moderately stratified mixtures of gravel, sand, silt and clay.

The economic importance of Quaternary deposits is explained by the occurrence of placer gold. In the Upper Koyukuk district occur three varieties of gold-bearing stream gravels (DILLON & REIFENSTUHL, 1990): active stream gravels (Qa), elevated bench gravels (Qa), and deeply buried gravels (Qg).

3.4 Quartz Veins

3.4.1 Deformed quartz veins

Deformed quartz veins are rare in the study area. One deformed vein has been mapped near Vermont Dome (Loc. 194), consisting of coarse crystalline white quartz. The vein has a width of 15 centimeters. A sample taken from this vein (S 11179) proves this vein to be barren in gold. Smaller deformed veins and veinlets were mapped on Midnight Dome.

3.4.2 Conformable quartz veins

These quartz veins dip gently, nearly conformable with the enclosing phyllites, schists, and quartz mica schists. Conformable quartz veins are quite common and occur in outcrops almost everywhere in the map area. They are a centimeter to more than 30 centimeters in width and consist of coarse white bull quartz and commonly contain some carbonate. Minor pyrite or iron oxide after pyrite may be present. Quartz crystals are common and may be up to several centimeters in size. An interesting feature often seen in the map area is the thickening of these conformable veins in fold noses. As a matter of fact, within these the white bull quartz forms big rounded blocks, sometimes interfingering in foliation planes (Fig.8). According to PROFFETT (1982) no gold has been found associated with these veins. Several samples taken of conformable quartz veins proved PROFFETT to be right.

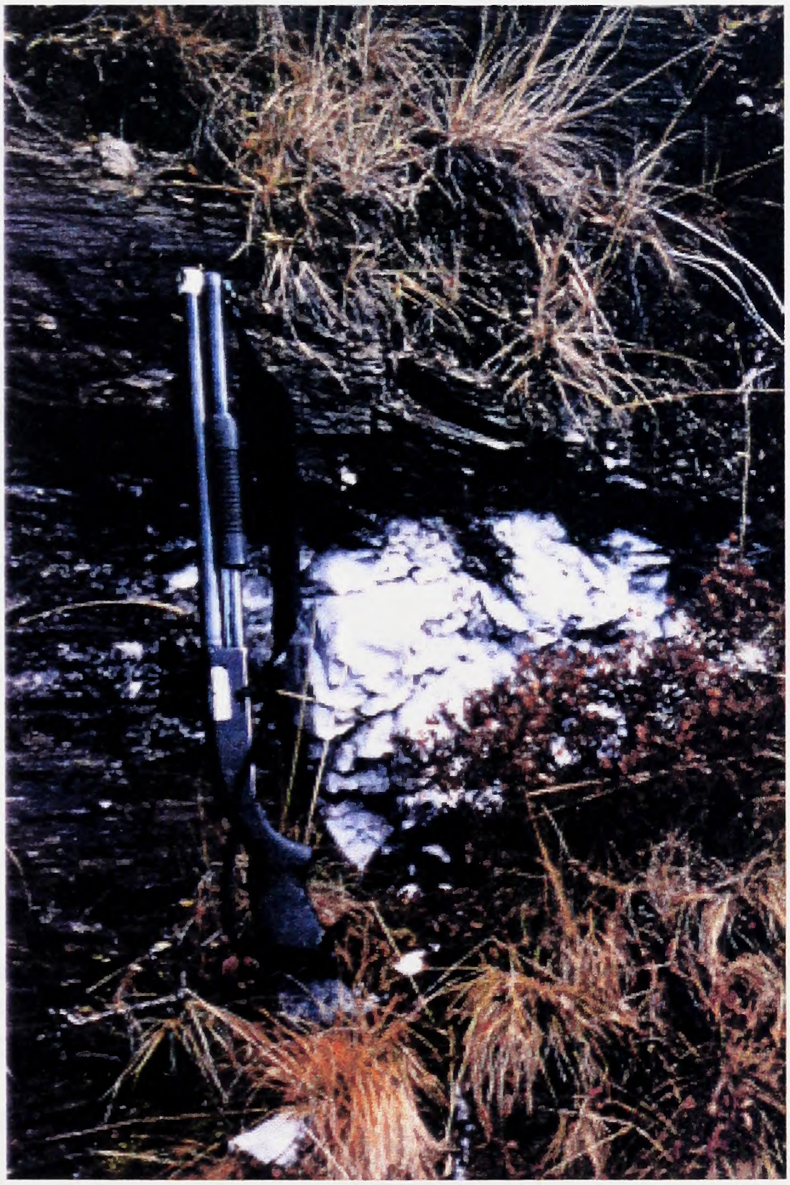

Fig. 8: Blocky, rounded bull quartz, Loc. 49.

3.4.3 Cross-cutting quartz veins

The other type of vein, which is common in the map area, consists of veins which cross cut the phyllites, schists, quartz mica schists, and quartzites at a high angle to foliation. Most of these strike west-northwest and dip steeply. They vary from 2 millimeters (veinlet) to more than 30 centimeters in width. They do not show alteration envelopes. The veins consist of white coarse to fine grained quartz and commonly contain calcite, ankerite, and minor dolomite as determined in thin sections and proven by X-ray diffraction. Pyrite, and in minor amounts hematite, chalcopyrite, pyrrhotite, and limonite occur in some of these veins.

A unique appearance of west-northwest, east-southeast striking quartz veins with enclosed rutile needles occurs south of Vermont Dome (Loc.195 to 198). These veins vary in width to more than 40 centimeters. Quartz crystals with enclosed rutile needles are common and may be up to several centimeters in size.

To the above described cross-cutting veins and veinlets also belong quartz-gold and quartz-stibnite-gold veins.
The vein mineralogy of these veins is briefly described below, a detailed description is presented in Chapter 8 of this thesis report.

3.4.3.1 Quartz-gold veins

These veins can be distinguished in quartz-gold and quartz-arsenopyrite-(gold) veins. Both vein types follow the same strike and show strong similarities, which gives evidence that they are of the same type.

Quartz gold veins are exposed near Friday the 13th Pup (Fig.9), in the Right Fork of Vermont Creek (Loc. 178 and 179), and within the "Fortress Formation". The veins consist of calcite, ankerite, dolomite, and white coarse quartz associated with pyrite, chalcopyrite, and minor arsenopyrite. Visible gold occurs in these veins, commonly along the vein margins between quartz and schist. These veins are up to 2 centimeters in width and strike northwest-southeast (210/80), dipping steeply.
Assay results from rock samples taken from these veins appear to be very encouraging, up to 63.56 ppm gold (S 10730).

Also belonging to this vein system are the quartz-calcite-ankerite veins which are very well exposed in the "Fortress Formation" (Loc. 42, 43, 44, 45, 348, and 349). Veins strike northwest-southeast, dipping steeply (210/80), reaching a width of up to 2 centimeters (Fig.10). Veins consist of white coarse quartz crystals and euhedral calcite crystals, and ankerite on vein margins, further pyrite and hematite after pyrite. Quartz occurs as crystals that fill cavities. The brownish color of calcite derived from limonite, which is present in microfractures.
Sample 10650 taken from a vein from the “Fortress” contained 8.3 ppm gold.

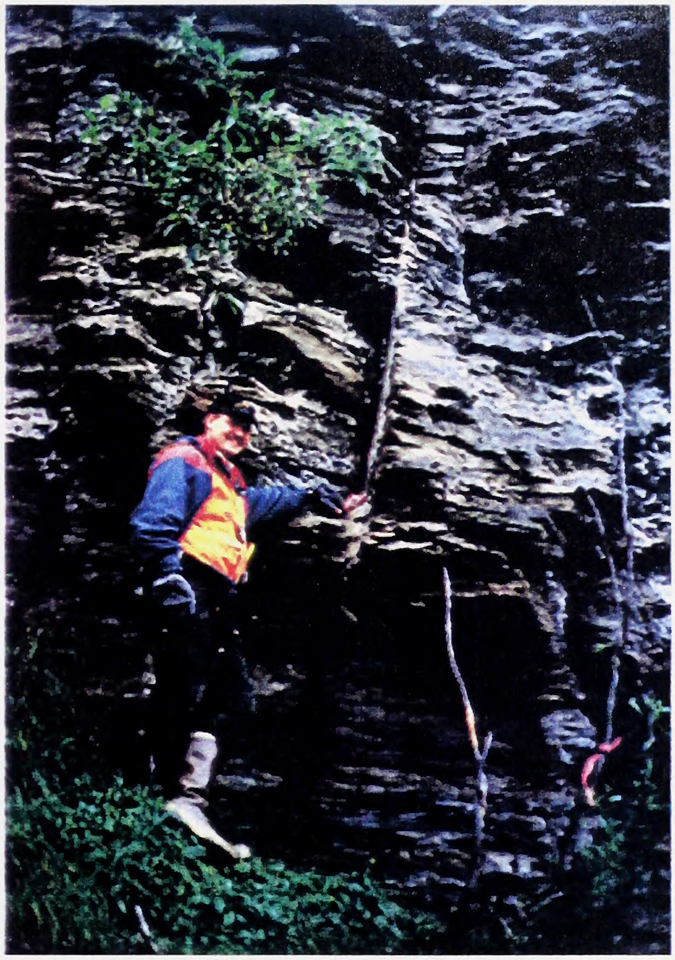

Fig.9: Quartz-gold veins near Friday the 13th Pup, in the Right Fork of Vermont Creek.

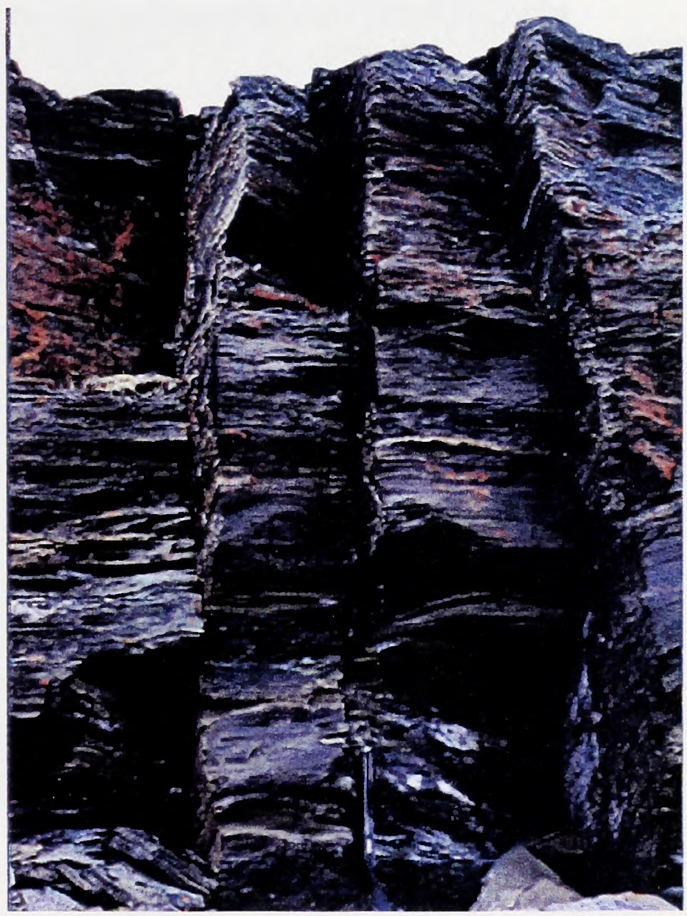

Fig.10: Quartz veins exposed in the "Fortress Formation".

Quartz-arsenopyrite-(gold) veins are exposed at Thompson Pup. Three veins have been found consisting of white coarse quartz associated with arsenopyrite. Veins vary in thickness from a few millimeters up to 50 centimeter, striking northwest-southeast, dipping steeply. According to HUBER (1995) these veins contain gold. However, assay results of these veins have not been encouraging. Therefore these veins are not noted on the Geologic map.
Massive quartz veins containing arsenopyrite and pyrite are exposed in a trench east of Thompson Pup south of the "Fortress" (Loc. 363). Veins strike east-west, dipping steeply. Pyrite and arsenopyrite are euhedral in open space filling voids or open space growth quartz.

Near thrust faults top of the southern ridge of Midnight Dome and west of Montana Mountain occurs massive quartz-calcite-ankerite-dolomite float with accessory pyrite (Fig.11). As float is quite massive, it must have come from veins of large thickness. I suggest these thick veins to belong to the quartz-gold vein type, though very little gold was detected (S 11174 contained 18 ppb gold, Loc.168).

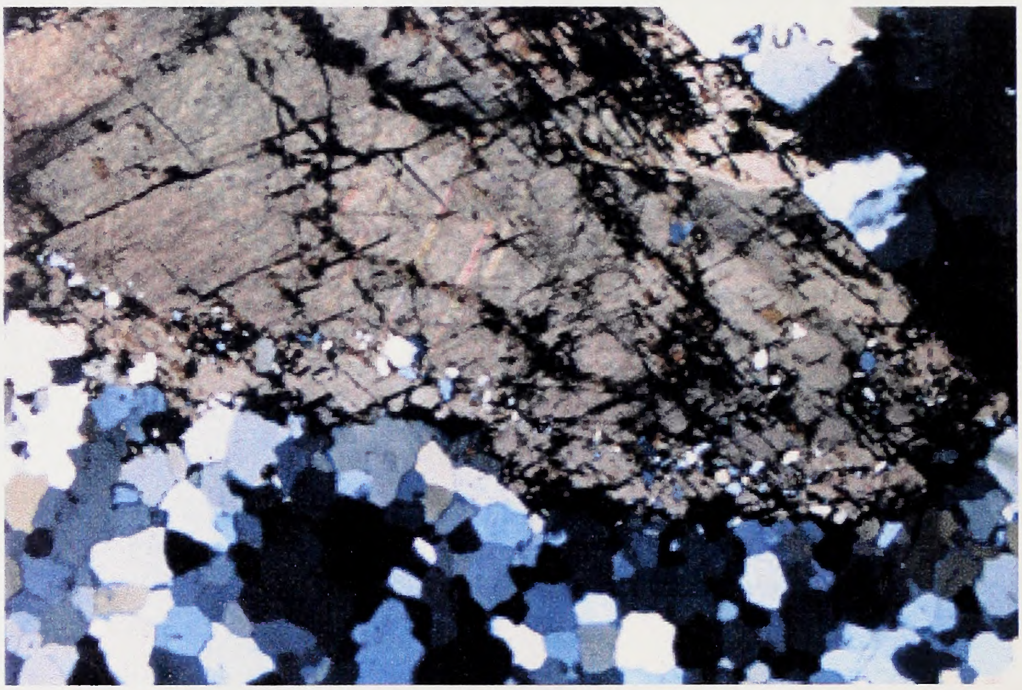

Fig.11: Crossed-polar photomicrograph of calcite-ankerite and quartz mineralization. Float sample (S 11174).
Bottom edge of picture is 5.6 millimeters in length.

3.4.3.2 Quartz-stibnite-gold veins

Quartz-stibnite-gold veins are exposed north and south of the mouth of Smith Creek (Workmen's Bench, Loc. 266), and north of it in a small pit (Loc. 359).
Further, in Smith Creek (Loc.116 and 122). COBB (1973) reports that during World War II about six tons of stibnite ore was mined from prospects on the east side of Nolan Creek.
Thickness of vein size varies. Veins exposed in Smith Creek (Loc.116 and 122) are 0.5 to 1.5 centimeters in width. Veins from Workmen's Bench (Fig.12) have a thickness of up to a few centimeters. That corresponds with veins exposed in the small pit north of the mouth of Smith Creek (Loc.359). The biggest vein found has a thickness of 15 centimeters.
The veins strike northeast-southwest, dipping steeply with roughly 80 degrees.
These veins consist of calcite, ankerite and minor dolomite on vein margins (examined in thin sections and proven by X-ray diffraction), of white coarse quartz, and further of stibnite and arsenopyrite. Gold is most common near vein margins in quartz, but rare in stibnite.
The veins do not show alteration envelopes. The quartz-stibnite-gold veins are cut by thin quartz-carbonate veinlets which represent a later stage mineralization.
Assay results from these veins appear to be very encouraging. Sample 10747 contained 12.2 ppm gold, S 11372 contained 1.8 ppm gold. Both samples were taken from a stibnite prospect at Workmen's Bench (Loc. 266). Another sample taken from a stibnite vein (S 11280) contained 9.84 ppm gold. BROSGÉ and REISER (1972) mention stibnite-gold veins from a small stibnite prospect at the head of Fay Creek. A sample collected by them from that prospect contained 9.2 ppm gold.

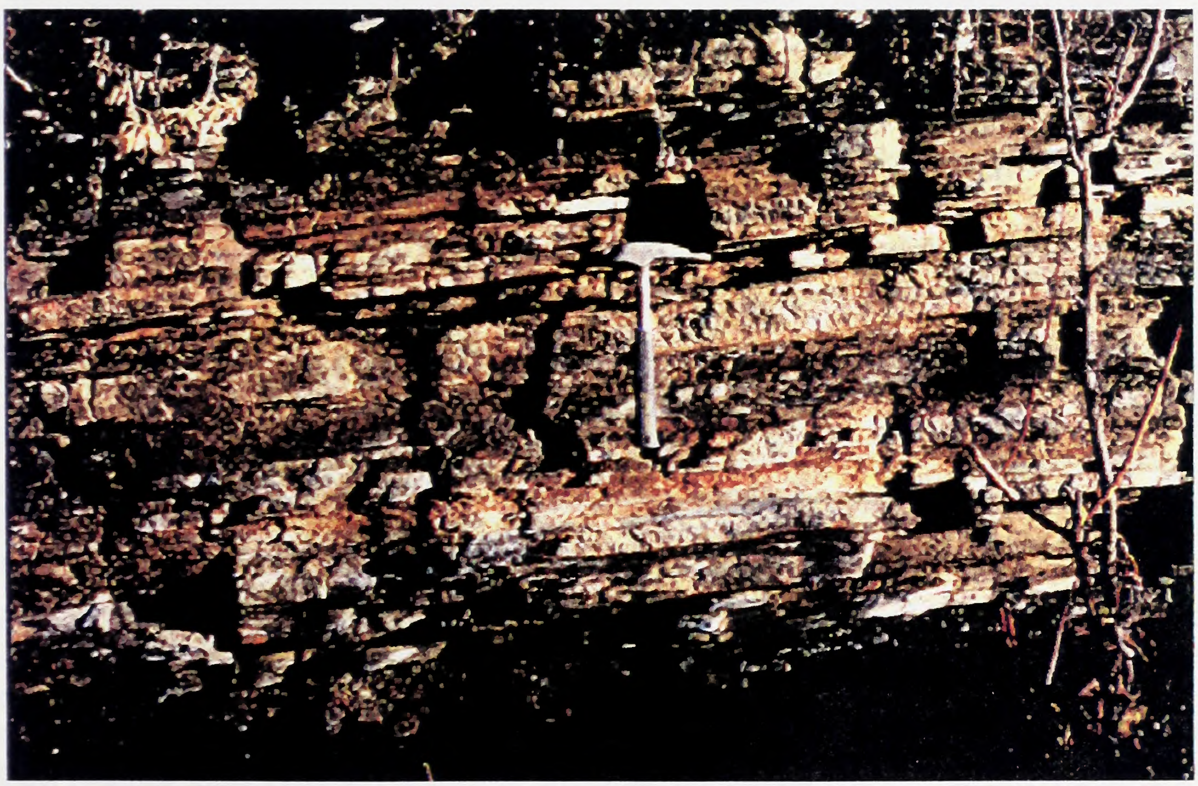

Fig.12: Stibnite-gold vein exposed at an old stibnite prospect at Workmen's Bench (Loc. 266).

3.5 Metamorphism

At least two episodes of regional metamorphism (M_2, and M_3) have affected the Devonian schist units with corresponding cleavages S_2 and S_3. Two cleavages (S_2 and S_3) are found in most outcrops, especially S_2.

The youngest metamorphic event (M_3) is represented by millimeter-spaced, semipenetrative, schistose, axial-plane cleavage (S_3). Cleavage is axial planar to major north-vergent isoclinal folds that were formed during thrusting, and probably occurred during Late Jurassic or Neocomian time (DILLON & REIFENSTUHL, 1990).
M_3 is defined by greenschist facies minerals, as typical greenschist facies minerals such as clinozoisite-epidote, chlorite, and actinolite recognized in thin sections prove. Mineral lineations trend north-south, parallel to the apparent thrust-transport direction.
The older metamorphic event (M_2) is evident from a penetrative schistosity (S_2) that is parallel to a lithologic layering and partially transposed the younger schistosity (S_3). Metamorphism M_2 is defined by epidote-amphibolite facies minerals (DILLON, LAMAL, HUBER, 1989), as garnet, tschermakite and amphiboles in general (hornblende) determined in thin sections, prove.
Therefore, schistosity S_2 was developed during an amphibolite-facies event, whereas schistosity S_3 was developed during a retrograde greenschist-facies event.
An older, pre-S_2 metamorphic event (M_1) is believed to be existing in the study area. Examination of thin sections discovered an older pre-S_2 cleavage (S_1).

4. Structure

All measuring data collected during field work are listed on Table 1. Data was taken with a Clar-compass.

4.1 Bedding

Due to thrusting, strike-slip faulting, reverse-, and normal faulting the study area is cut into several separate plates with different strikes and dips of bedding planes.

Within the south dipping thrust belt in the southern part of the study area, bedding of the metasedimentary units Dcc, Dcss, Dbss 1, and Dbss 2 strikes east-west dipping south. Due to thrusting and north-vergent folding, within each unit, strike and dip of bedding varies. On cross-section A-A' (Appendix 1) bedding was given an approximate dip of 40°, parallel to dip of the thrusts faults which corresponds with field data. Metasedimentary layers lie conform on top of each other and belong to a large north-vergent fold as small folds and axial plane cleavage within each unit indicate.

On Midnight Dome the Dbcs unit (Subunit 4) crops out consisting of very resistant quartzites and coarse grained quartz-mica schists which occur interlayered with softer phyllites and schists. The Dbcs unit stands out and clearly delineates the

sedimentary bedding, dipping gently with approximately 20° to the Northeast from Smith Creek to the Hammond River (Fig.13). The different layers lie concordant on top of each other, cut by normal faults.
Sedimentary bedding is well preserved in the quartzites and coarse grained quartz-mica schists. Southeast-vergent isoclinal and also recumbent folds occur within this unit.

Fig.13: View from Acme Creek towards Smith Creek Dome (on photo left) and Midnight Dome (on photo middle). The Dbcs unit stands out and clearly delineates the sedimentary bedding.

In Swift Creek the Dbcs layers (Subunit 3) dip gently to the Northeast with approximately 20°, striking northwest-southeast. Layers lie conform on top of each other.

The Dbcs layers in the Nolan-Hammond area (Subunit 3) dip gently northeast with approximately 20°, striking NW-SE. The only exception is the Fortress Formation north of Smith Creek Dome. The Fortress Formation dips gently east with approximately 20 degrees, striking N-S. This phenomena is believed to be an erosional effect, or caused by frost lifting. The layers of this subunit lie conform on top of each other.

On Smith Creek Dome (Subunit 5) strike and dip of Dbcs layers varies. Bedding is exposed in southeast-vergent folds in quartzites, similar to the ones on Midnight Dome. A northeasterly gentle dip of bedding is present on Smith Creek Dome. However, Smith Creek Dome does not conformable overlie the Dbcs layers of the Nolan-Hammond area (Subunit 2) and is therefore suggested to be a small separate thrust sheet.

On Butte Mountain the Dbcs layers dip gently to the Northeast with approximately 20° and discordantly underlie the Butte Mountain thrust which dips gently southeast.

Strike and dip of Dbs in the area between the Right Fork of Vermont Creek, Thompson Pup, Fay Creek, Archibald Creek, and the lower part of Smith Creek varies from N-S to NW-SE in strike and from 5° to 30° in dip. This phenomena can be explained by thrusting and reverse faulting which heavily disturbed this area. Evidence is given in Fay Creek where small north-vergent folds indicate thrust faults.

A drastic change in strike and dip of bedding occurs in Vermont Creek, Vermont Dome, and on Montana Mountain.
Bedding of Dbps 1-4 and Dbcs 1 strikes in the eastern part WNW-ESE, dipping very gently with 12 to 15° NNE. In the western part Dbps 1-4 and Dbcs strike WSW-ENE, dipping with 12 to 15° NNW. The centroclinal stike may indicate Vermont Dome to be part of a large north-south trending, gentle anticline.
Strike and dip of Dbss 2 on Montana Mountain is basically similar compared to Vermont Dome.

4.2 Folds

Three generations of very small and larger-scale folds occur in the study area.

The possibly oldest generation of folds in the study area is represented within the metasedimentary rocks of the Dbss 2 unit near the mouth of Fay Creek (Loc. 365).

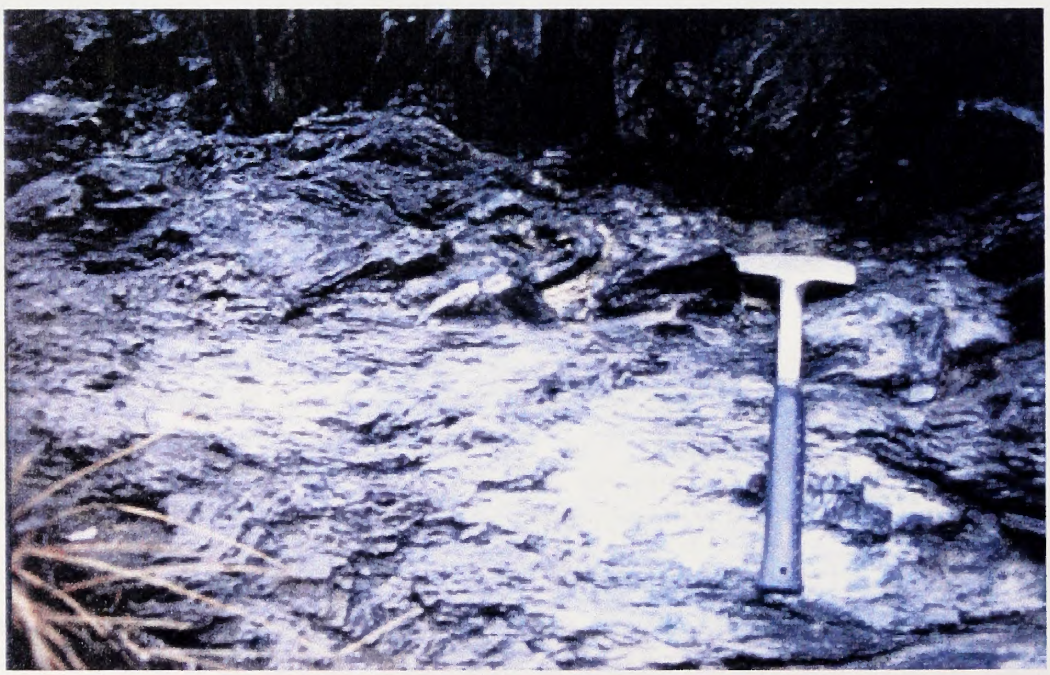

Fig.14: The possibly oldest generation of folds in the study area, outcropping near the mouth of Fay Creek (Loc. 365). This first folding event is represented in a flat lying fold with a flat fold axis plane dipping east.

This first folding event is represented in a flat lying fold with a flat fold axis plane dipping gently east (Fig.14). This may be related to regional metamorphism M_1.

In the thrust belt in the southern part of the study area small and larger north-vergent, isoclinal folds are present. Folds up to 15 meters in size and more can be seen on the southern ridge of Midnight Dome (Loc. 169).
These north-vergent, isoclinal folds are close to thrust faults with fold axes parallel to the regional east-west, east-northeast strike (Fig.15). Also buckle folds occur within these folds. In many outcrops these buckle folds form penetrative shear band cleavage (S_3). S_3 cleavage is axial-plane. In most outcrops where this fabric is developed, S_3 surfaces dip to the south and folds indicate a north-vergent shearing along these planes.
I strongly suggest these north-vergent folds to belong to larger scale north-vergent to northwest-vergent folds, possibly recumbent folds, though not defined by mapping. Evidence is given in the axial-planar semipenetrative cleavage to the mapped folds and according to DILLON and REIFENSTUHL (1990) folds of this size have been recognized in the Wiseman A-5, A-6, B-3, and B-6 Quadrangles. Small scale north-vergent folds are also exposed in Fay Creek. Moreover, another small north-vergent fold was mapped on Vermont Dome.

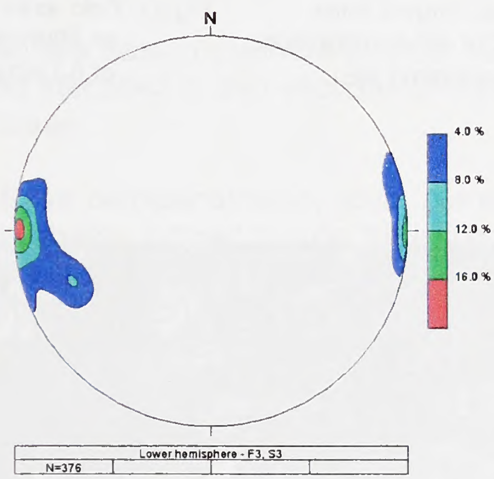

Fig.15: Fold axes of thrust related north-vergent folds on the southern ridge of Midnight Dome ("Cut all-construction of δ-Linears). Fold axes trend east-west.

Southeast-vergent, tight to isoclinal and recumbent folds occur on Midnight Dome and Smith Creek Dome (Fig.18). These vary in size from half a meter up to several meters. Fold axes trend with 40 to 60° NE-ENE, down plunging gently NE-ENE.
Fig. 16 and 17 show trending of fold axes determined by "cut all"-construction of δ-Linears (cleavage S_3 - bedding intersection) and ß-Linears (line of intersection of fold limbs).
Buckle folds within these folds form penetrative shear band cleavage (S_3). In most outcrops where this fabric is developed, S_3 surfaces dip northwest and folds indicate a south-vergent shearing along these planes. S_3 cleavage is axial-plane.
Further, crenulation cleavage occurs within folds
These southeast-vergent folds are presumed to be generated in the lower limb of a large scale north-vergent to northwest-vergent anticline, and can be seen as parasitic

folds within a large fold. Therefore these small folds are of the same generation as the north-vergent folds and belong to the same thrust related large north-vergent to northwest-vergent folds, possibly recumbent folds.

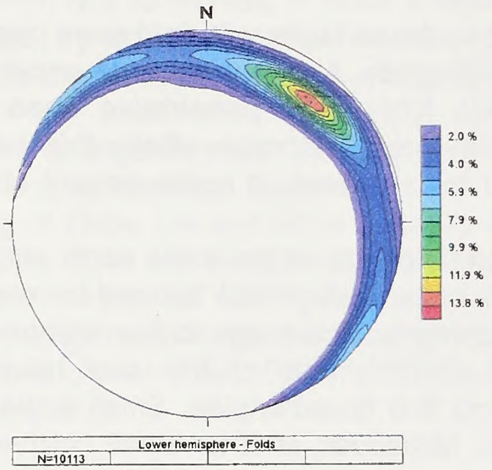

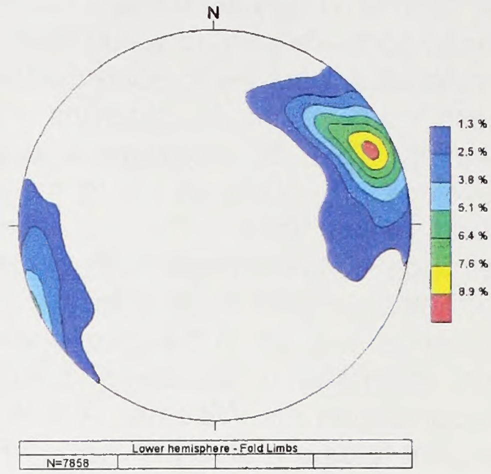

Fig.16: Fold axes of southeast-vergent folds on Midnight Dome ("Cut all"-construction of δ-Linears). Fold axes trend NE.

Fig.17: Fold axes of southeast-vergent folds on Midnight Dome ("Cut all"-construction of ß-Linears). Fold axes trend NE.

Fig.18: Southeast-vergent folds on Smith Creek Dome.

The youngest generation of folds is rarely developed in the study area and occurs near the head of Nutmeg Gulch (Loc. 289). Exposed folds are close and have a few millimeters up to 2 centimeters in wavelength with fold axes which trend north-south. Folds occur as thin close folds of quartz in black metasiltstone. A hand specimen given to me by Roger Burggraf (Tri-con Mining) from the former Eureka Pit (Nolan valley) of black metasiltstone with small close folds with wavelengths up to 1.5 centimeters suggests folds of this generation also to occur in Nolan valley.
I suggest that these small folds belong to larger north-south trending gentle folds with almost vertical axes planes. Evidence for larger north-south trending folds is given in Vermont Dome, which is probably part of a large north-south trending gentle anticline with a very gently north plunging fold axis. On Vermont Dome bedding dips gently to the north-northeast on the eastern side, and north-northwest on the western side (centroclinal strike). This indicates a large anticline.
A basically similar situation (centroclinal strike) is present on Montana Mountain. It cannot be ruled that the entire map area is part of a broad, north-south trending anticlinale structure.

4.3 Cleavage

Two cleavages (S_2 and S_3) are easy discernible in most outcrops in the study area. An older cleavage (S_1) was identified in thin sections of metasedimentary rocks from near the mouth of Smith Creek.

The youngest cleavage S_3 is semipenetrative, axial planar to major north-vergent isoclinal folds that were probably formed during thrusting. Mineral lineations trend north-south, parallel to the apparent thrust-transport direction. This is observed in north-vergent folds in the thrust belt on the south trending ridge of Midnight Dome.
S_3 strikes almost east-west, dipping with approximately 40° south.
On Midnight Dome, Smith Creek Dome, and Vermont Dome S_3 occurs axial planar to south-southeast vergent, isoclinal and recumbent folds, striking WSW-ENE, dipping with approximately 35° north-northwest.
As described in the previous chapter, these south-east vergent folds are presumed to be generated in the lower limb of a large scale north-vergent, possibly recumbent anticline.

The older penetrative cleavage S_2 is parallel to a lithologic layering and partially transposed by the younger cleavage (S_3). Cleavage S_2 is well exposed in the study area, especially on Midnight Dome. According to DILLON (1989) S_2 and S_3 are nearly coaxial in the southern Brooks Range. This is true on Vermont Dome and Montana Mountain, where S_2 and S_3 strike almost parallel, both dipping north. On Midnight Dome and Smith Creek Dome S_2 strikes northwest-southeast, dipping gently with approximately 20° northeast.
Schistosities S_2 and S_3 were developed during amphibolite- and retrograde greenschist-facies events.

Fig.19: Crossed-polar photomicrograph of S_1 and S_2 in quartz-mica schist next to a quartz vein. S_1 is folded and got partly destroyed by younger S_2-cleavage (on top of photo left). Picture is 5.6 mm in length.

The deformation to knotty texture and the occurrence of quartzite rods in quartzites and coarse grained quartz mica schists on Midnight Dome and Smith Creek Dome can be referred to the younger metamorphic events (M_2 and M_3). A strong penetrative cleavage (S_2) locally cuts across the quartzite-bands and deforms them into rods (Loc. 346), but in most places the cleavage parallels the banding; therefore, the banding might have formed penecontemporaneously with cleavage (S_2) during metamorphism M_2 (DILLON & REIFENSTUHL, 1990). The cleavage and banding are disrupted and partially transposed by semipenetrative cleavage (S_3) that is defined by middle greenschist-facies minerals (DILLON & REIFENSTUHL, 1990). The deformation of coarse grained quartz mica schists to knotty texture and the occurrence of quartzite rods can be explained by cutting of cleavage S_3 and S_2, and banding at high angles, resulting disruption of quartzite bands into rods and coarse grained quartz mica schist to knotty texture.

The oldest cleavage (S_1) can only be identified in thin sections (Fig.19 and 20). Cleavage S_1 got almost destroyed by later stage metamorphic and tectonic events.

Fig.20: Crossed-polar photomicrograph of S_1 and S_2 in phyllite. S_1 is folded and got partly destroyed by younger S_2-cleavage. Picture is 5.1 mm in length.

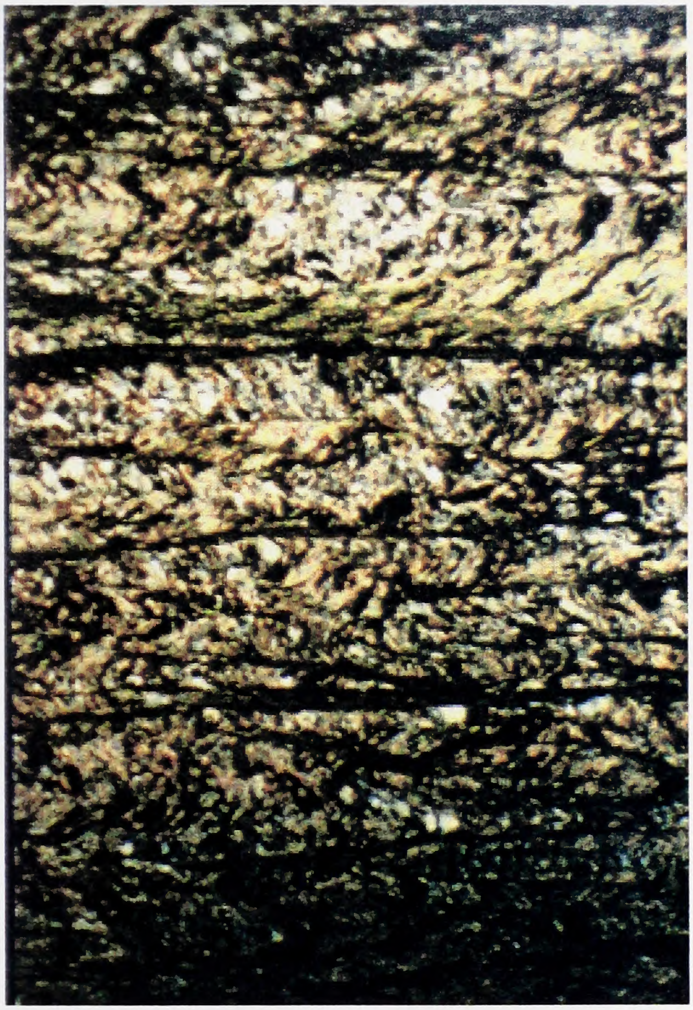

4.4 Faults

The study area is cut by several thrust faults, reverse faults, normal faults, and by one strike-slip fault. Although many of these faults have not been precisely located within the field, their approximate location is based on airphoto interpretation.

4.4.1 Thrust Faults

Three large-displacement thrusts occur in the southern part of the study area creating the large thrust belt. These thrusts faults are south dipping, striking east-west and juxtapose Middle Devonian rocks over Upper Devonian rocks (cross-section 1, Appendix 1). Evidence is given in mylonite shear zones along bedding planes.
The large-displacement thrust in the southeastern part of the study area (Bluff Gulch) belongs to the thrust belt described above. The only difference is given in a southeasterly dip of the thrust fault.

The Butte Mountain thrust sheet forms the top of Butte Mountain. Butte Mountain slate was juxtaposed north-northwest over younger metasedimentary rocks of the Dbcs unit (cross-section 1, Appendix 1). Evidence for this thrust is given in mylonite shear zones occurring along bedding planes on the northern or steeper side of the mountain, and secondly, there is a distinct anomaly in the southwestern flank. From the summit of Butte Mountain, the bedding dips smoothly southeast at an angle of approximately 25 degrees (Loc.209, 210, and 211). This is also reported by DRISCOLL (1987). On the south leading ridge (Loc. 212a), bedding of the Dbcs unit strikes generally northwest and dips northeast with approximately 20 degrees.

Fig.21: View from Nolan Camp towards Montana Mountain. Topographic changes on Montana Mountain indicate thrust faults.

Thrust faults of small-displacement compared to the ones described above occur on Montana Mountain (cross-section 2, Appendix 1). Their precise location is mapped from airphoto interpretation and due to topographic changes observed on Montana Mountain (Fig.21). Displacement is believed to vary between 100 ft up to 1000 ft (30 to 300 meters).

Smith Creek Dome has been mapped and given the status of a separate thrust sheet. Bedding is exposed in southeast-vergent folds in quartzites, similar to the ones on Midnight Dome. An approximate northeasterly gentle dip of bedding is present on Smith Creek Dome, but strike and dip vary locally. Mylonite shear zones were not observed near the top, but are assumed to be present on lower parts of Smith Creek Dome as topographic changes indicate. Therefore I suggest Smith Creek Dome to be a small separate thrust sheet.

4.4.2 Reverse Faults

Three parallel northeast trending, northwest dipping reverse faults striking parallel to Nolan Creek and the Right Fork of Vermont Creek have been mapped in the Nolan area. Two of them are obvious on aerial photographs. Due to placer mining activity in Archibald Creek in summer 1998, the westerly located fault of these two was exposed shortly, proving the interpretation of aerial photographs to be right and the faults to be existing. Amount of displacement could not be determined.
The westerly located fault can be followed further through the Right Fork of Vermont Creek. Due to late-stage extensional movement (uplift), this reverse fault was reactivated as a normal fault in the Right Fork area.
It should be noted here that the Koyukuk River valley (located southeast in the study area) runs precisely parallel to the strike of the reverse faults. There is likely to be a reverse fault existing in that valley. This reverse fault is dotted on the Structural Geologic map (Appendix 2).

4.4.3 Strike-Slip Faults

One almost vertical strike-slip fault has been mapped in the study area. This one is located in Vermont Creek, west-trending with a right-lateral separation. Unfortunately, the amount of displacement could not be determined. Interpretation of aerial photographs strongly suggests this fault to be right-lateral. Evidence for this fault is given south of Vermont Dome in a major zone of brittle, heavily disturbed gray-black micaceous schists and phyllites (Loc.195 to Loc.198), probably due to shearing. Within this zone appears massive quartz-float from thick outcropping veins. Strike of these veins could not exactly be determined, but is strongly assumed to be west-northwest, with a vertical dip.
Moreover, Vermont Creek itself runs east west and this dominant feature can be followed further to the other side of the Hammond River. On the east side of the Hammond River (Loc.205), an almost vertical, west-trending fault was mapped, steeply dipping with 80 degrees south with a brecciated fault contact. As this fault is located very close to the assumed right-lateral strike-slip fault, I presume this fault to belong to the strike-slip fault zone. This is further evidence for the existence of the right-lateral strike-slip-fault.

4.4.4 Normal Faults

Several normal faults have been mapped in the study area. Two of them are exposed in Thompson Pup. The first of the two of them is situated in the upper part of Thompson Pup (Loc. 243), west-trending and steeply dipping north . The second one is situated in the lower part of Thompson Pup (Loc.253) striking NW-SE, steeply dipping northeast (30/75). Thickness of fault zone is approximately 80 centimeters. Amount of displacement in both of them could not be determined.

A third normal fault is exposed near the head of Smith Creek (Loc. 121). This fault is north trending, steeply dipping east. Amount of displacement is minor, only 20 centimeters.

A high-angle normal fault was mapped on the northern flank of Midnight Dome. This fault strikes west-southwest and dips south-southeast. The amount of displacement could not be determined. Evidence for this fault is given in the topographic change on the northern flank of Midnight Dome and also in interpretation of aerial photographs, proving this normal fault to be existing. Its precise location is mapped due to interpretation of aerial photographs

CHIPP (1970) describes a prominent system of high-angle faults trending approximately N57W for the Chandalar quadrangle (east of the Wiseman quadrangle). This corresponds with the normal fault mapped in the lower part of Thompson Pup (Loc.253) striking with 120 degrees NW-SE, dipping with 75 degrees northeast.
In addition to that, the Wiseman Creek valley runs precisely NW-SE (120°), and is very linear. There is likely a normal fault there, related to those in the Chandalar quadrangle (DRISCOLL, 1987).
Further, the normal faults on Midnight Dome have almost the same strike, cutting Midnight Dome into a Horst and Graben-structure caused by late-stage extensional movement (uplift).

4.5 Joints

A large number of joint orientations were measured out in the field. Data compilation is plotted in a rose diagram (Fig. 22) showing strikes of joints and also in a lower hemisphere, equal-area plot for joint pole orientations (Fig. 23). More specific rose diagrams of strikes of joints are presented on the Structural Geologic map (Appendix 2).

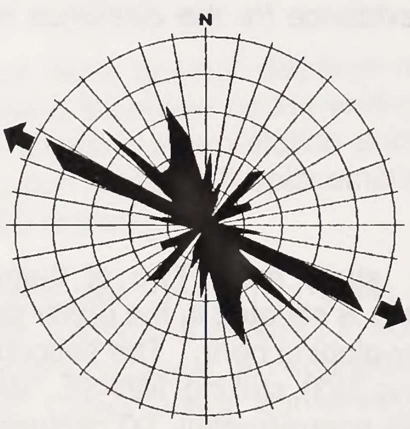

Fig.22: Rose diagram of strikes of joints for the Nolan area, N= 430

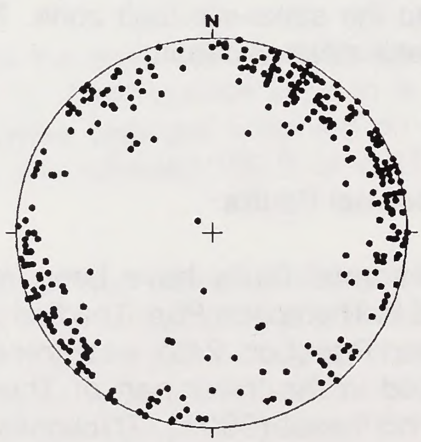

Fig.23: Lower-hemisphere, equal area plot showing joint pole orientations for the Nolan area, N= 430

A weak developed orthogonal joint system is present in the study area, as shown in the rose diagram (Fig.22). Its relation towards larger-scale folds could not be determined. Therefore it is impossible to define those joints into ac- and bc-joints.
The primary joint system developed in the sedimentary rocks was destroyed by later stage metamorphic events (M_2 and M_3).
The most prominent joint system in the study area strikes roughly with 120 degrees NW-SE (N60W), dipping steeply to the southwest. Moreover, a second prominent joint system is developed in the study area. This system strikes roughly 45 degrees northeast, dipping almost vertical. These joints cannot be defined with certainty. The NE striking joints could possibly be tensional fractures being supplementary to zones of shearing, and second order in origin.
The NW striking joints could most likely be tension fractures at right angles to the axis of a large scale NE striking fold.

These two prominent joint systems are often mineralized and important for gold mineralization as a comparison of joint orientations and orientation of gold-bearing veins shows (Fig.22 and Fig.24).

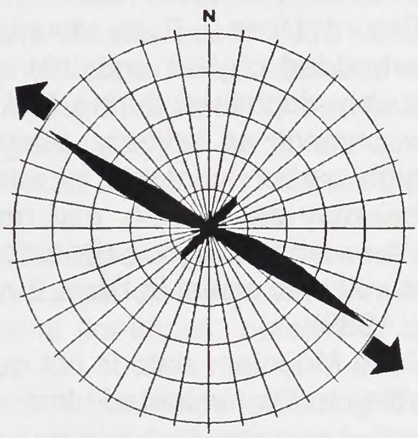

Fig. 24: Rose diagram of strikes of quartz veins for the Nolan area.

Mineralization of the quartz-gold veins took place in the NW-striking joint system, whereas emplacement of the quartz-stibnite-gold veins occurred in the NE-striking joint system.

5. Summary and Interpretation of Results

Rocks in the Nolan area are believed to be Middle to Upper Devonian in age. DILLON ET AL.(1986) mapped the area as Devonian, and though no fossils have been found in the immediate vicinity to substantiate this, there have been some found in adjacent regions that seem to constrain this area to be Devonian (DILLON ET AL., 1986, BROSGÉ AND REISER, 1964, 1971).
The metasediments of the Nolan area were originally deposited as siltstones, sandstones, graywackes, and conglomerates; shales, and limestones. They belong to the Coldfoot- and Hammond subterrane, which are two of four subterranes composing the Arctic Alaska terrane.

The siliceous metasedimentary rocks with carbonaceous interlayers form the structurally lowest units (Dcc and Dcss), belonging to the Cooldfoot subterrane. The metasedimentary Dcc and Dcss units are composed of sandstones and conglomerates with interbedded phyllite of Middle Devonian age, deposited in a lower shore face marine environment. The conglomerates belonging to these units possibly contain fragments of Lower Paleozoic rocks.
The metasedimentary units Dbss 1, Dbss 2, Butte Mountain Slate, and Dbs consist of black metasiltstone with interbedded phyllite and thin marble interlayers, phyllites, and slates. These were probably deposited during Middle to Upper Devonian in a deeper, quieter marine environment as primary siltstones and shales with thin limestone interlayers. The high carbon contents in some of these units (e.g. the graphitic schists and phyllites) may be organic, and result of deposition in a very anoxic environment, such as a swamp or lagoon (DRISCOLL, 1987). The interlayers of fine-grained calcareous felsic volcanic schist in Dbss 2 may have been derived from distal airfall tuff (DILLON ET AL.,1989).
The stratigraphic setting of Butte Mountain slate is not quite certain to determine. As this unit shows strong similarities to the laminated black metasiltstone of Dbss 2 and the black slate of the Dbs unit, I suggest that this unit may be located in between these two units, or interfingering between these.
The metasedimentary units Dbps 1 to 4, consisting of phyllite and pelitic mica schist, were also deposited in a deeper, quieter marine environment during Upper Devonian, probably as shale. Also within these units occur thin interlayers of felsic schist, believed to have been derived from a distal airfall tuff.
The chloritic quartzite and coarse grained quartz-mica schist of the Dbcs unit, with interlayers of phyllite and schist were deposited during Upper Devonian in a nearshore, shallow marine environment as sandstones, graywackes, and shales.

The age of the metabasite dyke is not quite certain to define. As the dyke intruded into the metasediments of the Dbcs unit of the Upper Devonian, it must be at least Upper Devonian in age. Further, the metabasite is schistose, therefore it must have been intruded before the two regional metamorphic events M_2 and M_3 have happened. Based on this conclusion I suggest the metabasite dyke to be Upper Devonian to Jurassic in age. ASHWORTH (1983) describes “greenstones” for the Chandalar district, dated as Devonian.

The possibly first tectonic event happened in the study area is recorded by a first period of folding within the metasedimentary unit Dbss 2 near the mouth of Fay

Creek (Loc. 365). This first folding event is represented in a flat lying fold with a flat fold axis plane dipping gently east. This may be may be related to regional metamorphism M_1.

A second tectonic event recorded by the Devonian metasediments is evident from a penetrative cleavage (S_2) that is parallel to a lithologic layering. This dominant cleavage is well exposed in the study area. According to ASHWORTH (1983) development of S_2 took place during the Late Triassic to Early Cretaceous.
The youngest metamorphic event (M_3) is represented by a semipenetrative, axial-plane cleavage (S_3) transposing the older cleavage S_2. DILLON & REIFENSTUHL (1990) suggest S_3 to have occurred during Late Jurassic or Neocomian time. Cleavages S_2 and S_3 were developed during two metamorphic events. S_2 formed under amphibolite-facies conditions, S_3 formed under a retrograde greenschist-facies event.

During Late Jurassic to Early Cretaceous time the Middle Devonian metasedimentary rocks of the Coldfoot subterrane (Dcc and Dcss in the study area), and Dbss 1 and Dbss 2 of the Hammond subterrane were thrust northward onto the Middle to Upper Devonian metasedimentary rocks of the Hammond subterrane of the Arctic Alaska terrane. This is represented by the large thrust belt in the southern part of the study area (cross-section A-A', Appendix 1). Thrusting and thrust related folding created the S_3 cleavage. Subordinate thrusts occur within the Dbss 2 and Dbs units on Montana Mountain and around Nolan Creek, but have no large-displacement (cross-section B-B', Appendix 1). In the thrust belt in the southern part of the study area small and larger north-vergent, isoclinal folds are present. These north-vergent, isoclinal folds are close to thrust faults with fold axes parallel to the regional east-west, east-northeast strike and deform the older cleavage S_2. From these observations, I inferred that the upper plates of the major thrust faults were probably moving northward while the younger cleavage was forming. Further evidence is given in north-south trending mineral lineations, parallel to the apparent thrust-transport direction.
I strongly suggest these north-vergent folds to belong to larger scale north-vergent to northwest-vergent folds, though not defined by mapping. Evidence is given in the in the axial-planar semipenetrative cleavage to the mapped folds and according to DILLON & REIFENSTUHL (1990) folds of this size have been recognized in other Wiseman Quadrangles.
A bit difficult to explain are the south-east vergent isoclinal, possibly recumbent folds on Midnight Dome and Smith Creek Dome. I interpret the south-east vergent folds on Midnight Dome to be generated in the lower limb of a large scale north-vergent to northwest-vergent anticline, possibly recumbent. Therefore they are interpreted to be parasitic folds within a large scale fold. This would fit with DILLON & REIFENSTUHL'S (1990) inference of large-scale north-vergent to northwest-vergent folds. Evidence is given in the intersection of the younger semipenetrative axial-planar cleavage (S_3) with the older, layer parallel penetrative cleavage (S_2), indicating the location of major fold axes.

The south-east vergent folds on Smith Creek Dome probably formed either in the lower limb of a large-scale recumbent anticline, or due to backthrusting. Field observations suggest that model A is preferable.
Butte Mountain slate was thrust north-westward onto metasedimentary rocks of the Upper Devonian.

According to DILLON (1989), thrusting and thrust related large-scale folding had its origin in the obduction of the oceanic rocks of the Angayucham terrane in the Koyukuk basin onto the continental rocks of the Arctic Alaska terrane. At this time the lithotectonic terranes of northern Alaska were sutured together. This event produced regional metamorphism of the continental rocks that were overridden and pervasive thrust faulting in both the continental and oceanic plates.

The last tectonic event in the southern Brooks Range is represented by post-Early Cretaceous (DILLON, 1989), high angle, west-trending, strike-slip faults that displace the thrust faults. These are related to post-thrust-folding. Within the study area one almost vertical, right-lateral, strike-slip fault has been mapped with large displacement. According to GOTTSCHALK (1987) the east-west compression reorients earlier structures related to north directed contraction. The ninety degree shift in the orientation of compressive stress from north-south to east-west may result from the onset of differential movement between the Siberian and Arctic Alaska Alaskan portions of the North American plate in the Late Cretaceous (PATTON AND TAILLEUR, 1977).

The west dipping reverse faults mapped in the region are interpreted to be post thrusting in age, caused eastwest-compressional tectonic movement. On the aerial photographs these faults can be followed further southwards across Smith Creek into the mountains south of Wiseman Creek. As these reverse faults cut the thrust faults in the study area they must be younger in age. An interesting phenomena is that these faults do not seem to cut the strike-slip fault in Vermont Creek, suggesting reverse faulting to have happened after thrusting and before strike-slip faulting.
However, it cannot totally be ruled out that the origin of these faults relates to thrusting caused by northward compression and reactivation as reverse faults during eastwest-compressional movement.

Due to east-west compression the latest phase of folding has produced a series of small folds of a few centimeters in wavelength (Loc.289) with north-south trending fold axes and almost vertical, north-south striking axes planes. These latest phase folds are rarely developed in the study area. I strongly suggest these small folds to belong to larger north-south trending gentle folds with almost vertical fold axes planes. Evidence for larger north-south trending folds is given in Vermont Dome, which is interpreted to be part of a large north-south trending gentle anticline with a very gently dipping north plunging fold axis. On Vermont Dome bedding dips gently to the north-northeast on the eastern side, and north-northwest on the western side. This centroclinal strike indicates a large, gentle anticline. Similar features can be observed on Montana Mountain.

Several normal faults have been mapped in the area. Late Jurassic to Early Cretaceous south to north-thrusting formed a series of allochthons now exposed in various locations across the Brooks Range (GOLDFARB ET AL., 1997). Coeval with latter stages of this contraction, regional Middle Cretaceous crustal extension affected the Brooks Range (MILLER AND HUDSON, 1991). Structural relationships suggest a cessation of extension by 112 Ma (GOTTSCHALK, 1990). Coeval contraction and extension favored normal faulting driven by compressional uplift of the high-pressure rocks of the southern Brooks Range (GOLDFARB ET AL., 1997).
I personally suggest that extensional movement caused by uplift also reactivated older fault systems (e.g. the Right Fork fault) and joint planes as normal faults.

Faults on Midnight Dome were possibly first developed as joint planes during thrusting, or after thrusting during eastwest compression. Uplift reactivated joint planes as normal faults. Evidence is given in parallel strike of joints to the normal faults (e.g. Union Gulch faults and Confederate Gulch fault). Late-stage extensional movement led to the Horst and Graben-structure of Midnight Dome.

At least three generations of quartz veins occur in the study area.
The oldest generation is represented by slightly deformed (Loc. 194), non schistose quartz veins which cross cut the metasediments. As deformation of these veins corresponds to north-vergent folding, I suggest these must have been formed during late stage tectonic movement, probably during late stage thrusting.
A younger generation of quartz veins is presented by veins which are nearly conformable with the enclosing metasediments. I suggest these veins to be post-thrusting in age and to have been derived from "sweated out" metamorphic quartz (segregation quartz). Due to regional metamorphism quartz grains of the metasediments got into solution and formed fluids which moved into foliation- and bedding planes of the enclosing metasediments. The thickening of these veins in fold noses can be explained by weakening and fracturing of the rocks in fold noses caused by stress. This leads to openings for fluids to circulate into with subsequent mineralization of quartz.
The youngest generation of quartz veins is represented by veins which cross-cut the metasediments at a high angle to foliation. These veins also cross-cut the conformable quartz veins as observed in Loc. 146, proving these veins to belong to the youngest generation. These quartz veins are related to fractures, and occur with different orientations.
The two prominent joint systems developed in the study area are related to folding and thrusting which occurred in Late Jurassic to Early Cretaceous. It cannot be ruled out that these fractures may have formed also during later stage east-west compressional tectonic movement. If not, they were possibly reactivated during east-west compression. I suggest the NE-striking joints to be tensional fractures being supplementary to zones of shearing, and second order in origin. Further, the NW-striking joints can be interpreted as tension fractures at right angles to the axis of a large scale NE striking fold. Fractures were reactivated during extensional movement (uplift).

Gold-bearing veins in the Brooks Range were most likely emplaced during uplift, as originally suggested by DILLON (1982). In addition, strike-slip movement may have played a role in vein genesis. According to GOLDFARB ET AL. (1997) there is strong evidence that gold vein formation across the southern Brooks Range was controlled in part, by Albian strike-slip movement. Gold-bearing quartz veins were emplaced during Albian and Campanian time (GOLDFARB ET AL., 1997).

Most of the cross cutting veins are barren of gold. Apparently gold only occurs along certain restricted parts of the veins (in "shoots") in two vein systems of different strike. The gold-quartz and stibnite-gold-quartz vein systems are mainly concentrated in a "corridor" from the south of Smith Creek through the Nolan Valley, along Thompson Pup and the "Fortress" into the Right Fork of Vermont Creek. The reason for this is the fact that this particular area was heavily disturbed by multistage faulting, shearing, and folding. Extensional movement (uplift) caused even more openings for mineralized fluids to circulate through with subsequent crystallization of quartz, stibnite, and gold. Further, the metasedimentary rocks in this area contain graphite and pyrite, which are favorable for precipitation of gold from hydrothermal fluids.

DRISCOLL (1987) describes some shearing along bedding planes after development of the joints, and after mineralization of the joints, as evidenced by offset of mineralized joints. This was also determined in thin sections, but this movement is believed to be minor.

Several episodes of glaciation with intervening interglacial and interstadial intervals are recognized in the Brooks Range (REED, 1938). Throughout the study area it appears that events of late Pleistocene glacial and nonglacial intervals played a dominant role in the formation of placer deposits.
During Quaternary, glaciation shaped and sculptured the region to its present erosional surface. Glaciers of at least three advances have trenched and filled the main through-going valleys of the southern Brooks Range and have left the lowland south of the range largely covered by drift and outwash (BROSGÉ & REISER, 1972). The oldest interval of glaciation in the area is represented by the Sagavanirtok River Glaciation. The youngest intervals of glaciation are represented by the Itillik Glaciation I to III (PROFFETT, 1982).

The gold placer deposits in the study area were derived from nearby lode occurrences. I suggest the gold-bearing veins of the area to be the source of placer gold as placer deposits surround these auriferous veins. Note that the origin of gold in both vein systems, the vein mineralization as well as the origin of placer gold will be described in Chapter III of this thesis report.
The preservation of gold placers is found in mountain valleys least affected by glaciation. The placer deposits are usually confined to Quaternary alluvium that overlies bedrock in deeply cut, non glaciated valleys (DILLON, LAMAL, HUBER, 1989). Cycles of erosion and deposition during the Quaternary Period coupled with the presence or absence of favorable gold sources in present and former drainage systems are responsible for the composite nature of placers formed in the area.
Three varieties of gold-bearing stream gravels occur in the Upper Koyukuk district (DILLON & REIFENSTUHL, 1990): (1) active stream gravels (Qa), (2) elevated bench gravels (Qa), and (3) deeply buried gravels (Qg?). Placer gold deposits are presented on the Geologic map (Appendix 1).

III. Gold Mineralization of the Nolan Area

6. Procedures

A total of 224 samples, consisting of rock samples, stream sediment samples, pan concentrates, and sluice concentrate samples were collected by AMRT during summer 1997, and by myself and AMRT during field season 1998.
Each sample was analyzed for 38 elements. Data of samples taken by AMRT will be used for this report with kind permission from Joseph Kurtak (BLM Alaska, AMRT).
Rock samples Nc1 to Nc4 were collected by Jack DiMarchi (Project Exploration Geologist, Teck Corp.) and myself in late summer 1998. Data will be used for this report with kind permission from Jack DiMarchi.
Electron microprobe work was carried out on placer gold from different creeks and benches in the study area as well as on lode gold. This was performed in co-operation with the University of Alaska-Fairbanks. Purpose was to compare placer gold from various creeks with each other as well as with lode gold.
Thin sections, polished sections, and polished thin sections were examined petrographically for mineral identification, and to establish mineral parageneses. This was performed at the Technical University of Clausthal in Germany.
X-ray diffraction was carried at the Colorado School of Mines (USA) for gangue mineral identification.
Fluid inclusion data on gold-bearing veins used for this report was obtained from BLM and by intense research of literature.

6.1 Sampling

Apart from rock samples, sampling in the Nolan area consisted of stream sediment, pan concentrate, and sluice concentrate sampling at a majority of the streams visited. These methods are often used to cover large land areas with relative efficiency. Coordinates of sample locations and assay data of taken samples are presented on Table 2c. Sample locations are also marked on the Sample Location map (Appendix 3).

6.1.1 Stream sediment samples

Stream sediment samples are composites of silt and clay material from the stream bed (KURTAK ET AL., in press). If there is mineralization within the basin, important ore and indicator elements will often be present in streambed fines at elevated concentrations. 400 to 500 g of wet silt and clay material was put in a water resistant paper bag for a representative stream sediment sample.

6.1.2 Pan concentrate samples

Pan concentrate samples are collections of coarse sand and gravel. It is important to collect the sample at the proper location. Often areas where the gradient changes from steep to relatively moderate will provide a depositional environment for heavy minerals (KURTAK ET AL., in press). Other locations include: plunge pools, crosscutting fractures, and crosscutting schists which act as natural riffles. When a suitable collection site was located, coarse material was heaped into a 14-inch plastic pan (KURTAK ET AL., in press). The material is was panned down to 0.75 fluid ounces (marked on each pan). The presence of heavy minerals such as gold, sulfides, magnetite, and garnet were noted in the field.

6.1.3 Sluice concentrate samples

For this report, I combined sluice samples in general, soil samples, and placer samples as sluice concentrate samples. Therefore, the term sluice concentrate sample is a generic term. Sluice samples are concentrate samples of the processing plants of local miners. The material collected for analysis was heavy material remaining in the processing plant after the gold had been removed (KURTAK ET AL., in press).
Soil samples taken from the thin C horizon, were washed through a sluice box to check for gold. The concentrate captured in the sluice box, representing the sample, was put in water resistant bags.
Placer samples were taken by AMRT from gold-bearing gravels on the east side of the Hammond River. Placer samples were processed in a sluice box.

6.1.4 Rock samples

Rock samples inevitably collected were differentiated into three types of rock samples: outcrop, rubblecrop, or float. An outcrop sample is a sample of bedrock; it is often referred to as 'in place'. Rubblecrop describes cobbles and boulders which are often frost jacked to the surface from underlying bedrock (which is not visible but implied). Float samples are simply cobbles with no discernable bedrock source (KURTAK ET AL., in press). Note that the sample site can also be tailings pile, or an existing trench.

Once the sample site was characterized, the sample type was described. There are several types of chip samples that are collected by hammer and chisel from outcrop exposures. Chip samples include: continuous chip, random chip, representative chip, and spaced chip (Table 2a). Finally, a grab sample is a more or less random collection; whereas, a select sample implies collecting from the highest grade of the exposed mineralization (KURTAK ET AL., in press).

Usually, approximately 1.5 kg of sample material was put in a bag for assaying. Problems occurred with sampling of veins and veinlets, where that much material could not be obtained. Especially sampling of veinlets led to contamination problems as often vein material could not be separated from surrounding wall rock.

6.1.5 Placer Gold samples (Nuggets)

Placer gold (nuggets), suitable for electron microprobe analysis, was taken from several creeks in the study area by gold panning and bucket sampling of stream sediments from plunge pools in creeks. Bucket samples of sediments were run through a sluice box and further through a gold saver to catch the fines. Also, placer gold was taken from benches (bench placer) and buried gravels (Swede underground) by washing the mud through a sluice box and further gold saver.

6.2 Analytical Procedures

6.2.1 Analytical procedures of stream sediment-, pan concentrate-, sluice concentrate samples, and rock samples

All samples were analyzed by Intertek Testing Services of Vancouver, Canada, except for rock samples Nc1 to Nc4, which were analyzed by Chemex Labs in Vancouver, Canada.

Samples sent to Intertek were analyzed for 38 elements, whereas samples sent to Chemex were analyzed for 32 elements. Both laboratories use the same analytical methods.

Pan concentrate and rock samples were ground to -150 mesh. (Pan cons were also silica cleaned). Stream sediment and soil samples (sluice concentrates) were ground to -80 mesh.

Gold was analyzed by a pre-concentration fire assay followed by an atomic absorption (AA) finish. Platinum and palladium were also analyzed by a pre-concentration fire assay followed by induction couple plasma (ICP) atomic emission spectroscopy.

All other elements (except for mercury) were digested in a (3:1) HCl-HNO_3 solution. Once in solution, the elements were measured by ICP atomic emission spectroscopy. The analysis for mercury was accomplished with (3:1) HCl-HNO_3 digestion followed by cold vapor measurement (KURTAK ET AL., in press).

Concentrations of gold which exceeded the upper detection limit (>10,000 ppb) for the AA finish were re-analyzed by fire assay gravimetric methods. Elevated concentrations of antimony, barium, bismuth, copper, iron, lead, and zinc were re-analyzed by multi acid digestion followed by atomic absorption.

A complete list of assay results and detection limits for each element assayed is presented on Table 2b and on Table 2c.

6.2.2 Electron microprobe analysis

Compositions of placer gold and visible gold from veins, determined by electron microprobe analysis was carried out in co-operation with the University of Alaska-Fairbanks.
Analyses were performed on the Chimeca SX-50 microprobe at the University of Alaska, Fairbanks during October 1998. Placer grains (nuggets) and vein gold were mounted in epoxy, ground to a uniform thickness, polished to ¼ micron, and examined under reflected light prior to microprobe analysis. A 30 kV, 30 mA, 1 micron beam was employed for all analyses (NEWBERRY & CLAUTICE, 1997). At least 6 analyses were performed on each grain, representing a minimum of 3 analyses from cores and 3 from rims of nuggets and gold grains in veins. Elements analyzed were Au, Ag, Hg, Sb, Bi, and Te. Gold analyses with analytical totals of less than 97% were discarded; most analyses totaled 99-102%.
Electron microprobe data is presented on Table 3. Data obtained from electron microprobe analyses was used to determine the "true fineness" of gold.
"True fineness" is the ratio of gold to gold plus silver multiplied by 1000 (BOYLE, 1979, p. 197). True fineness = (Au / (Au+Ag)) x 1000.

6.2.3 Fluid inclusion analysis

In 1995, two quartz samples from the Nolan area were submitted by the Alaska Field Operations Center (Bureau of Mines) to the Albany Research Center (Bureau of Mines) for fluid inclusion studies. Data will be used for this report with kind permission from Joseph Kurtak (BLM Alaska, former Bureau of Mines).
The two samples were prepared as doubly-polished thick sections. The sections were examined for fluid inclusions, mapped, broken into chips, and subjected to freezing and heating runs to estimate fluid characteristics.
All inclusions examined were contained in quartz. Efforts were made to crosscut the quartz crystals during sample preparation, when the crystal orientation was evident. All inclusions contained two phases - liquid and vapor. No solid phases or additional liquid or gaseous phases (such as CO_2) were seen.

6.2.4 Thin sections, polished thin sections, and polished sections

Thin sections, polished thin sections, and polished sections were commissioned from Mann Petrographis (New Mexico, USA). Reflected light petrography on polished sections and polished thin sections, as well as interpretation of thin and polished thin sections for mineral identification was undertaken at the Technical University of Clausthal in Germany.

6.2.5 X-Ray Diffraction

One sample for gangue mineral identification was handed to the Colorado School of Mines in Golden, Colorado, by BLM. Data will be used in this report with permission from Joseph Kurtak (BLM, AMRT).
For identification purposes the dry powder-method was used. The sample was ground into particles < 50 µm in size. The powder was put in a sample holder and leveled off with a ground glass slide. This is done to get a random mounted sample and therefore reduce the biasis of sheet silicates.

7. Geochemical Reconnaissance Sampling

Altogether, 228 samples were taken in the study area consisting of 30 pan concentrate samples, 25 stream sediment samples, 10 sluice concentrate samples, and 163 rock samples. Samples were taken by AMRT (BLM) during summer 1997, and by myself and AMRT during field season 1998. Location of samples with anomalous gold and those with anomalous concentrations of silver or some base metals will be described below. Concentrations described as anomalous are interpretive, but are at approximately at the 95th percentile levels of the continuous part of the frequency distribution for each metal.
All assay data is presented on Table 2c. Sample locations are presented on the Sample Location map (Appendix 3).

7.1 Results of pan concentrate sampling

To present results of pan concentrate sampling, the study area is divided into three areas: Nolan Creek Valley and its tributaries, Union Gulch, and the Hammond River and its tributaries.

Nolan Creek Valley and its tributaries: 14 pan concentrate samples were taken from Nolan Creek and its tributaries. Some samples contain anomalous gold concentrations.

Nolan Creek: Sample 8035, taken near Nolan Camp contains more than **10,000 ppb gold,** further 31 ppm Ag, 100 ppm As, and 196 ppm Sb. One sample (S 11117) taken in Nolan Creek further upstream, near the mouth of Fay Creek contains 11,740 ppb gold and 5.1 ppm Ag. Further upstream, near Montana Gulch and Vermont Pass, sample 11088 was assayed with 14.99 ppm gold, though no other elements are anomalous. Other samples taken in Nolan Creek are not anomalous in element concentrations.

Smith Creek: Pan concentrate sample (S 10744) taken near the head of Smith Creek is not anomalous in element concentrations.

Archibald Creek: Pan concentrate sample 11144 taken in Archibald Gully contains **217.63 ppm Au** and 6.1 ppm Ag. Sample 11069 taken from Archibald is not anomalous in element concentrations.

Acme Creek: Pan concentrate sample 11091 taken from Acme Creek is not anomalous in element concentrations.

Fay Creek: Pan concentrate sample 11067 which was taken in Fay Creek contains 1120 ppb Au and 100 ppm As. Sample 11133 shows an anomaly in its mercury concentration with 2.269 ppm Hg.

Thompson Pup: Thompson Pup is a tributary to Fay Creek. Pan concentrate sample 11063 was assayed with **15.80 ppm Au,** 3.2 ppm Ag, and 374 ppm As. Sample 11065 is anomalous with more than 10000 ppm As, 393 ppm Co, and 777 ppm Sb.

Union Gulch: Four pan concentrates were taken from Union Gulch. The highest detected was sample 11140 containing **17.24 ppm Au** and 209 ppm As.
Sample 11141 contains 1559 ppb Au, Sample 11139 contains 1471 ppb Au, though no other elements are anomalous in concentration. S 11137 was assayed with 1023 ppm As.

Hammond River and its tributaries: 12 pan concentrate samples were taken from the Hammond River and its tributaries.

Steep Gulch: Sample 11356 was assayed with 276 ppb Au, though no other elements are anomalous in concentrations.

Gold Bottom Gulch: Sample 11354 contains **407.59 ppm Au**, 27 ppm Ag, and 5.320 ppm Hg.

Lofty Gulch: Sample 11330 was assayed with **13.33 ppm Au**, though no other elements are anomalous in concentrations.

Swift Creek: Samples 11058 contains **5869 ppb Au**, 570 ppm As, and 1.070 ppm Hg. Sample 11052 is not anomalous in element concentrations.

Buckeye Gulch: Sample 11309 is not anomalous in element concentrations.

Muck Pup: Sample 11276 was assayed with **95.28 ppm Au**, 4.5 ppm Ag, 633 ppm As, and 1.160 ppm Hg.

Vermont Creek: Sample 10736 contains 398 ppb Au, though no other elements are anomalous in concentrations.

Right Fork: The Right Fork is a tributary to Vermont Creek. Sample 10732 contains **5993 ppb Au** and 369 ppm As. Sample 11268 contains 1170 ppb Au.
Samples 11260 and 11262 are not anomalous in element concentrations.

7.2 Results of stream sediment sampling

Altogether, 25 stream sediment samples were taken in the study area. Surprisingly, no anomalies in element concentrations can be noticed, except for sample S 11062 , taken from Thompson Pup, which contains 83 ppb Au. Stream sediment samples are normally best for base metals, i.e. copper, zinc, but in this case they don't seem to show any anomaly.

7.3 Results of sluice concentrate sampling

10 sluice concentrate samples were taken in the study area. Three sluice concentrates samples (S 10674 to S 10676) were collected near Nolan Camp. Sample 10676 contains 1964 ppb Au. Further this sample contains 99.9 ppm Ag, more than 10,000 ppm Pb, 228 ppm Bi, more than 10,000 ppm As, and 830 ppm Sb. The strong anomaly in lead is quite interesting and is possibly related to contamination, probably caused by bullets. Sample 10675 contains 294 ppm As. Sample 10674 is not anomalous in element concentrations.
Sluice concentrate sample 10764 ("soil sample") taken on Smith Dome Bench (Gobblers Knob) was assayed with 387.62 ppm Au. That is highly anomalous. Further, this sample is also high anomalous in silver (83,7 ppm), copper (161 ppm), lead (>10,000 ppm), Bi (135 ppm), As (737 ppm), Sb (199 ppm), and Fe (> 10 pct). Sample S 11247 ("soil sample") was also taken on Smith Dome Bench and contains 2.33 ppm Au.
Sluice concentrate sample 10763 was taken near the mouth the Hammond River. This sample is highly anomalous in gold (430,43 ppm). Further, it is anomalous in Ag (27.7 ppm), Pb (473 ppm), As (597 ppm), and 8.277 ppm Hg. The mercury anomaly is probably due to contamination.
Sluice concentrate sample 10765 was taken in Buckeye Gulch. This sample is not anomalous in gold concentration, but shows an anomalous copper (303 ppm) and Mo (152 ppm) concentrations.
Three sluice concentrate samples (S 11277 to S 11279) were collected of gold-bearing gravel terraces on the east side of the Hammond River. Samples were collected from the south wall of a gully exposing a 30 meter (90 ft) thick gravel unit overlying a phyllite bedrock. Sample 11277 was collected from shallow pits at 6.5 meter (20 ft) intervals up gully wall. Sample 11278 was collected from a single pit 50 meters (150 ft) upstream and on the same side. Sample 11279 was located below the two other placer samples near the gravel-bedrock contact (Robert Kliefort, written communication 1999). Sample 11277 was re-calculated to 0.0008 oz/cyd. The reason assay data for gold was put it in ounces per cubic yard is because the visible gold was separated before it got sent to the laboratory (Robert Kliefort, written communication 1999). Sample 11277 contained 15 fine colors (0.0012 grams). Sample 11279 contained 4 fine colors (tiny little flakes of gold) and 2 coarse colors (0.0189 grams). The lab results are: Sample 11277 had 0.55 ppm gold and sample 11279 had 11.38 ppm gold. Calculations to add the visible gold and the 'laboratory gold' together were undertaken by BLM.

7.4 Results of rock sampling

Altogether, 163 rock samples were taken in the study area. Most of the samples were taken from veins and veinlets, some from bedrock. As a result, an anomalous area in gold and base metal concentration seems to be apparent from Smith Creek, going northward through Nolan Creek Valley, Thompson Pup and the "Fortress" into the Right Fork of Vermont Creek.

Rock samples from veins and veinlets from **Smith Creek** contain anomalous gold, arsenic, and antimony concentrations.
The highest gold concentration contains sample 10747, taken from a stibnite vein the southern side near the mouth of Smith Creek from a former stibnite pit (Workmen's Bench, Loc. 266). This sample was assayed with **12.20 ppm Au**, 295 ppm As, 15.83% Sb, and 1.049 ppm Hg. A second sample taken from this pit (S 11372) was assayed with 1804 ppb Au, 1365 ppm As, and 2000 ppm Sb.
Rock samples taken from stibnite veins on the northern side of Smith Creek near its mouth also contain anomalous gold, arsenic, and antimony concentrations and therefore follow that specific trend. Sample 11280, which is a float sample of a stibnite vein taken near a stibnite prospect was assayed with **9836 ppb Au** (visible gold), further this sample contains 924 ppm As, and 42.42% Sb.
Sample 10725, S 10726, S 11402 to S 11404 taken from stibnite veins from a small stibnite pit are also high anomalous in gold, arsenic, and antimony concentration and follow the trend.
Further upstream towards the head of Smith Creek, rock samples taken from antimony veins and veinlets exposed in bedrock also show anomalous gold, arsenic, and antimony concentrations. Sample 11164 contains 463 ppb Au, 1028 ppm As, and more than 2000 ppm Sb. Sample 11165 was taken 4 meters further upstream from a veinlet. This sample contains 1532 ppb Au, 5772 ppm As, and more than 2000 ppm Sb. Sample 11166 was taken a bit further upstream from a thin vein. It contains 1958 ppb Au, 3933 ppm As, and more than 2000 ppm Sb. It should be noted that all these described antimony veins strike roughly NE, dipping steeply.

Sample 11167 was taken at the same location as S 11166, but from a WNW striking quartz vein. This sample contains anomalous silver (1.3 ppm) and zinc (4004 ppm).

Several rock samples were taken from veins and veinlets exposed in bedrock from **Fay Creek**. Sample 11211 taken from a NW striking quartz vein near the mouth of Fay Creek contains anomalous Pb (1033 ppm), and Sb (589 ppm). Sample Nc 2 taken from a NW striking vein contains anomalous As (938 ppm). This sample was collected 100 m below the mouth of Thompson Pup. Sample 11371 was taken further upstream from a NW striking quartz vein. This sample was assayed with 167 ppb Au.

Rock sample 11215, collected from a NW striking vein in **Thompson Pup,** contains anomalous arsenic (765 ppm). Sample 11061 is a float sample of quartz which contains anomalous 3059 ppm copper. Also, sample 11208 which contains 3062 ppm Cu is a quartz float sample. Sample 11207 was collected from a NW striking quartz vein. This sample is anomalous in As (434 ppm). Sample 10647 was taken from a NW striking quartz veinlet containing low gold (186 ppb), but contains 0.35% antimony.
Two float bedrock samples were collected north of Thompson Pup.

S 11213 contains anomalous copper (4768 ppm) . S 11214 contains 683 ppm As. Sample 10649 is a quartz float sample collected north of Thompson Pup. This sample contains 372 ppm Sb.
A bedrock sample 11214 from pyrite-bearing chloritic schist in Thompson Pup contains 65 ppb Au. It is likely that this sample has been contaminated with placer gold.

Four rock samples were collected from **Smith Creek Dome**. S 10720 was collected just south of Smith Creek Dome. The sample consists of quartz muscovite schist with iron staining, ½ inch quartz veinlets, and of euhedral pyrite cubes (<5mm). This sample contains **2234 ppb gold**, 7.2 ppm silver, and 3500 ppm lead. Veinlets strike NW.

Sample 10659 taken from a 2 cm thick quartz vein in phyllites from the **"Fortress"** (north of Smith Creek Dome) shows anomalous gold and arsenic concentrations. This sample was assayed with **8301 ppb Au** and 1134 ppm As. This vein strikes NW, dipping steeply. Samples S 10663 and Nc 4 were collected in a trench south of the Fortress. These are quartz samples and both anomalous in arsenic.
S 10663 was assayed with 3035 ppm As, Nc 4 with 4760 ppm As.
Further south towards Smith Creek Dome sample 10666 was taken in a trench, from a quartz stibnite vein. Strike of vein is probably NE as the trench shows this orientation. This sample was assayed with 436 ppb Au, 297 ppm As, and 28.09% Sb. A sample taken from the same locality by BROSGÉ & REISER (1972) contained **9.2 ppm Au**.

Rock samples from veins and veinlets taken in the **Right Fork** of Vermont Creek near Friday the 13th Pup are anomalous in gold, silver, and arsenic. Grab samples S 10727 and S 10728 taken from NW striking veins contain anomalous gold concentrations (S 10727 assayed with 1585 ppb Au and S 10728 with 521 ppb Au). Sample 10729 contains anomalous silver (1.3 ppm) and lead (1657 ppm).
Sample 10730 is also a grab sample taken from NW striking quartz veins from the same location and contains high anomalies in gold, silver, and mercury. This sample was assayed with **63.56 ppm Au**, 3.9 ppm Ag, and 1.359 ppm Hg. This anomaly led to the resampling of these veins and further sampling of veins in the nearby area. The resampling of veins (S 11264 to S 11266) confirms the high anomaly of gold concentration. Sample S 11264 contains 2948 ppb Au.
Sample 11265 was assayed with 415 ppb Au and 3802 ppm As. The highest "kick" in gold from the resampling contains sample 11266 with **17.82 ppm Au** and 4.4 ppm Ag. This sample contains visible gold.
Sample 11284 was collected from NW striking quartz veinlets below previous sample location. This sample contains anomalous **26.07 ppm Au**.

The bedrock sample 11175 from pyrite-bearing schists in **Vermont Creek** contains 73 ppb Au. It is likely that this sample has been contaminated with placer gold.

Sample 11376 was collected south of the mouth of **Swift Creek** from a NW striking quartz vein. This sample is anomalous in arsenic (2127 ppm).

Rock sample 11382 taken from a NW striking quartz vein in **Gold Bottom Gulch** contains anomalous copper (506 ppm) and mercury (2.112 ppm) concentrations.

Sample 11387 was collected from a quartz vein located on the ridge between **Confederate Gulch** and **Union Gulch**. It was assayed with 591 ppm As.

Several rock samples of veins and veinlets were collected on **Midnight Dome**. Sample 11162 was collected on the eastern part of Midnight Dome from a NW striking quartz vein. This sample contains **810 ppb Au**. Sample 10703 was taken from a NE striking quartz vein in a trench on Midnight Dome, northwest of the head of Union Gulch. This sample contains 33.13% Sb and 26.468 ppm Hg. Sample 10708 was taken from a quartz veinlet near the western ridgetop of Midnight Dome. This sample is high anomalous in copper (1469 ppm) and mercury (5 ppm). Also, sample 11358 taken from a quartz veinlet set striking NE near the previous sample location was assayed with **532 ppb Au**.
Sample 11173 was collected on Midnight Dome northeast of the head of Drinking Cup Gulch. This sample was taken from a NW striking thick quartz vein and contains 291 ppb Au and 317 ppm As.
Sample 11375 was collected from NW striking quartz veinlets. This sample was assayed with 1101 ppm Sb.

7.5 Discussion of Reconnaissance Sampling

It can be argued how representative reconnaissance sampling is, especially stream sediment sampling, as assay results do not show any anomalies. As mentioned previously, problems occurred with sampling of veins and veinlets. Often, sample contamination could not be prevented.

Pan concentrate and sluice concentrate samples confirm the existence of placer gold in creeks, gulches, and benches in the Nolan-Hammond area.

Stream sediment samples taken in the Nolan-Hammond area do not show any anomalous areas in element concentrations, apart from sample 11062 (Thompson Pup), which contains 83 ppb Au. At least anomalous antimony concentrations should be expected in the Smith Creek and Archibald Creek area. BROSGÉ AND REISER (1972) describe antimony anomalies in stream sediment samples taken in the Nolan area, up to 3000 ppm Sb.
This stands in total contrast with modern assay results from 1997 and 1998. I would assume that laboratory analyses in the 70's weren't as good as modern analytical techniques. Therefore the data should be looked at with care.

It is obvious that there seem to be two different compositions of gold-bearing veins in the Nolan-Hammond area: first of all northeast striking veins and secondly northwest striking veins and veinlets.
The first gold bearing vein system is characterized by a tensional fracture filling, roughly NE striking, vein system composed of quartz-calcite-ankerite-dolomite gangue with gold, stibnite, and arsenopyrite as the principal ore minerals, and probably galena and cinnabar as accessory minerals as geochemical results indicate. Gold occurs mainly in quartz near vein margins, but is rare in stibnite. These veins

are located in the Smith Creek - Nolan area and continue northward to Thompson Pup. Veins of this type show encouraging gold values up to 12.20 ppm Au (S 10747). Within this "corridor" there seems to be a sort of zoning of antimony and arsenic. In the southern part of the Nolan area the stibnite-arsenopyrite-gold mineralization is quite common. To the north the amount of antimony decreases towards Fay Creek and Thompson Pup. The concentration of arsenic seems to increase northwards. According to HUBER (1995) quartz-stibnite-gold nuggets were common in the Thompson Pup placer gold, suggesting gold-stibnite veins to be existent in the area. Further, according to ED ARMSTRONG and ROGER BURGGRAF, Tri-con Mining Alaska/ Silverado Mines (oral communication, 1998), placer concentrates from Thompson Pup always contained a lot of arsenopyrite crystals.

Stibnite pebbles (up to 3 cm in size) were also found in placer concentrates from Archibald Creek during mining activity in summer 1998, proving the existence of this vein system to be present. Placer concentrates from Swede underground mine (located south of Archibald Creek, on the western side of Gobblers Knob) have a large amount of stibnite in them in addition to some massive hematite (MIKE BALEN, written communication 1999). This also proves the stibnite-gold vein system to be existing in the area. Bedrock geochemical data from placer drilling carried out on benches between Smith and Archibald Creek proves the existence of the stibnite vein system.

Some gold concentrates from Vermont Creek contain angular pieces of gold-bearing stibnite-quartz vein material (DENNIS STACEY, oral communication 1998) suggesting the stibnite-gold vein system to continue further northwards than expected.

According to BROSGÉ & REISER (1972), antimony anomalies in stream sediment samples on and west of Acme Creek suggest the presence of veins west of Nolan Creek placer deposits. This could not be confirmed by recent stream sediment sampling.

The second gold bearing vein system is composed of fracture filling, roughly northwest striking, quartz calcite-ankerite gangue with gold, and traces of arsenopyrite, pyrite, galena, stibnite, and marcasite. The concentration of arsenic varies, significant is the high silver concentration associated with gold in those vein systems. Gold occurs in quartz near vein margins.

These vein systems are exposed in the Right Fork of Vermont Creek, where samples taken were assayed with up to encouraging 63.56 ppm Au (S 10730). The highest gold concentrations in veins and veinlets of this type were located in the Right Fork of Vermont Creek. These vein systems were also found on Smith Creek Dome (S 10720: 2234 ppb Au, 7.2 ppm Ag, and 3500 ppm Pb), in the "Fortress" north of Smith Creek Dome (S 10659, 8301 ppb Au) and on Midnight Dome (S 11358, containing 532 ppb Au).

It should be noted that the orientation of this vein system is parallel to the strike of the most prominent joint system developed in the area. Most joints of this orientation are filled with quartz mineralization and are widespread in the area, though most of these veins are barren in gold.

Apparently gold only occurs along certain restricted parts of the veins (in "shoots"). Most of these veins show anomalous concentrations of arsenic.

As arsenic is often associated with gold in both gold-bearing veins systems, I suggest that therefore arsenic may be a useful pathfinder element.

The occurrence of two different compositions of gold-bearing veins, and the occurrence of placer deposits around or nearby auriferous veins encouraged me for further continuing investigations on gold-bearing veins and placer gold.
The results and discussion will be illustrated in the following chapters.

8. Lode Gold Mineralization

8.1 The stibnite-gold-quartz vein system

As described in previous chapters, the stibnite-gold-quartz veins are well exposed north and south of the mouth of Smith Creek in prospects and trenches; and veins can be followed further upstream. The historic importance of these veins for antimony ore is described in the introduction of this thesis report.
South of the mouth of Smith Creek, veins of this type strike approximately with 44° NE (Workmen's Bench, Loc. 266), dipping almost vertical. North of the mouth of Smith Creek (Loc. 359) veins of this type strike with 55° NE, dipping almost vertical. Veins in Smith Creek (Loc. 116 and Loc. 122) follow the 55° trend in strike.
Veins of this type vary in width, from 2 centimeters up to 15 centimeters. That corresponds with widths of these veins described by EBBLY & WRIGHT (1948) in the Nolan area.

8.1.1 Mineralization

Mineralization of these veins took place in tension fractures. After opening of joints the first stage mineralization was deposition of calcite ($CaCO_3$), ankerite ($CaFe[CO_3]_2$), and dolomite ($CaMg[CO_3]_2$) as gangue minerals. Calcite and ankerite were recognized in examining thin sections, also ankerite and the presence of small amounts of dolomite were determined by X-ray diffraction. Tiny "flakes" of hematite can be observed in microfractures within calcite and ankerite crystals. The reddish color of the carbonates relates to the presence of iron in ankerite and ironhydroxides (goethite (FeOOH), limonite (FeOOH), see Fig.25) and hematite (Fe_2O_3) in microfractures in calcite, ankerite, and dolomite. Quartz of the first stage mineralization occurs as euhedral crystals that fill cavities.

The "main-stage" mineralization of vein emplacement is represented by injection of mineralized fluids into reopened joint planes and subsequent crystallization of quartz, stibnite (Sb_2S_3), arsenopyrite (FeAsS), and gold (Au). Further, galena (PbS) and cinnabar (HgS) as accessory minerals as geochemical results indicate, though not recognized in reflected light microscopy on polished sections. Subsequent movement along existing joints reopened space that permitted crystallization of the main-stage deposition.
The mineralization consists of masses of fibrous and columnar twinned euhedral crystals of stibnite (Fig.26). "Nests" of arsenopyrite can be observed in quartz, stibnite, and wall rock (Fig.27). Some arsenopyrite crystals show concentric zonation.

Gold occurs mainly in quartz of the second stage mineralization and is rare in stibnite (Fig.28). Gold occurs as wires, dendrites, and also as crystals in the main-stage quartz and in stibnite, though crystals are rare. The grain size of gold ranges from 1 micron to 0.6 millimeters (Fig.28) up to two or three millimeters (Fig.29).

Fig.25: Photomicrograph of ironhydroxides (FeOOH) in microfractures in calcite and ankerite. Reflected light on polished surface, oil imersion, crossed-polars. Bottom edge of picture is 0.28 mm in length.

Fig.26: Photomicrograph of euhedral stibnite (antimonite) mineralization. Reflected light on polished surface, oil imersion, crossed-polars. Bottom edge of picture is 0.7 mm in length.

Fig.27: Photomicrograph of euhedral arsenopyrite crystals in quartz and surrounding wall rock. Reflected light on polished surface, crossed-polars. Bottom edge of picture is 2.8 mm in length.

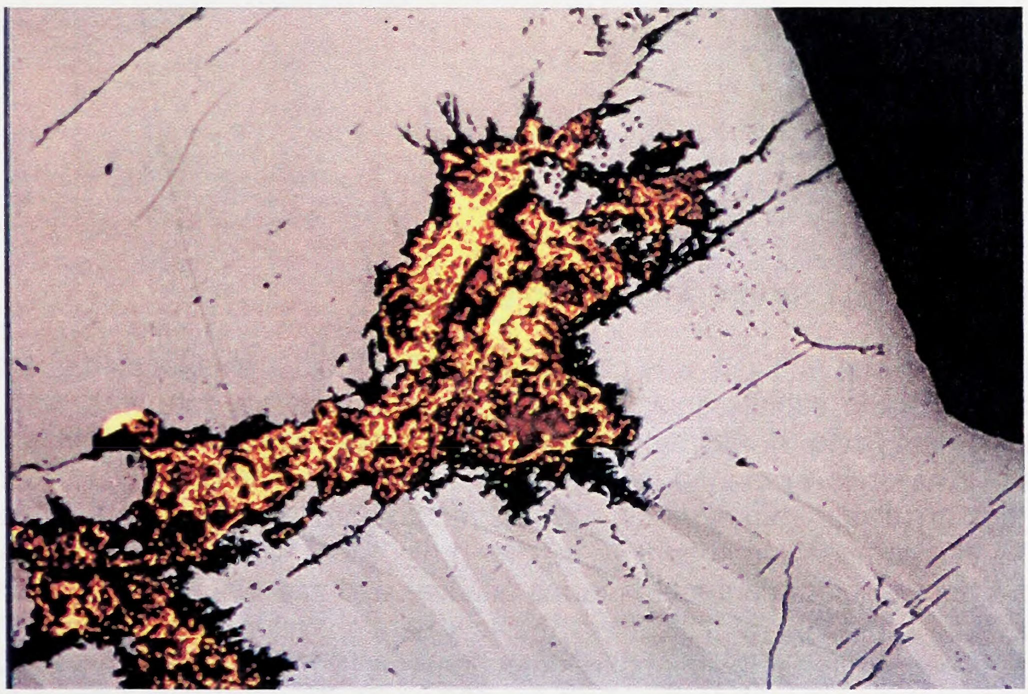

Fig.28: Photomicrograph of gold in stibnite. Reflected light on polished surface, oil imersion, crossed-polars. Bottom edge of picture is 0.7 mm in length.

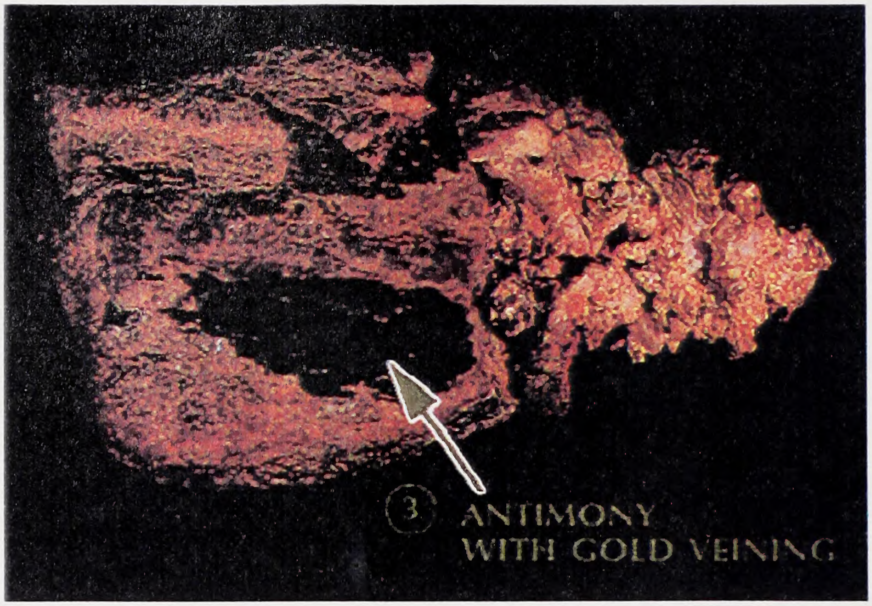

Fig.29: Antimony with gold veining. Photo enlarged to 2x of actual size. With permission from Silverado Mines Ltd.

The main-stage quartz occurs discontinuously and is finer grained than the first stage quartz.
There is no appreciable alteration of the wall rock or earlier vein material, which indicates thermal equillibrium between the wall rock and vein material (DILLON ET AL., 1989).

8.1.2 Electron microprobe analysis on gold grain

Electron microprobe analysis was carried out on four gold grains located in the main-stage quartz of the stibnite-gold vein, though representative data was only gained from one grain (Table 3). Gold analyses with analytical totals of less than 97% were discarded. The grain examined is wiry to dendritic in habit and nearly 1 millimeter in length. It is extremely homogenous, with respect to both silver and mercury contents. There is no compositional zoning in the grain, core and rim show the same composition of element contents in terms of silver and mercury (0.45% Ag and 3.3% Hg in average, Fig.30). Significant is the low concentration of silver and the high mercury concentration. Sb is above detection (ca.100 ppm) whereas Bi was not detected by microprobe (detection limit ca. 100 ppm). The calculated "true" fineness for this grain is 995, which is very high. "True fineness" is the ratio of gold to gold plus silver multiplied by 1000 (BOYLE, 1979; p.197).True fineness = (Au / (Au+Ag)) x 1000.

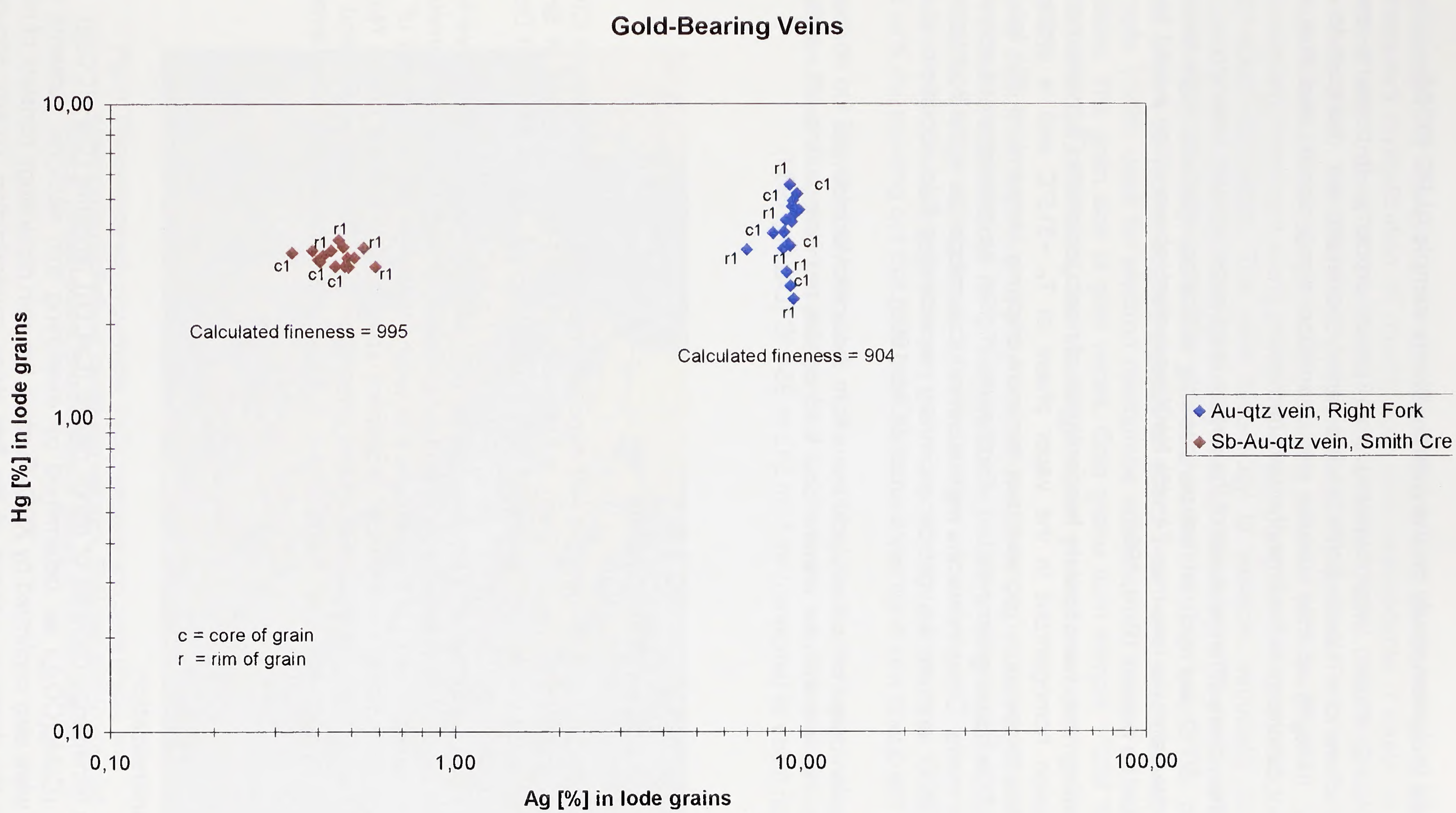

Fig.30: Compositions of vein gold from Smith Creek and the Right Fork.

8.1.3 Fluid inclusion study on the quartz stibnite sample ALRC #3384

Sample (ALRC #3384) was collected from Nolan property. It contains many inclusions of various sizes. Some of the larger inclusions are deduced to be secondary, because of their shapes and orientation along planes, and thus not indicative of conditions at the time of quartz formation.

Inclusion from three different areas of the section were super-cooled between -60°C and -80°C, but did not freeze, possibly indicating relatively high salinity. However, the salinity is less than 24 wt% NaCl equivalent, above which a solid halite phase would be present (BOM, 1995)

During heating runs, two separate temperatures of homogenization (T_h) were noted. One inclusion homogenized in the vapor phase at T_h ~315°C and is probably primary; this temperature represents a minimum trapping temperature (T_t) for the inclusion. True trapping temperature is somewhat higher; no corrections of pressure have been made. Other inclusions were observed to homogenize in the liquid phase at T_h ~ 224°C, and are thought be secondary, representing fluid conditions at the time after the quartz was originally formed (BOM, 1995).

Fluid inclusion-data from stibnite gold veins from Sukapak Mountain (25 km northeast of Nolan) indicate that the mineralizing fluid crystallized from boiling (?) carbon-dioxide-rich fluids at temperatures from 212 to 254 °C (DILLON, 1989).

8.2 The gold-quartz vein system

Fracture filling gold-quartz veins are well exposed in the Right Fork of Vermont Creek (located around Friday the 13th Pup), further within the "Fortress" (north of Smith Creek Dome), on the southern flank of Smith Creek Dome, and on Midnight Dome (Geologic map, Appendix 1).
Veins of this type strike with an average of 120° NW-SE, dipping almost vertical. Width varies from 1 millimeter to 1 centimeter (veinlets) and up to a few centimeters. Most of these veins are up 2 centimeters in width. Note that the orientation of this vein system is parallel to the most prominent striking joint system in the Nolan-Hammond area. Most of the joints of this orientation are filled with quartz and are widespread through the area, though most of these veins and veinlets are barren in gold.

8.2.1 Mineralization

The vein mineralogy consists of minor calcite ($CaCO_3$), ankerite ($CaFe[CO_3]_2$), and dolomite ($CaMg[CO_3]_2$) as determined by examining thin sections. Ankerite and dolomite were also confirmed by XRD. Further, the vein mineralogy consists of major quartz as the dominant gangue of the first stage mineralization. Quartz occurs as cavity filling crystals. The second stage mineralization (main-stage mineralization) is

represented by injection of mineralized fluids into reopened joint planes with subsequent crystallization of quartz, gold (Au), arsenopyrite (FeAsS, in changing amount) and traces of pyrite (FeS_2), marcasite (FeS_2), chalcopyrite ($CuFeS_2$), pyrrhotite (FeS), hematite (Fe_2O_3), sphalerite (ZnS), galena (PbS), and rutile (TiO_2). These minerals were recognized in examining polished sections (Fig.31).
Subsequent movement along joints reopened space, permitting crystallization of the main-stage deposition. The vein mineralogy is variable, especially in terms of accessory vein minerals. Stibnite is very rare in these veins. The main-stage quartz occurs discontinuously and is finer grained than the first stage quartz.
Gold occurs as (sharp edged) crystals in quartz near vein margins (visible gold in sample 11266, used for electron microprobe analysis) and is also associated with sulfides. The grain size of gold varies. Gold grains from sample 11266 have sizes from 0.5 to 0.8 millimeters, but also bigger sized grains have been reported (Fig.32 and 33).
Assay data from these veins show anomalous silver (Ag) concentrations. This may be related to argentiferous ($(Cu,Fe, Ag)_{12}Sb_4S_{13}$) which occurs along with galena and sphalerite, though not confirmed by reflected light microscopy.
Electron microprobe analysis carried out on a gold grain from sample 11266 detected 9.2 wt% Au, pointing out that gold itself contains silver.

There is no appreciable alteration of the wall rock or earlier vein material, which indicates thermal equillibrium between the wall rock and vein material (DILLON, 1989).

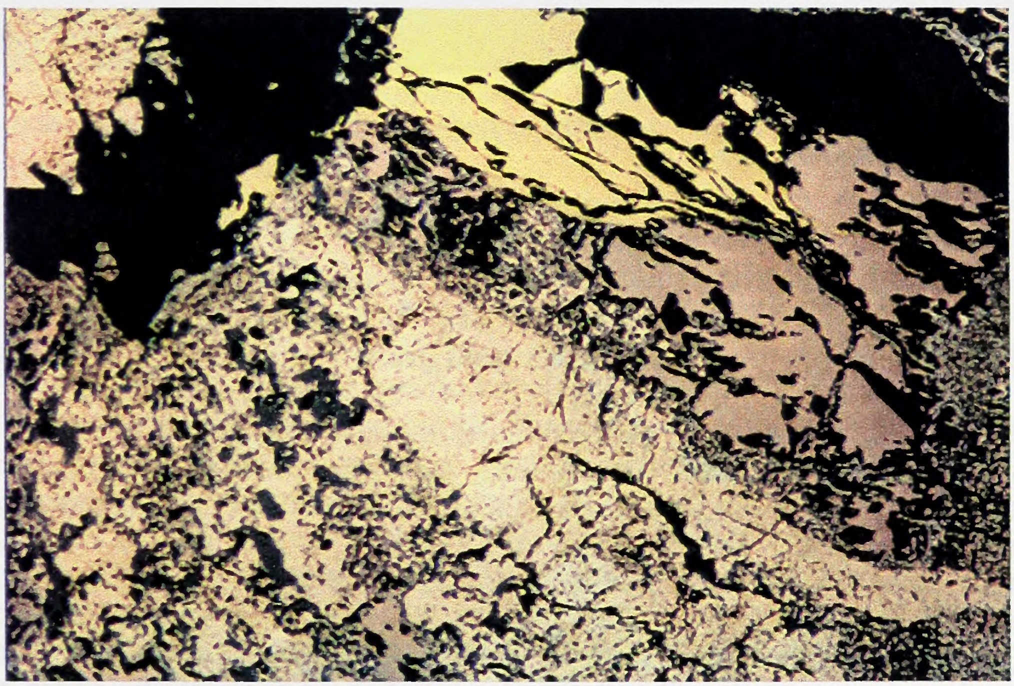

Fig.31: Photomicrograph of pyrrhotite (FeS), marcasite and pyrite (FeS_2), and chalcopyrite ($CuFeS_2$) in quartz and wall rock. Reflected light on polished surface, crossed-polars. Bottom edge of picture is 1.4 mm in length.

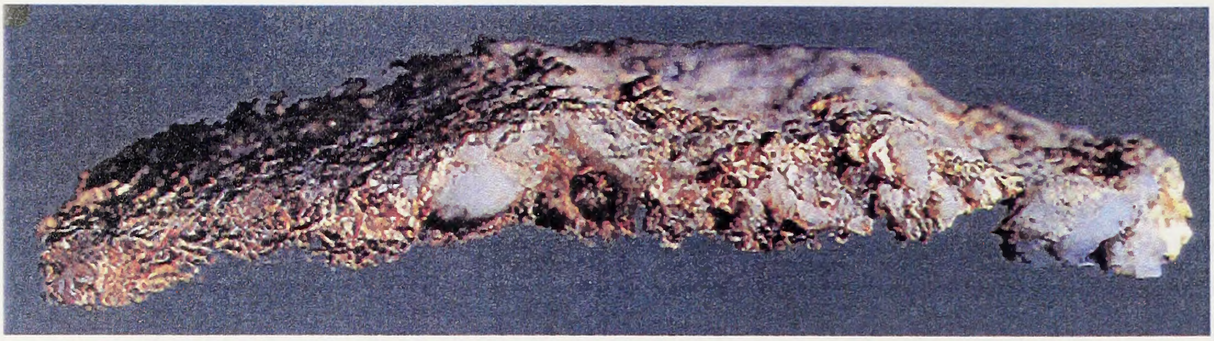

Fig.32: Quartz with gold. Photo enlarged to 2x of actual size. With permission from Silverado Mines Ltd.

Fig.33: Quartz with gold veining. Photo enlarged to 4x of actual size. With permission from Silverado Mines Ltd.

8.2.2 Electron microprobe analysis on gold grain

Sample 11266 contained two gold crystals, though one got lost during sample preparation. Therefore, electron microprobe analysis was carried out on one gold grain located in the main-stage quartz (Table 3). This grain is 0.6 millimeters in length and crystalline in habit.

There is no evidence for silver compositional zoning in the grain (Fig.30). Core and rim show the same average concentration (9.215% Ag in core; 9.327% Ag in rim). Further, there is no evidence for mercury compositional zoning in the grain. Core and rim show changing contents within themselves, but show basically the same average content (4.041% Hg in core; 4.632% Hg in rim). The high silver concentration is significant. Sb is below detection (interference from Au L-Xrays). The apparent Te content of the gold from this vein is at the same level than the gold from the stibnite-gold vein. No Bi was detected by microprobe (detection limit ca. 100 ppm). The calculated "true" fineness for this grain is 904, which is much lower than the grain examined from the stibnite-gold vein.

8.2.3 Fluid inclusion studies

Fluid inclusion work on NW striking veins with equal mineralization was carried out in the Chandalar mining district by ROSE, PICKTHORN, AND GOLDFARB (1987); at the Little Squaw Mines in the Chandalar mining district by ASHWORTH (1983); and on Sukapak Mountain in the Koyukuk mining district by DILLON ET AL. (1989). Their fluid inclusion work suggests that these veins were formed at temperatures of 300°C from a hydrothermal solution containing 4 to 5 % NaCl with 1 to 4% CO_2 and CH_4. Depth estimated from fluid inclusion are complicated by the presence of four phase fluids and range from 5 to 10 Kb (HUBER, 1995).

9. Placer Gold

Placer gold (nuggets) was taken from several creeks in the study area by gold panning and bucket sampling of stream sediments from plunge pools in creeks. Also, placer gold was taken from benches (bench placer) and buried channel gravels (Swede underground). All placer gold was taken from Tri-con Mining / Silverado Mines mining leases.

9.1 Smith Creek Placer

Six grains were examined from Smith Creek. The sample location is marked as P1 on the Sample Location map (Appendix 3). Grains are 2 to 3 millimeters in size, rounded to flattened with some coarse (crystalline) edges. Two grains have quartz fragments attached to them.
Grain 6 (Fig.34, Table 3) contains high Ag concentration. The core contains 7.35% Ag, and rim contains 7.42% Ag in average. As core and rim have the same Ag concentration there is no evidence for silver compositional zoning within the grain. The mercury content depletes from core (3.8% Hg) to rim (2.4% Hg). This grain also contains 0.043 % Te.
Grain 1 to 5 are low in silver concentration (1.4% to 3.5% Ag in range). Grain 2 shows depletion in Au from core to rim. The core contains 97.36% Au whereas the rim contains 94.94% Au in average. Further, within grain 2 the mercury content increases from core to rim . The core contains 1.01% Hg, whereas the rim contains 3.49% Hg in average. Grain 4 shows the same phenomena, depletion in Au from core to rim (97.08% Au in core to 94.58% Au in rim in average) and rise in mercury content from core to rim (0.84% Hg in core to 3.14% Hg in rim in average). Grain 3 contains 0.035% Sb. Bi was not detected by microprobe analysis.

Placer gold from Smith Creek seems to belong to two different populations of gold (Fig.34). The first population is characterized by its low silver content (1.4% to 3.5% Ag in average) and the second population by its high silver content (7.38% Ag). This corresponds with the two different populations of gold from the two different vein systems. Fineness of grains is presented in Figure 34. Population 1 (grain 1 to 5) has an average calculated fineness of 963, whereas population 2 (grain 6) has a calculated fineness of 925.

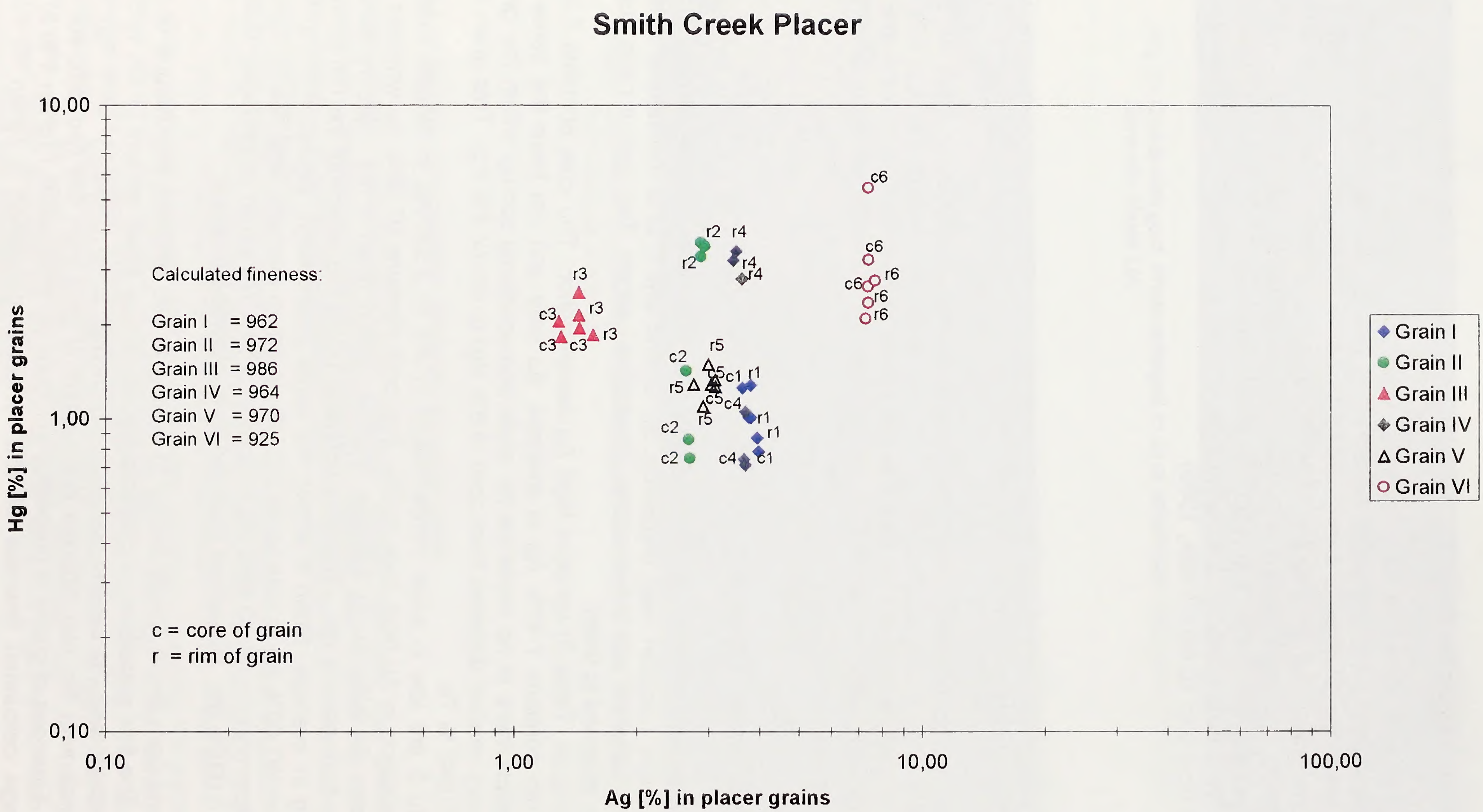

Fig.34: Compositions of placer gold grains from Smith Creek.

9.2 Swede Underground Placer

Three grains were examined from Swede channel (underground placer mine, leading into the hillside of Gobblers Knob). According to MIKE BALEN (written communication, 1999) the channel appears to have been glacially carved. The entire placer gold deposit was emplaced as a result of mass wasting processes (MIKE BALEN, written communication 1999). Sample location is marked as P2 on the Sample Location map (Appendix 3).
The grains are approximately 2 millimeters in size and rounded to flattened.
Grain 1 and 2 contain high silver concentrations (Fig.35). Grain 1 has an average silver content of 10.58%. Grain 2 has an average silver content of 10.20% Ag. There is no evidence for silver compositional zoning in both grains. In grain 1 the mercury content increases from core to rim. The core contains 1.42% Hg whereas the rim contains 2.92% Hg in average.
Grain 3 contains low silver concentration (2.20% Ag in average). There is also no evidence for silver compositional zoning in this grain. In all three grains, Sb and Te are below detection limit. Bi was not detected by electron microprobe analysis.

Swede underground placer contains two populations of placer gold (Fig.35). The first population is characterized by its low silver content (grain 3, 2.20% Ag), whereas the second population is therefore characterized by its high silver content (grains 1 and 2 contain 10.34% Ag in average). This corresponds with the two different populations of gold from the two different vein systems. Due to the remarkable difference in silver concentration, the fineness of placer grains of the two populations is different. Whereas grain 1 and 2 have calculated fineness of 893 and 897, grain 3 has a calculated fineness of 977.

9.3 Archibald Creek Placer

Two grains were microprobed from Archibald Creek. Sample location is marked as P3 on the Sample Location map (Appendix 3). Grain 1 is round and flattened, and 5 millimeters in diameter. Grain 2 is approximately 3 millimeters in length, crystalline with rounded edges and has a quartz crystal attached to it. Grain 2 seems to have been derived from a nearby vein as the grain itself is still crystalline in habit and attached to vein quartz.
Both grains are low in silver concentration. Grain 1 contains average 3.45% Ag, grain 2 contains 2.63% Ag in average (Fig.36). There is no evidence for silver compositional zoning (core to rim) within both grains. The mercury concentration does not seem to vary from core to rim in both of them and is therefore stable. Te is below detection limit (interference from Au L-Xrays). Grain 1 contains an average of 0.015% Sb. No Bi was detected by electron microprobe analysis.

Both grains belong to the same population which is characterized by its low silver concentration (Fig.36). Therefore these grains are of the same population as the low silver grain from Swede underground and the five grains from Smith Creek. Grain 1 has a calculated fineness of 965 and grain 2 of 973.

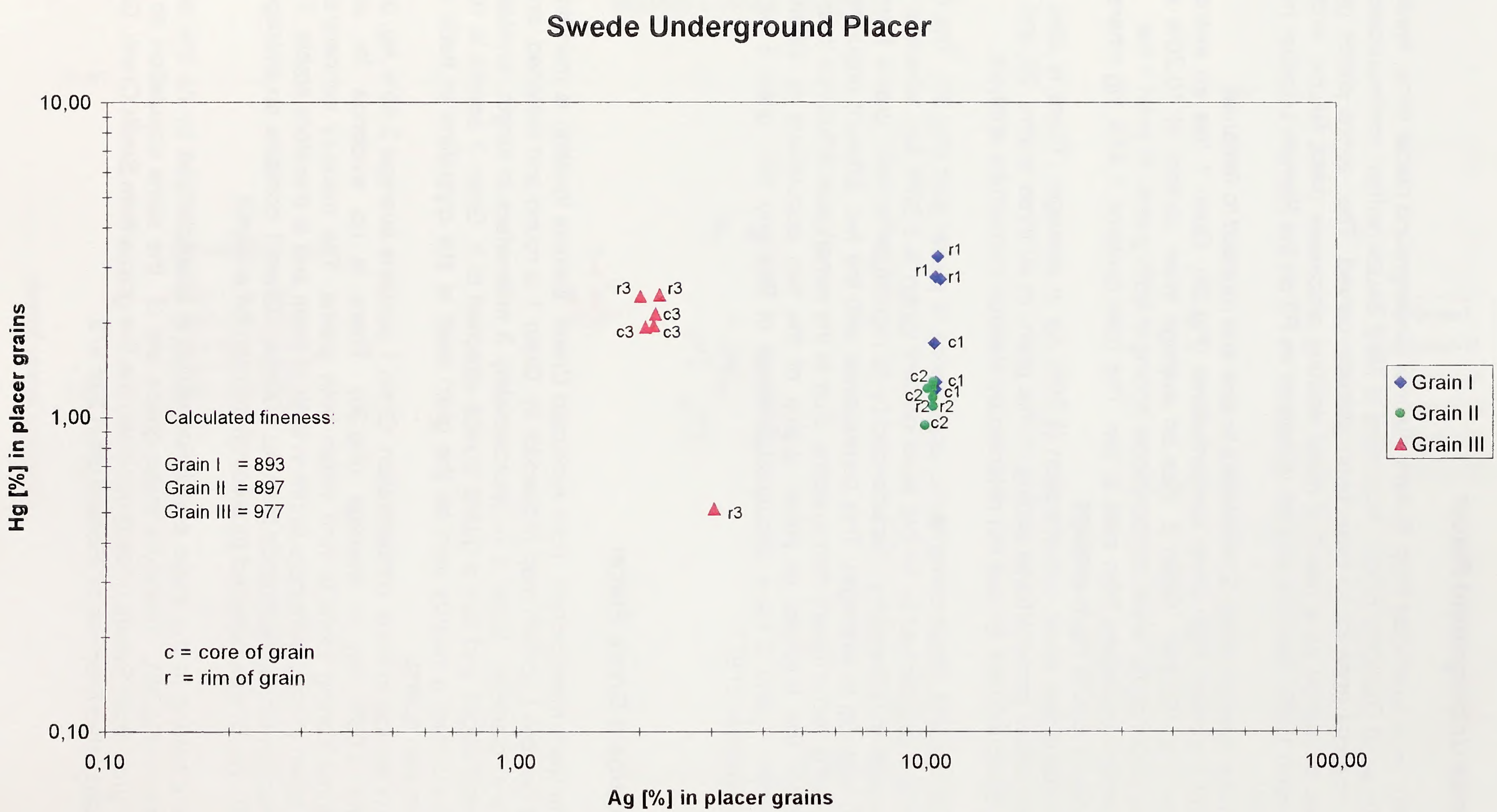

Fig.35: Compositions of placer gold grains from Swede Underground.

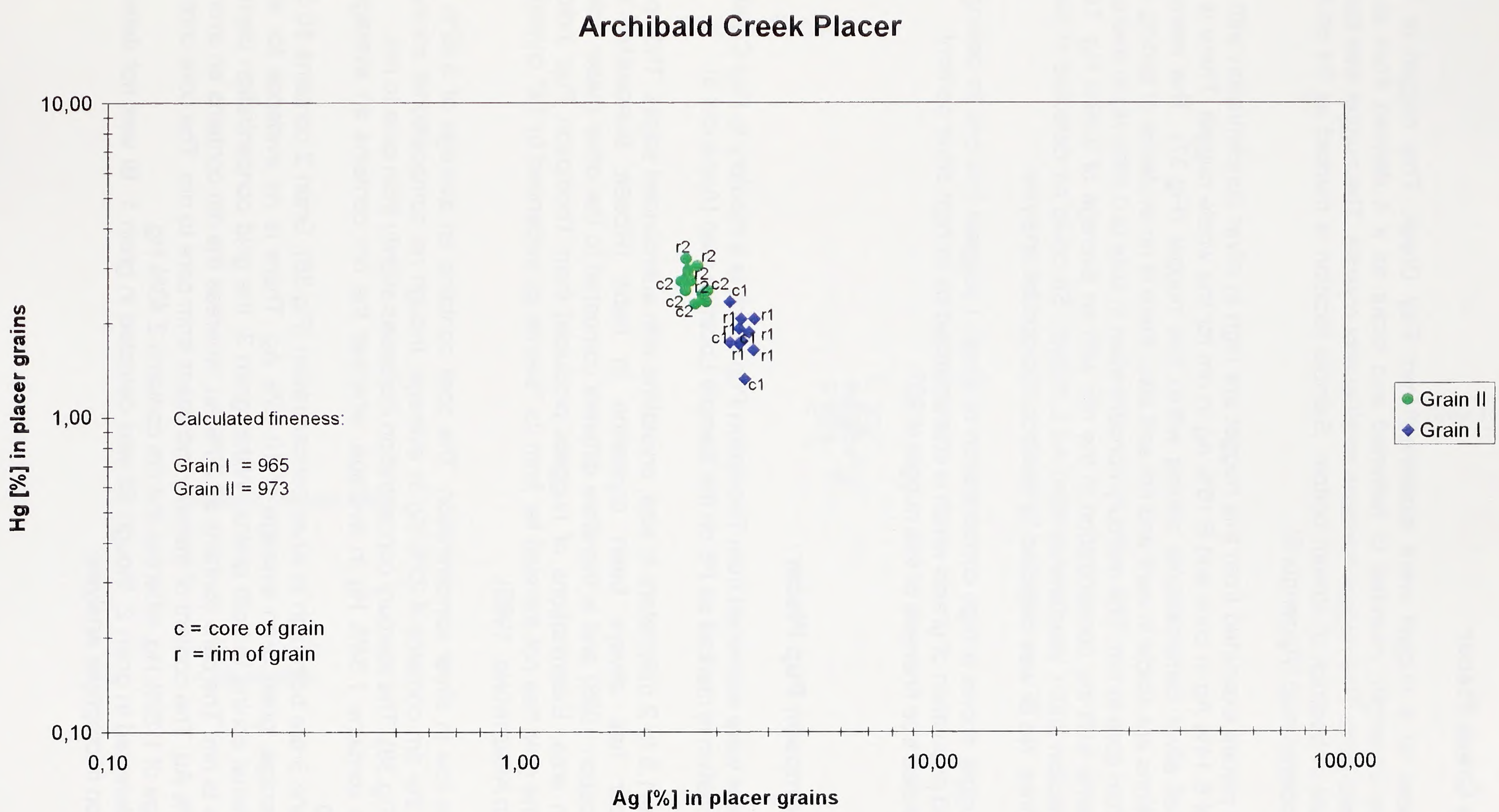

Fig.36: Compositions of placer gold grains from Archibald Creek.

9.4 Fay Creek Placer

Three pieces of a nugget were examined from Fay Creek. This nugget is 1.5 centimeters in length, rounded to flattened and looks as if it derived from stuck together wire gold. This nugget contains small quartz crystals. The nugget was found in a fracture in bedrock of stream bottom. Sample location is marked as P4 on the Sample Location map (Appendix 3).

The three pieces examined from this nugget are high in silver concentration with an average of 6.14% Ag in core and 6.18% Ag in rim for the whole nugget. There is no evidence of silver compositional zoning within this nugget (Fig.37). The mercury concentrations are stable in core and rim and also, there is no evidence of zoning of mercury from core to rim. The mercury concentration in core is 0.99% Hg in average, it is the same with the concentration in the rim with an average of 0.99% Hg. Te is below detection limit (interference from Au L-Xrays). Sb could be detected in piece two and three. No Bi was detected by electron microprobe analysis.

As this nugget shows a high concentration of silver, I suggest this one to belong to the second population of grains which is characterized by its high silver content.
The calculated true fineness of this nugget is 937.

9.5 Thompson Pup Placer

Three grains were examined from Thompson Pup which is a tributary to Fay Creek. Sample location is marked as P5 on the Sample Location map (Appendix 3).

Grains are 1.5 to 2 millimeters in size, crystalline with subrounded edges. Thompson Pup placer has always been crystalline in habit (Roger Burggraf, oral communication 1998) and is therefore different compared to the other placer gold in the Nolan area. Examinations of nuggets produced from Thompson Pup indicate some of the gold has not traveled far from its "source as evidenced by its" crystalline nature (Ed Armstrong, 1985).

Grain 1 is low in silver concentration. The core contains an average of 3.92% Ag, whereas the rim contains 4.22% Ag in average, though no compositional zoning is evident (Fig.38). The mercury concentration increases slightly from core to rim.
The core contains 1.34% Hg in average, whereas the rim contains an average of 1.80% Hg.
Grain 2 and 3 are both high in silver concentration (Fig.38). Grain 2 contains 10.50% Ag in average, grain 3 an average of 10.45% Ag. There is no evidence for silver compositional zoning in both grains. Within grain 3, the gold concentration depletes from core to rim. The core contains 89.20% Au, whereas the rim contains an average of 86.62% Au. The content of mercury increases from core to rim. The core contains an average of 1.26% Hg, whereas the rim contains 2.43% Hg.
Te was detected in grain 2, though Sb was detected in grain 1. Bi was not detected by electron microprobe analysis.

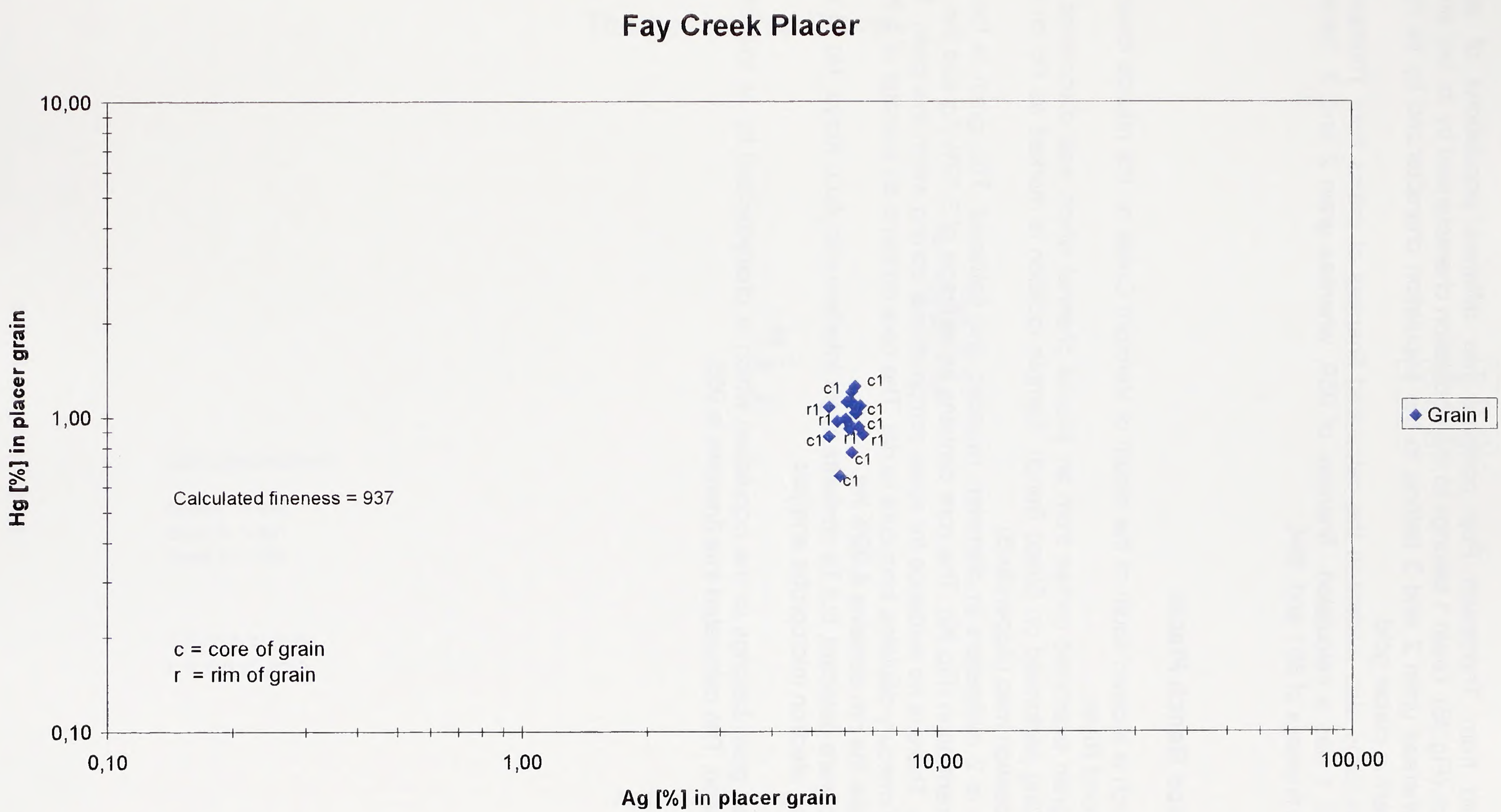

Fig.37: Composition of placer gold nugget from Fay Creek.

Placer gold from Thompson Pup contains two different populations of gold composition (Fig.38). Grain 1 belongs to the population characterized by its low silver content, whereas grain 2 and 3 belong to the population characterized by its high silver content in placer gold.
The difference is also evident in the calculated fineness of grains from Thompson Pup. Grain 1 has a calculated fineness of 959, whereas grain 2 and 3 have a calculated fineness of 891 and 894.

9.6 Slisco Bench Placer

Slisco Bench is located south of the mouth of Vermont Creek on the hillside towards the Hammond River.
The one grain examined comes from an alluvial channel which was discovered by placer drilling performed on Slisco Bench. Sample location is marked as P6 on the Sample Location map (Appendix 3).
The grain is 2 millimeters in diameter, rounded and flattened. This grain is low in silver concentration (Fig.39). The core contains an average of 3.19% Ag and the rim 3.22% Ag. There is no evidence for silver compositional zoning within this grain. The content of mercury depletes from core to rim. The core contains an average of 5.80% Hg, whereas the rim contains 4.99% Hg.
Te and Sb were detected, but Te contents might interfere with Au L-Xrays. No Bi was detected by electron microprobe analysis.

This placer grain belongs to the population which is characterized by its low silver concentration. The calculated true fineness is 966.

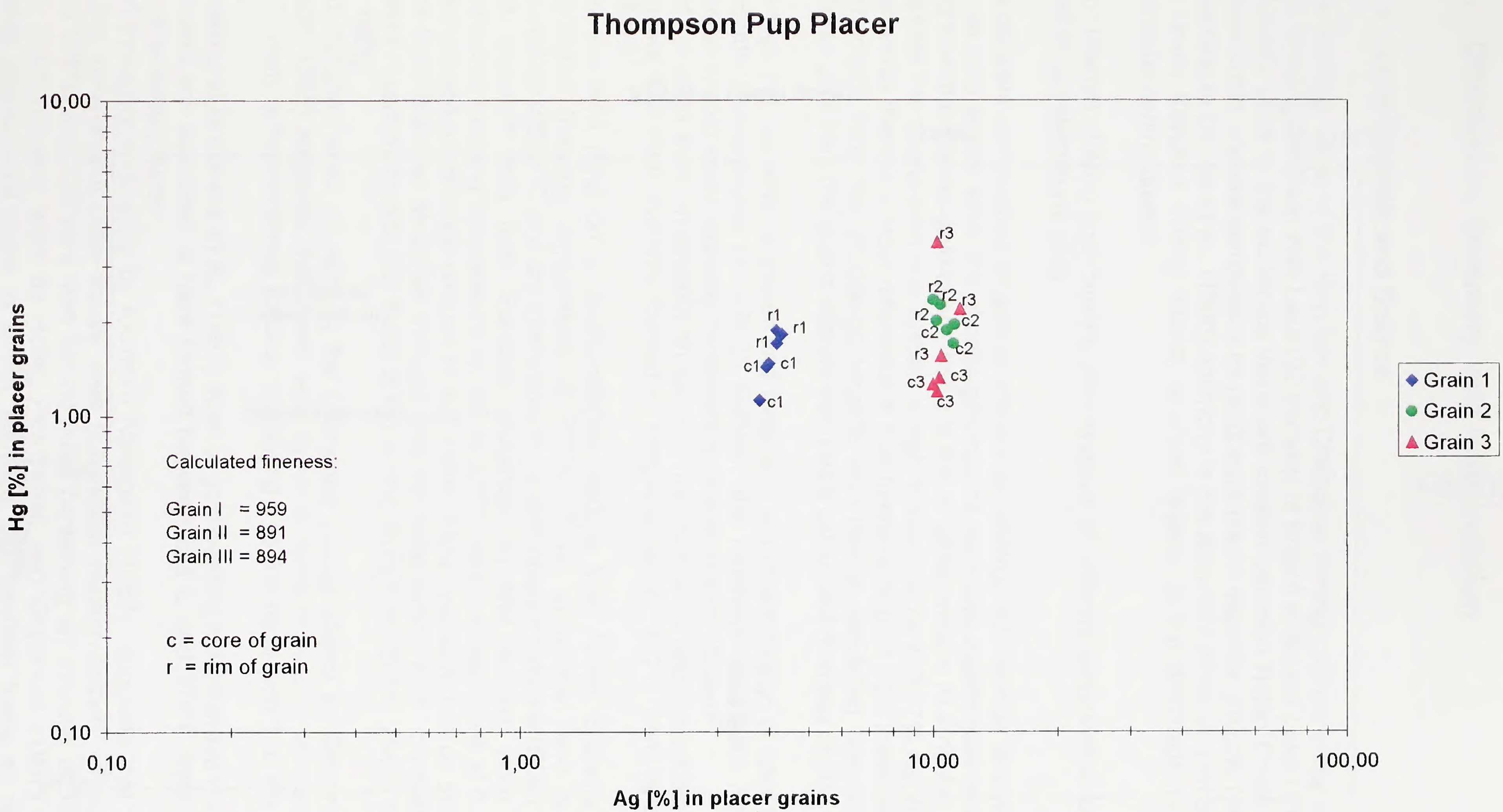

Fig.38: Compositions of placer gold grains from Thompson Pup.

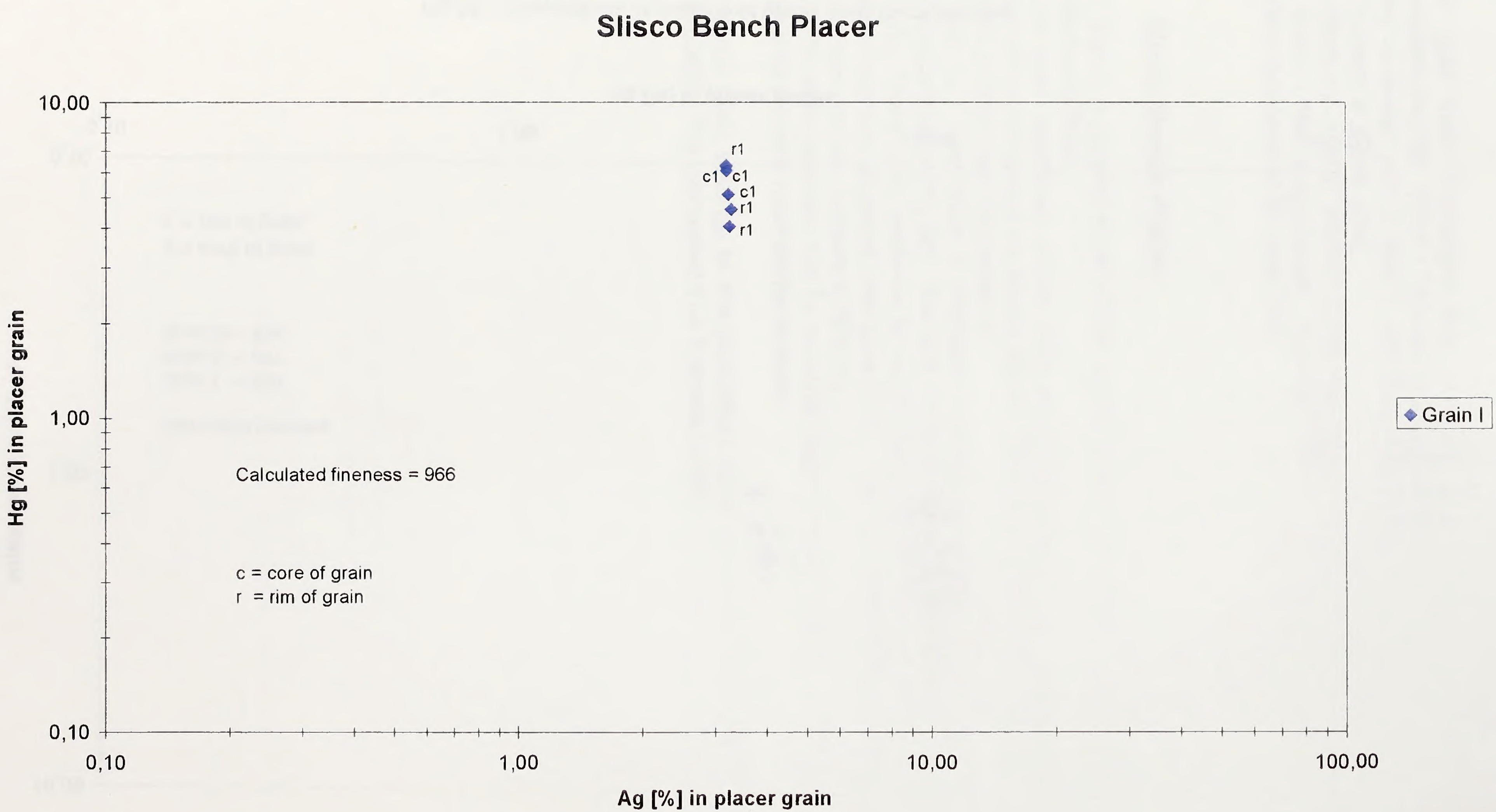

Fig.39: Composition of placer gold grain from Slisco Bench.

10. Discussion, Summary, and Interpretation

10.1 Lode Deposit and Source

Gold-bearing veins of the Koyukuk and Chandalar mining districts occur in an east-west-trending belt from Wild Lake (92 km west of Nolan) to Squaw Lake (100 km east of Nolan). Most of the auriferous veins are located between Nolan Creek and Little Squaw Creek and are surrounded by productive placer deposits (DILLON,1989).
According to DILLON ET AL. (1989) antimony is the dominant metal in vein deposits of the Upper Koyukuk mining district, whereas arsenic is the dominant metal in the Chandalar mining district.

Two different striking gold-bearing vein systems of different composition are located in the Nolan-Hammond area.

The different composition of gold is proven by electron microprobe analysis carried out on gold grains from the stibnite-gold-quartz vein and quartz-gold vein system. Gold from the stibnite-gold-quartz veins is low in silver content (0.45% Ag), whereas gold from the quartz-gold vein system is high in silver content (9.27% Ag) (Fig.30). In other words there is a clear difference in true fineness of gold from these veins. Gold microprobed from the stibnite-gold-quartz vein has a calculated fineness of 994, whereas gold from the quartz-stibnite vein has a calculated fineness of 904.

The high Hg contents of placer and lode gold are characteristic of gold formed at moderate temperatures (< 300°C). Further, the relatively consistent Ag and Hg contents in gold imply relatively consistent hydrothermal conditions.
Fluid inclusion work undertaken on veins in the study area and surrounding districts suggests that both systems formed at temperatures of 300°C from hydrothermal solutions.
Fluid inclusion data on a quartz-stibnite sample from Nolan property give an uncorrected trapping temperature of 315°C. Other inclusions have a trapping temperature of 224°C and are interpreted to be secondary inclusions (BOM, 1995).
Fluid inclusion data from Sukapak Mountain on NW striking veins give an uncorrected trapping temperature of 199 to 293°C and a composition of 6.5 percent by weight sodium chloride (DILLON ET AL., 1989). Fluid inclusion data on stibnite gold veins from Sukapak Mountain indicate that the mineralizing fluid crystallized from boiling (?) carbon-dioxide-rich fluids at the temperature from 212 to 254°C (DILLON ET AL., 1989).
Fluid inclusion work on veins in the Chandalar mining district by GOLDFARB (after HUBER, 1995) suggests that these vein systems were formed at temperatures of 300°C from a hydrothermal solution containing 4 to 5% NaCl with 1 to 4% CO_2 and CH_4.
According to GOLDFARB ET AL. (1997) most of gold-bearing mesothermal quartz veins in Alaska are estimated to have formed between 225°C and 375°C from the H_2O-CO_2, low-salinity fluids.
Fluid inclusion work done by KATHRYN ASHWORTH (1983) suggests that the gold-bearing veins in the Little Squaw area (Chandalar mining district) crystallized at about 275°C and 825 bars from boiling fluids containing an average of 18 mole % CO_2. Fluid inclusion work by ROSE, PICKTHORN, AND GOLDFARB (1987) identified variable gas-to-liquid ratios in similar samples, but interpret these as secondary

inclusions formed by necking down (ROEDDER, 1984) of former primary inclusions. They did not see any evidence for trapping of immiscible fluids or boiling.

It is this author's personal interpretation that the roughly NW striking quartz-gold vein system was formed from mesothermal solutions at a temperature of 250 to 300°C. The roughly NE striking stibnite-gold veins may have formed at a lower temperature, possibly around 200 to 250°C. Therefore, I interpret the stibnite gold vein system to be the younger one in age and to be the last gasp of the mineralizing system. This corresponds with fluid inclusion data on stibnite-gold veins from Sukapak Mountain as described above. The stibnite-gold veins may present the "borderline" from a mesothermal system to an epithermal system.
According to EVANS (1993), stibnite is a characteristic ore mineral of epithermal deposits.
Temperature of mineralization is below that of peak greenschist-facies metamorphism (M_3). This suggests that mineralization of veins took place during cooling from regional metamorphism.

Transport and Deposition Model:

Two possibilities of transport and deposition of gold can be suggested for the Nolan-Hammond area.

Model 1: The Bisulfide Complex $Au(HS)^-_2$ System

The low salinity, near neutral to slightly alkaline fluids, combined with the ore element association, high gold to base metal ratios, and intimate association of gold with iron sulfides all suggest reduced sulfur complexes (e.g. $HAu[HS]_2$) as the gold transporting agent (e.g. PHILLIPS AND GROVES, 1983). Temperatures in this zone range from 200 to 300°C, but average around 240°C. It is obvious that auriferous H_2O-CO_2, low salinity fluids were channeled up shear zones after post peak metamorphism (M_3). Temperature of mineralization is below that of peak greenschist-facies metamorphism (M_3). This suggests that mineralization of veins took place during cooling from regional metamorphism. Sulfidation reactions between hydrothermal fluids and wall rock destabilized gold-reduced sulfur complexes causing gold precipitation. There is no appreciable alteration of the wall rock or earlier vein material, which indicates thermal equilibrium between the wall rock and vein material (DILLON ET AL., 1989).
In low temperature hydrothermal precious metal deposits, there is a characteristic change in mineralogy over the vertical sequence.
The first stage of deposition of ore in NW striking fractures in the Nolan-Hammond area is therefore characterized by gold and arsenopyrite mineralization as the principal ore minerals and pyrite, marcasite, chalcopyrite, pyrrhotite, hematite, sphalerite, galena, and rutile as accessory minerals. Stibnite is rare in this system. Deposition of Au from solutions containing $Au(HS)_2^-$ complexes will occur in response to changes in temperature, pressure, pH, oxidation potential of the system, and total sulfur concentration (ASHWORTH, 1983). Decreasing temperature leads to deposition of gold and associated sulfides.
The second stage of deposition is characterized by lower temperature (200 to 250°C) mineralization of gold, stibnite, and arsenopyrite as the dominant ore minerals, and

galena as accessory mineral. Mineralization took place in NE striking tensional fractures. Subsequent movement along existing fractures reopened space, permitting crystallization of the second stage deposition.

This differentiation of mineralization is also reported by ROBINSON AND BUNDTZEN (1982) from the Scrafford Mine in the Fairbanks Mining district. Their data indicate that stibnite-gold mineralization may be a higher level expression of underlying gold-quartz vein mineralization.

Both vein systems in the Nolan-Hammond area underwent each at least two phases of mineralization, first stage and "main" stage mineralization.

As described in previous chapters, most veins in the Nolan-Hammond area are barren of gold. Gold seems only to occur in "shoots". A possible explanation which might control the location of shoots is that veins often cross cut graphite-rich and pyritic schists and phyllites. These are favorable for precipitation of gold from hydrothermal solutions. This might explain the anomaly of 63 ppb Au in pyritic schist in Vermont Creek (note that the anomaly may also be related to placer contamination as that particular sample was taken from bedrock in a mine site). It is also possible that gold is associated with, or related to arsenopyrite in veins.

The presence of stibnite in veins suggests that also antimony-complexes may have transported some gold in the hydrothermal fluids.

Model 2: The Au-Sb-S System

The two populations of gold may represent slightly different environments of formation in the Au-Sb-S system. NEKRASOV (1996) describes Au-Sb-S systems from metamorphic quartz-gold veins in northeast Russia.

In a low temperature, Sb-rich and Bi-poor hydrothermal system, aurostibite ($AuSb_2$) would be the first antimony mineral deposited. Aurostibite was not detected in reflected light and has not been reported from gold veins in the Brooks Range though. NEKRASOV (1996) describes the parageneses of berthierite and antimonite with gold and aurostibite. Deposition of low-grade gold (650-740) of an early generation precedes crystallization of antimonite and berthierite. The early gold has been segregated in the veins together with quartz and with pyrite and arsenopyrite. In the Nolan-Hammond area stibnite is rarely developed in the "older" gold-quartz veins, but pyrite and arsenopyrite are present. Note that fineness of gold from this vein system is 904, therefore it cannot be connected to the low-grade gold.

The high-grade gold of the second generation was either deposited together with antimonite, or is a decomposition of aurostibite (NEKRASOV, 1996). However, aurostibite is unstable and dissociates in Au + Sb_2S_3 (low Ag-group) as well as Au-Ag (higher Ag group) + Sb_2S_3 (RAINER NEWBERRY, written communication 1999). This might explain why aurostibite was not detected by reflected light. The dissociation in a low Ag and higher Ag-group totally corresponds with electron microprobe results of the two different compositional gold-bearing vein systems. The fact that a few of the microprobe analyses seem to indicate anomalous Sb in the low-Ag gold is compatible with this model, as is the common presence of both types in a single placer. There is absolutely no evidence that the differences in Ag content reflect any sort of leaching process.

Studies undertaken by NEKRASOV (1996) about the dependence of the composition of parageneses containing aurostibite on pH of solutions and H_2S activity in them suggest that with decreasing pH (neutral solutions) aurostibite is replaced by gold and antimonite paragenesis. According to his studies the stability field of aurostibite is narrow even in an intensely reducing environment. This phenomena is in satisfactory agreement with the relatively rare find of this mineral in gold-antimony ores. Further, NEKRASOV (1996) mentions that deposition of gold and antimonite in gold-antimony ores occurred at different times. In the background of decreasing pH of solutions and increasing aH_2S in them, gold crystallization commences initially. This is followed possibly by simultaneous deposition of Au + Sb_2S_3. The formation of massive, essentially stibnite ores, often barren with respect to gold, occurs only thereafter. This might explain why gold is rare in stibnite and occurs in quartz and "borderline" between quartz and stibnite in the Nolan-Hammond area.

Both gold transport mechanisms have the right to be responsible for gold mineralization in the Nolan-Hammond area, and probably occurred together in hydrothermal fluids that were responsible for establishing the two gold vein systems. However, the Au-Sb-S system seems more likely to be responsible for gold mineralization in the Nolan-Hammond area.
It is obvious that auriferous H_2O-CO_2, low salinity fluids were channeled up shear zones after post peak metamorphism (M_3), probably during uplift. Temperature of mineralization is below that of peak greenschist-facies metamorphism (M_3). This suggests that mineralization of veins took place during cooling from regional metamorphism. There is no appreciable alteration of the wall rock or earlier vein material, which indicates thermal equilibrium between the wall rock and vein material (DILLON ET AL., 1989).

Many theories have been developed to explain the origin of metamorphic fluids for the southern Brooks Range. As described in Chapters 3.5 and 5, the southern Brooks Range underwent regional high-pressure — low-temperature metamorphism in the Late Jurassic and Early Cretaceous following obduction of allochthonous oceanic crust (DUSEL-BACON, 1994). Vein-forming fluids were certainly not products of the regional metamorphic event (GOLDFARB ET AL., 1997). A study undertaken by PATRICK ET AL. (1994) suggests that at about 110 Ma warmer rocks from the core of the Brooks Range were thrust over the now widely exposed high-pressure — low-temperature sedimentary rocks. If this occurred throughout the southern Brooks Range, then large prograde fluid volumes required for hydrothermal ore formation could have been released during synkinematic footwall heating (GOLDFARB ET AL., 1997). ROSE ET AL. (1987) suggest a hydraulic fracturing model for the formation of the gold lodes. Rapid uplift due to tectonic unloading results in a decrease in lithostatic pressure. When the fluid pressure exceeds confining pressure, hydraulic fracturing and the release of metamorphic fluids will occur. Gold-bearing quartz veins were emplaced during Albian and Campanian time (GOLDFARB ET AL., 1997).

Source of Lode Gold:

As previously mentioned, gold deposits in the upper Koyukuk and Chandalar mining district form a nearly east-west trending belt from Little Squaw Lake to Wild Lake.
The gold-bearing veins in the Nolan area are younger than the exposed metasedimentary rocks and the metabasite dyke. It is the same in the Little Squaw Lake area, Sukapak Mountain and around Wild Lake. This suggests a regional phenomena with a widely distribution, probably caused by remobilization of a preexisting source (metamorphic origin) and not by a pluton-related source. As there

are no known and mapped granites in the Nolan area, according to PROFFETT (1982) the nearest granitic rocks mapped are 25 miles to the east and 60 miles to the west, is further evidence for gold remobilization from a deeper source by metamorphic fluids.

Final evidence, and also the strongest one, for this theory is given in the results of electron microprobe analyses carried out on placer gold and lode gold grains from the Nolan-Hammond area and from further away located placer deposits (Sawyer Creek, and Rye & Jay Creek, Fig.40). All gold grains (placer and lode grains) examined lack in Bi.

According to RAINER NEWBERRY (written communication, 1999) the absence of Bi in gold grains from both vein systems and also in placer gold suggests the absence of a pluton-related source. Also, placer gold from Sawyer Creek (22 km south of Nolan) and Rye & Joy Creek (76 km west of Nolan) can analogous be distinguished in the two prominent populations, suggesting this to be a regional phenomena for gold-mineralization and a region-wide source. This associates with metamorphic related gold mineralization. In comparison with lode and placer grains from the Fairbanks mining district (RAINER NEWBERRY, written communication 1999), every single lode and placer which has been investigated, regardless of distance from mineralized granite, has gold which is at least anomalous in Bi.

DILLON ET AL. (1989) suggest that gold may have been remobilized during metamorphic dewatering of the lower Paleozoic rocks. There is geochemical evidence for silver-arsenic-antimony-mercury-molybdenum-gold occurrences in the lower Paleozoic rocks of the Doonerak area, which is north of Nolan (CATHRALL AND OTHERS, 1984).

Alternatively, stibnite enrichments in veins in the Brooks Range may also reflect a high antimony background in fine-grained pelitic beds (GOLDFARB ET AL., 1997).

Another explanation as described by DILLON ET AL. (1989) might be remobilization of gold deposits, such as paleoplacers (quartz-rich metaconglomerates). Within the western Wiseman Quadrangle, there is a fair correlation between exposures of potential paleoplacer deposits that underlie and overlie the Skajit Limestone and the occurrence of present-day placers at Wild Lake and Crevice, Jay, Birch and Nolan Creeks. The metaconglomerates do not continue eastward to the Chandalar area from the productive Nolan Creek area; thus the paleoplacer hypothesis seems an incomplete explanation for the belt of gold deposits (DILLON ET AL., 1989).

According to ROSE, PICKTHORN, AND GOLDFARB (1987) gold in the Chandalar mining district is believed to have been mobilized from pelitic metasediments by metamorphic fluids. GOLDFARB ET AL. (1997) favor the theory that gold contained in mesothermal lodes was derived largely from metasedimentary rocks at lower crustal levels.

10.2 Source of Placer Gold

The fact that productive placer deposits are located around the gold-bearing veins in the Nolan-Hammond area suggests that placer gold has been derived from these auriferous veins. Nuggets found in the area are normally rounded, flattened and rough, coarse and crystalline. Wire gold is not that common. Some nuggets with relict crystal shape and attached pieces of quartz weigh up to 40 oz; these are particularly common close to gold-bearing veins (DILLON ET AL., 1989). Some of the gold from the Nolan area and Vermont Creek contain angular pieces of gold-bearing stibnite-quartz vein material that must have been derived directly from nearby lode deposits (oral communication with DENNIS STACEY and ROGER BURGGRAF, 1998). Further, other minerals found in placer concentrates, such as arsenopyrite, pyrite, and stibnite are typically associated with gold-bearing quartz-veins.
Note that REED (1938) provides a more detailed description of the placer deposits in the region.

Placer gold in the Nolan-Hammond area occurs as stream placer (Gulch and Creek placer) and as bench placer. The following description of these is adopted from the Technical Bulletin 4, published by BLM (1989).
"Gulch placers are characteristically small in area, have steep gradients and are usually confined to minor drainages in which a permanent stream may or may not exist. Creek placers have been important sources of gold and were most carefully prospected by the early miners and almost worked out. Bench placers are usually remnants of deposits formed during an earlier stage of stream development and left behind as the stream cuts downward. The abandoned segments, particularly those on the hillsides, are commonly referred to as "bench" gravels. Frequently, there are two or more sets of benches in which case the miners refer to them as "high" benches and "low" benches".
Bench placers are mining and exploration targets for placer gold in the Nolan-Hammond area with high potential.

To interpret the e-probe data on placer gold grains and lode gold I also consulted USGS OFR 86-345 (MOISER & LEWIS, 1986), which gives data on placer gold compositions. According to RAINER NEWBERRY and RICHARD GOLDFARB (written communication, 1999) the USGS gold data has to be interpreted with care as they were all done by emission spectrographic analyses, which have analytical uncertainties of +/- 50%. However, that data give at least semi-quantitative information on the gold. Further, because MOISER and LEWIS analyzed whole nuggets, their composition reflect that of the gold plus any included minerals (RAINER NEWBERRY, written communication 1999).

As discussed in Chapter 9, there does not seem to be any evidence for compositional changes in the gold due to surficial processes. The gold from bench, gulch and creek placers of the Nolan-Hammond area is not significantly different from that of the two vein systems in the area nor from the placer at Sawyer Creek and Rye & Jay Creek, which are located further away (Fig.40). Again, and as previously mentioned, there is no evidence for silver compositional zoning. The minor differences between core and rim Ag contents show no systematic pattern or either Ag-enrichment or Ag-depletion. The core-to-rim Ag compositional variations are no greater than within-grain variations shown by the quartz vein gold. There is a little variation in Hg content of the gold (from a minimum of 1% to a maximum of 6% Hg), but the apparent core-to-rim variations of individual nuggets are no greater than the variation of Hg contents within the quartz vein gold. Also, there is no systematic core-to-rim zoning: some cores are richer in Hg, some rims are richer. Consequently, the apparent zoning is due to compositional variations in the original vein gold, and a nugget is simply a sample of the variable Hg content (RAINER NEWBERRY, written communication 1999).

In comparing my data with work done by MOISER & LEWIS (1986), the high Hg contents measured by microprobe are compatible with values determined by emission spectrographic analyses. All the gold from the Nolan-Hammond area analyzed by MOISER & LEWIS (1986) is at least anomalous in Hg, and mostly in the 0.5 - 2% range.

No Bi was detected by microprobe (detection limit ca. 100 ppm). MOISER & LEWIS (1986) present many analyses with anomalous (> 10 ppm) Bi. This may be related to the strong correlation between Pb and Bi indicating that the Bi in their gold analyzed is due to Bi in galena inclusions in gold.

Several grains analyzed by microprobe yielded Sb contents apparently above detection (ca. 100 ppm). In consultation with RAINER NEWBERRY (written communication, 1999), the believable ones are those with values of 0.015% (Archibald Creek and stibnite vein sample) and 0.035% (grain 6 from Smith Creek). MOISER & LEWIS (1986) similarly give several analyses from Smith Creek and one from Archibald Creek with Sb above 0.01%. As nuggets analyzed by them with this Sb content also have high Pb contents, it can be argued that the anomalous Sb in their gold was due to either Sb in galena inclusions or small amounts of inclusion stibnite associated with galena.

The silver contents of the gold grains, as determined by both microprobe and emission spectrographic analyses, apparently indicates that several different populations are present. In particular, there seems to be a group with about 0.5% to 4% Ag (as represented by the stibnite vein sample) and a group of with about 6 to 11% Ag (represented by the quartz vein sample). This is presented in Figure 40. The emission spectrographic analyses data suggest an addition group with compositions of about 14 to 18% Ag, though not represented by the microprobe analyses. Because the Ag contents of individual grains vary so little and because so many grains were analyzed, the compositional "void" between 4 and 6% Ag is suggested to be real.

Placer samples from Thompson Pup, Smith Creek, and Swede underground contain both types or populations of gold, whereas Fay Creek, Archibald Creek, and Slisco Bench only contain one population. The apparent presence of only one type of gold is related to the small number of nuggets analyzed from these localities. Note that only one nugget was analyzed from Fay Creek and Slisco Bench, and two grains were examined from Archibald Creek. The emission spectrographic analyses data indicate a wide range of Ag in Archibald Creek.

I suggest that both types of gold are present in creeks, gulches, and benches in the Nolan-Hammond area as the presence of the two prominent vein systems indicates. Data from MOISER & LEWIS (1986) from the Hammond River and its tributaries support this.

Both types of gold also occur in Sawyer Creek and Rye & Jay Creek (Fig.40), which are located south and west-southwest of Nolan. Because their gold compositions are so similar to the Nolan-Hammond gold compositions, despite being far away, suggests a regional phenomena for the gold mineralization and a region-wide source.

Lode and Placer Gold from the Nolan area, Sawyer Creek, and Rye & Jay Creek

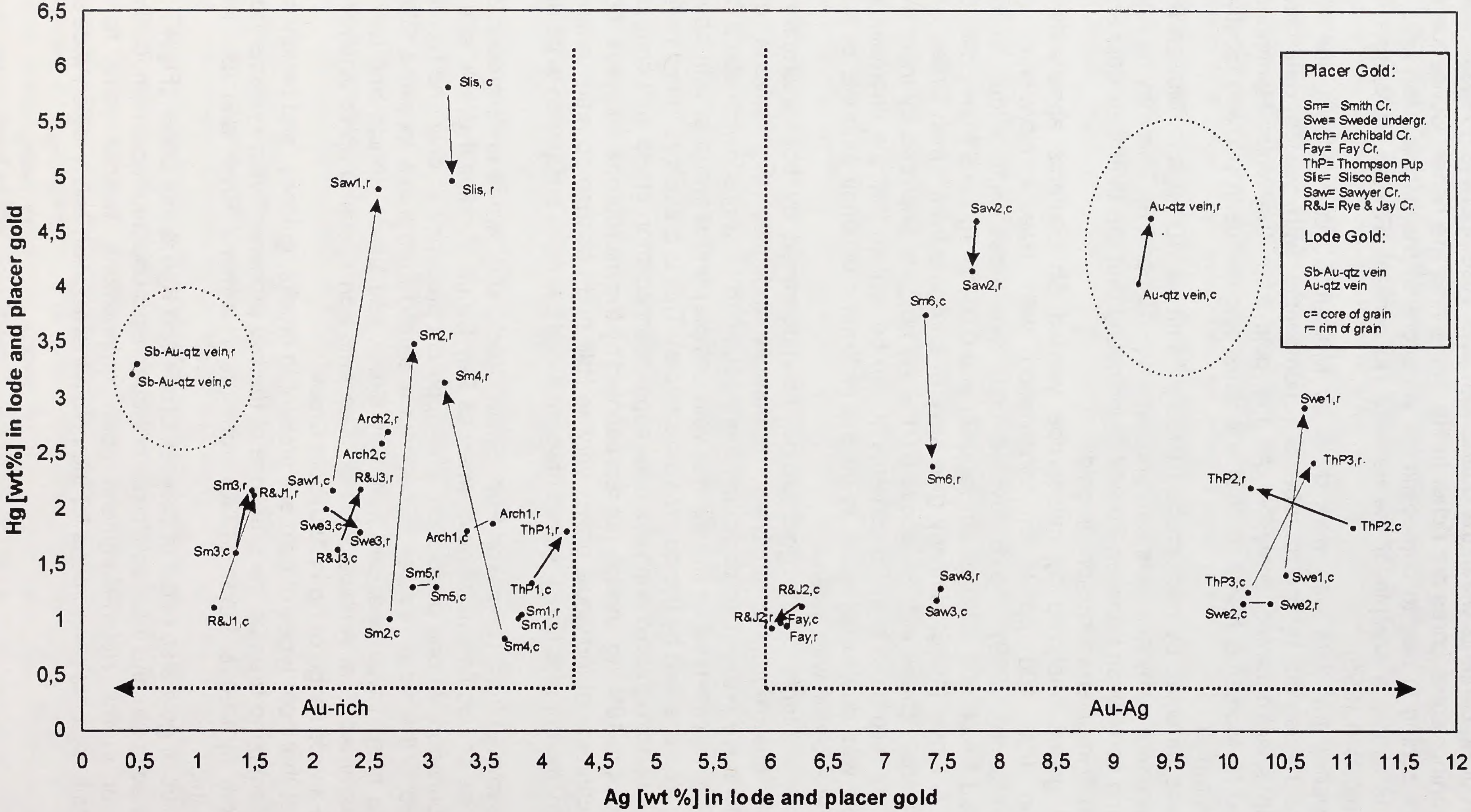

Fig.40: Compositions of lode and placer gold grains from the Nolan area, Sawyer Creek, and Rye & Jay Creek. Mean composition of core and rim for each grain. Arrowhead shows towards rim of grain

Therefore I suggest that placer gold located around gold-bearing veins in the Nolan-Hammond area has been derived from the two prominent gold-vein systems occurring in the area. The fact that there is no evidence for compositional changes from core to rim in placer grains from the area (no evidence for silver compositional zoning from core to rim) totally rules out that placer gold might have been transported from a distant source. According to BOYLE (1979), it has been repeatedly observed that there is an increase in the fineness of gold with increasing distance from the source. This is not the case in the Nolan-Hammond area. The two compositions of placer gold (two populations) can directly be related to the stibnite-gold vein system and to the quartz-gold vein system.

It is obvious that placer gold with stibnite fragments and/or with quartz crystals attached to them, or placer gold with relict crystal shape from the Nolan-Hammond area must have been derived directly from the nearby lode veins of the area. Further, as this gold is fresh and not water worn also suggests that is has been eroded from a nearby source. This gold, especially gold with relict crystal shape is reported from Thompson Pup and Archibald Creek (ED ARMSTRONG, 1985), and also found in Smith Creek.
On the other hand, well water worn placer gold has also been reported for the Nolan-Hammond area (PROFFETT, 1982), suggesting erosion from ore shoots on veins that have long since been eroded away.

The above discussed only explains the existence of small nuggets and larger ones up to a few ounces, but how about the "big ones" such as the 41.35 troy ounce nugget (Fig.41) found by Tri-con in 1994 at Nolan and the 139 ounce nugget found in late 1913 or early 1914 on the Hammond River?

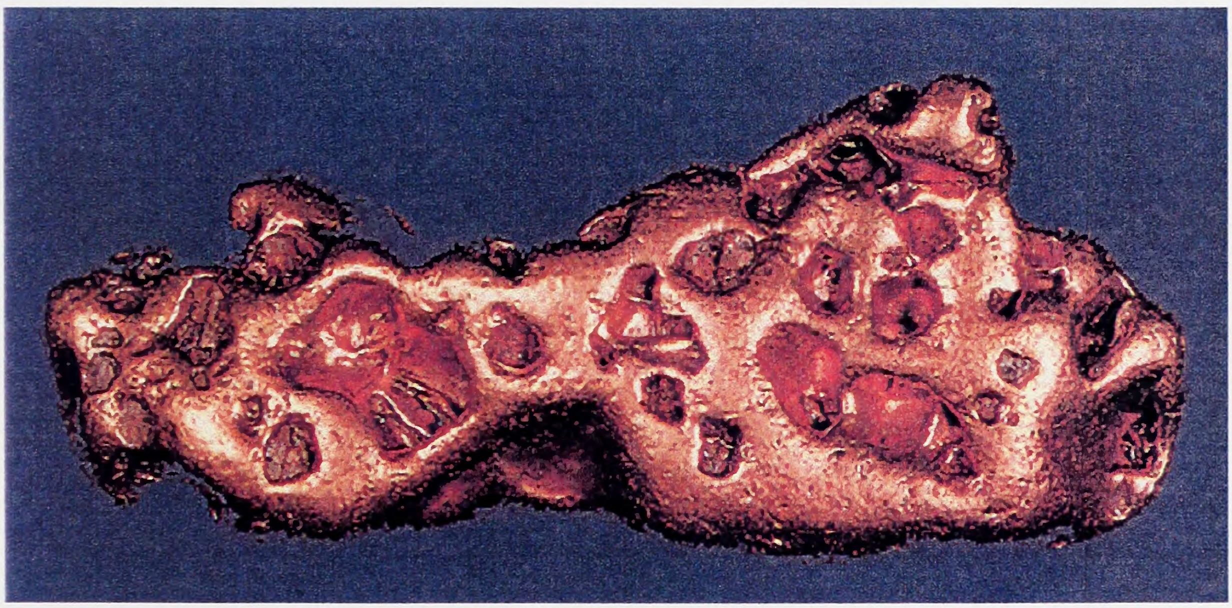

Fig.41: 41.35 troy ounce gold nugget with impressions of quartz crystals. Actual size. With permission from Silverado Mines Ltd.

DILLON ET AL. (1989) report that some nuggets with relict crystal shape and attached pieces of quartz found in the upper Koyukuk mining district and Chandalar mining

district weigh up to 40 ounces. As these are particularly common close to gold-bearing quartz veins suggests that these have been directly derived from those veins. However, unless big nuggets are not donated for scientific research, their origin can only be suspected.
The origin of gold nuggets has long been a subject of discussion (BOYLE, 1979). In fact, up to present, three main theories prevail as described by BOYLE (1979): "the first one holds that the nuggets are formed mainly by chemical accretion processes; the second one maintains that they are detrital in origin, had essentially the same weight as they now possess, but their shape and features are due to the rolling and hammering they have received as they have been moved along in the gravels". A third theory as described by BOYLE (1979) is a compromise holding that nuggets are partly detrital and partly chemical in origin.

11. Conclusion

Two different striking gold-bearing vein systems occur in the Nolan-Hammond area. The NW-striking quartz-gold and NE-striking stibnite-quartz-gold vein systems in the Nolan-Hammond area crystallized in post-metamorphic structures (fractures) at temperatures below 300°C. The predominant gold transport mechanisms in the hydrothermal fluids were the Au-Sb-S complex and the $Au(HS)^{-}_{2}$ complex systems, but arsenothio complexing may have also contributed to the transport of gold. Gold is believed to have been mobilized from metasedimentary rocks at lower crustal levels by metamorphic hydrothermal fluids. Gold-bearing vein systems were emplaced during Albian and Campanian time periods.
The composition of gold in both vein systems is different. Gold from the stibnite-quartz-gold veins is characterized by its low silver content (0.5% Ag), whereas gold from the quartz-gold veins shows high a silver content (9.25% Ag). The two different populations represent slightly different environments of formation in the Au-Sb-S system.
Both gold-bearing vein systems are mainly concentrated in a "corridor" from the south of Smith Creek through the Nolan Valley, along Thompson Pup and the "Fortress" into the Right Fork of Vermont Creek. The reason for this is the fact that this particular area was heavily disturbed by multistage faulting, shearing, and folding which led to fracturing of rocks. Especially late stage extensional movement (uplift) reactivated fractures which caused more space for mineralized fluids to circulate through with subsequent crystallization of quartz, stibnite, and gold. Further, the metasedimentary rocks in this area contain graphite and pyrite, which are favorable for precipitation of gold from hydrothermal fluids.

Placer gold from the Nolan-Hammond area can be related to the two different gold-bearing vein systems occurring in the area. Analogous to lode gold, placer gold can also be distinguished into two different populations characterized by a low silver type (0.5 to 4% Ag) and a high silver type (6 to 11% Ag). The fact that there is no evidence for compositional changes from core to rim in the gold grains due to surficial processes leads to the conclusion that placer gold from the area does not come from a distant source. Further evidence is given in the occurrence of placer gold with stibnite fragments and/or with quartz crystals attached to them, or placer gold with relict crystal shape. This must have been derived directly from nearby lode veins of the area. Finally, the fact that productive placer deposits in the Nolan-Hammond area are located around or nearby auriferous veins leads to the conclusion that placer gold in the Nolan-Hammond area has been derived by the erosion of the two different gold-bearing vein systems.

Recommendations

Exploration for lode deposits has to focus on both vein systems. As the potential area is expansive and covered extensively with tundra, and also with the existence of permafrost, it is questionable if trenching along strikes of known veins would be productive for bedrock exploration.

The only way to complete successful lode exploration in the Nolan-Hammond area is to develop and carry out a serious drilling program. Drilling has to be carried out to search for the horizontal extension as well as for the vertical extension (down-plunge continuity) of gold mineralization in both vein systems.

The hydrothermal system developed in the area, and especially the Au-Sb-S complex transport mechanism strongly suggest down-dip continuity of potential gold mineralization.

IV. REFERENCES

Armstrong, E.J. , 1985, Nolan Lode Project, Summary of Investigations completed during 1985. Internal Report prepared for Silverado Mines (U.S.) Inc.

Armstrong, E.J., Placer Geology of the Wiseman Area. Internal Report prepared for Silverado Mines (U.S.) Inc.

Armstrong, E.J., Nolan Creek Lode Claims, Geophysical and Geochemical Report. Internal Report prepared for Silverado Mines (U.S.) Inc.

Ashworth, K., 1983, Genesis of Gold Deposits at the Little Squaw Mines, Chandalar Mining District, Alaska. MSc. thesis Western Washington University, Bellingham, Washington, 64 p.

Berg, H.C., and Cobb, E.H., 1967, Metalliferous Lode Deposits of Alaska. U.S. Geol. Surv. Bull. 1246, 254 p.

BLM, 1989, Placer Examination, Principles and Practice, Technical Bulletin 4, BLM, pp. 1-24.

BOM, 1995, Report on Fluid Inclusion Studies, 3 p.

Boyle, R.W., 1979, The Geochemistry of Gold and its Deposits (together with a chapter on geochemical prospecting for the element. Geological Survey of Canada Bulletin 280, pp.333-386.

Boyle, R.W., 1987, Gold, History and Genesis of Deposits, Society of Economic Geologists, pp. 455-544.

Brosgé, W. P., and Reiser, H.N., 1964, Geologic map and section of the Chandalar quadrangle, Alaska: U.S. Geol. Surv. Misc. Geol. Inv. Map I-375, scale at 1:250,000.

Brosgé, W. P., and Reiser, H.N., 1971, Preliminary bedrock geologic map: Wiseman and eastern Survey Pass quadrangles, Alaska: U.S. Geol. Surv. Open File Map 479, scale 1:250,000:

Brosgé, W. P., and Reiser, H.N., 1972, Geochemical Reconnaissance In the Wiseman and Chandalar Districts and Adjacent Region, Southern Brooks Range, Alaska. U.S. Geological Survey Professional Paper 709, 21 p.

Cathrall, J.B., Dillon, J.T., and Chazin, B., 1984, Map of anomalous trace metals in rocks and stream sediment pebbles of the Wiseman 10' x 30' Quadrangle, Brooks Range, Alaska: U.S. Geological Survey Open-file Report OF-84-161-B, scale 1:250,000, 1 sheet.

Chipp, E.R., 1970, Geology and geochemistry of the Chandalar area, Brooks Range, Alaska: Alaska Div. Mines and Geology, Geologic Rpt. no. 42, 39 p.

Cobb, E.H., 1973, Placer Deposits of Alaska. U.S. Geological Survey Bull. 1374, pp. 111-114, 144-145, 155-160.

Dillon, J.T., 1982, Source of Lode and Placer Gold Deposits of the Chandalar and Upper Koyukuk Districts, Alaska. Alaska Div. of Geol. and Geophys. Surv. Open File Rpt. AOF-158, 22 p.

Dillon, J.T., Brosgé, W.P., and Dutro, J.T., 1986, Generalized Geologic Map of the Wiseman Quadrangle, Southcentral Brooks Range, Alaska. U.S. Geol. Surv. Open-file Report 86-219.

Dillon, J.T., Lamal, K.K., and Huber, J.A., 1989, Gold Deposits in the Upper Koyukuk and Chandalar Mining Districts, Alaska. In Alaska Div. of Geol. and Geophys. Surv. Guidebook 7, Vol. 2, pp. 196-201.

Dillon, J.T., Solie, D.N., Murphy, J.M., Bakke, A.A., and Huber, J.A., 1989, Road Log from South Fork Koyukuk River (mile 156.2) to Chandalar Shelf (mile 237.1). In Mull C.G., and Adams, K.E., eds., Dalton Highway, Yukon River to Prudhoe Bay, Alaska: Geology of eastern Koyukuk Basin, Central Brooks range, and East-central Arctic Slope: Div. of Geol. and Geophys. Surv. Guidebook 7, Vol. 1, pp. 74-100.

Dillon, J.T., 1989, Structure and Stratigraphy of the Southern Brooks Range and Northern Koyukuk Basin near the Dalton Highway. In Alaska Div. of Geol. and Geophys. Surv. Guidebook 7, Vol. 2, pp. 158-187.

Dillon, J.T., and Reifenstuhl, R.R., 1990, Geologic Map of the Wiseman B-1 Quadrangle, Southcentral Brooks Range, Alaska. Alaska Div. of Geol. and Geophys. Surv., Professional Rpt. 101.

Dillon, J.T., Reifenstuhl, R.R., and Harris, G.W., 1996, Geologic Map of the Chandalar C-5 Quadrangle, Southeastern Brooks Range, Alaska. Alaska Div. of Geol. and Geophys. Surv.

Driscoll, A., Jr., 1987, Geology and Economic Geology of the Wiseman Area, Koyukuk Mining District, Northern Alaska, Unpublished report to Alaska Mining Co., 25 p.

Dusel-Bacon, C., 1994, Metamorphic history of Alaska, in Plafker, G., and Berg, H.C., eds., The Geology of Alaska: Boulder, Colorado, Geological Society of America, v. G1, pp. 495-533.

Ebbly, N., Jr., and Wright, W.S., 1948, Antimony Deposits in Alaska. U.S. Bur. Mines Rpt. of Inv. 4173, 41 p.

Einaudi, M.T., and Hitzman, M.W., 1986, Mineral Deposits in Northern Alaska: Introduction, Economic Geology Vol. 81, No. 7, pp. 1583-1591.

Evans, A.M., 1993, Ore Geology and Industrial Minerals, An Introduction. Third Edition. Blackwell Science Ltd., pp. 99-103.

Goldfarb, R.J., Miller, L.D., Leach, D.L., and Snee, L.W., 1997, Gold Deposits in Metamorphic Rocks of Alaska. In Economic Geology, Monograph 9, pp. 151-190.

Gottschalk, R.R., Jr., 1987, Structural and Petrologic Evolution of the Southern Brooks Range near Wiseman, Alaska. Rice University Houston, Texas Ph.D. thesis, 263 p.

Gottschalk, R.R., Jr., 1990, Structural evolution of the schist belt, south-central Brooks Range fold and thrust belt, Alaska: Journal of Structural Geology, v. 12, pp. 453-469.

Groves, D.I., and Ho, S.E., 1990, A Short Review of Gold in the Yilgarn Block. In Geology of Mineral Deposits of Australia and Papua New Guinea. Vol. 1. Australian Institute of Mining and Metallurgy Monograph No. 14, pp.546-547.

Hamilton, T.D., 1989, Glacial Geology of the Brooks Range. In Alaska Div. of Geol. and Geophys. Surv. Guidebook 7, Vol. 1, pp. 23-26.

Hatcher, R.D., Jr., 1995, Structural Geology, Principles, Concepts, and Problems. Second Edition. Prentice- Hall, Inc., 523 p.

House, G.D., 1981, Nolan Creek Lode Claims, Preliminary Geological and Geophysical Report. Unpublished report to Silverado Mines Ltd.

Huber, J.A., 1995, Mineralization in Nolan Valley. Unpublished report to Silverado Mines Ltd.

Kurtak, J.M., Robert F. Klieforth, John M. Clark, and Earle M. Wiliams, Mineral Investigations in the Koyukuk Mining District. Northern Alaska-Progress Report. Bureau of Land Management Open File Report (in press).

Maddren, A.G., 1913, The Koyukuk-Chandalar region, Alaska. U.S. Geol. Surv. Bull. 532, 119 p.

Metz, P., 1981, A summary of Gold Fineness from Alaska Placer Deposits, MIRL Report No. 45, pp. 36-37.

Metz, P., 1991, Metallogeny of the Fairbanks Mining District, Alaska and Adjacent Areas, MIRL Report No. 90, pp. 22-23, 30-39, 70-101.

Miller, E.L., and Hudson, T.L., 1991, Mid-Cretaceous extensional fragmentation of a Jurassic-Early-Cretaceous compressional orogen, Alaska: Tectonics, v. 12, pp. 781-796.

Moiser, E.L., and Lewis, J.S., 1986, Analytical Results, Geochemical Signatures, and Sample Locality Map of Lode Gold, Placer Gold, and Heavy-Mineral Concentrates from the Koyukuk-Chandalar Mining District, Alaska. U.S. Geol. Survey Open-File Report 86-345, 1972 p.

Moiser, E.L., Cathrall, J.B., Antweiler, J.C., and Tripp, R.B., 1989, Geochemistry of placer gold, Koyukuk-Chandalar district, Alaska, Journal of Geochemical Exploration, 31, pp. 97-115.

Moore, T.E., Wallace, W.K., Bird, K.J., Karl, S.M., Mull, C.G., and Dillon, J.T., 1994, Geology of northern Alaska, In The Geology of North America, Vol. G-1, the Geological Society of America, pp. 50-140.

Muller, S.W., 1947, Permafrost or permanently frozen ground and related engineering problems: Ann Arbor, J.W. Edwards, Inc., 162 p.

Mull, C.G., and Adams, K.E., 1989, Dalton Highway, Yukon River to Prudhoe Bay, Alaska. Bedrock Geology of the eastern Koyukuk basin, central Brooks Range, and eastcentral Arctic Slope, Alaska Div. of Geol. and Geophys. Surv. Guidebook 7, Vol 1 and 2, 309 p.

Nekrasov, I.Ya., 1996, Geochemistry, Mineralogy and Genesis of Gold Deposits. A.A. Balkema, Rotterdam, Brookfield, pp. 141-185.

Newberry, R.J., and Clautice, K.H., 1997, Compositions of Placer Gold in the Rampart-Eureka-Manly-Tofty Area, Eastern Tanana and Western Livengood Quadrangles, central Interior Alaska, Determined by Electron Micrprobe Analysis. Alaska Div. of Geol. and Geophys. Surv. Public- Data File 97-49, 49 p.

Patrick, B., Till, A.B., and Dinklage, W.S., 1994, An inverted metamorphic field gradient in the central Brooks Range, Alaska, and implications for exhumation of high-pressure/low-temperature Metamorphic rocks: Lithos, v.33, pp. 67-83.

Patton, W.W., Jr., and Miller, T.P., 1973, Bedrock geologic map of Bettles and southern part of Wiseman Quadrangles: U.S. Geol. Surv. Miscellaneous Field Studies Map MF-492, scale 1:250,000.

Patton, W.W., Jr., and Tailleur, L.L., 1977, Evidence in the Bering Strait region for differential movement between North America and Eurasia: Geol. Soc. Am. Bull., v. 88, pp. 1298-1304.

Proffett, J.M., 1982, Preliminary Report on the Geology of the Hammond River - Vermont Creek Gold Placer Area, Wiseman District, Alaska. Unpublished report to Alaska Mining Co., 15 p.

Reed, I.McK., 1938, Upper Koyukuk region, Alaska. Alaska Dept. of Mines Misc. Rpt. No. 194-7, 169 p.

Robinson, M.S. and Bundtzen, T.K., 1982, Geology of the Scrafford antimony-gold lode deposit, Fairbanks mining district, Alaska: Alaska Division of Geological and Geophysical Surveys Open-file Report 173, 7 p., 1 sheet.

Roedder, E., 1984, Fluid-inclusion evidence bearing on the environments of gold deposition: Geological Society of Zimbabwe Special Publication 1, pp. 129-163.

Rose, S.C., Pickthorn, W.J., and Goldfarb, R.J., 1987, Gold Mineralization by Metamorphic Fluids in the Chandalar District, Southern Brooks Range - Fluid Inclusion and Oxygen-Istopic Evidence. In Geologic Studies in Alaska by U.S. Geological Survey, U.S. Geol. Surv. Circular 1016, pp. 81-84.

Silverado Gold Mines Ltd., 1993 Annual Report, 16 p.

Silverado Gold Mines Ltd., 1994 Annual Report, 21 p.

Silverado Gold Mines Ltd., 1997 Annual Report, 13 p.

Till, A.B., 1992, Detrital high-pressure/low-temperature metamorphic mineral assemblages in Early Cretaceous sediments of the foreland basin of the Brooks Range, Alaska and, implications for orogenic evolution: tectonics, v. 11, pp. 1207-1223.

Till, A.B., Box, S.E., Roeske, S.M., and Patton, W.W., Jr., 1993, Comment on "Mid-Cretaceous extensional fragmentation of a Jurassic-Early-Cretaceous compressional orogen, Alaska" by E.L. Miller and T.L. Hudson: Tectonics, v. 12, pp. 1076-1081.

Swainbank, R.C., Bundtzen, A.H., Henning, M.W., and Hansen, E.W., 1995, Alaska's Mineral Industry 1994, Div. of Geol. and Geophys. Surv. Special Report 49, 78 p.

Wilson, 1982, Introduction to Small Scale Geological Structures, pp. 24-29.

Wimmler, N.L., 1929, Placer Mining in Alaska in 1929. Alaska Terr. Dept. of Mines Misc. Rpt. MR-195-1, pp. 223-239.

V. LIST OF TABLES

Table 1: Field Measuring Data

Location	Bedding	Fold Limbs	Cleavage	Joints	Faults	Lineation	Quartz Veins	Rock Unit
1	53 / 08		S2: 53 / 08					Dbs 1
	53 / 04		S2: 53 / 04					
2	6 / 28						210 / 80	Dbs 1
	12 / 26							
3	30 / 30		S2: 30 / 30	18 / 85			214 / 65	Dbs 5
				18 / 80				
4	2 / 15							Dbs 5
	8 / 18							
5	10 / 20			222 / 85			190 / 89	Dbs 5
	8 / 25			8 / 25				
6			S3: 350 / 35				218 / 85	Dbs 5
			S3: 350 / 40				208 / 82	
							320 / 82	
							212 / 80	
7	32 / 15	2 / 45		240 / 85			218 / 85	Dbs 5
	18 / 22	12 / 25		242 / 85			55 / 80	
				132 / 85			135 / 85	
				132 / 81			25 / 90	
				242 / 86			340 / 20	
				242 / 88			202 / 85	
				160 / 85				
				170 / 85				
8	350 / 20						214 / 76	Dbs 5
	346 / 21						192 / 80	
9	350 / 15			212 / 75			211 / 85	Dbs 5
10	33 / 13						216 / 85	Dbs 5
	4 / 10						132 / 80	
11		32 / 25						
		30 / 55						
		38 / 65						
		32 / 65						
		32 / 26						
		202 / 25						
		36 / 25						
		194 / 25						
12		144 / 58	S2: 14 / 03	110 / 76		170 / 0	210 / 70	Dbcs 45
		148 / 54		110 / 75		180 / 0		
		140 /45		32 / 88		10 / 05		
		334 / 35						
		335 / 35						
		180 / 65						
		196 / 25						
		300 / 15						
		2 / 35						
		342 / 52						
		158 / 45						
13		164 / 75		42 / 85				Dbcs 45
		342 / 45		230 / 88				
14				248 / 85			164 / 35	Dbcs 45
				250 / 80			192 / 60	

Table 1: Field Measuring Data

Location	Bedding	Fold Limbs	Schistosity	Joints	Faults	Lineation	Quartz Veins	Rock Unit
15		0 / 90	S3: 340 / 25					Dbcs 45
		332 / 55					192 / 85	
		192 /45						
16		22 / 30						Dbcs 45
		340 / 80						
		10 / 36						
		10 / 30						
17	32 / 24		S2: 32 / 24	222 / 75			228 / 75	Dbcs 45
	22 / 25		S2: 22 / 25					
18						165 / 10		Dbcs 45
19			S3: 330 / 35	92 / 89			30 / 85	Dbcs 45
				108 / 85				
				256 / 74				
20		41 / 20					222 / 70	Dbcs 45
		158 / 85						
21	38 / 17		S2: 38 / 17	232 / 68				Dbcs 45
	40 / 20		S2: 40 / 20	130 /80				
22	344 / 30		S3: 342 / 30	60 / 85			192 / 82	Dbcs 45
	2 / 26		S3: 341 / 32	62 / 84			224 / 85	
	0 / 28						350 / 10	
							210 / 70	
							202 / 85	
							204 / 85	
23		48 / 50	S3: 350 / 30	50 / 84				Dbcs 45
		0 / 65	S3: 345 / 31					
24		128 / 25	S3:350 / 30			50 / 14	340 / 40	Dbcs 45
		136 / 60				48 / 12		
		138 / 86						
25			S3: 355 / 29	210 / 70				Dbcs 45
26		338 / 70	S3: 356 / 30	210 / 72		54 / 25	211 / 75	Dbcs 45
		114 / 62	S3: 350 / 30	210 / 72		50 / 21	210 / 75	
				72 / 90			210 / 70	
				76 / 80			212 / 75	
				75 / 89			318 / 80	
							102 / 10	
27		350 / 45	S3: 358 / 30	84 / 82			0 / 35	Dbcs 45
		338 / 38	S3: 358 / 30				10 / 80	
		170 / 64	S3: 342 / 20					
		168 / 60	S3: 350 / 30					
28			S3: 352 / 50	70 / 84			220 / 90	Dbcs 45
			S3: 340 / 30	316 / 78				
			S3: 350 / 25					
29		336 / 38	S3: 340 / 30	214 / 85			350 / 40	Dbcs 45
		152 / 65	S3: 340 / 35	204 / 75			208 / 80	
				116 / 85				
30		352 / 35					230 / 80	Dbcs 45
		120 / 38						
31			S3: 330 / 25	230 / 80				Dbcs 45
			S3: 326 / 30	208 / 75				
			S3: 346 / 20	210 / 75				

Table 1: Field Measuring Data

Location	Bedding	Fold Limbs	Cleavage	Joints	Faults	Lineation	Quartz Veins	Rock Unit
			S3: 345 / 20	284 / 75				
				285 / 70				
32							198 / 80	Dbcs 45
							198 / 85	
33			S3: 358 / 38	298 / 82			194 / 85	Dbcs 45
			S2: 50 / 30	198 / 75				
			S3: 358 / 30					
			S3: 356 / 26					
34	60 / 28						280 / 80	Dbcs 45
35	10 / 20							Dbcs 9
	12 / 18							
36	118 / 25						62 / 70	Dbcs 9
							190 / 90	
							192 / 89	
37	58 / 25			212 / 80			318 / 76	Dbcs 9
	54 / 25			208 / 75				
38	42 / 20		S2: 42 / 20	214 / 85				Dbcs 9
	44 / 22		S2: 44 / 22	212 / 75				
39	102 / 22			212 / 70				Dbcs 9
	108 / 22			200 / 75			180 / 90	
				90 / 83			185 / 89	
				210 / 85				
				60 / 65				
				68 / 70				
40	48 / 25		S2: 48 / 25	156 / 80			210 / 85	Dbcs 9
	40 / 25		S2: 40 / 25	342 / 80				
				280 / 78				
41	42 / 26							Dbcs 9
	52 / 30							
42	88 / 15						210 / 82	Dbcs 10
	110 / 20			194 / 80			204 / 83	
	88 / 25						210 / 85	
	40 / 20						208 / 85	
43	92 / 16			274 / 70			192 / 88	Dbcs 10
	98 / 20			292 / 85			210 / 88	
				272 / 80				
44	94 / 25			320 / 75				Dbcs 10
				196 / 83				
45	42 / 12		S2: 42 / 12	190 / 80				Dbcs 10
	42 / 10		S2: 42 / 10	190 / 68				
	44 / 12		S2: 44 / 12	258 / 88				
46	54 / 10			42 / 85				Dbcs 12
	80 / 10			44 / 85				
	50 / 10			230 / 85				
				290 / 85				
				294 / 85				
47	60 / 15							Dbcs 12
	60 / 25							
48	64 / 20			70 / 85			176 / 70	Dbcs 8
	50 / 15			126 / 78			0 / 85	

Table 1: Field Measuring Data

Location	Bedding	Fold Limbs	Cleavage	Joints	Faults	Lineation	Quartz Veins	Rock Unit
							170 / 65	
49	40 / 15			288 / 80			202 / 85	Dbs 9
	40 / 12			200 / 88			202 / 83	
	30 / 20			200 / 85				
				220 / 80				
				224 / 85				
				112 / 85				
				200 / 85				
50								Dbs un.
51								Dbs un.
52								Dbs un.
53	350 / 38						210 / 76	Dbs un.
	348 / 40							
54	42 / 20		S2: 42 / 20	194 / 76			196 / 79	Dbps 1
	43 / 20		S2: 43 / 20				198 / 85	
	44 / 22		S2: 44 / 22				202 / 85	
							208 / 75	
55	35 / 15						202 / 85	Dbps 1
							206 / 88	
							208 / 82	
56				222 / 75				Dbps 1
57	40 / 25		S2: 40 / 25	200 / 85			208 / 85	Dbps 1
	42 / 23		S2: 42 / 23	206 / 85				
	42 / 20		S2: 42 / 20					
58	32 / 25		S2: 32 / 25					Dbps 1
59			S2: 42 / 12				204 / 88	Dbps 1
			S2: 40 / 20					
			S2: 42 /22					
60			S2: 42 / 12					Dbps 1
			S2: 40 / 20					
			S2: 42 / 22					
61			S2: 42 / 12					Dbps 1
			S2: 40 / 20					
			S2: 42 /22					
62			S2: 42 / 12					Dbps 1
			S2: 40 / 20					
			S2: 42 /22					
63			S2: 42 / 12					Dbps 1
			S2: 40 / 20					
			S2: 42 / 22					
64			S2: 42 / 12					Dbps 1
			S2: 40 / 20					
			S2: 42 / 22					
65	42 / 16		S2: 42 / 16	138 / 88			210 / 88	Dbs 10
	40 / 20		S2: 40 / 20					
66	42 / 12		S2: 42 / 12					Dbps 1
	40 / 20		S2: 40 / 20					
	42 / 18		S2: 42 / 18					
	38 / 10		S2: 38 / 10					
	40 / 12		S2: 40 / 12					

Table 1: Field Measuring Data

Location	Bedding	Fold Limbs	Cleavage	Joints	Faults	Lineation	Quartz Veins	Rock Unit
67	42 / 12		S2: 42 / 12					Dbps 1
	40 / 20		S2: 40 / 20					
	42 / 18		S2: 42 / 18					
	38 / 10		S2: 38 / 10					
	40 / 12		S2: 40 / 12					
68	42 / 12		S2: 42 / 12					Dbps 1
	40 / 20		S2: 40 / 20					
	42 / 18		S2: 42 / 18					
	38 / 10		S2: 38 / 10					
	40 / 12		S2: 40 / 12					
69	42 / 12		S2: 42 / 12					Dbps 1
	40 / 20		S2: 40 / 20					
	42 / 18		S2: 42 / 18					
	38 / 10		S2: 38 / 10					
	40 / 12		S2: 40 / 12					
70	12 / 15			218 / 78			210 / 90	Dbps 1
	10 / 10			142 / 70			198 / 84	
				70 / 90				
71	22 / 10			272 / 84			210 / 90	Dbps 1
				258 / 82			198 / 84	
72	30 / 10		S2: 30 / 10				210 / 85	Dbps 1
	30 / 15		S2: 30 / 15				210 / 80	
73	30 / 10		S2: 30 / 10				210 / 85	Dbps 1
	30 / 15		S2: 30 / 15				210 /80	
74	30 / 10		S2: 30 / 10					Dbps 1
	30 / 15		S2: 30 / 15					
75	152 / 20			198 / 88				Dbcs 11
	94 / 15			210 / 82				
	130 / 12			250 / 82				
				246 / 81				
76	65 / 15			224 / 78				Dbcs 11
	68 / 18			234 / 76				
77	40 / 15						210 / 88	Dbps 1
	38 / 20						218 / 82	
	37 / 18						300 / 80	
							300 / 75	
78	40 / 15		S2: 40 / 15					Dbps 1
	38 / 20		S2: 38 / 20					
	36 / 19		S2: 36 / 19					
79	41 / 16		S2: 41 / 16					Dbps 1
	38 / 20		S2: 38 / 20					
	37 / 18		S2: 37 / 18					
80	40 / 15		S2: 40 / 15					Dbps 1
	38 / 20		S2: 38 / 20					
	39 / 18		S2: 39 / 18					
81	40 / 16		S2: 40 / 16					Dbps 1
	38 / 20		S2: 38 / 20					

Table 1: Field Measuring Data

Location	Bedding	Fold Limbs	Cleavage	Joints	Faults	Lineation	Quartz Veins	Rock Unit
	40 / 18		S2: 40 / 18					
82	40 / 15		S2: 40 / 15					Dbps 1
	36 / 17		S2: 36 / 17					
	39 / 18		S2: 39 / 18					
83	37 / 15		S2: 37 / 15					Dbps 1
	38 / 20		S2: 38 / 20					
	40 / 18		S2: 40 / 18					
84	40 / 16		S2: 40 / 16					Dbps 1
	35 / 16		S2: 35 / 16					
	36 / 17		S2: 36 / 17					
85	42 / 14			206 / 79				Dbss 2
	340 / 25			64 / 79				
				148 / 84				
				210 / 89				
86	22 / 21			200 / 80			142 / 86	Dbss 2
	42 / 08			332 / 70				
87	75 / 20			242 / 70				Dbcs 30
	60 / 20			242 / 68				
	68 / 40			52 / 85				
	68 / 35			54 / 80				
88								Dbcs 30
89		196 / 30						Dbcs 31
		148 / 85						
		330 / 65						
90		340 / 42		94 / 85				Dbcs 31
		346 / 46		270 / 85				
94								Dbcs 31
92								Dbcs 31
93	68 / 15			72 / 55				
	60 / 16							
94		18 / 36	S2: 40 / 20	264 / 82			200 / 65	Dbcs 43
		72 / 40		263 / 79			186 / 82	
				10 / 85			190 / 85	
				150 / 85				
95		10 / 22	S2: 42 / 28	136 / 84				Dbcs 43
		84 / 31	S2: 40 / 29	200 / 72				
				336 / 85				
96			S2: 45 / 25					Dbcs 44
			S2: 42 / 26					
97		310 / 30	S2: 46 / 15	210 / 70				Dbcs 44
		328 / 34	S2: 40 / 16	204 / 60				
			S2: 48 / 12	210 / 65				
				142 / 72				
				142 / 80				
98			S2: 46 / 15	210 / 70				Dbcs 44
			S2: 40 / 16	204 / 60				
			S2: 48 / 12	210 / 65				

Table 1: Field Measuring Data

Location	Bedding	Fold Limbs	Cleavage	Joints	Faults	Lineation	Quartz Veins	Rock Unit
				142 / 72				
				142 / 80				
99		118 / 65	S2: 42 / 20	200 / 78				Dbcs 43
		114 / 36	S2: 40 / 22	202 / 79				
		350 / 40	S3: 330 / 30	200 / 80				
		334 / 49	S3: 335 / 29	200 / 80				
				200 / 74				
				72 / 75				
				76 / 75				
				214 / 56				
				48 / 76				
				46 / 77				
				46 / 76				
100			S2: 42 / 20	200 / 78				Dbcs 43
			S2: 40 / 22	202 / 79				
			S3: 330 / 30	200 / 80				
			S3: 335 / 29	200 / 80				
				200 / 74				
				72 / 75				
				76 / 75				
				214 / 56				
				48 / 76				
				46 / 77				
				46 / 76				
101		0 / 35	S2: 30 / 20	258 / 85			210 / 80	Dbcs 43
		348 / 45	S2: 50 / 20	258 / 80			210 / 85	
		155 / 68		212 / 68			25 / 85	
102		0 / 35	30 / 20					Dbcs 44
		348 / 45	S2: 50 / 20					
		155 / 68						
103		40 / 35	S3: 348 / 26	148 / 76			312 / 82	Dbcs 43
		48 / 38	S2: 60 / 30	310 / 80			210 / 65	
		62 / 25	S2: 58 / 30					
104	40 / 29		S2: 40 / 30					Dbcs 43
105	40 / 30		S2: 40 / 30					Dbcs 44
106	40 / 30		S2: 40 / 30					Dbcs 44
107	40 / 30		S2: 40 / 30					Dbcs 44
108			S3: 342 / 35	242 / 80			212 / 80	Dbcs 43
			S3: 350 / 35	90 / 90			210 / 75	
			S3: 343 / 35	82 / 88			202 / 65	
109		330 / 79	S2: 70 / 20				210 / 85	Dbcs 43
		152 / 39						
		104 / 50						
		320 / 85						
110				238 / 89				Dbcs 2
				72 / 85				
				70 / 70				
				324 / 85				
111			S2: 30 / 20					Dbcs 2
112			S2: 30 / 20					Dbcs 2

Table 1: Field Measuring Data

Location	Bedding	Fold Limbs	Cleavage	Joints	Faults	Lineation	Quartz Veins	Rock Unit
113			S2: 30 / 20					Dbcs 2
114	14 / 18		S2: 14 / 18					Dbcs 2
	25 / 15		S2: 25 / 15					
115	68 / 15		S2: 68 / 15				258 / 50	Dbcs 2
	42 / 22		S2: 42 / 22					
	52 / 30		S2: 52 / 30					
116	32 / 16		S2: 32 / 16	98 / 82			150 / 90	Dbcs 2
	41 / 25		S2: 41 / 25	272 / 85			150 / 85	
				260 / 75			162 / 85	
							258 / 80	
117	20 / 20		S2: 20 / 20	248 / 80			310 / 83	Dbcs 3
	25 / 20		S2: 25 / 20	238 / 70			316 / 84	
				286 / 88				
118								Dbcs 3
119			S3: 0 / 40					Dbcs 2
			S3: 355 / 30					
			S2: 10 / 25					
120	30 / 20		S2: 30 / 20	64 / 89				Dbcs 4
				242 / 85				
				238 / 85				
121	60 / 26		S2: 60 / 26	254 / 85				Dbcs 4
	20 / 30		S2: 20 / 30	228 / 85				
	20 / 30		S2: 20 / 30					
	35 / 25		S2: 35 / 25					
			S3: 0 / 30					
122			S2: 50 / 20	88 / 85			150 / 90	Dbcs 2
			S2: 50 / 19	268 / 82			150 / 89	
				264 / 88				
123	48 / 15		S2: 48 / 15	2 / 85				Dbcs 2
	30 / 15		S2: 30 / 15	10 / 85				
				250 / 80				
				250 /82				
124			S2: 45 / 10	58 / 76			130 / 85	Dbs 3
			S2: 45 / 10	58 / 85			130 / 88	
			S2: 42 / 08	274 / 88			230 / 80	
				280 / 75				
125			S2: 12 / 16	45 / 85			132 / 84	Dbs 3
			S2: 12 / 16	45 / 85			212 / 85	
			S2: 45 / 10	74 / 89				
			S2: 50 / 20	75 / 90				
				132 / 88				
				212 / 85				
				310 / 85				
126			S2: 20 / 15	210 / 70				Dbs 5
			S2: 30 / 15	212 / 75				
				90 / 80				
				90 / 80				
127			S3: 322 / 30	44 / 85				Dbcs 9
			S3: 320 / 28	44 / 89				
128			S2: 90 / 30					Dbcs 9

Table 1: Field Measuring Data

Location	Bedding	Fold Limbs	Cleavage	Joints	Faults	Lineation	Quartz Veins	Rock Unit
			S2: 90 / 30					
129		304 / 74	S2: 50 / 17	204 / 89				Dbcs 18
		106 / 39	S2: 50 / 20	210 / 89				
130			S3: 350 / 20	220 / 65			240 / 85	Dbcs 16
			S3: 348 / 20					
131								Dbcs 13
132								Dbcs 13
133								Dbcs 14
134	40 / 15		S2: 40 / 14	210 / 75				Dbcs 14
	41 / 15		S2: 41 / 15	210 / 65				
				134 / 70				
				130 / 70				
135	48 / 26		S2: 48 / 26	204 / 75			210 / 60	Dbcs 5
	50 / 30		S2: 50 / 30	206 / 80			220 / 60	
				112 / 70				
136	48 / 26		S2: 48 / 26	204 / 75			204 / 75	Dbcs 5
	50 / 30		S2: 50 / 30	206 / 80			206 / 80	
				112 / 70			112 / 70	
137	40 / 20		S2: 40 / 20	210 / 90			210 / 90	Dbcs 17
	40 / 19		S2: 40 / 19	90 / 90			220 / 85	
138	100 / 15		S2: 100 / 15	210 / 85			210 / 85	Dbcs 18
	102 / 20		S2: 102 / 20	258 / 80				
	86 / 16		S2: 86 / 16					
	90 / 20		S2: 90 / 20					
139	42 / 18		S2: 42 / 12				212 / 80	Dbcs 18
	30 / 18		S2: 30 / 18					
	42 / 15		S2: 42 / 15					
140			S2: 20 / 15	68 / 90			220 / 75	Dbcs 43
			S2: 22 / 15	224 / 85				
			S2: 20 / 20	160 / 65				
				160 / 75				
141	44 / 16		S2: 44 / 16	220 / 75				Dbcs 43
	24 / 16		S2: 24 / 16					
	20 / 10		S2: 20 / 10					
	34 / 20		S2: 34 / 20					
142	50 / 20							Dbcs 37
143	44 / 17		S2: 44 / 17	224 / 70			270 / 78	Dbcs 37
	48 / 19		S2: 48 / 19	225 / 70				
				312 / 86				
				312 / 80				
144	44 / 17		S2: 44 / 17	224 / 70			270 / 80	Dbcs 37
	48 / 19		S2: 48 / 19	225 / 70				
				312 / 86				
				312 / 80				
145							310 / 77	Dbcs 37
							308 / 65	
146	46 / 10		S2: 46 / 10				210 / 80	Dbcs 33
	45 / 20		S2: 45 / 20				220 / 70	
	40 / 19		S2: 40 / 19					
147	50 / 20		S2: 50 / 20	310 / 75				Dbcs 33

Table 1: Field Measuring Data

Location	Bedding	Fold Limbs	Cleavage	Joints	Faults	Lineation	Quartz Veins	Rock Unit
				226 / 72				
148	40 / 20		S2: 40 / 20				216 / 75	Dbcs 36
	38 / 16		S2: 38 / 16					
149	60 / 20		S2: 60 / 20	220 / 60				Dbcs 32
				310 / 80				
150	50 / 20		S2: 50 / 20					Dbcs 32
	40 / 24		S2: 40 / 24					
151	50 / 19		S2: 50 / 19					Dbcs 32
	45 / 22		S2: 45 / 22					
	47 / 20		S2: 47 / 20					
152			S2: 55 / 22	290 / 85				Dbcs 41
153		130 / 15						Dbcs 41
		130 / 30		58 / 75				
				54 / 75				
154		108 / 25						Dbcs 41
		134 / 44						
		150 / 85						
		10 / 40						
155		330 / 35		230 / 82				Dbcs 41
		162 / 85		228 / 72				
		170 / 60						
156			S2: 64 / 15	218 / 75				Dbcs 40
				46 / 79				
				320 / 78				
157			S2: 60 / 25				225 / 85	Dbcs 40
			S2: 55 / 25					
158			S2: 60 / 20					Dbcs 39
159		138 / 64						Dbcs 39
		130 / 25						
		130 / 35						
160		148 / 80				10 / 15		Dbcs 29
161		350 / 25		222 / 85			238 / 80	Dbcs 29
							250 / 60	
162		112 / 45						Dbcs 28
163		124 / 20		62 / 80				Dbcs 28
				63 / 80				
				288 / 60				
164		340 / 60					280 / 75	Dbcs 28
165	122 / 12							Dbss 2
	155 / 25							
166		308 / 42						Dbss 2
		210 / 45						
167	190 / 29		S3: 190 / 29	54 / 75			290 / 60	Dbss 2
	140 / 40		S3: 140 / 40	56 / 70			300 / 60	
	150 / 35		S3: 150 / 35				304 / 65	
168		158 / 25						Dbss 2
169		220 / 45					310 / 89	Dcc
		210 / 35					308 / 89	
		164 / 55						
		184 / 48						

Table 1: Field Measuring Data

Location	Bedding	Fold Limbs	Cleavage	Joints	Faults	Lineation	Quartz Veins	Rock Unit
		190 / 45						
		172 / 62						
		170 / 40						
170	190 / 49			334 / 45				Dcss
	180 / 40			332 / 45				
	180 / 35			72 / 80				
				80 / 82				
				280 / 59				
171		155 / 30		320 / 65			262 / 50	Dbss 1
		150 / 30		340 / 80				
172								Dbs 10
173								Dbs 10
174	40 / 15							Dbs 10
	34 / 15							
	52 / 12							
175	12 / 15							Dbps 1
176	270 / 20			18 / 80			20 / 85	Dbps 1
	262 / 20			20 / 80				
				64 / 85				
				20 / 50				
177	40 / 10			88 / 78			202 / 85	Dbps 1
	30 / 10			250 / 75			198 / 85	
				90 / 90				
178	10 / 10			72 / 75			358 / 45	
				72 / 80			350 / 38	
				170 / 75			206 / 80	Dbps 1
				184 / 87			200 / 80	Dbps 1
				138 / 89				
179	10 / 10			184 / 85			350 / 45	
				184 / 80			202 / 85	Dbps 1
180	353 / 22			46 / 70				Dbcs 1
	352 / 25			190 / 75				
181	340 / 20		S2: 0 / 10	20 / 84			212 / 80	Dbcs 1
	352 / 15			40 / 85				
	0 / 10			32 / 85				
				148 / 47				
				90 / 80				
				48 / 90				
182							210 / 85	Dbcs 1
183		0 / 15		240 / 65			204 / 80	Dbcs 1
		358 / 30					206 / 75	
184		320 / 32	S3: 340 / 33	62 / 85				Dbcs 1
185	10 / 10		S2: 10 / 10	200 / 70				Dbsp 4
				140 / 50				
186	0 / 12		S2: 0 / 12					Dbps 3
187	350 / 15		S2: 350 / 15				220 / 80	Dbps 3
188	354 / 12		S2: 354 / 12	210 / 90				Dbps 3
				200 / 45				
189	350 / 08		S2: 350 / 08	78 / 90				Dbps 3
				220 / 89				

Table 1: Field Measuring Data

Location	Bedding	Fold Limbs	Cleavage	Joints	Faults	Lineation	Quartz Veins	Rock Unit
				260 / 80				
190	340 / 20		S3: 340 / 35					Dbps 2
	342 / 15		S2: 342 / 15					
191	10 / 10		S2: 10 / 10					Dbps 2
	12 / 15		S2: 12 / 15					
192	350 / 10		S2: 350 / 10	218 / 55		132 / 20	214 / 85	Dbcs 1
	350 / 12		S2: 350 / 12	164 / 89		132 / 21	210 / 85	
						130 / 20		
193	350 / 11		S2: 350 / 11	216 / 85			212 / 85	Dbcs 1
	330 / 15		S2: 330 / 15	72 / 80			212 / 84	
			S3: 330 / 30	70 / 88				
			S3: 340 / 31	140 / 55				
			S3: 350 / 33	136 / 50				
194	350 / 15		S3: 350 / 15	22 / 50				Dbps 3 / 4
				140 / 89				
195							190 / 90	Dbps 2 / 3
196							185 / 90	Dbps 2
197							190 / 90	Dbps 2
198							195 / 90	Dbps 2
199	18 / 10		S2: 18 / 10	260 / 80			216 / 80	Dbs un.
	340 / 10		S2: 340 / 10					
	340 / 15		S2: 340 / 15					
200	18 / 10		S2: 18 / 10	260 / 80				Dbs un.
	340 / 10		S2: 340 / 10					
	340 / 15		S2: 340 / 15					
201	350 / 15		S2: 350 / 15	80 / 87				Dbss 2
	350 / 15		S2: 350 / 15	194 / 75				
				192 / 76				
202	2 / 20		S2: 2 / 20	277 / 86				Dbs 1
	14 / 22		S2: 14 / 22	160 / 85				
	10 / 10		S2: 10 / 10	2 / 54				
				220 / 70				
				154 / 75				
				278 / 85				
				12 / 88				
				12 / 88				
203	10 / 10		S2: 10 / 10	142 / 80			142 / 85	Dbss 2
				212 / 75				
204	10 / 10		S2: 10 / 10	320 / 89			220 / 60	Dbps 1
	2 / 10		S2: 2 / 10	340 / 80			80 / 80	
				150 / 86				
205	10 / 10		S2: 10 / 10		182 / 66			Dbsp 1
					170 / 70			
					172 / 76			
206	10 / 10		S2: 10 / 10	264 / 88				Dbps 1
				48 / 89				
				320 / 89				
				8 / 81				
207	86 / 15	130 / 30	S2: 86 / 15	200 / 90			192 / 80	Dbcs 19
	96 / 25		S2: 96 / 25	272 / 89			192 / 80	

Table 1: Field Measuring Data

Location	Bedding	Fold Limbs	Cleavage	Joints	Faults	Lineation	Quartz Veins	Rock Unit
	96 / 15		S2: 96 / 15	272 / 80				
208	86 / 15		S2: 86 / 15				208 / 85	Dbcs 19
	96 / 25		S2: 96 / 25					
	96 / 15		S2: 96 / 15					
209	132 / 30		S2: 132 / 30	240 / 85				Butte Mt. Slate
	128 / 26		S2: 128 / 26	241 / 86				
				160 / 80				
				162 / 79				
	130 / 30		S2: 130 / 30	161 / 78				
210	142 / 25		S2: 142 / 25	260 / 85				Butte Mt. Slate
				259 / 84				
				255 / 85				
				160 / 80				
				161 / 79				
	142 / 25		S2: 142 / 25	140 / 75				
211	100 / 20		S2: 100 / 20	16 / 72				Butte Mt. Slate
	112 / 20		S2: 112 / 20	312 / 80				
	110 / 19		S2: 110 / 19	320 / 84				
				315 / 85				
				252 / 85				
				250 / 84				
				249 / 82				
				261 / 80				
				260 / 74				
212 a	48 / 25							Dbcs un.
212 b								Dbcs un.
213								Dbs 1
214								Dbs 2
215	60 / 20		S2: 60 / 20	140 / 84				Dbs 1
	59 / 20		S2: 59 / 20	138 / 82				
216	60 / 19		S2: 60 / 19				232 / 65	Dbcs 20
	60 / 25		S2: 60 / 25					
217								Dbcs 21
218	40 / 22		S2: 40 / 22	148 / 65			222 / 45	Dbcs 21
				154 / 70				
219		320 / 60						Dbcs 22
		130 / 75						
		320 / 42						
220								Dbcs 22
221							290 / 71	Dbcs 23
222	90 / 19		S2: 90 / 19				270 / 57	Dbcs 24 / 25
	70 / 20		S2: 70 / 20					
223	55 / 15		S2: 55 / 15					Dbcs 25
	45 / 20		S2: 45 / 20					
224	72 / 15		S2: 72 / 15					Dbcs 25
	60 / 20		S2: 60 / 20					
225	114 / 15			54 / 85				Dbcs 26
	124 / 32			50 / 75				
226								Dbcs 27
227								Dbcs 27

Table 1: Field Measuring Data

Location	Bedding	Fold Limbs	Cleavage	Joints	Faults	Lineation	Quartz Veins	Rock Unit
228	22 / 15		S2: 22 / 15				223 / 85	Dbcs 27
229							310 / 60	Dbcs 28
230	45 / 25		S2: 45 / 25				310 / 60	Dbcs 28
							262 / 55	
231	45 / 20		S2: 45 / 20					Dbcs 38
232								Dbcs 38
233	68 / 12		S2: 68 / 12					Dbcs 32
234	50 / 20	152 / 75	S2: 50 / 20	210 / 78				Dbcs 32
	40 / 24	134 / 20	S2: 40 / 24	210 / 89				
235	10 / 15		S2: 10 / 15	350 / 55			310 / 89	Dbcs 32
	20 / 12		S2: 20 / 12	214 / 84				
				144 / 80				
236	10 / 15		S2: 10 / 15					Dbcs 32
	20 / 12		S2: 20 / 12					
237	60 / 20		S2: 60 / 20	228 / 70			238 / 82	Dbcs 32
	50 / 20		S2: 50 / 20	310 / 80			236 / 85	
				310 / 75				
238	40 / 19		S2: 40 / 19					Dbcs 32
	20 / 15		S2: 20 / 15					
	38 / 15		S2: 38 / 15					
239								Dbcs 6
240								Dbcs 3
241	70 / 10		S2: 70 / 10	260 / 85				Dbs 8
	50 / 10		S2: 50 / 10					
242	45 / 10		S2: 45 / 10				200 / 90	Dbs 8
243	30 / 15		S2: 30 / 15		0 / 86			Dbs 8
	40 / 20		S2: 40 / 20		0 / 85			
244	12 / 12		S2: 12 / 12					Dbs 7
	30 / 15		S2: 30 / 15					
	30 / 18		S2: 30 / 18					
245							148 / 80	Dbs 7
							190 / 90	
248	55 / 22		S2: 55 / 22	252 / 81			310 / 81	Dbs 6
248	50 / 20		S2: 55 / 22				22 / 90	Dbs 6
	70 / 20						25 / 90	
248	100 / 25		S2: 100 / 25	210 / 75			208 / 84	Dbs 6
	86 / 18		S2: 36 / 18	212 / 85			210 / 85	
				250 / 90				
249	48 / 10		S2: 48 / 10	149 / 70			136 / 85	Dbs 6
	40 / 15		S2: 40 / 15				212 / 70	
250	22 / 24		S2: 22 / 24				210 / 70	Dbs 6
							200 / 85	
							200 / 85	
							140 / 80	
251							206 / 65	Dbs 6
							210 / 75	
							210 / 75	
252	42 / 16		S2: 42 / 16	266 / 75				Dbs 5
				262 / 80				
253	72 / 10		S2: 72 / 10		30 / 75			Dbs

Table 1: Field Measuring Data

Location	Bedding	Fold Limbs	Cleavage	Joints	Faults	Lineation	Quartz Veins	Rock Unit
	30 / 10		S2: 30 / 10		22 / 60			
254							222 / 78	Dbs 5
							220 / 80	
							210 / 80	
255							210 / 82	Dbs 5
256	38 / 10		S2: 38 / 10				212 / 75	Dbs 5
							210 / 70	
							210 / 75	
							210 / 75	
257							210 / 75	Dbs 5
258	52 / 10		S2: 52 / 10				214 / 75	Dbs 5
							210 / 78	
259								Dbs 5
260								Dbcs 4
261								Dbcs 4
262								Dbcs 5
263		115 / 40					200 / 75	Dbcs 5
		340 / 65					208 / 78	
		340 / 45						
		132 / 30						
264	30 / 10		S2: 30 / 10				0 / 80	Dbcs 5
							0 / 80	
265							228 / 55	Dbs 5
266	0 / 16		S2: 0 / 16	52 / 85			132 / 85	Dbss 2
	28 / 05		S2: 28 / 05	52 / 90			134 / 86	
	40 / 20		S2: 40 / 20	200 / 85				
	10 / 24		S2: 10 / 24					
267	58 / 15		S2: 58 / 15					Dbs 5
268	64 / 20		S2: 64 / 20					Dbs 5
269								Dcc
270							202 / 80	Dbss 1
271							278 / 52	Dcss
							272 / 55	
							274 / 53	
272							200 / 70	Dbcs 43
273 a	14 / 25	32 / 58	S3: 350 / 30	75 / 80			208 / 80	Dbcs 44
	20 / 20			80 / 75			208 / 85	
							210 / 80	
273 b							320 / 75	Dbcs 44
274								Dbcs 11
275	114 / 10		S2: 114 / 10					Dbcs 9
	132 / 12		S2: 132 / 12					
276	60 / 20		S2: 60 / 20				210 / 85	Dbcs 9
							210 / 80	
277	320 / 10		S2: 320 / 10					Dbcs 8
278							208 / 85	Dbcs 8
279	20 / 35		S2: 20 / 35				210 / 85	Dbcs 7
	30 / 30		S2: 30 / 30					
280	42 / 15		S2: 42 / 15					Dbcs 7

Table 1: Field Measuring Data

Location	Bedding	Fold Limbs	Cleavage	Joints	Faults	Lineation	Quartz Veins	Rock Unit
281								Dbcs 18
282	0 / 15		S2: 0 / 15				190 / 85	Dbcs 18
	38 / 15		S2: 38 / 15				196 / 78	
	30 / 20		S2: 30 / 20					
283	350 / 15		S2: 350 / 15					Dbss 2
284	350 / 15		S2: 350 / 15					Dbss 2
285	350 / 12		S2: 350 / 12	210 / 75				Dbss 2
	352 / 14		S2: 352 / 14	86 / 85				
286	350 / 12		S2: 350 / 12					Dbss 2
	352 / 14		S2: 352 / 14					
287	350 / 10		S2: 350 / 10					Dbs un.
288								Dbss 2
289	20 / 20		S2: 20 / 20	8 / 90				Dbss 2
	30 / 19		S2: 30 / 19	180 / 85				
				84 / 85				
				80 / 85				
				210 / 85				
				254 / 80				
290	40 / 15		S2: 40 / 15	210 / 85				Dbss 2
	32 / 15		S2: 32 / 15	130 / 85				
	32 / 15		S2: 32 / 15	160 / 75				
291								Dbss 2
292	36 / 13		S2: 36 / 13	0 / 70			138 / 85	Dbss 2
	40 / 20		S2: 40 / 20	208 / 85			140 / 80	
				22 / 89			136 / 86	
293	36 / 13		S2: 36 / 13					Dbss 2
	40 / 20		S2: 40 / 20					
294	60 / 21		S2: 60 / 21				210 / 80	Dbcs 43
	58 / 23		S2: 58 / 23					
295	52 / 22		S2: 52 / 55				210 / 85	Dbcs 43
							210 / 85	
296								Dbcs 43
297	44 / 25		S2: 44 / 25				210 / 85	Dbcs 43
298								Dbcs 43
299	100 / 20		S2: 100 / 20					Dbcs 43
300								Dbcs 44
301							88 / 85	Dbcs 44
30[illegible]				240 / 88			204 / 85	Dbcs 44
303								Dbcs 44
304								Dbcs 44
305								Dbcs 44
306	10 / 22		S2: 10 / 22					Dbcs 44
307	40 / 15		S2: 40 / 15					Dbcs 42
	40 / 20		S2: 40 / 20					
308	40 / 15		S2: 40 / 15					Dbcs 42
	40 / 20		S2: 40 / 20					
309	30 / 20		S2: 30 / 20	250 / 62			290 / 75	Dbcs 42
	40 / 15		S2: 40 / 15				285 / 77	
			S3: 350 / 30					
310							224 / 70	Dbcs 42

Table 1: Field Measuring Data

Location	Bedding	Fold Limbs	Cleavage	Joints	Faults	Lineation	Quartz Veins	Rock Unit
							134 / 80	
							135 / 80	
311	350 / 20		S3: 350 / 30				300 / 90	Dbcs 42
	0 / 20		S3: 0 / 25					
312				238 / 70				Dbcs 42
313	88 / 25		S2: 88 / 25				290 / 72	Dbcs 42
	76 / 25		S2: 76 / 25					
314	80 / 15		S2: 80 / 15				294 / 80	Dbcs 32
	76 / 15		S2: 76 / 15					
315	35 / 15		S2: 35 / 15	244 / 80			230 / 80	Dbcs 32
				10 / 75			300 / 70	
316	45 / 20		S2: 45 / 20					Dbcs 32
	40 / 20		S2: 40 / 20					
	50 / 20		S2: 50 / 20					
317	82 / 30						302 / 85	Dbcs 36
							274 / 82	
318	60 / 25		S2: 60 / 25					Dbcs 36
	55 / 20		S2: 55 / 20					
319	57 / 20		S2: 57 / 20					Dbcs 33
320	70 / 20		S2: 70 / 20					Dbcs 33
	70 / 21		S2: 70 / 21					
321								Dbcs 33
322			S2: 62 / 20				300 / 75	Dbcs 33
			S2: 55 / 20					
323	62 / 21		S2: 62 / 21					Dbcs 34
	66 / 23		S2: 66 / 23					
324								Dbcs 34
325								Dbs 1
326								Dbs 1
327								Dbs un.
328	108 / 20		S2: 108 / 20	212 / 90			195 / 85	Dbcs 6
	85 / 20		S2: 85 / 20				200 / 85	
329	12 / 10		S2: 12 / 10	200 / 84				Dbcs 7
	30 / 12		S2: 30 / 12	110 / 85				
330								Dbcs 7
331								Dbcs 7
332	62 / 30		S2: 62 / 30	4 / 85			130 / 85	Dbs 6
	60 / 25		S2: 60 / 25	350 / 72				
333								Dbs 8
334	12 / 14		S2: 12 / 14	45 / 80				Dbss 2
335	310 / 08		S2: 310 / 08	182 / 87			190 / 90	Dbps 1
	310 / 10		S2: 310 / 10	250 / 85				
				210 / 90				
336	310 / 08		S2: 310 / 08				200 / 75	Dbps 1
	310 / 10		S2: 310 / 10					
337	52 / 08		S2: 52 / 08				210 / 85	Dbps 1
	60 / 09		S2: 60 / 09				210 / 80	
							206 / 80	
							208 / 84	
338	32 / 09		S2: 32 / 09	278 / 74				Dbps 1

Table 1: Field Measuring Data

Location	Bedding	Fold Limbs	Cleavage	Joints	Faults	Lineation	Quartz Veins	Rock Unit
				278 / 78				
339	30 / 10		S2: 30 / 10					Dbps 2
340	12 / 10		S2: 12 / 10					Dbps 1
	11 / 09		S2: 11 / 09					
341	10 / 10		S2: 10 / 10					Dbps 1
	12 / 09		S2: 12 / 09					
342	75 / 15		S2: 75 / 15					Dbps 1
	75 / 12		S2: 75 / 12					
343	20 / 12		S2: 20 / 12	180 / 85				Dbps 1
	15 / 12		S2: 15 / 12	190 / 85				
				220 / 80				
				250 / 87				
				140 / 85				
344	16 / 10		S2: 16 / 10					Dbps 1
	14 / 12		S2: 14 / 12					
345	11 / 10		S2: 11 / 10					Dbps 1
	12 / 10		S2: 12 / 10					
346								Dbps 1
347	114 / 35		S2: 114 / 35				210 / 80	Dbcs 10
	80 / 20		S2: 80 / 20					
348	78 / 29		S2: 78 / 29	320 / 70				Dbcs 10
	60 / 20		S2: 60 / 20					
349	100 / 15		S2: 100 / 15	290 / 65			208 / 86	Dbcs 10
	90 / 20		S2: 90 / 20	210 / 85				
350	70 / 15		S2: 70 / 15					Dbcs 10
351	64 / 16		S2: 64 / 16					Dbcs 9
352								Dbcs 9
353								Dbcs 9
354	62 / 15		S2: 62 / 15					Dbcs 45
355							200 / 75	Dbcs 45
356								Dbcs 45
357								Dbcs 45
358							220 / 85	Dbcs 45
359	14 / 21						330 / 79	Dbs 4
	38 / 21						330 / 85	Dbs
							330 / 80	Dbs
360							210 / 85	Dbs 5
361								Dbs 5
362								Dbs 5
363								Dbcs 9
364	75 / 08						220 / 80	Dbs 5
365								Dbss 2
366								Dbss 2
367								Dbss 2
368								Dcss
369								Dbss 1
370								Dcss

TABLE 2a: ASSAY DATA - SAMPLE RECORD ABBREVIATIONS

Sample Site

core	drill core
drum	55 gallon drum
flt	float
otc	outcrop
rub	rubblecrop
tail	mine tailings
trn	trench

Placer gold: size classification

v. fine	< 0.5 mm
fine	0.5 - 1.0 mm
coarse	1 -2 mm
v. coarse	> 2 mm

Footnotes:

Bold numbers indicate multiple erratic results, which were averaged.
IS denotes insufficient sample volume for analysis of all elements.
Results for Au are reported in ppb unless other units are stated.

Sample Type

cont	continuous chip
grab	grab sample
pan	pan sample
plac	placer sample
rand	random chip
rep	representative chip
sed	sediment sample
sel	select
slu	sluice concentrate
soil	soil sample
spac	spaced chip

Sample Description

abu	abundant
Ag	silver
alt	altered, alteration
amph	amphibole
ank	ankerite
apy	arsenopyrite
Au	gold
az	azurite
ba	barite
bio	biotite
blk	black
bn	bornite
box	boxworks
brn	brown
ca	calcite
calc	calcareous
carb	carbonate
cc	chalcocite
cgl	conglomerate
ch	chlorite
comp	composite
con	concentrate
cont	continuous
cpy	chalcopyrite
cst	cassiterite
Cu	copper
cv	covellite
diss	disseminated
ep	epidote
feld	feldspar
ft	foot (12 inches)
gar	garnet
gn	galena
gwy	graywacke
hbl	hornblende
hem	hematite
hfls	hornfels
Hg	mercury
hydro	hydrothermal
in	inch
intr	intrusive

Sample Description

lim	limonite
ls	limestone
lt	light
mag	magnetite
mal	malachite
mdst	mudstone
meta	metamorphic
MnO	manganese oxide
Mo	molybdenum
mod	moderate
monz	monzonite
musc	muscovite
oz/cyd	ounces per cubic yard
oz/st	ounces per short ton
po	pyrrhotite
ppb	parts per billion
ppm	parts per million
psuedo	psuedomorph
py	pyrite
qtz	quartzite
qz	quartz
sch	scheelite
sco	scorodite
sed	sediment
ser	sericite
serp	serpentinized
sid	siderite
sl	sphalerite
slts	siltstone
ss	sandstone
stb	stibnite
tet	tetrahedrite
tm	tourmaline
tr	trace
v	very
val	valentinite
volc	volcanic
w/	with
xcut	crosscutting
xln	crystalline
xls	crystals

Elements

Ag	silver
Al	aluminum
As	arsenic
Au	gold
Ba	barium
Bi	bismuth
Ca	calcium
Cd	cadmium
Co	cobalt
Cr	chromium
Cu	copper
Fe	iron
Ga	gallium
Hg	mercury
K	potassium
La	lanthanum
Li	lithium
Mg	magnesium
Mn	manganese
Mo	molybdenum
Na	sodium
Nb	niobium
Ni	nickel
Pb	lead
Pd	palladium
Pt	platinum
Sb	antimony
Sc	scandium
Sn	tin
Sr	strontium
Ta	tantalum
Te	tellurium
Ti	titanium
V	vanadium
W	tungsten
Y	yttrium
Zn	zinc
Zr	zirconium

TABLE 2b: ASSAY DATA - ANALYTICAL PROCEDURES

Intertek Testing Services - Bondar Clegg - Vancouver, Canada. Standard Fire Assay Analysis for Gold, Platinum, and Palladium

Element	Element	Minimum Detection	Finish Method
Au	gold	5 ppb	atomic absorption
	gold	1 ppb	ICP
Pt	platinum	5 ppb	ICP
Pd	palladium	1 ppb	ICP

Minimum Detections for ICP - Atomic Emission Analyses (Standard Run)

Element	Element	Minimum Detection	Element	Element	Minimum Detection
Ag	silver	0.2 ppm	Mo	molybdenum	1 ppm
Al	aluminum	0.01 %	Na	sodium	0.01 %
As	arsenic	5 ppm	Nb	niobium	1 ppm
Ba	barium	1 ppm	Ni	nickel	1 ppm
Bi	bismuth	5 ppm	Pb	lead	2 ppm
Ca	calcium	0.01 %	Sb	antimony	5 ppm
Cd	cadmium	0.2 ppm	Sc	scandium	5 ppm
Co	cobalt	1 ppm	Sn	tin	20 ppm
Cr	chromium	1 ppm	Sr	strontium	1 ppm
Cu	copper	1 ppm	Ta	tantalum	10 ppm
Fe	iron	0.01 %	Te	tellurium	10 ppm
Ga	gallium	2 ppm	Ti	titanium	0.01 %
K	potassium	0.01 %	V	vanadium	1 ppm
La	lanthanum	1 ppm	W	tungsten	20 ppm
Li	lithium	1 ppm	Y	yttrium	1 ppm
Mg	magnesium	0.01 %	Zn	zinc	1 ppm
Mn	manganese	1 ppm	Zr	zirconium	1 ppm

Methods and Minimum Detections for Ore Grade Runs

Element	Element	Method	Minimum Detection
Ag	silver	fire assay, gravimetric finish	0.7 ppm
Au	gold	fire assay, gravimetric finish	0.17 ppm
Bi	bismuth	atomic absorption low level assay	0.005 %
Ba	barium	atomic absorption	0.01 %
Cu	copper	atomic absorption low level assay	0.01 %
Fe	iron	atomic absorption low level assay	0.01 %
Pb	lead	atomic absorption low level assay	0.01 %
Sb	antimony	atomic absorption low level assay	0.01 %
W	tungsten	ICP - peroxide sinter extraction	0.01 %
Zn	zinc	atomic absorption low level assay	0.01 %

TABLE 2c1: ASSAY DATA - GEOCHEMICAL RECONNAISSANCE SAMPLING

Field No.	Latitude	Longitude	Location	Sample Site	Sample Type	Au ppb	Pt ppb	Pd ppb	Ag ppm	Cu ppm	Pb ppm	Zn ppm	Mo ppm	Ni ppm	Co ppm
8035	67.4771	150.2302	Nolan Ck, Tri-Con		pan	> 10000			31			< 390	38	390	130
10647	67.4958	150.1732	Palisades	otc	rand	186			0.4	55	13	22	5	20	6
10648	67.4958	150.1732	Palisades	otc	rand	122			< 0.2	78	20	142	3	62	27
10649	67.4958	150.1732	Palisades	flt	sel	< 5			< 0.2	6	< 2	10	2	13	3
10650	67.4960	150.1549	Palisades	otc	cont	8301			< 0.2	62	5	40	3	49	31
10651	67.5024	150.1378	Palisades	otc	rand	< 5			< 0.2	22	13	38	< 1	23	11
10652	67.5119	150.1189	Slisco Bench	flt	sel	< 5			0.5	4	7	8	3	9	1
10653	67.5206	150.2330	Vermont Ck	otc	rand	< 5			< 0.2	13	14	83	1	28	16
10654	67.5198	150.2298	Vermont Ck	flt	sel	< 5			< 0.2	14	31	14	2	10	4
10663	67.4906	150.1614	Palisades	trn	sel	27			< 0.2	10	< 2	4	5	18	4
10664	67.4906	150.1614	Palisades	trn	rand	< 5			< 0.2	5	< 2	< 1	1	6	< 1
10665	67.4872	150.1598	Smith Ck Dome	flt	sel	93			< 0.2	12	< 2	4	5	14	1
10666	67.4838	150.1572	Smith Ck Dome	trn	sel	436			< 0.2	36	< 2	13	< 1	< 1	< 1
10674	67.4771	150.2302	Nolan Ck, Tri-Con		slu	20			0.2	38	59	5	4	102	425
10675	67.4771	150.2302	Nolan Ck, Tri-Con		slu	79			5.0	137	136	23	47	144	33
10676	67.4771	150.2302	Nolan Ck, Tri-Con		slu	1964			99.9	35	> 10000	4	6	258	122
10701	67.4823	150.1582	Smith Ck Dome	otc	sel	11			< 0.2	175	18	468	2	10	5
10702	67.4677	150.1477	Midnight Dome	otc	sel	11			0.6	152	29	76	1	12	6
10703	67.4610	150.1519	Midnight Dome	trn	sel	14			< 0.2	25	< 2	24	< 1	< 1	2
10704	67.4610	150.1519	Midnight Dome	rub	sel	37			< 0.2	50	61	53	1	18	7
10705	67.4598	150.1557	Midnight Dome, SW	flt	sel	< 5			< 0.2	62	6	25	5	16	3
10706	67.4591	150.1639	Midnight Dome, SW	otc	sel	< 5			< 0.2	67	36	66	2	37	29
10707	67.4591	150.1639	Midnight Dome, SW	otc	rand	< 5			0.3	17	13	23	2	10	6
10708	67.4591	150.1639	Midnight Dome, SW	flt	sel	179			0.6	1469	35	34	2	9	4
10709	67.4594	150.0167	Midnight Dome, SW	rub	sel	< 5			< 0.2	27	82	15	6	16	5
10718	67.4759	150.1736	Smith Ck Dome	otc	sel	< 5			< 0.2	27	178	65	114	45	5
10719	67.4818	150.1663	Smith Ck Dome	flt	sel	70			< 0.2	27	7	34	2	27	17
10720	67.4739	150.1683	Smith Ck Dome	otc	sel	2234			7.2	171	3500	95	4	44	28
10725	67.4750	150.2194	Nolan, Smith Ck	pit	sel	1115			< 0.2	40	< 2	44	< 1	< 1	2
10726	67.4750	150.2194	Nolan, Smith Ck	otc	sel	151			0.6	26	8	32	2	11	5
10727	67.5076	150.1494	Right Fork	otc	grab	1585			0.2	22	29	32	2	19	7
10728	67.5076	150.1494	Right Fork	otc	grab	521			< 0.2	11	22	77	4	23	8
10729	67.5076	150.1494	Right Fork	otc	sel	6			1.3	< 1	1657	269	< 1	6	3
10730	67.5076	150.1494	Right Fork	otc	grab	63.56 ppm			3.9	6	114	23	6	25	5
10731	67.5087	150.1491	Right Fork	flt	grab	38			0.3	33	18	63	< 1	25	9
10732	67.5158	150.1383	Right Fork		pan	5993			0.3	81	23	84	2	57	30

TABLE 2c1: ASSAY DATA - GEOCHEMICAL RECONNAISSANCE SAMPLING

Field No.	Cd ppm	Bi ppm	As ppm	Sb ppm	Hg ppm	Fe pct	Mn ppm	Te ppm	Ba ppm	Cr ppm	V ppm	Sn ppm	W ppm	La ppm	Al pct	Mg pct	Ca pct
8035	< 50		100	196.0		> 10.0		< 200	520	760		< 2000	445	11			
10647	< 0.2	< 5	73	0.35 %	0.358	1.64	3452	< 10	76	234	3	< 20	< 20	5	0.20	0.62	1.42
10648	0.5	< 5	294	204	0.116	2.72	4992	< 10	70	155	5	< 20	< 20	8	0.41	0.18	1.01
10649	< 0.2	< 5	23	372	0.062	0.69	515	< 10	13	290	2	< 20	< 20	1	0.08	0.02	0.10
10650	1.0	< 5	1134	68	0.705	2.18	1690	< 10	52	176	10	< 20	< 20	5	0.35	0.10	0.16
10651	< 0.2	< 5	16	35	0.079	2.03	1697	< 10	64	107	13	< 20	< 20	11	0.85	0.46	0.43
10652	< 0.2	< 5	6	27	0.026	0.76	332	< 10	8	137	2	< 20	< 20	2	0.14	0.34	7.27
10653	< 0.2	< 5	15	18	0.043	6.06	1928	< 10	31	78	60	< 20	< 20	14	2.19	2.59	3.89
10654	< 0.2	< 5	8	36	0.023	1.33	1153	< 10	10	212	5	< 20	< 20	3	0.25	0.52	1.90
10663	2.4	< 5	3035	44	0.069	0.61	179	< 10	6	277	< 1	< 20	< 20	< 1	0.04	0.02	0.04
10664	< 0.2	< 5	44	17	0.015	0.26	67	< 10	3	247	< 1	< 20	< 20	< 1	0.02	< 0.01	< 0.01
10665	< 0.2	< 5	226	23	0.030	0.36	60	< 10	< 1	268	< 1	< 20	< 20	< 1	< 0.01	< 0.01	< 0.01
10666	2.6	< 5	297	28.09 %	0.794	0.46	234	< 10	13	101	< 1	< 20	26	< 1	0.10	< 0.01	0.11
10674	< 0.2	< 5	99	19	0.073	> 10.00	45	< 10	< 1	111	2	< 20	< 20	3	0.17	0.02	0.06
10675	0.7	< 5	294	91	0.010	> 10.00	59	< 10	< 1	74	< 1	< 20	< 20	< 1	0.04	0.03	0.09
10676	275.3	228	> 10000	830	< 0.010	> 10.00	168	101	< 1	102	< 1	< 20	< 20	7	0.06	< 0.01	0.06
10701	2.4	< 5	37	7	0.580	0.63	212	< 10	145	182	4	< 20	< 20	9	0.39	0.01	0.62
10702	0.6	< 5	25	7	0.152	3.06	10816	< 10	46	20	6	< 20	< 20	13	0.45	3.93	> 10.00
10703	2.5	< 5	< 5	33.13 %	26.468	0.26	199	14	11	80	< 1	< 20	29	< 1	0.20	< 0.01	0.04
10704	0.2	< 5	46	25	1.020	2.05	980	< 10	54	201	6	< 20	< 20	11	0.41	0.05	0.10
10705	< 0.2	< 5	23	7	0.046	0.56	874	< 10	6	246	2	< 20	< 20	1	0.13	0.05	0.10
10706	< 0.2	< 5	15	< 5	0.048	3.75	7765	< 10	31	137	18	< 20	< 20	14	1.23	0.96	0.82
10707	< 0.2	< 5	8	< 5	0.019	1.87	10141	< 10	9	83	4	< 20	< 20	7	0.14	1.76	4.54
10708	0.2	< 5	16	230	5.090	0.68	388	< 10	2	270	< 1	< 20	< 20	< 1	0.03	0.09	0.24
10709	< 0.2	< 5	15	31	0.044	0.92	1463	< 10	81	183	3	< 20	< 20	4	0.21	0.17	0.69
10718	0.7	< 5	81	9	0.483	1.23	171	< 10	89	211	8	< 20	< 20	3	0.33	0.07	0.01
10719	< 0.2	< 5	56	13	0.122	2.83	2905	< 10	126	147	7	< 20	< 20	15	0.45	0.12	0.32
10720	0.3	23	123	156	0.920	3.79	3371	< 10	248	150	7	< 20	< 20	9	0.43	0.50	0.51
10725	2.6	< 5	16	41.28 %	0.175	1.51	715	< 10	16	60	< 1	< 20	28	< 1	0.21	0.62	0.52
10726	0.5	< 5	702	483	0.100	3.93	3746	< 10	15	78	7	< 20	< 20	4	0.23	3.72	8.80
10727	0.3	< 5	412	748	0.057	2.08	959	< 10	34	161	5	< 20	< 20	10	0.31	0.86	2.99
10728	0.3	< 5	368	46	0.075	1.27	2017	< 10	5	202	2	< 20	< 20	< 1	0.05	0.55	1.25
10729	0.9	< 5	15	61	0.339	4.82	> 20000	< 10	8	77	< 1	< 20	< 20	5	0.07	2.68	9.92
10730	< 0.2	< 5	183	62	1.359	0.73	401	< 10	15	252	1	< 20	< 20	2	0.07	0.12	0.78
10731	< 0.2	< 5	149	20	0.111	3.52	1173	< 10	36	40	8	< 20	< 20	11	0.58	1.44	5.28
10732	< 0.2	< 5	369	11	0.285	5.82	4667	< 10	120	91	24	< 20	< 20	15	0.83	0.82	0.89

TABLE 2c1: ASSAY DATA - GEOCHEMICAL RECONNAISSANCE SAMPLING

Field No.	Na pct	K pct	Sr ppm	Y ppm	Ga ppm	Li ppm	Nb ppm	Sc ppm	Ta ppm	Ti pct	Zr ppm	Comments
8035	< 0.12							3.3	< 1		< 1500	sluice con
10647	< 0.01	0.10	113	4	< 2	2	< 1	< 5	< 10	< 0.01	2	qz veinlets in phyllite w/ FeO
10648	0.01	0.12	72	11	< 2	5	< 1	< 5	< 10	< 0.01	2	qz veinlet in phyllite w/ lim
10649	< 0.01	0.04	10	< 1	< 2	2	< 1	< 5	< 10	< 0.01	1	massive qz w/ py, po
10650	0.02	0.10	78	1	< 2	4	< 1	< 5	< 10	< 0.01	3	qz vein in phyllite w/ hem, py
10651	0.01	0.16	27	4	< 2	9	< 1	< 5	< 10	< 0.01	2	phyllite
10652	< 0.01	0.02	210	3	< 2	2	< 1	< 5	< 10	< 0.01	< 1	meta-qz cobbles w/ FeO
10653	0.02	0.18	131	8	< 2	33	2	6	< 10	0.05	2	phyllite w/ siliceous nodules, FeO
10654	0.01	0.04	67	5	< 2	5	< 1	< 5	< 10	< 0.01	< 1	massive qz w/ FeO
10663	< 0.01	0.01	10	< 1	< 2	< 1	< 1	< 5	< 10	< 0.01	1	meta-qz w/ apy, FeO
10664	< 0.01	< 0.01	< 1	< 1	< 2	< 1	< 1	< 5	< 10	< 0.01	< 1	meta-qz w/ apy, FeO
10665	< 0.01	< 0.01	< 1	< 1	< 2	< 1	< 1	< 5	< 10	< 0.01	1	qz w/ apy, FeO
10666	< 0.01	0.03	6	< 1	< 2	8	< 1	< 5	< 10	< 0.01	< 1	qz vein w/ stb, yellow alt mineral
10674	< 0.01	0.07	5	2	< 2	< 1	< 1	< 5	< 10	< 0.01	4	py cubes from sluice con
10675	< 0.01	0.02	3	< 1	< 2	< 1	< 1	< 5	< 10	< 0.01	2	py concretions from sluice con
10676	< 0.01	0.03	30	2	< 2	< 1	< 1	< 5	< 10	< 0.01	3	apy xls from sluice con
10701	< 0.01	0.11	106	14	< 2	2	< 1	< 5	< 10	< 0.01	2	qz mica schist w/ ba (?), lim
10702	0.05	0.22	244	20	< 2	1	3	< 5	< 10	< 0.01	2	qtz lense w/ tr py
10703	< 0.01	0.03	3	< 1	< 2	21	< 1	< 5	< 10	< 0.01	< 1	massive stb w/ yellow alt mineral
10704	0.01	0.26	14	3	< 2	7	< 1	< 5	< 10	< 0.01	1	qz veinlet w/ < 1% py, FeO
10705	< 0.01	0.03	5	2	< 2	1	< 1	< 5	< 10	< 0.01	1	qz w/ unknown metallic, lim
10706	0.04	0.26	79	6	< 2	18	< 1	< 5	< 10	0.03	4	qz mica schist w/ 5% py
10707	0.02	0.08	357	5	< 2	2	1	< 5	< 10	< 0.01	1	carb-qz lense w/in schist
10708	< 0.01	0.01	8	< 1	< 2	< 1	< 1	< 5	< 10	< 0.01	< 1	qz w/ py, mal, lim
10709	0.02	0.09	34	2	< 2	1	< 1	< 5	< 10	< 0.01	< 1	schistose qtz w/ py, FeO
10718	0.01	0.11	5	2	< 2	3	< 1	< 5	< 10	< 0.01	6	schistose qtz w/ tr py, FeO
10719	0.02	0.21	38	6	< 2	4	< 1	< 5	< 10	< 0.01	2	qz veinlet in qz musc schist
10720	0.01	0.27	66	3	< 2	4	< 1	< 5	< 10	< 0.01	2	qz musc schist w/ py cubes, FeO
10725	< 0.01	0.12	22	2	< 2	1	< 1	< 5	< 10	< 0.01	< 1	1.5 " stb vein w/ val
10726	0.02	0.09	510	11	< 2	2	3	< 5	< 10	< 0.01	2	qz veinlet w/ ank margins
10727	0.02	0.21	85	5	< 2	2	< 1	< 5	< 10	< 0.01	2	qz veinlets w/ py, po, FeO
10728	< 0.01	0.02	68	2	< 2	< 1	< 1	< 5	< 10	< 0.01	2	qz veinlet w/ py, po (?), apy (?)
10729	0.01	0.04	509	10	< 2	1	2	< 5	< 10	< 0.01	< 1	qz lense in phyllite w/ stb
10730	0.01	0.04	41	2	< 2	< 1	< 1	< 5	< 10	< 0.01	1	qz veinlet
10731	0.02	0.27	211	8	< 2	6	< 1	< 5	< 10	< 0.01	2	phyllite w/ py
10732	0.02	0.13	54	6	< 2	12	< 1	< 5	< 10	< 0.01	3	

TABLE 2c1: ASSAY DATA - GEOCHEMICAL RECONNAISSANCE SAMPLING

Field No.	Latitude	Longitude	Location	Sample Site	Sample Type	Au ppb	Pt ppb	Pd ppb	Ag ppm	Cu ppm	Pb ppm	Zn ppm	Mo ppm	Ni ppm	Co ppm
10733	67.5158	150.1383	Right Fork		sed	14			< 0.2	36	13	66	1	32	17
10734	67.5150	150.1364	Right Fork	otc	rand	29			< 0.2	77	8	84	2	42	22
10735	67.5142	150.1383	Vermont Ck		sed	< 5			0.2	35	12	66	2	28	16
10736	67.5142	150.1383	Vermont Ck		pan	398			< 0.2	56	11	79	< 1	31	16
10741	67.4739	150.1683	Smith Ck Dome	otc	sel	46			< 0.2	47	23	39	2	16	9
10742	67.4731	150.1762	Smith Ck Dome	otc	sel	9			< 0.2	62	17	17	10	25	9
10743	67.4717	150.1956	Smith Ck	otc	rep	< 5			0.4	34	6	65	1	12	11
10744	67.4686	150.1682	Smith Ck		pan	22			< 0.2	45	14	63	2	45	20
10745	67.4686	150.1682	Smith Ck		sed	< 5			< 0.2	23	11	57	1	25	12
10746	67.4706	150.2079	Smith Ck	otc	rep	7			< 0.2	54	21	60	1	18	9
10747	67.4721	150.2279	Nolan, Smith Ck	trn	sel	12.20 ppm			< 0.2	22	< 2	33	< 1	< 1	2
10748	67.4741	150.2220	Nolan, Smith Ck	drum	sel	577			0.6	13	< 2	3	< 1	< 1	< 1
10749	67.4741	150.2220	Nolan, Smith Ck	otc	rep	8			< 0.2	64	15	75	3	35	20
10763	67.4861	150.0433	Hammond River		slu	430.43 ppm			27.7	70	473	165	2	44	23
10764	67.4786	150.2000	Smith Dome Bench		slu	387.62 ppm			83.7	161	> 10000	73	2	69	50
10765	67.4982	150.1089	Buckeye Gulch		slu	259			1.0	303	21	20	152	37	3
11050	67.4823	150.1455	Swift Ck	otc	sel	10			< 0.2	165	140	40	< 1	13	12
11051	67.4814	150.1366	Swift Ck		sed	5			< 0.2	33	8	51	1	31	16
11052	67.4814	150.1366	Swift Ck		pan	5	1	< 5	< 0.2	54	8	92	4	44	23
11053	67.4884	150.1215	Swift Ck		sed	4			< 0.2	23	6	44	< 1	23	13
11054	67.4884	150.1215	Swift Ck		pan	25	3	11	< 0.2	72	5	139	4	58	26
11055	67.4884	150.1215	Swift Ck	otc	rand	3			0.2	24	4	99	2	77	26
11056	67.4884	150.1215	Swift Ck	flt	sel	5			< 0.2	76	123	24	6	19	12
11057	67.4886	150.1122	Swift Ck	otc	rep	29			0.3	51	19	53	1	26	11
11058	67.4918	150.1048	Swift Ck		pan	5869	2	5	< 0.2	75	6	159	3	47	22
11059	67.4718	150.1043	Midnight Dome	otc	sel	62			< 0.2	19	4	51	2	26	14
11060	67.4929	150.1729	Thompson Pup	flt	sel	4			0.4	2	31	50	1	16	10
11061	67.4896	150.1875	Thompson Pup	flt	sel	25			< 0.2	3059	20	88	1	6	8
11062	67.4888	150.1887	Thompson Pup		sed	82			< 0.2	33	7	45	1	22	15
11063	67.4888	150.1887	Thompson Pup		pan	15.80 ppm	3	7	3.2	108	25	262	6	44	23
11064	67.4885	150.1914	Thompson Pup	otc	rep	9			0.7	3	< 2	37	2	2	2
11065	67.4885	150.1914	Thompson Pup		pan	IS	IS	IS	0.3	42	17	141	7	245	393
11066	67.4872	150.1898	Fay Ck		sed	4			< 0.2	29	7	43	1	26	16
11067	67.4872	150.1898	Fay Ck		pan	1120	3	< 5	< 0.2	49	5	130	3	26	11
11068	67.4825	150.2152	Archibald Ck		sed	5			< 0.2	32	7	53	< 1	30	18
11069	67.4825	150.2152	Archibald Ck		pan	14	3	< 5	< 0.2	107	7	223	3	41	22

TABLE 2c1: ASSAY DATA - GEOCHEMICAL RECONNAISSANCE SAMPLING

Field No.	Cd ppm	Bi ppm	As ppm	Sb ppm	Hg ppm	Fe pct	Mn ppm	Te ppm	Ba ppm	Cr ppm	V ppm	Sn ppm	W ppm	La ppm	Al pct	Mg pct	Ca pct
10733	< 0.2	< 5	54	< 5	0.085	2.82	2234	< 10	23	10	13	< 20	< 20	14	0.63	0.55	0.55
10734	< 0.2	< 5	51	14	0.069	5.83	1835	< 10	46	65	46	< 20	< 20	11	3.02	2.25	0.90
10735	< 0.2	< 5	10	< 5	0.029	3.56	1731	< 10	11	17	22	< 20	< 20	19	1.19	1.15	0.72
10736	< 0.2	< 5	23	< 5	0.063	5	1545	< 10	27	74	34	< 20	< 20	17	1.96	1.7	0.7
10741	< 0.2	< 5	47	31	0.168	2.34	2096	< 10	112	122	8	< 20	< 20	15	0.49	0.56	0.47
10742	< 0.2	< 5	153	46	0.057	0.96	288	< 10	35	174	3	< 20	< 20	5	0.18	0.08	0.05
10743	< 0.2	< 5	89	42	0.125	4.52	1613	< 10	22	86	8	< 20	< 20	7	0.27	2.71	6.76
10744	< 0.2	7	57	15	0.16	7.96	2252	< 10	44	114	53	< 20	< 20	21	0.70	0.34	0.12
10745	< 0.2	< 5	15	10	0.192	2.27	1363	< 10	28	13	15	< 20	< 20	15	0.71	0.53	0.13
10746	< 0.2	< 5	64	22	0.135	4.29	3232	< 10	60	38	15	< 20	< 20	19	0.65	1.79	2.33
10747	1.8	< 5	295	15.83 %	1.049	1.17	1077	< 10	24	97	< 1	< 20	< 20	2	0.17	0.49	0.93
10748	4.7	< 5	15	66.41 %	0.465	0.08	30	< 10	4	20	< 1	40	56	< 1	0.02	0.02	0.15
10749	< 0.2	< 5	40	30	0.127	4.12	2252	< 10	30	107	16	< 20	< 20	7	0.96	1.07	1.10
10763	< 0.2	7	597	< 5	8.277	5.35	1920	< 10	86	91	36	< 20	47	22	1.19	0.98	2.85
10764	< 0.2	135	737	199	IS	> 10.00	1226	33	9	129	35	38	37	56	1.12	0.84	1.13
10765	< 0.2	9	207	10	0.229	> 10.00	13	< 10	< 1	51	< 1	< 20	< 20	< 1	0.04	< 0.01	0.01
11050	< 0.2	< 5	14	< 5	< 0.010	7.92	> 20000	< 10	16	75	< 1	< 20	< 20	7	0.40	1.85	2.95
11051	< 0.2	< 5	28	< 5	0.045	2.54	2679	< 10	22	14	11	< 20	< 20	10	0.47	0.32	0.35
11052	< 0.2	< 5	73	143	0.031	4.78	1587	< 10	114	287	28	< 20	< 20	15	1.29	0.37	0.17
11053	< 0.2	< 5	27	< 5	0.027	2.16	2040	< 10	15	8	9	< 20	< 20	11	0.36	0.25	0.24
11054	0.9	< 5	344	168	4.285	6.32	1864	< 10	226	488	53	< 20	< 20	23	3.26	0.43	0.27
11055	< 0.2	< 5	31	< 5	0.034	5.56	1694	< 10	43	121	24	< 20	< 20	9	0.72	1.82	3.52
11056	< 0.2	< 5	10	< 5	< 0.010	1.23	790	< 10	123	207	11	< 20	< 20	4	0.61	0.49	0.26
11057	2.6	< 5	874	11	0.033	3.39	1062	< 10	45	84	9	< 20	< 20	5	0.94	0.97	5.46
11058	1.3	< 5	520	55	1.070	5.56	2355	< 10	130	315	43	< 20	< 20	15	2.13	0.87	0.49
11059	< 0.2	< 5	70	8	0.595	2.93	2526	< 10	79	215	8	< 20	< 20	7	0.40	0.55	1.13
11060	< 0.2	< 5	7	< 5	< 0.010	4.49	10454	< 10	12	71	6	< 20	< 20	1	0.05	5.78	> 10.00
11061	0.3	< 5	46	< 5	0.205	> 10.00	> 20000	< 10	3	114	< 1	< 20	< 20	1	0.06	0.90	0.63
11062	< 0.2	< 5	65	< 5	0.036	2.30	2805	< 10	20	7	12	< 20	< 20	8	0.44	0.33	0.67
11063	1.1	< 5	374	104	1.070	8.00	5114	< 10	160	398	69	< 20	< 20	12	1.85	0.52	0.91
11064	< 0.2	< 5	94	< 5	0.034	9.95	3497	< 10	3	8	5	< 20	< 20	< 1	0.07	4.90	> 10.00
11065	406.2	< 5	> 10000	777	0.081	> 10.00	129	70	< 1	272	3	< 20	< 20	5	0.20	0.04	0.39
11066	< 0.2	< 5	30	8	0.059	2.44	2139	< 10	23	10	14	< 20	< 20	10	0.55	0.43	0.42
11067	< 0.2	< 5	100	35	0.048	3.65	1518	< 10	97	298	32	< 20	< 20	9	2.16	1.16	2.66
11068	< 0.2	< 5	21	18	0.038	2.60	1837	< 10	18	12	16	< 20	< 20	8	0.81	0.62	0.43
11069	< 0.2	< 5	34	45	0.035	5.15	3968	< 10	118	364	52	< 20	< 20	9	2.10	0.96	0.58

TABLE 2c1: ASSAY DATA - GEOCHEMICAL RECONNAISSANCE SAMPLING

Field No.	Na pct	K pct	Sr ppm	Y ppm	Ga ppm	Li ppm	Nb ppm	Sc ppm	Ta ppm	Ti pct	Zr ppm	Comments
10733	< 0.01	0.03	37	5	< 2	11	< 1	< 5	< 10	< 0.01	1	
10734	0.02	0.25	60	5	4	36	2	< 5	< 10	< 0.01	2	phyllite w/ py
10735	< 0.01	0.03	43	7	< 2	20	< 1	< 5	< 10	0.02	1	
10736	0.01	0.12	40	5	< 2	28	< 1	< 5	< 10	0.03	2	
10741	< 0.01	0.18	89	4	< 2	3	< 1	< 5	< 10	< 0.01	2	qz vein cutting qz mica schist
10742	0.01	0.09	9	1	< 2	2	< 1	< 5	< 10	< 0.01	3	schistose qtz w/ py, mal (?)
10743	0.02	0.15	619	11	< 2	1	1	< 5	< 10	< 0.01	1	qz vein xcut qz mica schist
10744	0.01	0.10	20	5	< 2	6	1	< 5	< 10	< 0.01	3	minor mag, no visible Au
10745	< 0.01	0.03	24	5	< 2	9	< 1	< 5	< 10	< 0.01	< 1	
10746	0.03	0.30	154	6	< 2	5	< 1	< 5	< 10	< 0.01	1	qz musc schist w/ lim
10747	< 0.01	0.08	57	3	< 2	< 1	< 1	< 5	< 10	< 0.01	< 1	stb vein in schist
10748	< 0.01	< 0.01	15	< 1	< 2	< 1	< 1	< 5	< 10	< 0.01	< 1	massive stb w/ yellow alt mineral
10749	0.02	0.19	53	5	< 2	12	< 1	< 5	< 10	< 0.01	7	qz musc schist w/ tr py, FeO
10763	0.02	0.11	106	8	< 2	16	< 1	< 5	< 10	0.05	3	sluice con
10764	0.02	0.11	65	7	3	13	< 1	< 5	< 10	0.01	4	colluvial soil
10765	< 0.01	0.03	2	< 1	< 2	< 1	< 1	< 5	< 10	< 0.01	< 1	py concretions from sluice con
11050	0.01	0.05	151	14	< 2	2	< 1	< 5	14	< 0.01	< 1	schist w/ black nodules
11051	< 0.01	0.03	22	5	< 2	5	< 1	< 5	< 10	< 0.01	< 1	
11052	0.04	0.30	23	6	< 2	11	< 1	< 5	< 10	< 0.01	< 1	no mag, no visible Au
11053	< 0.01	0.02	17	4	< 2	4	< 1	< 5	< 10	< 0.01	< 1	
11054	0.07	1.02	45	8	4	22	< 1	7	< 10	< 0.01	< 1	tr mag, from bedrock
11055	0.03	0.26	131	6	< 2	10	< 1	< 5	< 10	< 0.01	< 1	black qz mica schist w/ py (?)
11056	0.02	0.06	9	5	< 2	5	< 1	< 5	< 10	0.03	< 1	qtz w/ 1% diss py, cpy (?)
11057	0.02	0.30	270	8	< 2	12	< 1	< 5	< 10	< 0.01	< 1	blk qz mica schist w/ py
11058	0.09	0.50	42	7	3	19	< 1	6	< 10	< 0.01	< 1	1 v fine Au
11059	0.03	0.22	86	4	< 2	2	< 1	< 5	< 10	< 0.01	< 1	qz vein w/ euhedral py, FeO
11060	0.01	0.03	351	5	< 2	3	< 1	< 5	< 10	< 0.01	< 1	multiple phase alt qz w/ FeO
11061	0.01	0.02	10	5	< 2	1	< 1	< 5	15	< 0.01	< 1	qtz w/ 3% py, cpy (?), FeO
11062	< 0.01	0.02	36	5	< 2	6	< 1	< 5	< 10	< 0.01	< 1	
11063	0.14	0.41	62	15	< 2	17	< 1	7	< 10	0.03	< 1	4 v fine Au, minor mag
11064	0.02	0.03	1166	19	< 2	2	< 1	12	< 10	< 0.01	< 1	multiple phase qz vein
11065	0.04	0.06	35	2	< 2	< 1	< 1	< 5	< 10	0.02	5	apy concentrate
11066	< 0.01	0.03	27	6	< 2	7	< 1	< 5	< 10	< 0.01	< 1	
11067	0.09	0.53	136	8	3	22	< 1	< 5	< 10	0.02	< 1	1 fine Au, from bedrock
11068	< 0.01	0.04	27	6	< 2	11	< 1	< 5	< 10	0.01	< 1	
11069	0.14	0.36	33	15	2	21	< 1	9	< 10	0.1	< 1	tr mag, no visible Au

TABLE 2c1: ASSAY DATA - GEOCHEMICAL RECONNAISSANCE SAMPLING

Field No.	Latitude	Longitude	Location	Sample Site	Sample Type	Au ppb	Pt ppb	Pd ppb	Ag ppm	Cu ppm	Pb ppm	Zn ppm	Mo ppm	Ni ppm	Co ppm
11087	67.4994	150.1950	Nolan Ck		sed	3			< 0.2	29	3	59	< 1	25	16
11088	67.4994	150.1950	Nolan Ck		pan	14.99 ppm	2	< 5	0.8	39	15	112	2	29	17
11089	67.4994	150.1950	Vermont Pass		sed	6			< 0.2	30	5	67	1	28	18
11090	67.4823	150.2299	Acme Ck		sed	4			< 0.2	30	10	57	1	26	15
11091	67.4823	150.2299	Acme Ck		pan	25	3	< 5	< 0.2	47	< 2	139	3	33	16
11116	67.4867	150.2160	Nolan Ck	otc	ran	4			0.2	93	36	51	4	29	12
11117	67.4906	150.2032	Nolan Ck		pan	11740	1	< 5	5.1	43	32	115	3	31	18
11118	67.4906	150.2032	Nolan Ck		sed	2			< 0.2	25	4	55	< 1	23	15
11119	67.4928	150.2001	Nolan Ck	flt	grab	3			0.2	89	< 2	39	1	41	21
11120	67.4956	150.1966	Nolan Ck	flt	grab	2			< 0.2	126	< 2	58	1	25	26
11121	67.4990	150.1943	Webster Gulch		pan	26	< 1	< 5	< 0.2	30	< 2	106	2	23	17
11122	67.4990	150.1943	Webster Gulch		sed	4			< 0.2	27	7	72	< 1	25	17
11123	67.5022	150.2000	Montana Gulch		sed	2			< 0.2	39	6	67	1	31	19
11124	67.5022	150.2000	Montana Gulch		pan	10	3	< 5	< 0.2	94	9	121	3	46	33
11132	67.4867	150.1780	Fay Ck		sed	8			< 0.2	20	6	40	< 1	18	11
11133	67.4867	150.1780	Fay Ck		pan	28	2	< 5	< 0.2	113	13	219	6	52	33
11134	67.4935	150.1600	Palisades	otc	rep	30			< 0.2	21	4	37	3	14	6
11135	67.4935	150.1600	Palisades	otc	rep	5			< 0.2	18	63	31	1	11	9
11136	67.4957	150.1553	Palisades	otc	rep	9			< 0.2	29	< 2	26	2	13	4
11137	67.4563	150.1070	Union Gulch	flt	sel	13			< 0.2	20	5	13	2	15	7
11138	67.4569	150.1090	Union Gulch		sed	6			< 0.2	23	7	54	< 1	23	13
11139	67.4569	150.1090	Union Gulch		pan	1471	3	< 5	< 0.2	98	8	188	4	52	27
11140	67.4583	150.1117	Union Gulch		pan	17.24 ppm	2	< 5	0.7	84	8	159	4	74	40
11141	67.4597	150.1184	Union Gulch		pan	1559	5	9	< 0.2	79	11	346	4	54	40
11142	67.4597	150.1184	Union Gulch		sed	2			< 0.2	24	6	57	< 1	24	13
11143	67.4556	150.1051	Union Gulch	otc	grab	5			< 0.2	31	7	89	1	33	14
11144	67.4808	150.2229	Archibald Gully		pan	217.63 ppm	3	< 5	6.1	58	10	161	5	38	27
11155	67.4878	150.1949	Fay Ck	otc	sel	4			< 0.2	43	8	50	2	31	23
11156	67.4880	150.1931	Fay Ck	otc	sel	7			< 0.2	83	22	52	4	66	39
11157	67.4881	150.1918	Fay Ck	otc	sel	40			0.2	18	16	23	2	14	9
11158	67.4764	150.1767	Smith Ck Dome	otc	sel	11			< 0.2	10	< 2	33	2	16	10
11159	67.5060	150.1932	Nolan Ck	otc	ran	< 5			< 0.2	13	34	10	4	19	4
11160	67.5090	150.1919	Nolan Ck	otc	ran	< 5			0.3	11	19	21	2	19	6
11161	67.4744	150.1061	Midnight Dome	otc	ran	< 5			< 0.2	16	< 2	20	4	22	4
11162	67.4719	150.0777	Midnight Dome	otc	sel	810			< 0.2	55	6	24	8	36	14
11163	67.4692	150.1970	Smith Ck	otc	sel	13			< 0.2	72	22	58	4	44	18

TABLE 2c1: ASSAY DATA - GEOCHEMICAL RECONNAISSANCE SAMPLING

Field No.	Cd ppm	Bi ppm	As ppm	Sb ppm	Hg ppm	Fe pct	Mn ppm	Te ppm	Ba ppm	Cr ppm	V ppm	Sn ppm	W ppm	La ppm	Al pct	Mg pct	Ca pct
11087	< 0.2	< 5	8	< 5	0.026	3.66	1098	< 10	14	20	28	< 20	< 20	13	1.33	0.93	0.39
11088	< 0.2	< 5	13	< 5	0.350	5.05	2843	< 10	169	258	74	< 20	< 20	11	2.51	1.35	0.77
11089	< 0.2	< 5	10	< 5	0.046	4.00	2085	< 10	27	26	40	< 20	< 20	11	1.47	1.11	0.56
11090	< 0.2	< 5	7	< 5	0.035	3.66	994	< 10	11	23	30	< 20	< 20	16	1.43	1.17	0.82
11091	< 0.2	< 5	9	< 5	0.046	5.22	1664	< 10	134	247	77	< 20	< 20	12	3.33	1.68	0.86
11116	< 0.2	< 5	26	6	0.016	2.02	2211	< 10	26	260	9	< 20	< 20	3	0.41	0.69	0.94
11117	< 0.2	< 5	38	11	0.770	5.01	3965	< 10	107	293	78	< 20	< 20	14	2.58	1.25	0.79
11118	< 0.2	< 5	15	< 5	0.026	3.27	1362	< 10	16	19	30	< 20	< 20	10	1.15	0.86	0.40
11119	< 0.2	< 5	< 5	< 5	< 0.010	3.77	625	< 10	17	94	74	< 20	< 20	< 1	3.12	1.69	2.21
11120	< 0.2	< 5	< 5	< 5	< 0.010	4.43	632	< 10	25	67	95	< 20	< 20	3	2.18	1.33	1.17
11121	< 0.2	< 5	42	< 5	0.024	4.52	1775	< 10	89	208	91	< 20	< 20	9	2.22	1.32	1.00
11122	< 0.2	< 5	59	< 5	0.046	3.56	1382	< 10	23	21	42	< 20	< 20	8	1.22	0.95	0.56
11123	< 0.2	< 5	17	< 5	0.034	3.96	1945	< 10	20	21	29	< 20	< 20	10	1.41	1.02	0.40
11124	< 0.2	< 5	42	< 5	0.038	5.51	5896	< 10	110	255	55	< 20	< 20	14	2.57	1.33	0.57
11132	< 0.2	< 5	29	10	0.139	1.60	1403	< 10	43	8	10	< 20	< 20	8	0.39	0.24	0.17
11133	< 0.2	< 5	84	23	2.269	6.08	9569	< 10	229	490	44	< 20	< 20	19	1.87	0.23	0.48
11134	< 0.2	< 5	41	9	0.081	1.64	3390	< 10	35	170	4	< 20	< 20	2	0.18	1.00	2.93
11135	< 0.2	< 5	< 5	< 5	0.034	2.27	> 20000	< 10	45	132	1	< 20	< 20	6	0.25	1.84	6.34
11136	< 0.2	< 5	44	< 5	0.027	1.84	3090	< 10	48	207	6	< 20	< 20	6	0.26	0.04	0.16
11137	3.1	< 5	1023	12	< 0.010	0.65	1933	< 10	3	286	< 1	< 20	< 20	< 1	0.02	0.09	0.35
11138	< 0.2	< 5	36	5	0.107	2.65	1021	< 10	12	15	14	< 20	< 20	16	1.03	0.73	0.30
11139	< 0.2	< 5	72	< 5	0.099	> 10.00	1332	< 10	108	249	124	< 20	< 20	17	2.40	0.87	0.20
11140	0.4	< 5	209	< 5	0.330	> 10.00	933	< 10	68	220	297	< 20	< 20	16	1.52	0.47	0.10
11141	0.3	< 5	128	< 5	0.130	> 10.00	1219	< 10	114	334	123	< 20	< 20	15	2.49	0.82	0.14
11142	< 0.2	< 5	43	< 5	0.059	2.79	887	< 10	13	15	15	< 20	< 20	16	1.12	0.79	0.25
11143	< 0.2	< 5	10	< 5	0.019	4.43	463	< 10	61	39	13	< 20	< 20	10	1.66	0.90	1.56
11144	< 0.2	< 5	58	25	3.220	6.67	2924	< 10	110	309	54	< 20	< 20	9	1.95	0.82	1.20
11155	< 0.2	< 5	15	< 5	0.049	3.45	4936	< 10	34	106	15	< 20	< 20	3	0.85	1.10	1.14
11156	< 0.2	< 5	32	< 5	0.033	3.87	19649	< 10	51	132	13	< 20	< 20	8	0.51	1.37	3.63
11157	< 0.2	< 5	90	< 5	0.048	3.40	3677	< 10	16	160	7	< 20	< 20	< 1	0.30	1.23	3.76
11158	< 0.2	< 5	12	< 5	0.226	1.23	2133	< 10	88	230	3	< 20	< 20	< 1	0.12	0.49	1.09
11159	< 0.2	< 5	< 5	< 5	0.018	0.69	714	< 10	14	310	4	< 20	< 20	1	0.20	0.16	0.22
11160	< 0.2	< 5	< 5	< 5	< 0.010	1.34	439	< 10	29	207	12	< 20	< 20	< 1	0.58	0.32	3.37
11161	< 0.2	< 5	6	< 5	0.261	0.81	399	< 10	29	367	4	< 20	< 20	1	0.15	0.10	0.21
11162	< 0.2	< 5	28	22	0.320	2.13	1610	< 10	166	268	12	< 20	< 20	8	0.47	0.23	0.29
11163	< 0.2	< 5	23	9	0.052	3.66	1830	< 10	51	108	16	< 20	< 20	4	0.93	1.00	0.96

TABLE 2c1: ASSAY DATA - GEOCHEMICAL RECONNAISSANCE SAMPLING

Field No.	Na pct	K pct	Sr ppm	Y ppm	Ga ppm	Li ppm	Nb ppm	Sc ppm	Ta ppm	Ti pct	Zr ppm	Comments
11087	< 0.01	0.06	23	8	< 2	22	< 1	< 5	< 10	0.01	< 1	
11088	0.12	0.37	39	17	3	27	< 1	10	< 10	0.22	< 1	
11089	< 0.01	0.07	36	8	< 2	17	1	< 5	< 10	0.01	< 1	
11090	< 0.01	0.04	40	8	< 2	19	< 1	< 5	< 10	0.02	< 1	
11091	0.16	0.67	54	12	5	30	< 1	10	< 10	0.15	< 1	tr mag, no visible Au
11116	0.03	0.11	61	2	< 2	5	< 1	< 5	< 10	< 0.01	< 1	qz veinlets xcut phyllite
11117	0.15	0.42	40	20	4	24	< 1	11	< 10	0.19	< 1	1 fine and 12 v fine Au, no mag
11118	< 0.01	0.06	24	6	< 2	17	< 1	< 5	< 10	0.02	< 1	
11119	0.05	0.04	25	8	3	20	< 1	< 5	< 10	0.24	< 1	diorite w/ tr po
11120	0.06	0.03	30	11	< 2	14	< 1	< 5	< 10	0.29	< 1	diorite w/ <1% fine py, FeO
11121	0.17	0.28	55	14	3	20	< 1	10	< 10	0.2	< 1	no mag
11122	< 0.01	0.06	34	5	< 2	15	< 1	< 5	< 10	0.02	< 1	
11123	< 0.01	0.06	26	6	< 2	22	< 1	< 5	< 10	< 0.01	< 1	
11124	0.08	0.49	36	13	3	24	< 1	8	< 10	0.05	< 1	mod po and py, minor mag
11132	< 0.01	0.03	15	3	< 2	5	< 1	< 5	< 10	< 0.01	< 1	
11133	0.09	0.43	53	29	< 2	15	< 1	10	< 10	0.01	< 1	minor mag
11134	0.01	0.07	221	4	< 2	3	< 1	< 5	< 10	< 0.01	< 1	qz vein w/ py-hem psuedo, sid
11135	0.02	0.13	187	7	< 2	3	< 1	< 5	< 10	< 0.01	< 1	qz vein w/ hem, py
11136	0.01	0.13	21	2	< 2	3	< 1	< 5	< 10	< 0.01	< 1	qz vein w/ py
11137	< 0.01	< 0.01	20	< 1	< 2	< 1	< 1	< 5	< 10	< 0.01	< 1	qz vein w/ tr py, FeO
11138	< 0.01	0.04	22	8	< 2	12	< 1	< 5	< 10	< 0.01	< 1	
11139	0.12	0.61	36	9	< 2	22	< 1	6	< 10	0.06	< 1	1 v fine Au, 1 py cube, abu mag
11140	0.11	0.43	26	7	< 2	15	< 1	< 5	< 10	0.04	< 1	abu mag
11141	0.14	0.66	32	9	< 2	22	< 1	6	< 10	0.07	< 1	mod sulfides, abu mag
11142	< 0.01	0.04	18	8	< 2	13	< 1	< 5	< 10	< 0.01	< 1	
11143	0.02	0.32	74	5	< 2	28	< 1	< 5	< 10	< 0.01	< 1	blk mica schist w/ 3% py
11144	0.11	0.38	56	13	< 2	21	< 1	7	< 10	0.07	< 1	1 fine and 1 coarse Au, mod py
11155	0.03	0.17	44	5	< 2	14	< 1	< 5	< 10	< 0.01	< 1	phyllite w/ euhedral py
11156	0.04	0.23	231	8	< 2	2	< 1	< 5	< 10	< 0.01	< 1	folded qtz w/ abu py
11157	0.02	0.06	229	8	< 2	4	< 1	< 5	< 10	< 0.01	< 1	qz vein w/ sulfides
11158	< 0.01	0.08	106	3	< 2	2	< 1	< 5	< 10	< 0.01	< 1	qz vein w/ py
11159	0.01	0.04	8	< 1	< 2	2	< 1	< 5	< 10	< 0.01	< 1	folded quartz
11160	0.02	0.16	158	3	< 2	7	< 1	< 5	< 10	0.05	< 1	qz vein
11161	0.01	0.05	19	< 1	< 2	1	< 1	< 5	< 10	< 0.01	< 1	met qz w/ sulfides
11162	0.02	0.22	49	4	< 2	3	< 1	< 5	< 10	< 0.01	< 1	qz vein w/ py-hem psuedo
11163	0.03	0.20	52	3	< 2	15	< 1	< 5	< 10	< 0.01	< 1	blk schist w/ euhedral py

TABLE 2c1: ASSAY DATA - GEOCHEMICAL RECONNAISSANCE SAMPLING

Field No.	Latitude	Longitude	Location	Sample Site	Sample Type	Au ppb	Pt ppb	Pd ppb	Ag ppm	Cu ppm	Pb ppm	Zn ppm	Mo ppm	Ni ppm	Co ppm
11164	67.4692	150.1970	Smith Ck	otc	sel	463			< 0.2	6	3	67	4	12	2
11165	67.4692	150.1970	Smith Ck	otc	ran	1532			< 0.2	30	43	41	3	17	8
11166	67.4689	150.1947	Smith Ck	otc	ran	1958			< 0.2	23	29	25	7	13	4
11167	67.4689	150.1947	Smith Ck	otc	sel	14			1.3	22	359	4004	7	20	6
11168	67.4828	150.2136	Archibald Ck	otc	sel	27			0.3	14	5	15	5	20	3
11169	67.4833	150.1455	Swift Ck	otc	sel	18			< 0.2	28	131	20	9	24	9
11170	67.4884	150.1215	Swift Ck	otc	sel	< 5			< 0.2	11	301	39	4	19	4
11171	67.4747	150.1193	Midnight Dome	otc	sel	11			< 0.2	3	< 2	4	3	15	2
11172	67.4719	150.1284	Midnight Dome	otc	sel	37			< 0.2	4	6	30	6	18	6
11173	67.4569	150.1466	Midnight Dome	otc	sel	291			< 0.2	8	87	21	3	26	16
11174	67.4533	150.1360	Midnight Dome	flt	grab	18			0.2	30	64	14	3	14	3
11175	67.5150	150.1364	Right Fork	otc	sel	73			< 0.2	87	5	86	2	30	18
11176	67.5315	150.2159	Vermont Dome	otc	sel	6			< 0.2	33	16	107	< 1	52	33
11177	67.5292	150.2045	Vermont Dome	otc	sel	< 5			0.7	5	15	9	< 1	3	1
11178	67.5303	150.1911	Vermont Dome	otc	sel	< 5			0.2	19	62	19	7	18	4
11179	67.5244	150.2345	Vermont Dome	otc	sel	< 5			0.4	20	52	9	< 1	5	4
11206	67.4994	150.1950	Vermont Pass		pan	47	2	6	< 0.2	72	6	170	4	48	23
11207	67.4929	150.1729	Thompson Pup	otc	cont	152			< 0.2	23	< 2	49	2	20	10
11208	67.4924	150.1738	Thompson Pup	flt	sel	12			< 0.2	3062	11	79	2	21	26
11209	67.4878	150.1949	Fay Ck	otc	ran	7			< 0.2	43	213	49	2	23	11
11210	67.4878	150.1949	Fay Ck	otc	sel	16			0.3	117	59	25	2	41	20
11211	67.4878	150.1949	Fay Ck	otc	sel	60			1	170	1033	23	3	100	58
11212	67.4881	150.1918	Fay Ck	otc	sel	26			0.2	102	60	53	5	61	37
11213	67.4885	150.1914	Thompson Pup	flt	sel	11			< 0.2	4768	8	108	< 1	7	7
11214	67.4929	150.1729	Thompson Pup	flt	sel	65			< 0.2	60	31	44	4	47	33
11215	67.4929	150.1729	Thompson Pup	otc	sel	30			0.4	116	12	76	4	32	19
11216	67.4955	150.1662	Palisades	otc	sel	8			< 0.2	35	3	40	2	9	4
11217	67.4935	150.1600	Palisades	otc	ran	58			< 0.2	22	116	46	3	26	13
11218	67.4907	150.1613	Palisades	otc	sel	31			< 0.2	29	8	23	3	23	14
11247	67.4777	150.1954	Smith Dome Bench		soil	2.33 ppm	< 0.07 ppm	< 0.07 ppm	< 0.2	41	14	92	1	34	22
11259	67.5042	150.1637	Right Fork		sed	< 5			< 0.2	18	10	53	< 1	21	12
11260	67.5042	150.1637	Right Fork		pan	40	6	7	< 0.2	50	13	78	4	57	23
11261	67.5042	150.1637	Right Fork		sed	< 5			< 0.2	37	14	82	< 1	45	18
11262	67.5042	150.1637	Right Fork		pan	43	6	7	< 0.2	40	13	155	3	42	20
11263	67.5075	150.1608	Right Fork	otc	sel	9			< 0.2	59	23	52	< 1	23	16
11264	67.5075	150.1608	Right Fork	otc	ran	2948			0.9	56	34	29	< 1	15	5

TABLE 2c1: ASSAY DATA - GEOCHEMICAL RECONNAISSANCE SAMPLING

Field No.	Cd ppm	Bi ppm	As ppm	Sb ppm	Hg ppm	Fe pct	Mn ppm	Te ppm	Ba ppm	Cr ppm	V ppm	Sn ppm	W ppm	La ppm	Al pct	Mg pct	Ca pct
11164	2.4	< 5	1028	> 2000	0.124	1.05	727	< 10	14	272	3	< 20	< 20	< 1	0.11	0.76	1.71
11165	12.3	< 5	5772	> 2000	0.079	1.47	1201	< 10	21	246	4	< 20	< 20	2	0.22	0.49	1.15
11166	9.0	< 5	3933	> 2000	0.068	1.15	266	< 10	18	249	4	< 20	< 20	2	0.21	0.15	0.26
11167	16.9	< 5	54	48	5.685	1.40	867	< 10	7	397	1	< 20	< 20	< 1	0.06	0.16	0.34
11168	< 0.2	< 5	37	150	0.095	0.94	71	< 10	18	393	5	< 20	< 20	3	0.20	0.01	0.04
11169	0.3	< 5	99	66	0.031	1.46	2952	< 10	32	253	5	< 20	< 20	4	0.26	0.25	0.58
11170	< 0.2	< 5	18	148	0.041	3.73	2590	< 10	7	249	2	< 20	< 20	< 1	0.06	0.96	3.33
11171	< 0.2	< 5	9	21	0.034	0.43	154	< 10	6	341	< 1	< 20	< 20	< 1	0.03	< 0.01	0.01
11172	< 0.2	< 5	26	6	0.025	2.09	3298	< 10	25	177	11	< 20	< 20	4	0.31	0.68	1.94
11173	0.7	< 5	317	30	0.010	0.90	492	< 10	15	271	7	< 20	< 20	4	0.32	0.21	0.08
11174	< 0.2	< 5	15	45	0.029	1.69	1215	< 10	6	265	2	< 20	< 20	< 1	0.14	0.57	1.83
11175	1.6	< 5	799	8	0.018	5.85	2286	< 10	51	65	36	< 20	< 20	15	2.33	1.75	1.46
11176	< 0.2	< 5	< 5	< 5	0.010	6.89	1405	< 10	42	80	30	< 20	< 20	19	3.20	1.47	0.13
11177	< 0.2	< 5	< 5	< 5	< 0.010	1.32	7054	< 10	18	11	3	< 20	< 20	3	0.24	0.57	> 10.00
11178	< 0.2	< 5	< 5	< 5	< 0.010	3.11	1674	< 10	7	235	2	< 20	< 20	< 1	0.07	0.81	2.14
11179	< 0.2	< 5	< 5	6	< 0.010	1.55	3333	< 10	7	47	6	< 20	< 20	4	0.28	0.43	> 10.00
11206	< 0.2	< 5	15	< 5	0.036	4.38	6650	< 10	150	424	45	< 20	< 20	14	2.13	0.89	0.29
11207	1.2	< 5	434	5	0.148	2.03	2925	< 10	87	180	8	< 20	< 20	6	0.38	0.37	0.77
11208	0.8	< 5	191	< 5	0.171	> 10.00	> 20000	< 10	12	148	< 1	< 20	< 20	3	0.11	0.46	0.51
11209	< 0.2	< 5	19	95	0.089	2.46	8810	< 10	41	113	6	< 20	< 20	17	0.37	0.85	2.02
11210	< 0.2	< 5	25	< 5	0.133	1.88	3362	< 10	17	210	7	< 20	< 20	9	0.24	0.47	1.52
11211	0.4	6	163	589	0.751	3.16	1116	< 10	1	255	< 1	< 20	< 20	< 1	.0.02	0.22	0.38
11212	< 0.2	< 5	35	< 5	0.080	5.19	7732	< 10	57	75	30	< 20	< 20	4	1.28	1.21	2.33
11213	0.3	< 5	28	< 5	0.249	> 10.00	> 20000	< 10	15	111	< 1	< 20	< 20	3	0.09	0.73	0.47
11214	2.1	< 5	683	19	0.093	2.73	9418	< 10	94	161	4	< 20	< 20	3	0.30	0.73	2.52
11215	2.3	< 5	765	16	0.201	2.32	8629	< 10	64	257	5	< 20	< 20	6	0.35	0.44	1.66
11216	< 0.2	< 5	28	7	0.134	1.83	3395	< 10	59	217	4	< 20	< 20	4	0.27	0.83	1.71
11217	< 0.2	< 5	51	89	0.069	1.89	2880	< 10	57	239	7	< 20	< 20	6	0.32	0.19	1.02
11218	0.4	< 5	138	32	0.092	1.20	1401	< 10	27	286	2	< 20	< 20	2	0.09	0.19	0.56
11247	< 0.2	< 5	111	96	0.230	5.79	1354	< 10	63	207	80	< 20	< 20	9	2.01	1.26	1.11
11259	< 0.2	< 5	24	< 5	0.023	2.20	2681	< 10	14	8	10	< 20	< 20	15	0.59	0.40	1.06
11260	< 0.2	< 5	51	< 5	0.090	5.64	3974	< 10	134	585	47	< 20	< 20	11	1.96	0.63	1.45
11261	< 0.2	< 5	16	< 5	0.050	3.13	1490	< 10	17	10	9	< 20	< 20	14	0.65	0.48	0.67
11262	< 0.2	< 5	24	< 5	0.105	4.79	3897	< 10	187	405	47	< 20	< 20	12	1.80	0.76	1.18
11263	< 0.2	< 5	54	10	0.032	3.16	3532	< 10	44	107	13	< 20	< 20	10	1.01	1.11	1.79
11264	0.3	< 5	181	20	0.100	1.29	535	< 10	28	161	3	< 20	< 20	2	0.19	0.61	1.99

TABLE 2c1: ASSAY DATA - GEOCHEMICAL RECONNAISSANCE SAMPLING

Field No.	Na pct	K pct	Sr ppm	Y ppm	Ga ppm	Li ppm	Nb ppm	Sc ppm	Ta ppm	Ti pct	Zr ppm	Comments
11164	< 0.01	0.02	172	2	< 2	< 1	< 1	< 5	< 10	< 0.01	< 1	qz vein
11165	0.01	0.08	95	2	< 2	1	1	< 5	< 10	< 0.01	< 1	qz vein w/ sulfides, Sb
11166	0.01	0.07	53	< 1	< 2	2	< 1	< 5	< 10	< 0.01	1	qz vein w/ sulfides, Sb
11167	0.02	0.02	16	< 1	< 2	< 1	< 1	< 5	< 10	< 0.01	< 1	qtz w/ euhedral py
11168	< 0.01	0.06	10	< 1	< 2	1	< 1	< 5	< 10	< 0.01	4	qz vein w/in blk py schist
11169	0.01	0.08	54	3	< 2	2	< 1	< 5	< 10	< 0.01	< 1	qz vein w/ lim
11170	< 0.01	0.04	378	12	< 2	< 1	< 1	< 5	< 10	< 0.01	< 1	qz vein
11171	< 0.01	0.01	2	< 1	< 2	< 1	< 1	< 5	< 10	< 0.01	< 1	qz vein
11172	0.03	0.11	128	3	< 2	2	< 1	< 5	< 10	< 0.01	< 1	qz vein w/ py-hem psuedo
11173	0.01	0.08	11	1	< 2	3	< 1	< 5	< 10	< 0.01	< 1	qz vein w/ py voids
11174	< 0.01	0.03	59	3	< 2	2	< 1	< 5	< 10	< 0.01	< 1	qz vein w/ sid, py
11175	0.02	0.28	93	10	3	27	< 1	< 5	< 10	< 0.01	< 1	micaceous schist w/ euhedral py
11176	0.03	0.23	9	12	5	64	< 1	< 5	< 10	< 0.01	< 1	ch phyllite w/ py
11177	< 0.01	0.04	1747	18	< 2	3	< 1	< 5	< 10	< 0.01	< 1	met qz
11178	< 0.01	0.03	225	7	< 2	1	< 1	< 5	< 10	< 0.01	< 1	met qz w/ py-hem psuedo
11179	< 0.01	0.02	990	5	< 2	3	< 1	< 5	< 10	< 0.01	< 1	qz vein w/ sid
11206	0.11	0.40	32	18	3	15	< 1	8	< 10	0.04	< 1	
11207	0.02	0.17	41	3	< 2	4	< 1	< 5	< 10	< 0.01	< 1	qz vein w/ metallic mineral
11208	0.01	0.05	88	6	< 2	< 1	< 1	< 5	12	< 0.01	< 1	vein qz (?) w/ tr cpy (?)
11209	0.05	0.18	116	5	< 2	3	< 1	< 5	< 10	< 0.01	< 1	qz vein w/ 10% sid and tr cpy, sl, stb
11210	< 0.01	0.07	97	9	< 2	7	< 1	< 5	< 10	< 0.01	< 1	qz vein w/ stb, gn, py, cpy (?), sl (?)
11211	< 0.01	< 0.01	43	2	< 2	< 1	< 1	< 5	< 10	< 0.01	< 1	qz vein w/ py, po, tr stb and cpy
11212	0.03	0.30	164	3	< 2	13	< 1	< 5	< 10	< 0.01	< 1	phyllite w/ 5% po
11213	0.02	0.06	17	5	< 2	1	< 1	< 5	16	< 0.01	< 1	silicified schist w/ py, po, sid
11214	0.01	0.21	102	4	< 2	2	< 1	< 5	< 10	< 0.01	< 1	ch schist w/ 5% py, po
11215	< 0.01	0.16	130	9	< 2	6	< 1	< 5	< 10	< 0.01	< 1	qz vein w/ py, po, ch partings
11216	0.02	0.16	184	4	< 2	4	< 1	< 5	< 10	< 0.01	< 1	qz veinlet w/ 20% sid
11217	< 0.01	0.13	65	4	< 2	5	< 1	< 5	< 10	< 0.01	< 1	qz veinlets
11218	< 0.01	0.03	39	1	< 2	2	< 1	< 5	< 10	< 0.01	< 1	qz vein w/ 1% py, FeO
11247	0.08	0.19	70	8	5	29	< 1	9	< 10	0.01	< 1	soil from Smith Creek Dome bench
11259	< 0.01	0.03	35	6	< 2	9	< 1	< 5	< 10	< 0.01	< 1	
11260	0.13	0.53	81	10	3	21	< 1	6	< 10	0.01	< 1	abu euhedral mag
11261	< 0.01	0.04	31	7	< 2	15	< 1	< 5	< 10	< 0.01	< 1	
11262	0.13	0.46	77	8	3	20	< 1	5	< 10	< 0.01	< 1	tr mag, tr py
11263	0.03	0.18	132	5	< 2	16	< 1	< 5	< 10	< 0.01	< 1	qz veinlet w/ minor hem and py
11264	0.02	0.11	61	3	< 2	1	< 1	< 5	< 10	< 0.01	< 1	qz veinlet

TABLE 2c1: ASSAY DATA - GEOCHEMICAL RECONNAISSANCE SAMPLING

Field No.	Latitude	Longitude	Location	Sample Site	Sample Type	Au ppb	Pt ppb	Pd ppb	Ag ppm	Cu ppm	Pb ppm	Zn ppm	Mo ppm	Ni ppm	Co ppm
11265	67.5075	150.1608	Right Fork	otc	ran	415			< 0.2	12	112	14	< 1	9	4
11266	67.5075	150.1608	Right Fork	otc	ran	**17.82 ppm**			4.4	16	24	32	< 1	21	5
11267	67.5088	150.1492	Fri 13th Pup		sed	< 5			< 0.2	25	9	52	< 1	24	13
11268	67.5088	150.1492	Fri 13th Pup		pan	1750	9	7	< 0.2	63	20	88	4	59	29
11275	67.5248	150.1018	Muck Pup		sed	7			< 0.2	30	7	55	< 1	21	14
11276	67.5248	150.1018	Muck Pup		pan	95.28 ppm	< 0.07 ppm	< 0.07 ppm	4.5	23	9	83	2	30	16
11277	67.5238	150.0985	Muck Pup		plac	0.0004 oz/cyd	< 0.07 ppm	< 0.07 ppm	< 0.2	31	12	82	2	33	16
11278	67.5238	150.0985	Muck Pup		plac	0.07 ppm	< 0.07 ppm	< 0.07 ppm	< 0.2	40	12	73	1	28	17
11279	67.5238	150.0985	Muck Pup		plac	0.006 oz/cyd	< 0.07 ppm	< 0.07 ppm	1.9	38	16	78	2	31	18
11280	67.4738	150.2202	Nolan, Smith Ck	otc	sel	9836			< 0.2	69	< 2	51	< 1	< 1	5
11281	67.5018	150.1608	Right Fork	otc	sel	6			0.5	28	44	43	< 1	19	6
11282	67.5018	150.1608	Right Fork	flt	sel	10			0.3	38	8	65	< 1	33	11
11283	67.5018	150.1608	Right Fork	flt	sel	13			< 0.2	29	4	75	< 1	30	13
11284	67.5018	150.1608	Right Fork	otc	ran	**26.07 ppm**			< 0.2	7	154	31	< 1	17	4
11307	67.5143	150.1260	Vermont Ck	otc	sel	< 5			< 0.2	81	11	11	4	18	10
11308	67.4982	150.1089	Buckeye Gulch		sed	< 5			< 0.2	52	11	65	< 1	44	29
11309	67.4982	150.1089	Buckeye Gulch		pan	28	10	8	< 0.2	72	7	93	2	64	30
11329	67.4854	150.0886	Lofty Gulch		sed	< 5			< 0.2	28	11	57	< 1	26	14
11330	67.4854	150.0886	Lofty Gulch		pan	13.33 ppm	16	14	0.8	62	12	74	4	60	23
11344	67.5233	150.2345	Vermont Dome	flt	sel	< 5			0.9	25	355	11	2	11	3
11345	67.5228	150.2345	Vermont Dome	flt	rand	< 5			< 0.2	41	16	4	2	10	2
11346	67.5219	150.2345	Vermont Dome	flt	rand	< 5			0.4	262	116	24	3	25	11
11347	67.5214	150.2348	Vermont Dome	flt	rand	< 5			< 0.2	15	< 2	6	1	11	4
11348	67.5167	150.0994	Hammond River	otc	sel	93			< 0.2	155	96	45	< 1	59	34
11349	67.4603	150.2403	Midnight Dome	otc	sel	< 5			< 0.2	7	< 2	37	3	26	13
11350	67.4594	150.1644	Midnight Dome	flt	rand	< 5			0.3	34	99	4	1	7	1
11351	67.4854	150.0886	Lofty Gulch	flt	sel	< 5			< 0.2	44	19	58	1	43	21
11352	67.4862	150.0857	Lofty/ Gold Bottom G.	rub	rand	< 5			< 0.2	79	< 2	44	< 1	88	25
11353	67.4857	150.0819	Gold Bottom Gulch		sed	< 5			< 0.2	35	12	58	< 1	29	16
11354	67.4857	150.0819	Gold Bottom Gulch		pan	407.59 ppm	9	14	27.0	53	11	66	3	48	22
11355	67.4847	150.0648	Steep Gulch		sed	8			< 0.2	43	12	64	< 1	34	20
11356	67.4847	150.0648	Steep Gulch		pan	276	8	8	< 0.2	142	9	76	4	50	21
11357	67.4861	150.0433	Hammond River	flt	sel	< 5			< 0.2	4	3	2	6	5	< 1
11358	67.4591	150.1639	Midnight Dome	otc	rand	**532**			< 0.2	67	7	33	< 1	37	19
11359	67.4701	150.1477	Midnight Dome	otc	sel	6			< 0.2	12	< 2	50	2	19	12
11360	67.4929	150.1729	Thompson Pup	otc	sel	< 5			< 0.2	17	26	21	3	19	8

TABLE 2c1: ASSAY DATA - GEOCHEMICAL RECONNAISSANCE SAMPLING

Field No.	Cd ppm	Bi ppm	As ppm	Sb ppm	Hg ppm	Fe pct	Mn ppm	Te ppm	Ba ppm	Cr ppm	V ppm	Sn ppm	W ppm	La ppm	Al pct	Mg pct	Ca pct
11265	9.1	< 5	3802	33	0.023	1.42	799	< 10	22	127	1	< 20	< 20	< 1	0.06	0.38	1.26
11266	0.6	< 5	289	7	0.795	1.40	818	< 10	14	149	2	< 20	< 20	1	0.14	0.42	1.73
11267	< 0.2	< 5	24	< 5	0.054	2.68	1777	< 10	22	13	16	< 20	< 20	14	0.84	0.53	0.32
11268	0.5	< 5	199	< 5	0.173	5.67	5504	< 10	145	424	41	< 20	< 20	12	1.80	0.79	0.69
11275	< 0.2	< 5	81	< 5	0.020	3.15	724	< 10	23	19	31	< 20	< 20	10	1.18	0.88	0.53
11276	< 0.2	< 5	633	< 5	1.160	5.51	1165	< 10	67	294	80	< 20	< 20	9	2.43	1.47	0.82
11277	< 0.2	< 5	17	< 5	0.440	4.53	1100	< 10	52	187	47	< 20	< 20	5	1.35	0.94	1.53
11278	< 0.2	< 5	13	< 5	0.063	5.20	1604	< 10	33	108	47	< 20	< 20	10	1.68	1.48	2.99
11279	< 0.2	< 5	678	< 5	0.630	5.48	1125	< 10	57	213	61	< 20	< 20	9	1.90	1.37	1.22
11280	2.3	< 5	924	42.42%	0.457	1.08	912	< 10	< 1	69	2	< 20	< 20	< 1	0.06	0.68	1.89
11281	< 0.2	< 5	17	161	0.047	2.14	822	< 10	25	66	6	< 20	< 20	3	0.52	0.80	> 10.00
11282	< 0.2	< 5	47	16	0.034	3.58	658	< 10	31	47	11	< 20	< 20	6	1.04	1.21	5.52
11283	< 0.2	< 5	70	7	0.064	3.99	821	< 10	39	37	12	< 20	< 20	10	1.00	1.55	3.96
11284	0.3	< 5	126	80	0.128	0.69	208	< 10	10	211	2	< 20	< 20	1	0.06	0.07	0.31
11307	< 0.2	< 5	31	< 5	0.036	1.04	554	< 10	51	127	9	< 20	< 20	7	0.27	0.08	0.13
11308	< 0.2	< 5	27	9	0.048	2.95	3647	< 10	34	12	15	< 20	< 20	13	0.67	0.46	0.24
11309	< 0.2	< 5	25	7	0.049	5.68	5382	< 10	154	323	57	< 20	< 20	17	2.43	1.11	0.29
11329	< 0.2	< 5	38	< 5	0.075	2.30	1970	< 10	42	10	15	< 20	< 20	10	0.59	0.35	0.39
11330	0.6	< 5	176	< 5	0.540	9.04	9063	< 10	107	454	71	< 20	< 20	15	1.59	0.31	0.44
11344	< 0.2	< 5	< 5	< 5	< 0.010	1.74	2320	< 10	3	190	1	< 20	< 20	1	0.04	0.74	2.57
11345	< 0.2	< 5	< 5	< 5	< 0.010	0.65	157	< 10	4	349	2	< 20	< 20	< 1	0.07	0.03	0.18
11346	< 0.2	< 5	< 5	< 5	< 0.010	2.93	2340	< 10	9	207	9	< 20	< 20	4	0.57	0.61	2.73
11347	< 0.2	< 5	< 5	< 5	< 0.010	1.46	1310	< 10	5	196	2	< 20	< 20	1	0.06	0.54	2.35
11348	0.4	< 5	161	24	0.321	5.27	17637	< 10	20	155	7	< 20	< 20	4	0.29	1.91	5.88
11349	< 0.2	< 5	19	8	0.113	1.49	1575	< 10	34	206	5	< 20	< 20	5	0.28	0.05	0.16
11350	< 0.2	< 5	< 5	< 5	0.047	0.45	160	< 10	2	208	1	< 20	< 20	< 1	0.07	0.04	0.12
11351	< 0.2	< 5	45	< 5	0.019	2.42	2729	< 10	48	66	20	< 20	< 20	11	1.06	0.62	0.31
11352	< 0.2	< 5	23	< 5	< 0.0100	4.09	677	< 10	9	147	46	< 20	< 20	< 1	2.79	2.78	2.13
11353	< 0.2	< 5	35	< 5	0.054	2.74	2228	< 10	26	10	14	< 20	< 20	12	0.51	0.45	0.80
11354	0.3	< 5	154	< 5	5.320	5.10	3452	< 10	133	373	42	< 20	< 20	12	1.38	0.70	0.89
11355	< 0.2	< 5	30	< 5	0.036	3.16	2996	< 10	28	12	17	< 20	< 20	15	0.72	0.49	0.51
11356	0.2	< 5	76	< 5	0.037	5.08	3609	< 10	110	429	44	< 20	< 20	13	1.79	0.74	0.52
11357	< 0.2	< 5	< 5	< 5	0.288	0.23	18	< 10	100	128	31	< 20	< 20	5	0.14	0.02	0.03
11358	< 0.2	< 5	44	29	0.232	2.70	2556	< 10	49	140	10	< 20	< 20	7	0.38	0.55	0.91
11359	< 0.2	< 5	50	19	0.086	3.42	1838	< 10	5	154	5	< 20	< 20	2	0.09	2.17	5.87
11360	< 0.2	< 5	61	20	0.045	1.93	6614	< 10	46	368	5	< 20	< 20	7	0.24	0.39	0.95

TABLE 2c1: ASSAY DATA - GEOCHEMICAL RECONNAISSANCE SAMPLING

Field No.	Na pct	K pct	Sr ppm	Y ppm	Ga ppm	Li ppm	Nb ppm	Sc ppm	Ta ppm	Ti pct	Zr ppm	Comments
11265	0.01	0.03	36	2	< 2	< 1	< 1	< 5	< 10	< 0.01	< 1	qz veinlet w/ 5% py
11266	0.01	0.07	63	3	< 2	1	< 1	< 5	< 10	< 0.01	< 1	qz veinlet w/ 1% py, visible Au
11267	< 0.01	0.04	21	6	< 2	12	< 1	< 5	< 10	< 0.01	< 1	
11268	0.08	0.42	59	8	3	19	< 1	< 5	< 10	0.02	< 1	minor py and mag
11275	< 0.01	0.06	26	7	2	15	< 1	< 5	< 10	0.02	< 1	
11276	0.09	0.30	35	10	5	27	< 1	7	< 10	0.11	< 1	1 fine and 2 v fine Au
11277	0.02	0.13	51	6	< 2	20	< 1	< 5	< 10	0.06	< 1	3 fine and 5 v fine Au
11278	0.03	0.16	133	11	3	22	< 1	< 5	< 10	0.06	< 1	2 v fine Au, tr mag
11279	0.03	0.17	48	9	3	23	< 1	< 5	< 10	0.08	< 1	3 coarse, 4 fine, 6 v fine Au flakes
11280	< 0.01	0.02	163	2	< 2	< 1	< 1	< 5	< 10	< 0.01	< 1	qz veinlets w/ 50% Sb, 10% sid
11281	0.02	0.14	733	16	< 2	10	< 1	< 5	< 10	< 0.01	< 1	qz veinlets w/ 50 % ca
11282	0.02	0.22	309	9	< 2	20	< 1	< 5	< 10	< 0.01	< 1	phyllite w/ 2% euhedral py
11283	0.02	0.27	135	5	< 2	18	< 1	< 5	< 10	< 0.01	< 1	phyllite w/ 2% euhedral py
11284	0.01	0.03	26	2	< 2	< 1	< 1	< 5	< 10	< 0.01	< 1	qz veinlet
11307	0.02	0.16	11	1	< 2	2	< 1	< 5	< 10	< 0.01	3	mica qz schist w/ <5% py
11308	< 0.01	0.05	23	5	< 2	8	< 1	< 5	< 10	< 0.01	< 1	
11309	0.07	0.48	35	10	4	22	< 1	7	< 10	0.05	< 1	
11329	< 0.01	0.04	25	5	< 2	8	< 1	< 5	< 10	< 0.01	< 1	
11330	0.06	0.30	37	26	< 2	11	< 1	10	< 10	0.03	< 1	1 v fine Au, abu mag, from cutbank
11344	< 0.01	< 0.01	112	4	< 2	< 1	< 1	< 5	< 10	< 0.01	1	qz float
11345	< 0.01	0.01	7	1	< 2	1	< 1	< 5	< 10	< 0.01	2	loose vein qz
11346	0.01	0.03	124	7	< 2	10	< 1	< 5	< 10	< 0.01	2	loose vein qz
11347	< 0.01	0.01	135	8	< 2	< 1	< 1	< 5	< 10	< 0.01	2	loose vein qz
11348	< 0.01	0.06	365	13	< 2	5	< 1	< 5	< 10	< 0.01	2	qz w/ py and other sulfides
11349	0.01	0.12	18	2	< 2	2	< 1	< 5	< 10	< 0.01	2	vein qz
11350	< 0.01	< 0.01	9	< 1	< 2	< 1	< 1	< 5	< 10	< 0.01	1	loose vein qz
11351	0.02	0.11	14	4	< 2	9	< 1	< 5	< 10	< 0.01	< 1	greenstone w/ fine, euhedral py
11352	0.03	0.02	27	6	< 2	21	< 1	< 5	< 10	0.22	< 1	greenstone, greenschist w/ py, po
11353	< 0.01	0.04	43	6	< 2	7	< 1	< 5	< 10	< 0.01	< 1	
11354	0.08	0.29	50	11	< 2	13	< 1	5	< 10	0.03	< 1	2 coarse, 3 fine, 3 v fine Au, abu mag
11355	< 0.01	0.05	35	6	< 2	9	< 1	< 5	< 10	< 0.01	< 1	
11356	0.07	0.39	39	8	2	17	< 1	5	< 10	0.02	< 1	tr mag
11357	< 0.01	0.07	2	< 1	< 2	1	< 1	< 5	< 10	< 0.01	3	phyllite w/ mag properties (?)
11358	0.02	0.14	77	3	< 2	3	< 1	< 5	< 10	< 0.01	1	qz w/ py, lim
11359	< 0.01	0.03	506	5	< 2	< 1	< 1	< 5	< 10	< 0.01	1	qz w/ py, lim
11360	0.02	0.10	59	3	< 2	2	< 1	< 5	< 10	< 0.01	4	vein qz

TABLE 2c1: ASSAY DATA - GEOCHEMICAL RECONNAISSANCE SAMPLING

Field No.	Latitude	Longitude	Location	Sample Site	Sample Type	Au ppb	Pt ppb	Pd ppb	Ag ppm	Cu ppm	Pb ppm	Zn ppm	Mo ppm	Ni ppm	Co ppm
11361	67.4929	150.1729	Thompson Pup	otc	sel	< 5			< 0.2	13	< 2	12	1	9	3
11362	67.4914	150.1771	Thompson Pup	otc	sel	6			< 0.2	10	< 2	11	4	16	3
11363	67.4911	150.1790	Thompson Pup	otc	rand	< 5			< 0.2	13	8	26	1	11	6
11364	67.4896	150.1875	Thompson Pup	otc	sel	13			< 0.2	12	< 2	35	1	32	10
11365	67.4887	150.1900	Thompson Pup	otc	rand	17			< 0.2	11	4	20	2	14	6
11366	67.4887	150.1900	Thompson Pup	otc	rand	8			< 0.2	20	12	26	2	20	8
11367	67.4887	150.1900	Thompson Pup	otc	rand	83			< 0.2	24	45	74	1	20	11
11368	67.4887	150.1900	Thompson Pup	otc	sel	38			< 0.2	14	< 2	< 1	4	19	3
11369	67.4886	150.1672	Fay Ck	otc	sel	44			< 0.2	18	45	64	< 1	15	8
11370	67.4875	150.1680	Fay Ck	otc	sel	< 5			< 0.2	14	31	69	1	15	7
11371	67.4886	150.1672	Fay Ck	otc	sel	167			< 0.2	45	29	39	2	30	15
11372	67.4721	150.2279	Smith Ck	otc	sel	1804			< 0.2	16	< 2	34	< 1	< 1	3
11373	67.4490	150.1316	Midnight Dome, south	flt	rand	< 5			< 0.2	4	< 2	19	1	16	4
11374	67.4467	150.1307	Midnight Dome, south	otc	sel	< 5			< 0.2	13	< 2	2	3	13	1
11375	67.4475	150.1273	Midnight Dome, south	otc	sel	19			< 0.2	12	< 2	16	< 1	10	3
11376	67.4908	150.0890	Hammond River	otc	sel	23			< 0.2	5	18	1	1	14	6
11377	67.4860	150.0597	Steep Gulch	otc	sel	< 5			0.2	36	< 2	55	1	113	28
11378	67.4917	150.2621	Acme Ck	otc	sel	6			0.4	25	85	17	2	12	3
11379	67.4892	150.2083	Nolan Ck	otc	rand	37			0.3	17	10	13	4	11	1
11380	67.4861	150.0792	Gold Bottom Gulch	otc	sel	< 5			< 0.2	48	3	57	1	41	20
11381	67.4861	150.0792	Gold Bottom Gulch	otc	sel	33			< 0.2	91	4	44	2	22	9
11382	67.4861	150.0792	Gold Bottom Gulch	otc	sel	61			0.6	506	9	101	3	25	6
11383	67.4644	150.0909	Confederate Gulch	otc	rand	27			0.5	6	37	43	2	57	9
11384	67.4650	150.0928	Confederate Gulch	otc	sel	11			0.2	21	3	37	2	25	6
11385	67.4650	150.0928	Confederate Gulch	flt	sel	< 5			0.3	25	5	53	1	72	10
11386	67.4661	150.0985	Confederate Gulch	otc	sel	11			< 0.2	11	7	48	2	20	7
11387	67.4611	150.1061	Confederate Gulch	otc	sel	9			< 0.2	6	< 2	24	2	16	5
11388	67.4611	150.1083	Confederate Gulch	otc	sel	33			< 0.2	8	9	21	2	10	3
11389	67.4622	150.1083	Confederate Gulch	otc	sel	13			< 0.2	48	13	29	2	27	10
11390	67.4622	150.1083	Confederate Gulch	otc	rand	< 5			< 0.2	37	< 2	29	2	28	19
11391	67.4650	150.1159	Confederate Gulch	otc	rand	< 5			0.9	< 1	9	13	< 1	3	< 1
11392	67.5058	150.2358	Montana Mountain	flt	sel	< 5			< 0.2	4	10	32	2	5	4
11393	67.4982	150.1089	Buckeye Gulch	otc	sel	< 5			< 0.2	35	55	20	3	21	7
11394	67.4982	150.1089	Buckeye Gulch	otc	sel	< 5			< 0.2	13	6	15	2	22	6
11395	67.4921	150.1710	Thompson Pup	flt	sel	9			< 0.2	7	7	21	2	10	3
11396	67.5158	150.1364	Vermont Ck	otc	sel	17			< 0.2	4	3	27	3	34	10

TABLE 2c1: ASSAY DATA - GEOCHEMICAL RECONNAISSANCE SAMPLING

Field No.	Cd ppm	Bi ppm	As ppm	Sb ppm	Hg ppm	Fe pct	Mn ppm	Te ppm	Ba ppm	Cr ppm	V ppm	Sn ppm	W ppm	La ppm	Al pct	Mg pct	Ca pct
11361	< 0.2	< 5	< 5	< 5	< 0.010	1.02	599	< 10	36	215	4	< 20	< 20	3	0.34	0.29	1.86
11362	< 0.2	< 5	52	5	< 0.010	1.00	1216	< 10	32	309	3	< 20	< 20	2	0.12	0.18	0.39
11363	< 0.2	< 5	36	5	0.050	2.96	3775	< 10	39	196	16	< 20	< 20	3	0.39	1.85	4.72
11364	0.4	< 5	113	8	0.034	2.61	1811	< 10	29	245	10	< 20	< 20	5	0.64	0.58	0.57
11365	< 0.2	< 5	51	9	0.044	3.29	2431	< 10	26	126	7	< 20	< 20	5	0.32	2.06	6.46
11366	< 0.2	< 5	36	14	0.056	4.10	5940	< 10	31	145	9	< 20	< 20	4	0.28	2.16	5.30
11367	< 0.2	< 5	41	56	0.134	3.77	5911	< 10	35	128	13	< 20	< 20	5	0.73	1.39	6.27
11368	< 0.2	< 5	18	< 5	0.014	0.82	546	< 10	3	323	< 1	< 20	< 20	< 1	0.03	0.16	0.52
11369	< 0.2	< 5	35	23	0.084	5.43	2459	< 10	264	95	15	< 20	< 20	6	0.53	3.02	8.23
11370	0.2	< 5	59	21	0.285	2.07	2462	< 10	67	227	6	< 20	< 20	7	0.34	0.41	0.87
11371	< 0.2	< 5	21	15	0.041	4.50	3281	< 10	231	146	22	< 20	< 20	6	0.89	1.83	3.80
11372	5.2	< 5	1365	2000	0.234	1.30	1088	< 10	18	138	3	< 20	< 20	1	0.13	0.53	1.42
11373	< 0.2	< 5	< 5	158	< 0.010	1.55	760	< 10	15	228	8	< 20	< 20	4	0.71	0.52	3.87
11374	< 0.2	< 5	< 5	28	< 0.010	0.39	234	< 10	8	276	2	< 20	< 20	< 1	0.06	0.04	0.14
11375	0.3	< 5	88	1101	0.010	1.51	348	< 10	10	117	2	< 20	< 20	4	0.15	0.19	> 10.00
11376	4.1	< 5	2127	18	0.034	1.24	714	< 10	14	248	4	< 20	< 20	3	0.24	0.31	0.61
11377	< 0.2	< 5	6	< 5	< 0.010	4.96	755	< 10	18	154	59	< 20	< 20	< 1	3.17	3.24	2.56
11378	< 0.2	< 5	< 5	62	0.012	0.59	171	< 10	17	280	1	< 20	< 20	< 1	0.09	0.04	0.07
11379	< 0.2	< 5	14	27	0.086	0.84	99	< 10	21	200	8	< 20	< 20	5	0.19	0.09	0.04
11380	< 0.2	< 5	< 5	< 5	0.010	3.33	1946	< 10	226	115	20	< 20	< 20	13	0.85	0.56	0.48
11381	< 0.2	< 5	37	52	0.362	2.53	3035	< 10	199	134	6	< 20	< 20	4	0.46	0.68	1.34
11382	< 0.2	< 5	19	338	2.112	1.79	2033	< 10	40	357	4	< 20	< 20	3	0.20	0.44	0.59
11383	0.3	< 5	88	7	0.016	4.65	1753	< 10	20	123	16	< 20	< 20	1	1.11	2.74	8.11
11384	< 0.2	< 5	49	6	0.014	3.19	962	< 10	30	78	10	< 20	< 20	1	0.74	1.73	4.51
11385	< 0.2	< 5	55	13	0.021	5.16	1188	< 10	24	112	23	< 20	< 20	< 1	1.77	3.49	5.93
11386	< 0.2	< 5	30	6	0.023	2.16	817	< 10	19	199	9	< 20	< 20	5	0.72	0.55	0.70
11387	2.9	< 5	591	< 5	0.026	1.65	1649	< 10	27	180	3	< 20	< 20	2	0.22	0.60	1.32
11388	< 0.2	< 5	5	< 5	< 0.010	2.51	2518	< 10	4	175	3	< 20	< 20	1	0.20	0.93	3.23
11389	0.6	< 5	101	28	0.025	1.55	1943	< 10	25	175	5	< 20	< 20	4	0.31	0.26	0.63
11390	0.2	< 5	47	6	0.032	2.94	1278	< 10	26	143	12	< 20	< 20	10	0.52	0.28	0.19
11391	< 0.2	< 5	19	< 5	0.014	1.13	281	< 10	22	24	2	< 20	< 20	< 1	0.10	0.40	> 10.00
11392	< 0.2	< 5	< 5	< 5	< 0.010	7.27	5641	< 10	< 1	61	1	< 20	< 20	1	0.03	3.29	9.44
11393	< 0.2	< 5	7	< 5	0.016	1.69	3783	< 10	25	252	9	< 20	< 20	2	0.35	0.15	0.37
11394	< 0.2	< 5	< 5	< 5	0.020	1.17	2651	< 10	26	247	6	< 20	< 20	2	0.32	0.13	0.12
11395	< 0.2	< 5	16	< 5	< 0.010	2.24	6409	< 10	15	161	6	< 20	< 20	< 1	0.05	1.77	4.43
11396	0.5	< 5	103	11	0.045	4.26	3064	< 10	13	160	9	< 20	< 20	< 1	0.49	2.44	6.00

TABLE 2c1: ASSAY DATA - GEOCHEMICAL RECONNAISSANCE SAMPLING

Field No.	Na pct	K pct	Sr ppm	Y ppm	Ga ppm	Li ppm	Nb ppm	Sc ppm	Ta ppm	Ti pct	Zr ppm	Comments
11361	0.01	0.03	45	3	< 2	4	< 1	< 5	< 10	< 0.01	< 1	qz w/ py, lim
11362	< 0.01	0.04	24	< 1	< 2	< 1	< 1	< 5	< 10	< 0.01	2	vein qz
11363	0.03	0.07	139	7	< 2	8	1	< 5	< 10	< 0.01	5	vein qz
11364	0.02	0.13	29	3	< 2	10	< 1	< 5	< 10	< 0.01	5	vein qz
11365	0.02	0.15	332	9	< 2	3	< 1	< 5	< 10	< 0.01	1	qz w/ py, apy
11366	0.02	0.11	410	6	< 2	3	< 1	< 5	< 10	< 0.01	2	qz w/ py, lim
11367	0.02	0.18	512	16	< 2	8	< 1	< 5	< 10	< 0.01	< 1	vein qz
11368	< 0.01	0.01	30	1	< 2	< 1	< 1	< 5	< 10	< 0.01	< 1	metamorphic qz
11369	0.03	0.17	552	14	< 2	5	< 1	< 5	< 10	< 0.01	2	qz w/ py, lim
11370	0.01	0.12	61	2	< 2	6	< 1	< 5	< 10	< 0.01	2	vein qz
11371	0.03	0.21	292	6	< 2	9	1	< 5	< 10	< 0.01	2	qz w/ lim
11372	< 0.01	0.06	122	2	< 2	< 1	< 1	< 5	< 10	< 0.01	< 1	qz w/ stb
11373	< 0.01	0.08	233	7	< 2	8	< 1	< 5	< 10	< 0.01	1	qz w/ sid
11374	< 0.01	0.01	8	< 1	< 2	< 1	< 1	< 5	< 10	< 0.01	1	metamorphic qz
11375	< 0.01	0.08	1340	8	< 2	< 1	< 1	< 5	< 10	< 0.01	3	qz w/ py, sid, hem, lim
11376	< 0.01	0.07	47	1	< 2	3	< 1	< 5	< 10	< 0.01	< 1	vein qz
11377	0.02	0.06	46	6	< 2	36	2	< 5	< 10	0.20	< 1	porphyry greenstone w/ py
11378	< 0.01	0.02	2	< 1	< 2	< 1	< 1	< 5	< 10	< 0.01	< 1	metamorphic qz
11379	0.03	0.08	10	1	< 2	1	< 1	< 5	< 10	< 0.01	5	qz veinlets in graphitic schist
11380	0.04	0.17	34	9	< 2	10	< 1	< 5	< 10	0.01	< 1	qtz schist w/ py
11381	0.01	0.18	134	4	< 2	4	< 1	< 5	< 10	< 0.01	< 1	qz vein in banded graphitic schist
11382	< 0.01	0.08	58	2	< 2	3	< 1	< 5	< 10	< 0.01	< 1	qz vein
11383	0.02	0.17	476	13	< 2	19	< 1	< 5	< 10	< 0.01	< 1	qz vein
11384	0.02	0.21	229	10	< 2	8	< 1	< 5	< 10	< 0.01	< 1	qz vein w/ sid, lim
11385	0.01	0.18	288	6	< 2	32	< 1	5	< 10	< 0.01	< 1	qz vein w/ lim
11386	0.02	0.12	51	3	< 2	7	< 1	< 5	< 10	< 0.01	< 1	qz vein
11387	0.01	0.12	95	2	< 2	1	< 1	< 5	< 10	< 0.01	< 1	qz w/ lim after py
11388	< 0.01	0.03	333	26	< 2	3	< 1	< 5	< 10	< 0.01	< 1	metamorphic qz
11389	0.01	0.13	34	2	< 2	2	< 1	< 5	< 10	< 0.01	< 1	qz vein
11390	0.01	0.13	12	3	< 2	4	< 1	< 5	< 10	< 0.01	< 1	qz vein w/ sid, lim after py
11391	< 0.01	0.06	1029	8	< 2	< 1	< 1	< 5	< 10	< 0.01	< 1	qz vein w/ sid
11392	< 0.01	0.01	616	35	< 2	1	< 1	8	< 10	< 0.01	< 1	qz vein w/ sid, hem
11393	0.01	0.08	39	4	< 2	3	< 1	< 5	< 10	< 0.01	< 1	qz vein
11394	0.01	0.08	14	2	< 2	3	< 1	< 5	< 10	< 0.01	< 1	metamorphic qz
11395	< 0.01	0.02	142	3	< 2	1	< 1	< 5	< 10	< 0.01	< 1	qz w/ sid, py
11396	0.01	0.10	640	13	< 2	10	< 1	6	< 10	< 0.01	< 1	qz w/ carbonate, lim

TABLE 2c1: ASSAY DATA - GEOCHEMICAL RECONNAISSANCE SAMPLING

Field No.	Latitude	Longitude	Location	Sample Site	Sample Type	Au ppb	Pt ppb	Pd ppb	Ag ppm	Cu ppm	Pb ppm	Zn ppm	Mo ppm	Ni ppm	Co ppm
11397	67.5164	150.1369	Vermont Ck	otc	rand	78			0.3	10	13	41	3	19	5
11398	67.4963	150.1513	Palisades	otc	sel	52			< 0.2	23	15	6	< 1	6	1
11399	67.4935	150.1600	Palisades	otc	sel	14			< 0.2	3	3	11	< 1	6	6
11400	67.4808	150.1629	Smith Creek Dome	otc	sel	< 5			< 0.2	6	11	11	< 1	12	4
11401	67.4814	150.1629	Smith Creek Dome	otc	sel	8			< 0.2	63	< 2	35	< 1	21	11
11402	67.4750	150.2194	Smith Ck	otc	sel	1716			< 0.2	4	3	21	< 1	< 1	1
11403	67.4750	150.2194	Smith Ck	otc	rand	393			0.3	7	7	35	2	7	2
11404	67.4750	150.2194	Smith Ck	otc	sel	501			0.4	10	< 2	30	< 1	< 1	< 1

TABLE 2c1: ASSAY DATA - GEOCHEMICAL RECONNAISSANCE SAMPLING

Field No.	Cd ppm	Bi ppm	As ppm	Sb ppm	Hg ppm	Fe pct	Mn ppm	Te ppm	Ba ppm	Cr ppm	V ppm	Sn ppm	W ppm	La ppm	Al pct	Mg pct	Ca pct
11397	0.2	< 5	55	9	0.066	3.13	1901	< 10	11	174	8	< 20	< 20	2	0.56	1.53	4.29
11398	< 0.2	< 5	26	9	0.042	0.91	1378	< 10	19	116	2	< 20	< 20	1	0.10	0.30	0.75
11399	< 0.2	< 5	16	< 5	0.041	1.60	3525	< 10	10	79	2	< 20	< 20	< 1	0.06	1.29	3.34
11400	< 0.2	< 5	< 5	25	0.085	0.60	735	< 10	22	139	2	< 20	< 20	< 1	0.10	0.04	0.08
11401	< 0.2	< 5	20	24	0.153	2.74	2221	< 10	111	69	9	< 20	< 20	11	0.29	0.04	0.12
11402	5.9	< 5	1207	> 2000	0.066	1.22	961	< 10	5	109	3	< 20	< 20	< 1	0.12	0.85	2.12
11403	2.0	< 5	441	169	0.079	3.42	1550	< 10	14	144	8	< 20	< 20	< 1	0.33	3.31	7.12
11404	2.3	< 5	51	> 2000	0.153	0.81	661	< 10	3	43	1	< 20	32	< 1	0.06	0.71	1.45

TABLE 2c1: ASSAY DATA - GEOCHEMICAL RECONNAISSANCE SAMPLING

Field No.	Na pct	K pct	Sr ppm	Y ppm	Ga ppm	Li ppm	Nb ppm	Sc ppm	Ta ppm	Ti pct	Zr ppm	Comments
11397	0.01	0.06	338	9	< 2	11	< 1	< 5	< 10	< 0.01	< 1	qz vein w/ sid, hem (?), py
11398	< 0.01	0.05	55	1	< 2	2	< 1	< 5	< 10	< 0.01	< 1	qz vein w/ sid after py
11399	< 0.01	0.02	215	4	< 2	1	< 1	< 5	< 10	< 0.01	< 1	qz vein w/ sid
11400	< 0.01	0.04	7	1	< 2	1	< 1	< 5	< 10	< 0.01	< 1	qz vein w/ lim
11401	0.01	0.14	10	4	< 2	2	< 1	< 5	< 10	< 0.01	< 1	qz vein w/ lim
11402	0.01	0.05	147	4	< 2	< 1	< 1	< 5	< 10	< 0.01	< 1	qz vein w/ stb, carbonate
11403	0.02	0.13	623	7	< 2	1	< 1	< 5	< 10	< 0.01	< 1	qz vein w/ stb, carbonate
11404	< 0.01	0.02	87	2	< 2	< 1	< 1	< 5	< 10	< 0.01	< 1	qz vein w/ stb, carbonate

ASSAY DATA 2c2: GEOCHEMICAL RECONNAISSANCE SAMPLING

Field No.	Sample Site Type	Au ppb	Ag ppm	AL ppm	As ppm	Ba ppm	Bi ppm	Ca ppm	Cd ppm	Co ppm
Nc1	otc rep	65	<0.2	0.25	44	10	<2	0.97	<0.5	13
Nc2	otc rep	50	0.2	0.27	938	20	<2	2.63	<0.5	106
Nc3	flt sel	60	0.2	0.1	54	10	<2	0.03	<0.5	6
Nc4	trn sel	90	0.2	0.09	4760	20	<2	0.24	<0.5	7

Field No.	Sample Site Type	Cr ppm	Cu ppm	Fe %	Ga ppm	Hg ppm	K %	La ppm	Mg %	Mn ppm
Nc1	otc rep	467	32	1.93	<10	<1	0.09	<10	0.65	2270
Nc2	otc rep	486	167	6.35	<10	<1	0.07	<10	1.15	>1000
Nc3	flt sel	427	13	0.89	<10	<1	0.03	<10	0.01	1095
Nc4	trn sel	257	16	1.31	<10	<1	0.03	<10	0.18	580

Field No.	Sample Site Type	Mo ppm	Na %	Ni ppm	P ppm	Pb ppm	Sb ppm	Sc ppm	Sr ppm	Ti %
Nc1	otc rep	1	0.03	11	100	4	6	1	63	<0.01
Nc2	otc rep	<1	<0.01	211	330	6	60	4	244	<0.01
Nc3	flt sel	1	<0.01	11	70	6	4	<1	8	<0.01
Nc4	trn sel	1	<0.01	13	40	<2	14	<1	36	<0.01

Field No.	Sample Site Type	Te ppm	U ppm	V ppm	W ppm	Zn ppm
Nc1	otc rep	<10	<10	7	<10	130
Nc2	otc rep	<10	<10	9	<10	40
Nc3	flt sel	<10	<10	3	<10	12
Nc4	trn sel	<10	<10	3	<10	8

TABLE 3: MICROPROBE DATA FOR LODE AND PLACER GOLD GRAINS - IN WEIGHT PERCENT

Line Number	AU e%	Ag e%	Hg e%	Sb e%	Bi e%	Te e%	Totals e%
Slisco Bench, core							
332	91.76600	3.17954	6.05487	0.00000	0.00000	0.00000	101.000
333	92.06870	3.20759	5.10346	0.05866	0.00000	0.05746	100.496
334	90.94810	3.16868	6.25343	0.00000	0.00000	0.00000	100.370
Slisco Bench, rim							
335	92.96720	3.25620	4.57506	0.00000	0.00000	0.02760	100.826
336	90.67470	3.17515	6.29672	0.00000	0.00000	0.00000	100.147
337	92.83130	3.22344	4.03241	0.00000	0.00000	0.01163	100.099
Rye&Jay Creek 1, core							
338	99.33900	1.15883	1.13111	0.00000	0.00000	0.00000	101.629
339	98.35860	1.12218	1.05954	0.01435	0.00000	0.01653	100.571
340	99.29360	1.17103	1.15400	0.00000	0.00000	0.00165	101.620
Rye&Jay Creek 1, rim							
341	97.44830	1.58439	2.14192	0.00000	0.00000	0.00412	101.179
342	95.98440	1.71798	2.24261	0.00000	0.00000	0.00576	99.951
343	96.98580	1.43901	1.98474	0.03261	0.00000	0.00000	100.442
Rye&Jay Creek 2, rim							
344	94.62540	6.26024	1.16133	0.00000	0.00000	0.00408	102.051
345	95.19950	5.74653	0.98406	0.00000	0.00000	0.00000	101.930
346	93.65710	6.01865	0.64002	0.00000	0.00000	0.00000	100.316
Rye&Jay Creek 2, core							
347	93.05090	6.09877	1.22049	0.00000	0.00000	0.00489	100.375
348	93.64820	6.36597	1.19927	0.00000	0.00000	0.02036	101.234
349	94.50640	6.35431	0.96625	0.00504	0.00000	0.01466	101.847
Rye&Jay Creek 3, core							
350	97.35840	2.22840	1.77173	0.01011	0.00000	0.05382	101.422
351	97.10180	2.20047	1.68809	0.00000	0.00000	0.04648	101.037
352	97.01030	2.23779	1.44812	0.00000	0.00000	0.04239	100.739
Rye&Jay Creek 3, rim							
353	96.25560	2.31224	2.09121	0.00000	0.00000	0.00000	100.659
354	96.10270	2.61594	2.21330	0.00000	0.00000	0.00000	100.932
355	96.80470	2.33935	2.29907	0.00000	0.00000	0.00000	101.443
Archibald Creek 2, core							
356	95.44760	2.84910	2.52254	0.05127	0.00000	0.03887	100.909
357	95.13810	2.45950	2.70383	0.00102	0.00000	0.00000	100.302
358	97.52860	2.56085	2.93021	0.00000	0.00000	0.02063	103.040
359	96.66160	2.66167	2.28779	0.00102	0.00000	0.03873	101.651
360	96.46870	2.52058	2.52288	0.00000	0.00000	0.03622	101.548
Archibald Creek 2, rim							
361	96.02490	2.53158	3.18013	0.00408	0.00000	0.00000	101.741
362	96.59680	2.59882	2.71401	0.00000	0.00000	0.00000	101.910
363	96.04950	2.55207	2.80141	0.00916	0.00000	0.00985	101.422
364	95.23120	2.82681	2.32770	0.00000	0.00000	0.00000	100.386

TABLE 3: MICROPROBE DATA FOR LODE AND PLACER GOLD GRAINS - IN WEIGHT PERCENT

Line Number	AU e%	Ag e%	Hg e%	Sb e%	Bi e%	Te e%	Totals e%
365	95.03440	2.69253	3.02872	0.00000	0.00000	0.00000	100.756
366	96.06850	2.77179	2.45127	0.02741	0.00000	0.00901	101.328
Smith Creek 1, core							
367	97.05080	3.62188	1.25882	0.00000	0.00000	0.02045	101.952
368	96.53870	3.97754	0.78509	0.00202	0.00000	0.01144	101.315
369	97.12840	3.80180	1.00901	0.02532	0.00000	0.02287	101.987
Smith Creek 1, rim							
370	96.09690	3.93674	0.86741	0.00000	0.00000	0.00408	100.905
371	96.15430	3.79396	1.28207	0.00000	0.00000	0.00000	101.230
372	96.61140	3.75882	1.01315	0.00000	0.00000	0.04236	101.426
Smith Creek 2, rim							
373	94.94210	2.93021	3.54447	0.00000	0.00000	0.00000	101.417
374	95.15570	2.86838	3.64117	0.00000	0.00000	0.00000	101.665
375	94.72990	2.86749	3.28702	0.00000	0.00000	0.00000	100.884
Smith Creek 2, core							
376	97.18460	2.63778	1.42568	0.00000	0.00000	0.00000	101.248
377	97.61570	2.68242	0.85873	0.00303	0.00000	0.00000	101.160
378	97.29110	2.69993	0.74762	0.00000	0.00000	0.02358	100.762
Smith Creek 3, core							
379	97.51600	1.29892	1.82590	0.02018	0.00000	0.07811	100.739
380	97.74560	1.28304	2.04556	0.07160	0.00000	0.00000	101.146
381	97.61250	1.44075	1.94468	0.00000	0.00000	0.00000	100.998
Smith Creek 3, rim							
382	97.31600	1.55519	1.84868	0.04132	0.00000	0.00000	100.761
383	96.67650	1.43604	2.13806	0.05241	0.00000	0.01057	100.314
384	96.75460	1.43430	2.52769	0.03426	0.00000	0.00000	100.751
Smith Creek 4, core							
385	96.96750	3.68760	1.05605	0.00000	0.00000	0.01073	101.722
386	97.31600	3.65665	0.74145	0.00817	0.00000	0.00000	101.722
387	96.95500	3.69505	0.71203	0.01123	0.00000	0.00000	101.373
Smith Creek 4, rim							
388	94.26470	3.43422	3.20248	0.01020	0.00000	0.00000	100.912
389	94.49860	3.61096	2.79678	0.00000	0.00000	0.00000	100.906
390	94.98180	3.49300	3.42195	0.01832	0.00000	0.00000	101.915
Smith Creek 5, rim							
391	96.32650	2.98737	1.49770	0.02339	0.00000	0.00000	100.835
392	95.94080	2.75078	1.29107	0.00000	0.00000	0.00410	99.987
393	97.21420	2.90312	1.09905	0.00406	0.00000	0.00000	101.220
Smith Creek 5, core							
394	96.38170	3.03493	1.29108	0.00000	0.00000	0.00000	100.708
395	96.56670	3.11002	1.27101	0.00000	0.00000	0.00000	100.948
396	96.93580	3.10717	1.33358	0.00000	0.00000	0.00000	101.377

TABLE 3: MICROPROBE DATA FOR LODE AND PLACER GOLD GRAINS - IN WEIGHT PERCENT

Line	AU	Ag	Hg	Sb	Bi	Te	Totals
Number	e%	e%	e%	e%	e%	e%	e%
Smith Creek 6, core							
397	91.39660	7.34686	2.63553	0.01210	0.00000	0.07241	101.463
398	89.12590	7.35981	5.43103	0.01512	0.00000	0.02279	101.955
399	92.00370	7.35239	3.20451	0.00000	0.00000	0.05448	102.615
Smith Creek 6, rim							
400	91.17280	7.36104	2.33899	0.02316	0.00000	0.00000	100.896
401	92.33110	7.24793	2.08475	0.00000	0.00000	0.01219	101.676
402	91.65510	7.64178	2.75059	0.00000	0.00000	0.09499	102.142
Swede Underground 1, core							
403	90.18580	10.51760	1.22585	0.02107	0.00000	0.04130	101.992
404	88.78210	10.45800	1.71930	0.02508	0.00000	0.00000	100.984
405	88.14240	10.53690	1.29306	0.04713	0.00000	0.01781	100.037
Swede Underground 1, rim							
406	87.35770	10.64560	3.23657	0.00000	0.00000	0.01457	101.254
407	87.57780	10.81600	2.74564	0.00000	0.00000	0.00000	101.139
408	87.74160	10.52680	2.79181	0.00000	0.00000	0.04694	101.107
Swede Underground 2, rim							
409	89.53390	10.37330	1.15344	0.03306	0.00000	0.00000	101.094
410	89.73980	10.34360	1.23845	0.00000	0.00000	0.00000	101.322
411	89.64640	10.39580	1.08164	0.05105	0.00000	0.10261	101.277
Swede Underground 2, core							
412	89.96150	10.40080	1.29374	0.00000	0.00000	0.00000	101.656
413	89.62060	9.93295	0.94007	0.00000	0.00000	0.05818	100.552
414	89.44500	10.06630	1.23132	0.00000	0.00000	0.00000	100.743
Swede Underground 3, core							
415	97.27730	2.15195	1.95192	0.00000	0.00000	0.01137	101.393
416	96.20550	2.17475	2.12210	0.00000	0.00000	0.00000	100.502
417	96.06590	2.05469	1.92920	0.00000	0.00000	0.00650	100.056
Swede Underground 3, rim							
418	95.78960	2.22192	2.44344	0.00000	0.00000	0.00000	100.455
419	96.02140	1.99734	2.41311	0.03218	0.00000	0.00000	100.464
420	96.18670	3.03042	0.51119	0.00000	0.00000	0.04052	99.769
Thompson Pup 1, core							
421	95.12760	4.00090	1.46947	0.00000	0.00000	0.03218	100.630
422	94.82020	3.94134	1.43184	0.00000	0.00000	0.00000	100.193
423	94.03780	3.79064	1.12105	0.00000	0.00000	0.01567	98.965
Thompson Pup 1, rim							
424	94.05640	4.17737	1.70006	0.02042	0.00000	0.01154	99.966
425	93.24330	4.17204	1.87008	0.01736	0.00000	0.00577	99.308
426	94.74650	4.30008	1.81637	0.00000	0.00000	0.00000	100.863

TABLE 3: MICROPROBE DATA FOR LODE AND PLACER GOLD GRAINS - IN WEIGHT PERCENT

Line Number	AU e%	Ag e%	Hg e%	Sb e%	Bi e%	Te e%	Totals e%
Thompson Pup 2, rim							
427	86.71850	9.99872	2.33250	0.00000	0.00000	0.07793	99.128
428	88.53290	10.40260	2.25218	0.00000	0.00000	0.00574	101.193
429	87.47430	10.18520	2.00085	0.02031	0.00000	0.00000	99.681
Thompson Pup 2, core							
430	86.99970	11.27450	1.94912	0.00000	0.00000	0.04096	100.264
431	85.13590	10.80460	1.86956	0.00812	0.00000	0.00000	97.818
432	87.83800	11.19700	1.69472	0.00000	0.00000	0.08189	100.812
Thompson Pup 3, core							
433	88.90900	10.34050	1.31777	0.00000	0.00000	0.02376	100.591
434	88.63140	9.97720	1.25753	0.00000	0.00000	0.02786	99.894
435	90.05300	10.22170	1.19189	0.00000	0.00000	0.00000	101.467
Thompson Pup 3, rim							
436	85.70960	11.59450	2.18492	0.05269	0.00000	0.00000	99.542
437	86.29810	10.20490	3.54036	0.00000	0.00000	0.00901	100.052
438	87.85910	10.43490	1.55076	0.00000	0.00000	0.00000	99.845
Archibald Creek 1, core							
439	95.88600	3.38458	1.71673	0.01325	0.00000	0.00329	101.004
440	95.31270	3.50402	1.32295	0.00713	0.00000	0.04358	100.190
441	95.30270	3.22740	1.73170	0.03362	0.00000	0.00494	100.300
442	95.08720	3.22890	2.33241	0.07742	0.00000	0.01480	100.741
443	95.20500	3.40056	1.91862	0.00000	0.00000	0.00000	100.524
Archibald Creek 1, rim							
444	95.09730	3.45545	1.74752	0.00000	0.00000	0.00000	100.300
445	94.43950	3.68629	1.63727	0.00917	0.00000	0.00000	99.772
446	95.01040	3.44150	2.05685	0.00000	0.00000	0.00000	100.509
447	94.68510	3.69822	2.05951	0.00000	0.00000	0.01644	100.459
448	95.05610	3.59436	1.86369	0.00000	0.00000	0.00000	100.514
Au from Au-qtz vein, core							
449	88.54180	8.92785	3.90256	0.00000	0.00000	0.00000	101.372
450	88.45310	9.30535	3.53722	0.00000	0.00000	0.07152	101.367
451	89.03610	9.19588	3.58356	0.00000	0.00000	0.00000	101.815
452	87.34400	9.43472	4.70884	0.00000	0.00000	0.02711	101.515
453	87.10580	9.47463	4.90992	0.00000	0.00000	0.00000	101.490
454	86.09390	9.74380	5.17059	0.00000	0.00000	0.05170	101.060
455	80.17790	8.30308	3.87901	0.00000	0.00000	0.02708	92.387
456	88.74710	9.33307	2.63279	0.00000	0.00000	0.00738	100.720
Au from Au-qtz vein, rim							
457	89.19180	9.54392	2.38741	0.00000	0.00000	0.02869	101.152
458	63.46820	6.96176	3.43583	0.00000	0.00000	0.03196	73.898
459	86.87460	9.48750	4.40872	0.00000	0.00000	0.04916	100.820
460	87.29130	9.38901	4.21164	0.06896	0.00000	0.06224	101.023
461	88.25840	8.89484	3.46455	0.00000	0.00000	0.00000	100.618
462	88.68830	9.09160	2.91787	0.00000	0.00000	0.00000	100.698
463	87.41600	9.03881	4.26576	0.00101	0.00000	0.04588	100.767

TABLE 3: MICROPROBE DATA FOR LODE AND PLACER GOLD GRAINS - IN WEIGHT PERCENT

Line Number	AU e%	Ag e%	Hg e%	Sb e%	Bi e%	Te e%	Totals e%
464	85.65430	9.29302	5.52327	0.00000	0.00000	0.02622	100.497
465	82.48660	9.87660	4.59933	0.00000	0.00000	0.00000	96.963
Fay Creek Nugget, piece 1, core							
486	93.33170	6.07020	1.11498	0.00000	0.00000	0.00000	100.517
487	87.53800	5.50881	1.07437	0.00000	0.00000	0.00000	94.121
488	94.06090	6.25462	0.77040	0.00000	0.00000	0.00941	101.095
Fay Creek Nugget, piece 1, rim							
489	94.39450	6.16052	0.91651	0.02991	0.00000	0.00000	101.501
490	93.44100	5.50250	0.86322	0.00000	0.00000	0.05249	99.859
491	93.87070	5.76638	0.96745	0.00771	0.00000	0.03444	100.647
Fay Creek Nugget, piece 2, rim							
492	91.83980	6.30938	1.09057	0.00000	0.00000	0.00626	99.246
493	92.49540	6.35189	1.25139	0.04139	0.00000	0.02737	100.167
494	91.48220	6.36427	1.03003	0.00000	0.00000	0.01564	98.892
Fay Creek Nugget, piece 2, core							
495	92.94620	6.55046	1.08536	0.01251	0.00000	0.00000	100.594
496	92.27310	6.23871	1.20261	0.00000	0.00000	0.07422	99.789
497	93.25250	6.26621	1.11239	0.00000	0.00000	0.01953	100.651
Fay Creek Nugget, piece 3, core							
498	90.55890	6.04512	0.98420	0.00000	0.00000	0.00000	97.588
499	86.18710	5.85334	0.64796	0.03554	0.00000	0.00000	92.724
500	93.04080	6.49462	0.92796	0.00000	0.00000	0.00000	100.463
Fay Creek Nugget, piece 3, rim							
501	91.59640	6.63043	0.87878	0.01632	0.00000	0.00000	99.122
502	91.51110	6.40070	1.02603	0.00000	0.00000	0.00624	98.944
503	93.12190	6.20248	0.94141	0.00000	0.00000	0.06159	100.327
Sawyer Creek 1, core							
504	96.45660	2.02926	1.72594	0.00000	0.00000	0.05161	100.263
505	96.73120	2.33992	2.41591	0.02214	0.00000	0.00000	101.509
506	95.99590	2.16776	2.37442	0.00000	0.00000	0.04065	100.579
Sawyer Creek 1, rim							
507	92.21250	2.61046	5.59658	0.00000	0.00000	0.00000	100.420
508	94.01660	2.62739	4.53116	0.00000	0.00000	0.00391	101.179
509	94.00070	2.49681	4.53797	0.00000	0.00000	0.00000	101.036
Sawyer Creek 2, rim							
510	89.84540	7.31497	3.44384	0.00000	0.00000	0.00000	100.604
511	89.69190	8.05110	3.94450	0.00191	0.00000	0.00000	101.689
512	88.30720	7.93080	5.05453	0.01149	0.00000	0.00000	101.304
Sawyer Creek 2, core							
513	89.11790	7.91665	4.26967	0.03350	0.00000	0.00000	101.338
514	90.59490	8.10771	3.15448	0.00000	0.00000	0.02799	101.885
515	83.21760	7.36697	6.40704	0.00000	0.00000	0.01089	97.002

TABLE 3: MICROPROBE DATA FOR LODE AND PLACER GOLD GRAINS - IN WEIGHT PERCENT

Line Number	AU e%	Ag e%	Hg e%	Sb e%	Bi e%	Te e%	Totals e%
Sawyer Creek 3, core							
516	91.97430	7.31753	1.11816	0.00000	0.00000	0.00622	100.416
517	92.87740	7.53352	1.29274	0.03634	0.00000	0.00000	101.740
518	92.34640	7.51099	1.14567	0.01912	0.00000	0.06291	101.085
Sawyer Creek 3, rim							
519	92.71110	7.71190	1.25255	0.02485	0.00000	0.01786	101.718
520	92.52830	7.32093	1.34265	0.00000	0.00000	0.00000	101.192
521	93.22130	7.43142	1.26992	0.00000	0.00000	0.00389	101.927
Large Au grain from Sb-Au-qtz vein, core							
522	97.14060	0.40343	3.14184	0.00000	0.00000	0.00000	100.686
523	96.62640	0.50684	3.24076	0.00000	0.00000	0.00000	100.374
524	98.09270	0.47565	3.03734	0.03156	0.00000	0.01923	101.656
525	97.08630	0.48777	3.03011	0.00000	0.00000	0.01522	100.619
526	95.88750	0.39793	3.18654	0.06608	0.00000	0.00000	99.538
527	97.34450	0.33426	3.36111	0.00197	0.00000	0.00000	101.042
528	97.42510	0.41170	3.29418	0.00000	0.00000	0.08730	101.218
529	94.08520	0.43424	3.41686	0.00000	0.00000	0.03605	97.972
Large Au grain from Sb-Au-qtz vein, rim							
530	96.88820	0.53945	3.48476	0.00000	0.00000	0.00000	100.912
531	97.54080	0.48429	3.23639	0.00000	0.00000	0.00000	101.261
532	97.04640	0.44771	3.04062	0.06506	0.00000	0.04804	100.648
533	97.75670	0.45648	3.69408	0.00000	0.00000	0.01121	101.918
534	96.02080	0.58340	3.03322	0.03053	0.00000	0.04320	99.711
535	89.90440	0.44567	3.04200	0.00000	0.00000	0.01600	93.408
536	93.90390	0.38353	3.41092	0.00689	0.00000	0.00000	97.705
537	93.13680	0.47106	3.50508	0.04133	0.00000	0.00080	97.155
Small Au grains from Sb-Au-qtz vein							
538	92.64670	2.06598	1.44897	0.00000	0.00000	0.00637	96.168
539	0.09098	0.00000	0.09610	59.30970	0.00000	0.00000	59.497
540	52.84860	0.76820	0.66900	0.19070	0.00000	0.00000	54.477
Minimum	0.09098	0.00000	0.09610	0.00000	0.00000	0.00000	
Maximum	99.33900	11.59450	6.40704	59.30970	0.00000	0.10261	
Average	92.29649	5.00237	2.26204	0.32363	0.00000	0.01561	
Median	94.03780	3.69822	1.96833	0.00000	0.00000	0.00408	

APPENDIX 2: STRUCTURAL GEOLOGIC MAP OF THE NOLAN AREA.

By Karsten Eden 1998

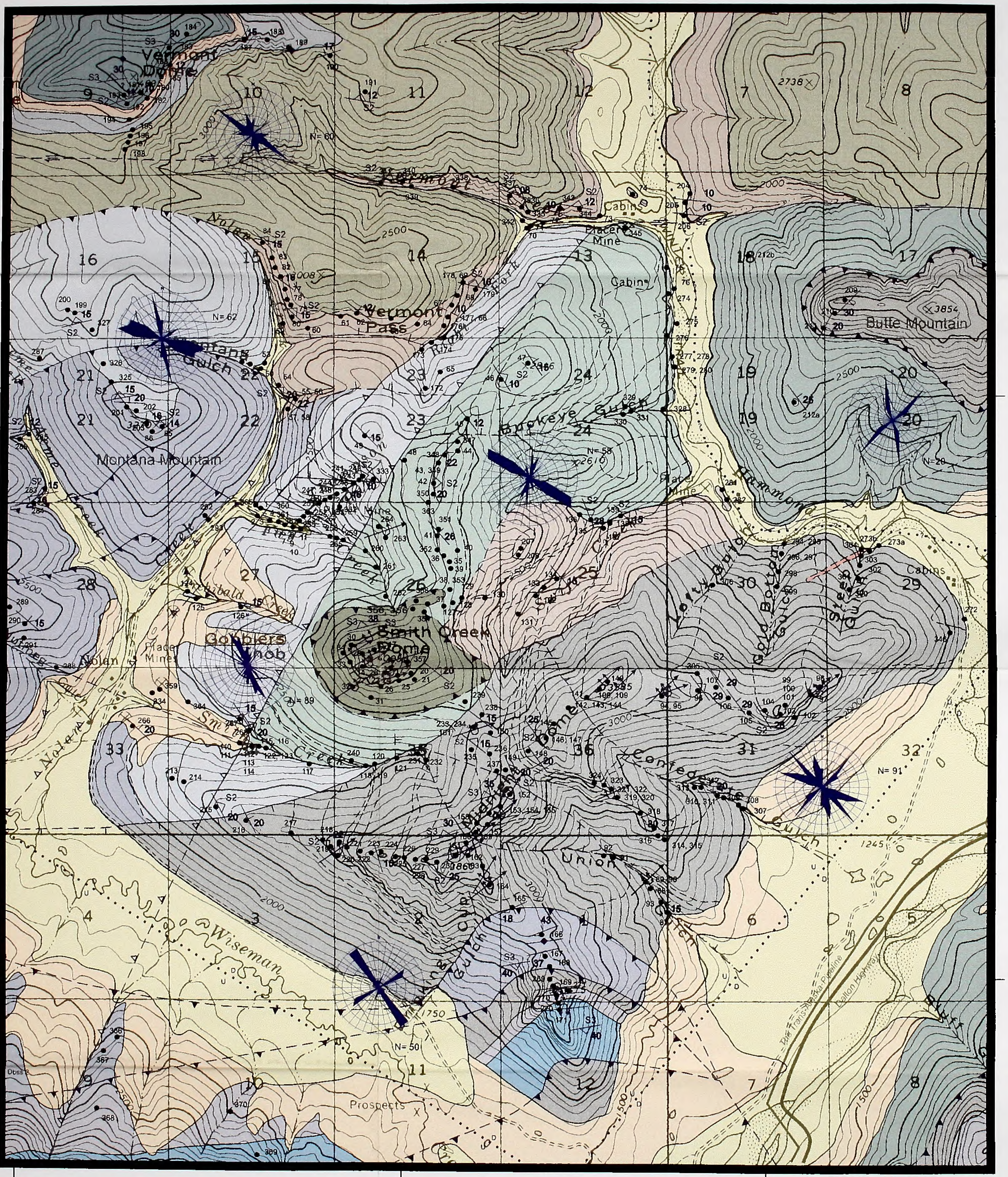

Topographic base map from U.S. Geological Survey Wiseman B1 and C1 quadrangles

Scale 1: 21, 000

0 1 2 3 4 MILES

0 1 2 3 4 Km

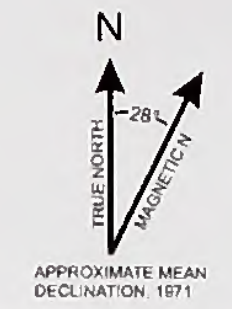

GEOLOGIC MAP SYMBOLS

- Geologic contact - Solid where located; dashed where approximately located
- Concealed fault; U = upthrown side, D = downthrown side
- Strike-slip fault - Solid where located; dashed where approximately located
- Normal fault - Solid where located; dashed where approximately located
- Reverse fault - Sawteeth on upper plate; solid where located; dashed where approximately located
- Thrust fault - Sawteeth on upper plate; solid where located; dashed where approximately located
- Overturned anticline - Showing direction of dip of limbs and plunge of axis
- Overturned anticline - Showing direction of dip of limbs
- Axis of antiform
- 29 Strike and dip of bedding
- 20 Strike and dip of schistosity, S2 = schistosity two, S3 = schistosity three
- 346 Location of outcrop / subcrop exposure
- Rose diagram of strikes of joints N = number of joints

QUATERNARY DEPOSITS

- Oa; ALLUVIAL DEPOSITS, UNDIFFERENTIATED
- Og; GLACIAL DEPOSITS, UNDIFFERENTIATED

TWICE METAMORPHOSED DEVONIAN SEDIMENTARY AND IGNEOUS ROCKS

- Dbcs, UNDIFFERENTIATED, BEAUCOUP FORMATION; UPPER DEVONIAN
- Dbcs, SMITH CREEK DOME SUBUNIT (5), BEAUCOUP FORMATION; UPPER DEVONIAN
- Dbcs, MIDNIGHT DOME SUBUNIT (4), BEAUCOUP FORMATION; UPPER DEVONIAN
- Dbcs, SWIFT CREEK SUBUNIT (3), BEAUCOUP FORMATION; UPPER DEVONIAN
- Dbcs, NOLAN-HAMMOND SUBUNIT (2) BEAUCOUP FORMATION; UPPER DEVONIAN
- Dbcs, VERMONT DOME SUBUNIT (1), BEAUCOUP FORMATION; UPPER DEVONIAN
- Dbps 4, BEAUCOUP FORMATION; UPPER DEVONIAN
- Dbps 3, BEAUCOUP FORMATION; UPPER DEVONIAN
- Dbps 2, BEAUCOUP FORMATION; UPPER DEVONIAN
- Dbps 1, BEAUCOUP FORMATION; UPPER DEVONIAN
- Dbs, UNDIFFERRENTIATED, BEAUCOUP FORMATION; UPPER DEVONIAN
- Butte Mt. Slate, BEAUCOUP FORMATION?; MIDDLE TO UPPER DEVONIAN
- Dbss 2, BEAUCOUP FORMATION?; MIDDLE TO UPPER DEVONIAN
- Dbss 1, BEAUCOUP FORMATION?; MIDDLE TO UPPER DEVONIAN
- Dcss; MIDDLE DEVONIAN
- Dcc; MIDDLE DEVONIAN
- METABASITE; DEVONIAN-JURASSIC?

APPENDIX 3: SAMPLE LOCATION MAP.

By Karsten Eden 1998

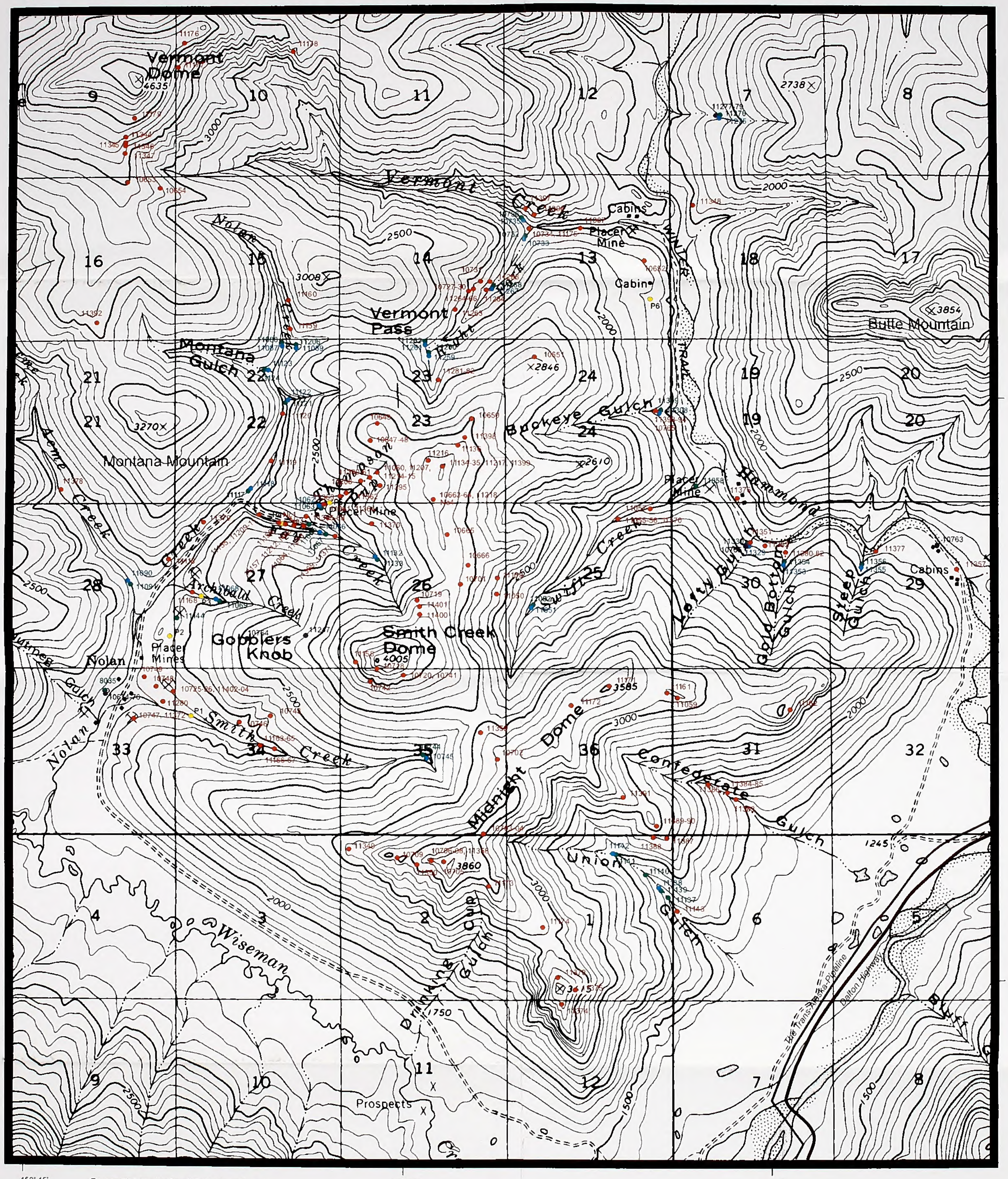

150° 15' — 150° 10' — 150° 05'

Topographic base map from U.S. Geological Survey Wiseman B1 and C1 quadrangles

Scale 1: 21, 000

0 1 2 3 4 MILES

0 1 2 3 4 Km

11349	ROCK SAMPLE
11090	STREAM SEDIMENT SAMPLE
11091	PAN CONCENTRATE SAMPLE
10674	SLUICE CONCENTRATE SAMPLE
P1	PLACER GOLD SAMPLE

APPENDIX 1: GEOLOGIC MAP OF THE NOLAN AREA.

By Karsten Eden 1998

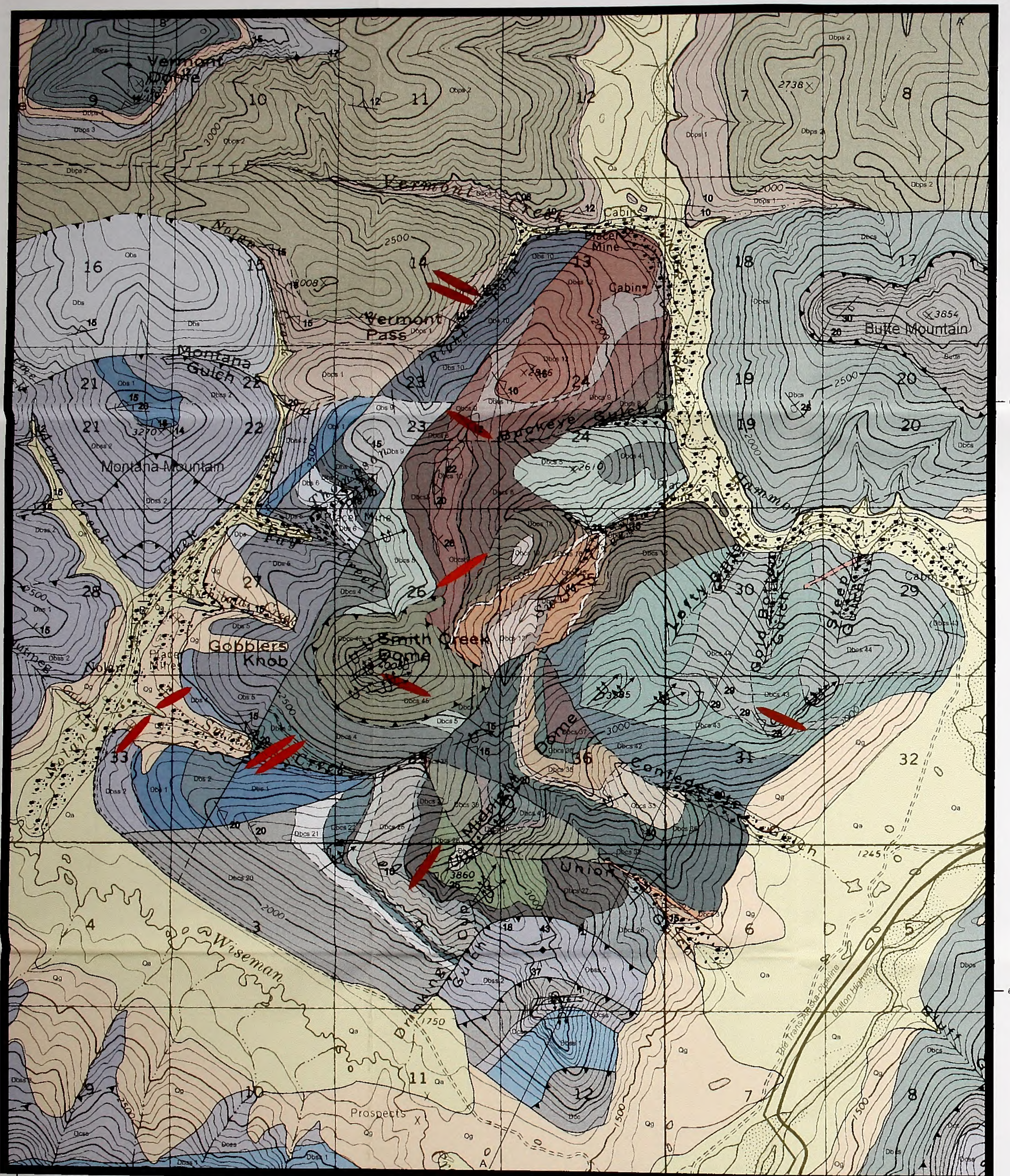

150° 15' 150° 10' 150° 05'

Topographic base map from U.S. Geological Survey Wiseman B1 and C1 quadrangles

Scale 1: 21, 000

0 1 2 3 4 MILES

0 1 2 3 4 Km

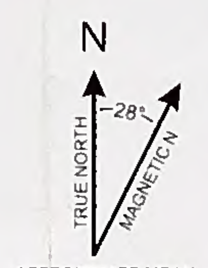

APPROXIMATE MEAN DECLINATION, 1971

GEOLOGIC MAP SYMBOLS

- Geologic contact - Solid where located; dashed where approximately located
- Fault - Solid where located; dashed where approximately located
- Thrust fault - Sawteeth on upper plate; solid where located; dashed where approximately located
- Overturned anticline - Showing direction of dip of limbs and plunge of axis
- Overturned anticline - Showing direction of dip of limbs
- Axis of antiform
- 29 Strike and dip of bedding
- 20 Strike and dip of foliation
- A A' Location of cross section

CORRELATION OF MAP UNITS

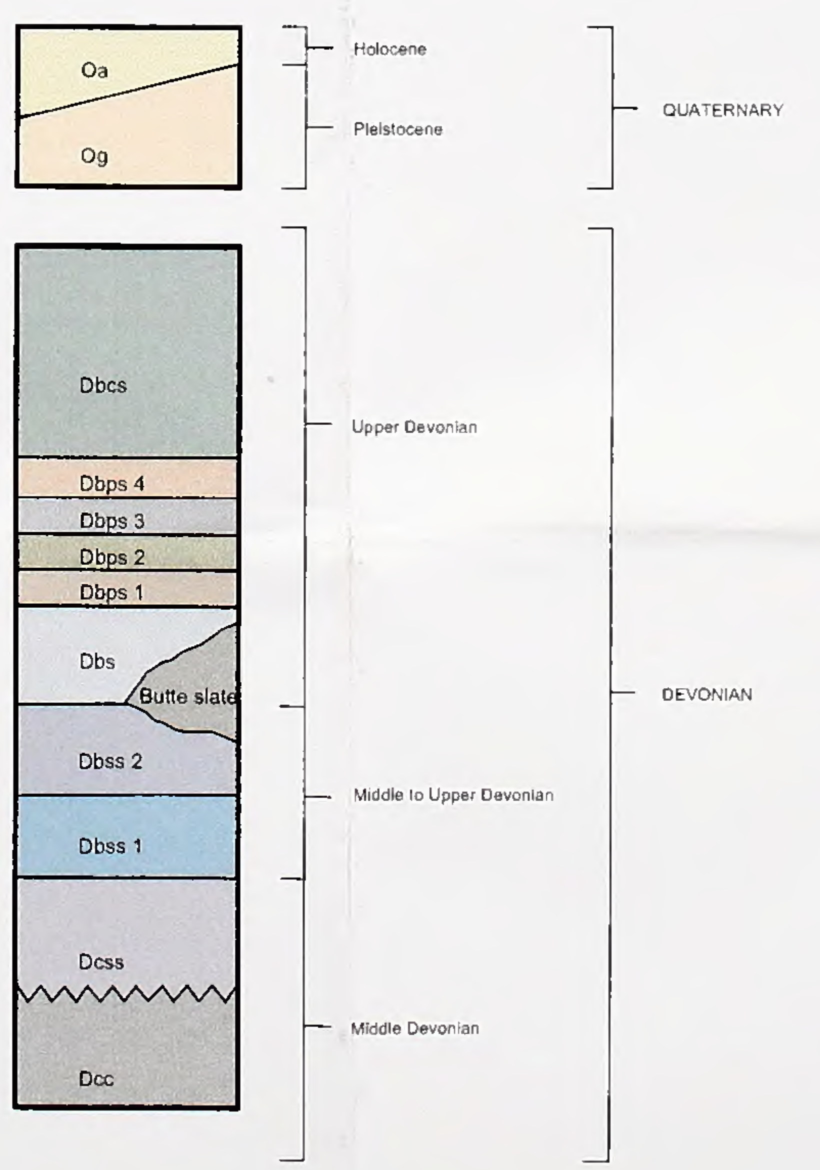

QUATERNARY DEPOSITS

Qa	ALLUVIAL DEPOSITS, UNDIFFERENTIATED
Qg	GLACIAL DEPOSITS, UNDIFFERENTIATED

TWICE METAMORPHOSED DEVONIAN SEDIMENTARY AND IGNEOUS ROCKS

Dbcs	CHLORITIC QUARTZITE AND COARSE GRAINED QUARTZ-MICA SCHIST, INTERLAYERED WITH PHYLLITE, SCHIST; AND CHLORITIC METASILTSTONE BEAUCOUP FORMATION; UPPER DEVONIAN
Dbps 4	BROWN-YELLOW PHYLLITE AND PELITIC MICA SCHIST, BEAUCOUP FORMATION; UPPER DEVONIAN
Dbps 3	GRAY PHYLLITE PELITIC MICASCHIST, BEAUCOUP FORMATION; UPPER DEVONIAN
Dbps 2	GRAY BLACK PHYLLITE AND PELITIC MICA SCHIST, BEAUCOUP FORMATION; UPPER DEVONIAN
Dbps 1	BROWN-YELLOW PHYLLITE AND PELITIC MICA SCHIST, BEAUCOUP FORMATION; UPPER DEVONIAN
Dbs	PHYLLITE, PELITIC SCHIST, AND BLACK SLATE, BEAUCOUP FORMATION; UPPER DEVONIAN
Butte Mt	BLACK SLATE AND BLACK METASILTSTONE, BEAUCOUP FORMATION?; MIDDLE TO UPPER DEVONIAN
Dbss 2	BLACK METASILTSTONE AND PHYLLITE, BEAUCOUP FORMATION?; MIDDLE TO UPPER DEVONIAN
Dbss 1	BLACK METASILTSTONE WITH INTERLAYERS OF PHYLLITE AND FINE GRAINED BLACK QUARTZITE; BEAUCOUP FORMATION?; MID. TO UP. DEVONIAN
Dcss	CHLORITIC SANDSTONE AND CONGLOMERATE; MIDDLE DEVONIAN
Dcc	CHLORITIC AND CARBONATE METASEDIMENTARY ROCKS; MIDDLE DEVONIAN
	METABASITE ("GREENSTONE"); UPPER DEVONIAN-JURASSIC?

LODE VEINS

- Au-Sb-Qtz VEIN SYSTEM
- Au-Qtz VEIN SYSTEM

GOLD - PLACER DEPOSITS

DESCRIPTION OF MAP UNITS

Dbcs differentiated

Smith Creek Dome Subunit (5)	Dbcs 45	Banded quartzite, interbedded with chloritic quartzite and quartz mica schist
Midnight Dome Subunit (4)	Dbcs 44	Chloritic quartzite, interlayered with banded quartzite, siltstone, phyllite
	Dbcs 43	Quartz mica schist, interlayered with chlorite schist and phyllite
	Dbcs 42	Quartz mica schist, interlayered with chlorite schist, phyllite, and metasiltstone
	Dbcs 41	Quartzite schist, chloritic quartzite interbedded with gray-brown schist and phyllite
	Dbcs 40	Gray-brown micaceous schist
	Dbcs 39	Chloritic quartzite, interbeded with phyllite and schist
	Dbcs 38	Brown quartz mica schist
	Dbcs 37	Brown micaceous schist
	Dbcs 36	Chloritic quartzite, banded quartzite
	Dbcs 35	Micaceous brown-green schist
	Dbcs 34	Gray-black-brown schist
	Dbcs 33	Brown schist
	Dbcs 32	Gray-brown micaceous schist, thinly bedded
	Dbcs 31	Gray-black phyllite, quartzite schist, in lower part of Union Gulch black pyrite schist
	Dbcs 30	Gray phyllite, micaceous black schist
	Dbcs 29	Chloritic quartzite
	Dbcs 28	Banded chloritic quartzite, interbedded with chloritic schist
	Dbcs 27	Black-green chloritic schist
	Dbcs 26	Chloritic quartz mica schist
	Dbcs 25	Chloritic schist, thinly bedded
	Dbcs 24	Gray-brown quartz mica schist
	Dbcs 23	Black schist
	Dbcs 22	Chloritic quartz schist, gray-black schist
	Dbcs 21	Chloritic metasiltstone
	Dbcs 20	Gray-green quartz schist
Swift Creek Subunit (3)	Dbcs 19	Gray-black quartz mica schist, black quartzite
	Dbcs 18	Brown-gray chlorite mica schist
	Dbcs 17	Black quartz mica schist with pyrite, interbedded with chlorite schist
	Dbcs 16	Gray-brown phyllite
	Dbcs 15	Gray-brown quartz mica schist
	Dbcs 14	Black micaceous schist with pyrite
	Dbcs 13	Gray-brown phyllite, quartz mica schist
Nolan-Hammond Subunit (2)	Dbcs 12	Gray phyllite, thinly bedded
	Dbcs 11	Gray-black micaceous schist, thinly bedded
	Dbcs 10	Brown chloritic quartz mica schist, coarse grained, "Fortress Formation"
	Dbcs 9	Gray-black-brown micaceous schist, phyllite, quartz mica schist
	Dbcs 8	Phyllite and quartz mica schist
	Dbcs 7	Biotite quartzite
	Dbcs 6	Chloritic quartzite, at Buckeye Gulch with pyrite
	Dbcs 5	Banded quartz mica schist, interbedded with phyllite and chlorite schist
	Dbcs 4	Gray micaceous schist, phyllite
	Dbcs 3	Chlorite schist, micaceous
	Dbcs 2	Gray-black micaceous schist, phyllite
Vermont Dome Subunit (1)	Dbcs 1	Chloritic quartzite, chlorite schist

Dbs differentiated

Dbs 10	Gray-black phyllite with pyrite, gray-black micaceous schist, and black slate
Dbs 9	Gray-brown micaceous schist, phyllite, with pyrite, thinly bedded
Dbs 8	Brown micaceous schist, metasiltstone
Dbs 7	Chlorite schist
Dbs 6	Gray-black micaceous schist, metasiltstone
Dbs 5	Gray-black -green schist and phyllites, various colours
Dbs 4	Brown micaceous schist, phyllite, thinly bedded
Dbs 3	Black micaceous schist, minor pyrite
Dbs 2	Gray-black slate, brown slate
Dbs 1	Gray-black phyllite, black slate, black metasiltstone

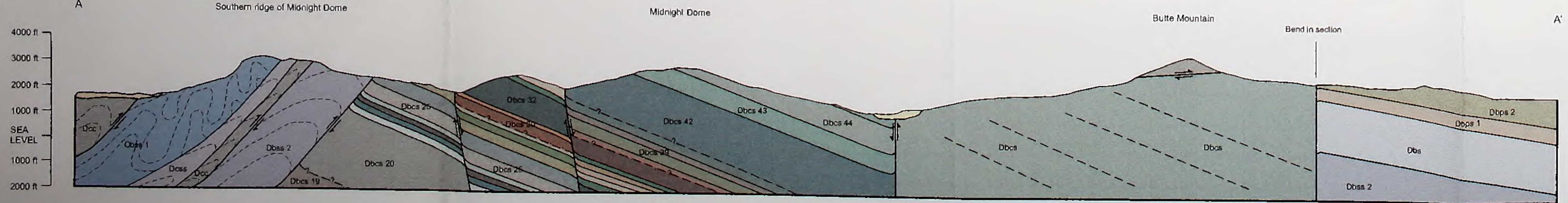

(-0.7) x VERTICAL EXAGGERATION